Vibration Transmission through Structural Connections in Beams

By

Ir. Saiddi A.F.M. Ishak

A Doctoral Thesis

Supervisors: Dr Jane L Horner & Dr Stephen J Walsh

Aeronautical & Automotive Department

Loughborough University

13th May 2018

Acknowledgement

I am grateful to Allah for His blessings, without which none of my work would have been possible.

I am deeply indebted to a lot of people who have contributed towards the completion of this Thesis. Dr Jane L Horner whom proposed this area of research for me to explore and have been guiding me tirelessly. Dr Stephen J Walsh who has been the co-supervisor to guide, support and ensuring the completion of this thesis. To all the Aero & Auto Dept. Loughborough University staff which supports the administrations and activities during my work there.

My wife Siti Aminah who have been struggling even during sickness and toughest times, to continue believing as well as supporting me mentally and spiritually. To my children, M Affiq Firdaus, M Arrif Firdaus and M Addib Firdaus, who has always been there to enhance my strength when I was weak, filling me when I was empty and without which this could never happen.

My parents, M Ishak & Alawiah for all their prayers for me as well as moral encouragement and they have always believed that I could accomplish this task. My siblings, S.N Izura and Zulkiflee Zain along with their families, thank you for your support when I was away and back, for this study. My prayers for the soul of our youngest sister Siti NorAdilah, may Allah grant you Jannah and be amongst the chosen there.

And finally, thousands of thanks to all my friends and those who have provided guidance and support for me to get through with this journey.

………………

2010-2017

Abstract

Analysis of vibration transmission and reflection in beam-like engineering structures requires better predictive models to optimise structural behaviour further. Numerous studies have used flexural and longitudinal structural wave motion to model the vibrational response of angled junctions in beam-like structures, to better understand the transmission and reflection properties. This study considers a model of a variable joint angle which joins two semi-infinite rectangular cross-section beams. In a novel approach, the model allows for the joint to expand in size as the angle between the two beams is increased. The material, geometric and dynamics properties were consistently being considered. Thus, making the model a good representation of a wide range of angles. Predicted results are compared to an existing model of a joint between two semi-infinite beams where the joint was modelled as a fixed inertia regardless of the angle between the beams, thus limiting its physical representation, especially at the extremes of angle (two beams lay next to each other at 180^{o} joint). Results from experimentation were also compared to the modelling, which is in good agreement for the range of angles investigated. Optimum angles for minimum vibrational power transmission are identified in terms of the frequency of the incoming flexural or longitudinal wave. Extended analysis and effect of adding stiffness and damping (rubber material) at the joint are also reported.

Abbreviations

EA	Young's modulus x area of the beam
EI	Young's modulus x second moment of area (inertia)
A	cross-sectional area
I	second moment of area (inertia)
m_j	mass of joint
J_w	width of joint
L	thickness of the beam
w	width of beam
t	time
F	resultant force
V	shear force
M	moment acted
D	longitudinal stiffness (for quasi-longitudinal wave)
U	displacement due to longitudinal in 'x' or lateral direction
W	displacement due to flexural in 'y' or vertical direction
FF	Flexural incidence wave, Flexural reflected/transmitted wave
LL	Longitudinal incidence wave, Longitudinal reflected/transmitted wave
FL	Flexural incidence wave, Longitudinal reflected/transmitted wave
LF	Longitudinal incidence wave, Flexural reflected/transmitted wave
$A_{I,\ L,2,4}$	wave amplitude in Alpha, section in-between force and joint (transmitted)
$B_{L,1,3}$	wave amplitude in Alpha, section in-between force and joint (reflected)
$C_{L,2,4}$	wave amplitude in Beta, section after the joint
$D_{L,1,3}$	wave amplitude in Gamma, section of the other side after the force

List of Symbols

μ	Poisson's ratio
ρ	density of the material
ω	radius frequency of vibration
π	180 degree in radian
θ	angle of beam joint
c_L	velocity of propagation of the longitudinal displacement
k_L	longitudinal wavenumber
λ_L	longitudinal wavelength
c_F	velocity of propagation of the flexural displacement
k_F	flexural wavenumber
λ_F	flexural wavelength

Table of Contents

List of Figures

List of Tables

Chapter 1: Introduction

A fundamental understanding of wave propagations in built-up structures is one of the key areas in engineering acoustics and vibrations. Any continuous system such as an aircraft structure, a pipeline or a car chassis has its masses and elastics forces continuously distributed. The structures comprise coupled cables, rods, beams, plates, shells, etc., all of which are neither rigid nor mass-less (W.T.Thomson 2002). These systems consist of an infinitely substantial number of particles and hence require an infinitely considerable number of coordinates, or degrees of freedom to describe the motion, and hence an infinite number of natural frequencies and an infinite number of natural modes of vibration are present.

It is observed and understood that any built-up structures need a model of a joint for a complete assembly, and vibration level study for the damping and transmission coefficient at the joints are still a great area of unknown. Statistical Energy Analysis (SEA) being dealing with estimating the coefficient to represent certain built-up structures. However, for beams joined together, the behaviour of vibration with regards to the different joint types requires research and understanding. This study will look at a joint model and be comparing results to real structures and estimate the vibration level for the benefit of understanding the behaviour of vibration transmission and reflection.

Vibration phenomena involving diverse types of structures and products have been an expanding area of studies. Vibrations being examined and observed using several behaviours such as through displacements due to any arbitrary input, its easiness to vibrate and the rate of change of vibration, those which are known in terminology as receptance, mobility and accelerance (Cremer 2005). A continuous system should be modelled with distributed mass, stiffness and damping such that the motion of each point in the system can be specified as a function of time and displacement. The resulting partial differential equations which describe the particle motion are also called the wave equations, which describes the propagation of waves in solids.

Generally, on knowing the factors relates to a certain situation by defining the source, path and receiver of a problem would provide a better approach to deal with vibration phenomena. Signal and system analysis defines two separate distinctions for solving acoustic and vibration problems. The process of determining the response of a system, due to some generally unknown excitation is called signal analysis and the technique for determining the inherent properties of a system by simulating the system with measurable force and studying the response/force ratio is called system analysis (Dossing 1988). Hence, this work presented would be dealing with system analysis by understanding the governing equations, modelling and validations through experimentations.

As for the problem overview, characteristics of vibration through wave analysis is very much in advantage especially dealing with structural joints or assembly. The knowledge will ensure a more reliable behaviour and prediction. Such study was needed to provide a closer understanding of vibration transmission and reflection to the current literature. Hence, this encourages a realistic model of mathematical to be established along with the required analysis and practical verifications. Consideration of damping for the material in the work have increased the complexity and method to deal with it and all other parameters being elaborated progressively in this thesis.

1.1 Aims and Objectives

There are three broad aims of this study.

1) Extending knowledge on using wave analysis in vibration reflection and transmissions.
2) Extending techniques used in the measurement of vibration power.
3) Improving the knowledge of vibration power in the angled jointed beam with a comparable mathematical model and measurements.

Accordingly, the objectives of this study are:

1) Modelling the joint in beam such that estimates of vibration levels give realistic values.

2) Analyze the modelling obtained with suitable measurement technique to eventually conclude a good agreement from the results.

1.2 Motivation

The progress of structure analysis requires closer to realistic prediction towards its behaviour; hence this work would contribute modelling of joint in beam structures for vibrational effect. Development of mathematical equation to represent the variable joint was a motivational challenge which the author believes would provide a significant addition to the knowledge. Steps from equation development into the modelling using MATLAB, and finally to ensure validation of result have been a driving effort to achieve a better understanding of vibration power reflected and transmitted in beams.

1.3 Contributions

The contribution of the research described in this thesis comprises as follows:

1) Model of an angled joint which varies in mass and inertia with respect to the two beams connection assembly.
2) Comparison with measurement result which validates the novel variable joint model.
3) The enhanced model of joint for variation of beam cross-section and joint material types.

1.4 Thesis Layout

This thesis is organised into nine chapters from this introduction until the summary and conclusions. Chapter 2 which is 'Review of Previous Works' covers various area of analysis for vibration transmission and reflections. Consideration of Euler-Bernoulli and its advantage against Timoshenko beam were part of the highlights.

Chapter 3 of the 'Modelling of vibration in a uniform beam' discuss the background of equation origins and deriving it for the analysis especially on the further chapters by using wave approach for vibration power. Moving on to the Chapter 4, 'Analysis of Variable Joint Modelling' would be the core information on the contribution for a realistic model of joint for beam were being derived. Analysis of output power against the input power was investigated to obtain validation of the model and the equations used.

Chapter 5 of 'Force Application for Beam Joint' elaborates the actual application with a complete spectrum of input waves from displacement, force and moments. This will also derive the equations governing the modelling of involving 12x12 matrix. Comparison to the measurements would then be done in Chapter 6 'Experimental Apparatus and Measurement Method'. Set-up and equipment used were detailed out and the result captured from the activities were explained for the validation of work.

Chapter 7 of 'Comparison of modelling and measurement due to rubber sheet hysteresis damping effect' would extend further advantages of behaviours in the variable joint model for added damping material into the beam-joint arrangement. And lastly, the summary and conclusion of this work, contributions, and future works are provided in Chapter 8.

Chapter 2: Review of previous works

Recent progress and trends in aeronautical and automotive vehicles have shown an exponential growth of demands for power, speed and reliability. This has also introduced several risks (R.Whalley 1998) and attempts to reduce those risks require investigation and research. As an example, aircraft wing structure (R.Martinez-Val n.d.) experience large variation in the frictional and stiffness parameters as a function of velocity, which these changes occur in proportion to aircraft velocity and velocity invariant characteristics which is entirely dependent upon the structural properties of the wing assembly, in terms of such as the mass-inertia, natural damping and stiffness. This has resulted in the increased interest to predict these vibration characteristics of built-up structures before the damage occurs.

Several papers involving wave characteristics in terms of transmission and reflection from a discontinuity have been published to provide further in-depth information and offer solutions for predicting and/or control of vibration behaviour in structures. Research relating to the modelling of ***wave motion through junctions*** and methods for ***measuring transmission properties*** of vibration is the area of interest for this study.

The vibrational behaviour of beam systems can be expressed in terms of waves of both propagating and near-field types. A propagating wave incident upon a discontinuity gives rise to reflected and transmitted waves of both kinds whose amplitudes may be found from well-known reflection and transmission coefficients. A paper by B.R.Mace (1984) extends to the case of the incident near-field waves, reflection and transmission matrices which are derived for the cases of a point support, change in section, reflection at a boundary and the effects of applied excitations. He also, however, noted that incident near fields can give rise to substantial propagating components, but this would be dismissed for the case of time-averaged power as well as an infinite section of both sides of beams or structure.

J.F.Doyle (1987) stated that analysis of the propagation of stress waves through a framed structure was also complicated by the presence of joints which act as both filters and sources of new waves. That is, an incident flexural wave can generate new flexural waves as well as longitudinal and torsional waves. A methodology detailed in the paper was quite successful in predicting the effects of an arbitrary T-joint, on the propagation of flexural waves. The joint was modelled as a rigid cylinder with independently specified diameter and density. It was assumed that the flexural waves have a Bernoulli-Euler beam dispersion relation, longitudinal waves are non-dispersive, and the joint was a rigid mass was clearly stated to the support result gained comparing with higher order theories such as Timoshenko beam.

J.L.Horner (1990) & (1991) was concerned with the prediction of vibrational power transmission through bends or joints in beam-like structures, impinged on by either flexural or longitudinal waves. Models have been developed which determine the wave type which carries most power in each section of the system. The research was also successful in predicting behaviours of vibration transmission at different angles of the joint upon various combinations of beam arrangement and ratio dimensions. This was used as the main reference to produce the estimated vibration levels in this work for comparing with the measurement taken in the laboratory.

Y.P.Guo (1995) studies the interactions between incident flexural waves and a structural joint that connects two identical elastic beams at an arbitrary angle. The beams are described by classical beam theory and the joint is modelled with stiffness, dissipation, and mass, all in three degrees of freedom, namely, in longitudinal and flexural displacement as well as rotation. Coefficients of flexural wave transmission, reflection, dissipation, and conversion to longitudinal waves were derived, and are analysed to reveal the functional dependence of these coefficients on parameters such as frequency, joint angle, and various joint parameters. Some potential ways of minimizing flexural wave transmission through a joint were also discussed.

With regards to the related input, the statistical energy analysis (SEA) method for two coupled plates, (R.S.Langley 2010) noted that the fraction of the energy that passes through the junction of the plates is governed by the power transmission coefficient; therefore, the power transmitted will be possible to measure. Determination of power transmission behaviour would not be achievable without knowing the coefficient value and it is vital to further develop the SEA method. Therefore, an in-depth investigation of this study of vibration power prediction will further assist next or future works of transmission/reflection at the joint due to vibration. To find the transmission coefficient, the subsystem of the junction is easier to be assumed as ‘semi-infinite’ and ***transmission coefficient is defined as the ratio of the power in a transmitted wave to the power in the incident wave.***

SEA uses energy as the parameter of interest and has always recognized that power is the key parameter, but with SEA modelling it is very difficult to predict the power transmission coefficient. Hence a better insight into the modelling of joint parameters from this thesis will lead to better prediction of power transmission coefficient and better SEA modelling.

T.Y.Li (2001) considered vibrational power flow analysis for *damaged beam structures.* The damage was modelled as a joint of a local spring. The damage point transfer matrix and the beam element transfer matrix are deduced, and then the relation of the vibrational power flow, the position and the characteristic size of the damage are obtained combined with periodic structure theory. The damage was modelled as a joint of a local spring and concluded that it can be analysed by comparing the vibrational power flow of beam structures with and without damage in further related research works.

Jonas et al (2008) stated, for a wave propagating in a beam, it enters a discontinuity and will be partly reflected and partly transmitted. Using Euler-Bernoulli theory, the application investigates a junction of two beams with rectangular cross-section and concludes that non-reflective junction of the right-side beam can be chosen in such a way that the active force (force to associate with power summation) and beam configuration always draw power from the left-side beam.

A paper by J.M.Muggleton (2007) stated that several approaches to estimating the reflection and transmission coefficients of joint from measured data were developed. Measurements were made on a beam with a mass/moment of inertia discontinuity and on a pipe with a right-angled bend, both with flexural excitation, to demonstrate the procedures and to highlight some of the inherent difficulties.

2.1 Euler Bernoulli application

In addition to the earlier reference related to Euler-Bernoulli beam theory, it is essential to further support the simplicity provided by this application in terms of a systematic and recursive procedure.

An alternative wave-based analysis technique from above beam theory were introduced for the dynamic response solutions, in terms of the transfer function, of one-dimensional distributed parameter systems with arbitrary supporting conditions which does not require Eigensolution as a priori or initial (B.Kang ,April 2007). The spatial amplitude variations of individual waves were presented by the field transfer matrix and the distortions of the wave amplitudes at point discontinuities due to constraints or boundaries are described by the wave reflection and transmission matrices.

Further investigation using Euler-Bernoulli theory was also considered by (C.Mei 2005) & (Hyungmi Oh 2004) for lighter structures and from the wave vibration standpoint. Wave reflection and transmission matrices were described for wave amplitudes at point discontinuities. Spectral element method used with the beam theory has also been compared with finite element solutions for vibration characteristics, wave characteristics and the static and dynamic stabilities.

Various other papers have also considered the Euler-Bernoulli beam as the mathematical model despite the neglected shear effects in the deformable solution it provides, compared to Timoshenko's shear-deformable model solution. The thin beam definition of Euler-Bernoulli (B.R.Mace 1987) was also used in an active control of disturbances propagating along a waveguide regarding the control of flexural vibration. The Euler-Bernoulli beam application nevertheless would always be easier to be manipulated and hence provide comparable required results.

2.2 Timoshenko Beam application

Consideration for higher frequencies, typically when the transverse dimensions are not negligible with respect to the wavelength, have ruled out Euler-Bernoulli beam theory as secondary after Timoshenko beam applications

C.Mei (Dec 2008) concerns in-plane vibration analysis of coupled bending and longitudinal vibrations in H- and T-shaped planar frame structures. Exact analytical solutions were obtained using wave vibration approach using Timoshenko beam theory, which considers the effects of rotary inertia and shear distortion. Reflection and transmission matrices corresponding to incident waves of flexural vibrations in the planar frame arriving at the "T" joint from various directions were also obtained.

In another paper by C.Mei (August 2005), concerns wave reflection, transmission and propagation in Timoshenko beam together with wave analysis of vibrations in Timoshenko beam structures. These papers have both shown good employment to complex structures and would be a related comparison to the future research conducted in this report.

Wave reflection and transmission in composite beams containing a semi-infinite delamination (Wan-Chun Yuan 2008), wave propagation in a split beam (T.N.Farris 1989), flexural-torsional-coupled vibration analysis of axially loaded closed-section composite beam using DTM (differential transform method) (M.O.Kaya Sept 2007), and free vibration analysis of axially loaded cracked beam using dynamic stiffness method (E.Viola 2007), have all employed the Timoshenko beam structure theory to take into account the coupling effects of shear deformation exist between the material layers. Such complexities in the solution were shown to be difficult to be treated in recursive numerical-modelling and experimentation activities.

2.3 Vibrational energy, velocity and displacement

Wave motion in thin, uniform, curved beams with constant curvature was considered in a paper by S.K.Lee (2007). The beams are assumed to undergo only in-plane motion, which is described by the sixth-order coupled differential equations based on Flugge's theory. The energy can be transported independently by the propagating waves and by the interaction of a pair of positive and negative going wave components which are non-propagating, i.e. the wave numbers are imaginary or complex. It also suggested that a further transformation can be made to power wave, which can transport energy independently. The first concerns power transmission and reflection through U-shaped connector between two straight beams, while the second concerns the free vibration of finite curved beams.

Another method for studying the vibrational energy flows through structures based on receptance theory (K.Shankar 1997), stated that the variation of the recovered internal damping coefficients as compared to the specified values was used as an indicator of benefit in SEA work. Vibration energy transfers, impedance approach and energy-based control strategy by (K.Renji 2006), (L.C.Chow 1987), (F.Fariborzi June (1997)), were further applied as a technique to various free and forced structural vibration issues.

2.4 Power measurements

Power measurement was applied by S.K.Lee (2004) was used in a vehicle using isolators to attenuate the vibrational transmission from an engine to a car body. Vibration power flow through these isolators gives information on the flow of the vibrational energy generated from an engine or induced from the road. The measurement of vibrational power flow at each isolator identifies the vibration transmission path in a vehicle. A simple equation was derived for the calculation of vibration power flow at the isolator of a passenger car. The equation was used for the measurement of the vibrational power flow at several isolators of the test car. From these results, the vibrational transmission path of the test car was identified and extended to the reduction of the structure-borne noise in the compartment of the test car

Vibrational power transmission in curved beams (S.J.Walsh 2000) & (S.J.Walsh 2001), seating of a vibration isolated motor (R.J.Pinnington 1987), and from a finite source beam to an infinite receiver beam via a continuous complaint mount (R.J.Pinnington 1990), were also successfully employed by all the papers above and giving clear comparison with power measurements formulation in experimentation.

In addition to that, the use of the effective point mobility concepts allows distribution of power flow and vibration over a contact region to be determined (J.Dai 1999), because power, force and velocity are easily related to mobility. So, it is convenient and efficient for handling problems concerning vibration transmission. Various other papers by (Albert.L.Stiehl 1996), (Chun-Chuan Liu 2010), (R.S.Langley 1995), also adapts the power flow analysis technique for beam members with multiple waves types, power transmission in a one-dimensional periodic structure subjected to single-point excitation and active control of power flow transmission in a finite connecting plate.

2.5 Experimentation consideration

An article by T.Eck (2000) which uses a novel method to measure the point mobility and resulting vibrational energy of a beam subjected to moment excitation were presented with reliable experimentation rig. Using finite-difference approximation, the rotational motion of the beam at the point of excitation was calculated. Moment excitation is induced by its specially designed impact rig which applies two equal and opposite forces on two-moment arms that are perpendicularly attached to the beam. The technique also showed good agreement over a wide frequency range between the measured input energy and the measured transmitted flexural wave energy along the beam.

A paper by R.J.Pinnington and R.G.White (1981) derived the expression for power input to a structure and comparing the experimentation with theoretical result. It also further illustrated the experimental condition to simulate an infinite beam where each end of beam embedded in sandboxes along with rubber foam. In such it's being designed to be anechoic termination while suspended by piano wires.

M.Petyt et al, (1977) has further described the experimental measurements using Perspex model, J.W.Verheij (1980) elaborates for measuring power flow in longitudinal and torsional waves on beam-like structures, R.S.Langley (1989) added good agreement of result of beams which rest on multiple simple support and C.J.Wu (1995) also further describe the expression for vibrational power input to a structure.

In a paper by L.Gaul (October 1983), excitation by incident flexural waves, as well as longitudinal waves were discussed for characteristics of wave transmission, reflection, and energy dissipation of jointed beams. The influence of different model of the joint was compared with a proposed setup for experimental verifications.

Multi-mode transmission at an L-junction of thin rods has been investigated theoretically and experimentally by B.M.Gibbs et al (Oct 1987). Various driver and accelerometer configurations for excitation and detection of different modes of vibration which for compressional, torsional, and bending waves were illustrated for the measurement techniques.

2.6 Wave measurements

Vibration can be described as a linear combination of the modes of a structure (C.Mei October 2002). An alternative approach is to describe vibration as propagating waves travelling in the structure. Papers by M.Meo et al (2005) and R.S.Langley (1990), (1994) & (1996) deals with the beam, plate, layered structures, pipes, curved panels and sandwich plates for a solution in wave analysis.

This approach provides a better understanding to predict vibrational behaviour where each longitudinal, flexural and torsional displacement being derived from wave amplitudes and its travelling directions (either positive or negative). The application in the frequency domain by using the wave equation (being of second order) is amenable to both numerical and analytical solution than the standard fourth order differential equations (R.S.Langley 1991).

This is also advantageous rather than the conventional differential equations of motion, provided that certain assumptions are made regarding the response of the system in the vicinity of a structural discontinuity. The wave approach is also a convenient framework for calculating the coupling loss factors which appear in the SEA, via a combination of wave transmission analysis and diffuse wave theory. Additionally, wave analysis can yield great physical insight, particularly when applied to the interactions of fluid and structures (R.S.Langley 2010).

A work (Renno and Mace 2013) for wave approach in vibration reflection and transmission, presents a hybrid method combining a finite element (FE) and a wave & finite element (WFE) model to determine the coefficient. It has successfully predicted the simplified model of the analytical and numerical results, for L-frame beam with the joint modelled using standard finite element.

2.7 Concluding remarks

Several of the papers stated the advantages of using Timoshenko beam theory as to account for higher modes, giving better results than Euler-Bernoulli beam theory. The objective of this study is to better estimate vibration power in structural joint, taking the advantage of Euler-Bernoulli thin beam theories of its simplicity on modelling the problem into a mathematical equation. Approaches using wave equations were the most convenient and much applicable in measuring the vibration transmission and power. Several set-ups for experiment purposes were also noted as an area to be considered for next step in this work.

The current model is considering flexural and longitudinal (in-plane) without damping or stiffness in joint. Further development in the model has considered improvements from lumped mass rigid joint into a variable rigid size joint and measuring the input-output and transmission-reflections from power or structural intensity. The cross-coupling effect between longitudinal and flexural was also being investigated in this model.

A more realistic joint will further include the damping and stiffness in the beam, particularly for in-plane incident waves. The flexural and longitudinal power would be further considered to gain closer comparison to the experimental work. Measurement method will include a different combination of transducers and using the model to simulate responses with error signals expected from experimental work and tabulate error contribution in each measurement method. This will aid the further definition of the experimental set-up for next model of joint.

Work Produced in this thesis would be categorised in Euler Bernoulli beam application with experimental validation. Further expanding the joint types, cross sections and material changes would contribute to the literature of vibration in jointed beams.

Chapter 3: Modelling of vibration in a uniform beam

3.1 Vibration analysis – wave approach

It is convenient to think of the physics of the response in the low-frequency region when the response of a system to excitation can be represented in terms of a summation of modes, but for higher frequency, there are advantages in representing the responses as the sum of waves (R.S.Langley 2010). The following sections discuss the structural waves considered in this research work as well as providing a basic understanding of beam-lumped mass joint configuration used in the literature. Areas for improvements would be noted, and in the end, chapter to lay the required steps on improving the method used for better prediction of vibration reflection and transmission.

3.2 Wave Types

There are three main types of waves considered in the previous work related to vibration transmission of structural connections (W.T.Thomson 2002), which were longitudinal waves, lateral waves and torsional waves. Only two wave types as Figure 3-1 that will be further elaborated in terms of mathematical and analysis throughout this thesis for its relationship to force applications, which are longitudinal and lateral. Furthermore, torsional waves could be similarly obtained from longitudinal wave steps of derivation for next consideration of research work.

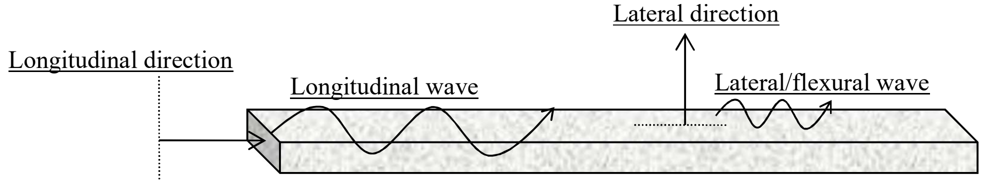

Figure 3-1: Wave types for longitudinal and lateral in the beam

3.2.1 Longitudinal wave

Longitudinal or compressive waves are waves in which the direction of the particle displacements coincides with the direction of wave properties. *Quasi-longitudinal waves* should be considered for bars or plates that are having one or more outer surface free from constraint due to Poisson contraction phenomena.

3.2.2 Lateral waves

Lateral / Bending or Flexural waves occurs due to the existence of both bending moment and shear force on an element. The behaviour of material with regards to flexural waves are very common especially in a built-up structure and its joints. This wave type would be the focus throughout this work where limitations on measurements for longitudinal waves being considered.

3.3 Development of wave equation

Propagation of acoustic/vibration power is governed by wave equations referring to the above wave types. Considering a single wave propagates in the structure, the wave equation is derived to produce solutions in terms of displacement, for both longitudinal and lateral vibration of the slender beam.

3.3.1 Longitudinal vibration of the beam

From Figure 3-2, an element of length dx on a long, slender and uniform beam with longitudinal displacement $u(x,t)$ at x will have displacement $u + \left({du}/{dx}\right)dx$ at $x + dx$.

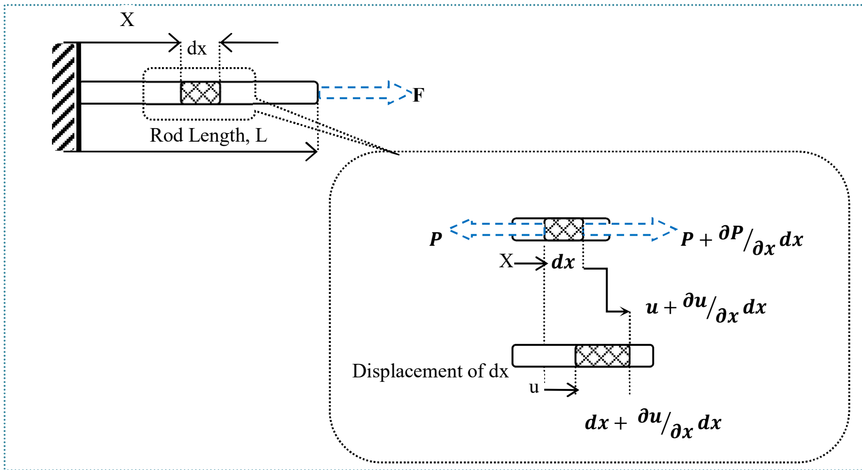

Figure 3-2: Forces and displacement along rod element (W.T.Thomson 2002)

Where the unit strain is $\partial u/_{\partial x}$. From Hooke's law (Cremer 2005), the stress-strain relation is,

$$P/_{A} = D\ \partial u/_{\partial x}$$

Equation 3-1

where P is the force at x, A the cross-sectional area, and D is the longitudinal stiffness (for quasi-longitudinal wave) given by,

$$D = \frac{E}{(1-\mu-2\mu^2)/_{(1-\mu)}} = \frac{E(1-\mu)}{(1+\mu)(1-2\mu)}$$

Equation 3-2

here μ as the Poisson's ratio defined as the ratio of the magnitude of the lateral strain to the longitudinal strain, but for pure longitudinal wave (slender and uniform beam), only modulus Young, E would be significant due to consideration of deformation for single plane and differentiation with respect to x for Equation 3-1 yields

$$\partial P/_{\partial x} = AE\ \partial^2 U/_{\partial x^2}$$

Equation 3-3

Application of Newton's law to the element gives

$$\boldsymbol{\rho A dx\, \partial^2 U/_{\partial t^2} = \left(P + \partial P/_{\partial x}\right) - P}$$

Equation 3-4

Elimination of $\partial P/_{\partial x}$ between (3) and (4) gives,

$$\partial^2 U/_{\partial t^2} = (E/_\rho)\, \partial^2 U/_{\partial x^2}$$

Equation 3-5

Let, $c_L = \sqrt{(E/_\rho)}$, then

$$\left[\!\left[\partial^2 U/_{\partial x^2} = (1 \,/\, c_L{}^2)\, \partial^2 U/_{\partial t^2}\right]\!\right]$$

Equation 3-6

where c_L is the velocity of propagation of the longitudinal displacement or stress/compressive wave in the rod. It is seen that the velocity increases with increasing modulus E, and decreases with increasing density ρ.

The longitudinal wave number is defined as

$$k_L = \frac{\omega}{c_L} = \frac{2\pi}{\lambda_L}$$

Equation 3-7

where ω is the radius frequency of vibration, and λ_L is the wavelength. Since the frequency, $f = \omega/_{2\pi}$, then

$$\lambda_L = \frac{c_L}{f}$$

Equation 3-8

3.3.2 Lateral vibration of the beam

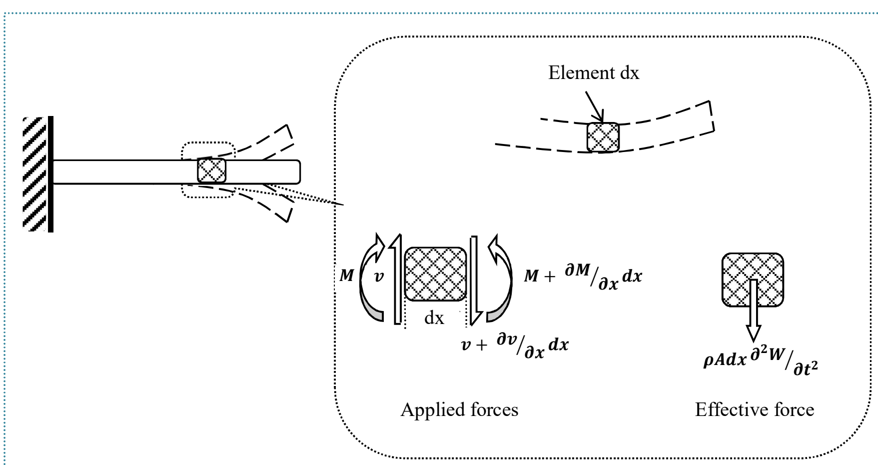

Figure 3-3: Forces and moments along rod element (W.T.Thomson 2002)

The lateral beam deflection in Figure 3-3, is assumed to be due to bending only as in the classical Euler–Bernoulli beam (W.T.Thomson 2002), which considers an element of the beam of length dx. Application of Newton's law to the element of lateral force gives

$$F = V + {\partial V}/{\partial x}\, dx - V = \rho A dx\, {\partial^2 W}/{\partial t^2}$$

Equation 3-9

where F, resultant force and V, shear force.

$$\text{or, } {\partial V}/{\partial x} = \rho A\, {\partial^2 W}/{\partial t^2}$$

Equation 3-10

Summing the moments on the centre of elements gives

$$\cancel{M} + \underbrace{V\frac{\partial x}{2} + V\frac{\partial x}{2}}_{V\partial x} + \underbrace{\frac{\partial V}{\partial x}dx\frac{dx}{2}}_{\approx 0} = \cancel{M} + \frac{\partial M}{\partial x}dx$$

Equation 3-11

where M, moment acted on the element.

With further simplification to the above equation,

$$Vdx = \frac{\partial M}{\partial x}dx$$

$$V = \frac{\partial M}{\partial x}$$

Equation 3-12

Differentiation with respect to x gives

$${\partial V}/{\partial x} = {\partial^2 M}/{\partial x^2}$$

Equation 3-13

It follows from Equation 3-10 and Equation 3-13,

$${\partial^2 M}/{\partial x^2} = \rho A\, {\partial^2 W}/{\partial t^2}$$

Equation 3-14

It is known from mechanics of materials (H.Tongue 2002) that,

$$M = -EI \, {}^{\partial^2 W}\!/_{\partial x^2}$$

Equation 3-15

Where *EI* is a constant value of Young's modulus, *E* (material property) and second moment of area or moment of inertia, *I* (material size/cross-section).

Differentiate twice with respect to x then gives

$$\frac{\partial^2 M}{\partial x^2} = -EI \frac{\partial^4 W}{\partial x^4}$$

Equation 3-16

Finally, from Equation 3-14 and Equation 3-16,

$$\frac{\partial^4 W}{\partial x^4} + \frac{\rho A}{EI} \frac{\partial^2 W}{\partial t^2} = 0$$

Equation 3-17

Let, $C_F = \left(\sqrt[2]{\omega}\right)\left(\sqrt[4]{{}^{EI}\!/_{\rho A}}\right)$, then

$$\left[\!\left[{}^{\partial^4 W}\!/_{\partial x^4} = -(1 \,/\, c_F{}^4) \, {}^{\partial^2 W}\!/_{\partial t^2} \right]\!\right]$$

Equation 3-18

where c_F is the velocity of propagation of the flexural displacement or bending wave in the rod. The flexural wave number is defined as

$$k_F = \frac{\omega}{c_F} = \frac{2\pi}{\lambda_F}$$

Equation 3-19

where ω is the radius frequency of vibration, and λ_F is the wavelength. Since the frequency $f = {}^{\omega}\!/_{2\pi}$, then

$$\lambda_F = \frac{c_F}{f}$$

Equation 3-20

3.4 Mathematical Model of Joint

Transmitted and reflected power in a slender and uniform beam being considered for a component of the full solution, which is equivalent motion in a semi-infinite system. Motions in longitudinal and lateral directions are derived for the relationship between propagating wave and the power in the wave.

3.4.1 Longitudinal wave motion

Referring to Figure 3-2 and Equation 3-1, longitudinal motion was contributed by the rate of work done, X_U from stress force P acting along the uniform beam

$$X_U = -P\dot{u} = \underbrace{-EA\frac{\partial U}{\partial x}}_{P}.\frac{\partial U}{\partial t}$$

Equation 3-21

Where $U(x,t)$, is the longitudinal displacement solution to the longitudinal wave equation above, whereby it is the general solution to Equation 3-6 and can be written as: -

$$U(x,t) = A_l \sin(\omega t - k_l x) = A_l[\sin(\omega t)\cos(k_l x) - \cos(\omega t)\sin(k_l x)]$$

Equation 3-22

Where A_l, k_l, are amplitude and wave number for longitudinal direction, which the equation above represents as a single wave propagating in the positive direction.

Differentiation of U with respect to x and t

$$\therefore \frac{\partial \boldsymbol{U}}{\partial \boldsymbol{x}} = -\boldsymbol{A_l k_l}\cos(\boldsymbol{\omega t} - \boldsymbol{k_l x})$$

Equation 3-23

$$\therefore \frac{\partial \boldsymbol{U}}{\partial \boldsymbol{t}} = \boldsymbol{A_l \omega}\cos(\boldsymbol{\omega t} - \boldsymbol{k_l x})$$

Equation 3-24

Finally, Equation 3-23 and Equation 3-24 into Equation 3-21 gives

$$X_U = -EA\frac{\partial U}{\partial x}.\frac{\partial U}{\partial t} = -EA(-A_l k_l \cos(\omega t - k_l x)).(A_l \omega \cos(\omega t - k_l x))$$

$$= EAA_l^2\omega\, k_l \cos^2(\omega t - k_l x)$$

Equation 3-25

So, time-averaged power for a longitudinal wave is given by,

$$\langle P\rangle_l = \frac{1}{T}\int_0^T X\, dt = \frac{EAA_l^2\omega k_l}{T}\int_0^T \cos^2(\omega t - k_l x)\; dt$$

$$= 0.5\, \frac{EAA_l^2\omega k_l}{T}\left[\underbrace{\frac{\sin(2\omega t - 2k_l x)}{2\omega}}_{\approx 0} + T\right]$$

$$= 0.5\, \frac{EAA_l^2\omega k_l}{T}[T]$$

Which finally,

$$\langle P\rangle_l = \frac{1}{T}\int_0^T X\, dt = [\![\underline{\underline{\boldsymbol{0.5EAk_lA_l^2\omega}}}]\!]$$

Equation 3-26

3.4.2 Flexural wave motion

Similarly for flexural motion, referring to Figure 3-3 and Equation 3-12 and Equation 3-15, the rate of work done, X_W for the flexural motion were contributed by both, the shear forces (V) and bending/moment (M), therefore;

$$X_W = \underbrace{V}_{\substack{shear\\ force}}\ \dot{W} - \underbrace{M\frac{\partial}{\partial x}}_{\substack{force\ from\\ moment}}\ \dot{W} = V\frac{\partial W}{\partial t} - M\frac{\partial^2 W}{\partial x \partial t} = \underbrace{EI\frac{\partial^3 W}{\partial x^3}}_{V}\frac{\partial W}{\partial t} - \underbrace{EI\frac{\partial^2 W}{\partial x^2}}_{M}\frac{\partial^2 W}{\partial x \partial t}$$

Equation 3-27

Where $W(x,t)$, is the lateral displacement solution to the flexural wave equation above and assuming that the near field component has decayed to zero, whereby it is the general solution to Equation 3-18 and can be written as: -

$$W(x,t) = A_f \sin(\omega t - k_f x) = A_f[\sin(\omega t)\cos(k_f x) - \cos(\omega t)\sin(k_f x)]$$

Equation 3-28

Where A_f, k_f, are amplitude and wave number for flexural direction, which the equation above represents as a single wave propagating in the positive direction.

Differentiation for x,

$$\frac{\partial}{\partial x}W = A_f\left[\left\{\sin(\omega t)\left(\frac{\partial}{\partial x}\cos(k_f x)\right) + \underbrace{\left(\frac{\partial}{\partial x}\sin(\omega t)\right).\cos(k_f x)}_{\approx 0}\right\}\right.$$
$$\left. - \left\{\cos(\omega t)\left(\frac{\partial}{\partial x}\sin(k_f x)\right) + \underbrace{\left(\frac{\partial}{\partial x}\cos(\omega t)\right).\sin(k_f x)}_{\approx 0}\right\}\right]$$
$$= -A_f k_f \cos(\omega t - k_f x)$$

Equation 3-29

So, from,

$$\frac{\partial}{\partial x}W = -A_f k_f \cos(\omega t - k_f x)$$
$$\therefore \frac{\partial^2}{\partial x^2}W = -A_f k_f\left[\left\{\underbrace{\sin(\omega t)\left(\frac{\partial}{\partial x}\sin(k_f x)\right)}_{=0} + \left(\frac{\partial}{\partial x}\sin(\omega t)\right).\sin(k_f x)\right\}\right.$$
$$\left. + \left\{\underbrace{\cos(\omega t)\left(\frac{\partial}{\partial x}\cos(k_f x)\right)}_{=0} + \left(\frac{\partial}{\partial x}\cos(\omega t)\right).\cos(k_f x)\right\}\right]$$
$$= -A_f k_f^2 \sin(\omega t - k_f x)$$

Equation 3-30

Moreover, from,

$$\frac{\partial^2}{\partial x^2}W = -A_f k_f^2 \sin(\omega t - k_f x)$$

$$\therefore \frac{\partial^3}{\partial x^3}W = \frac{\partial}{\partial x}\left(-A_f k_f^2 \sin(\omega t - k_f x)\right)$$

$$= A_f k_f^3 \cos(\omega t - k_f x)$$

Equation 3-31

Differentiate W with respect to time, t

$$\frac{\partial}{\partial t}W = \frac{\partial}{\partial x}A_f \sin(\omega t - k_f x) = \frac{\partial}{\partial x}A_f\left[\sin(\omega t)\cos(k_f x) - \cos(\omega t)\sin(k_f x)\right]$$

$$\frac{\partial}{\partial t}W = A_f\left[\left\{\sin(\omega t)\left(\frac{\partial}{\partial t}\cos(k_f x)\right) + \left(\frac{\partial}{\partial t}\sin(\omega t)\right).\cos(k_f x)\right\}\right.$$
$$\left. - \left\{\cos(\omega t)\left(\frac{\partial}{\partial t}\sin(k_f x)\right) + \left(\frac{\partial}{\partial t}\cos(\omega t)\right).\sin(k_f x)\right\}\right]$$
$$= A_f \omega \cos(\omega t - k_f x)$$

Equation 3-32

Differentiate $\frac{\partial}{\partial t}W$, with respect to x,

$$\therefore \frac{\partial}{\partial x}\frac{\partial}{\partial t}W = A_f \omega k_f \sin(\omega t - k_f x)$$

Equation 3-33

From equation (30), (31). (32) and (33) into Equation 3-27 gives

$$X_W = \underbrace{EI\frac{\partial^3 W}{\partial x^3}}_{V}\frac{\partial W}{\partial t} - \underbrace{EI\frac{\partial^2 W}{\partial x^2}}_{M}\frac{\partial^2 W}{\partial x \partial t}$$

$$X_W = EI\left[\left\{A_f k_f^3 \cos(\omega t - k_f x).A_f \omega \cos(\omega t - k_f x)\right\}\right.$$
$$\left. - \left\{-A_f k_f^2 \sin(\omega t - k_f x).A_f \omega k_f \sin(\omega t - k_f x)\right\}\right]$$

Using basic trigonometry relationship, the equation for X_W were reduced to, $\boldsymbol{EIk_f^3 A_f^2 \omega}$**.**

So, time-averaged power for flexural wave,

$$\langle P\rangle_f = \frac{1}{T}\int_0^T X_W \, dt = \underline{\underline{[\![\boldsymbol{EIk_f^3 A_f^2 \omega}]\!]}}$$

Equation 3-34

3.5 Wave motion in a non-collinear beam

A semi-infinite structure is considered which allows for a joint to be included. The impinging flexural waves will result in reflected and transmitted near field and propagating flexural waves while impinging compressive waves will result in reflected and transmitted compressive waves. B.R.Mace (1984), for wave reflection and transmission in beams, provides the basis for the notation of wave equation and parameters for the joint. Cross-coupling of wave conversion for flexural to longitudinal, and longitudinal to flexural would also be analysed.

3.5.1 Lumped Mass of Rigid joint

In the analysis of this joint, torsional vibration were ignored and only planar excitations are considered. The axial force, shear force and bending moments are considered for the summation of forces and the continuity of the system.

Figure 3-4, shows both longitudinal $U(x,t)$ and flexural $W(x,t)$ motion of the displacement. Assume a beam is bent through angle θ, and both incident side of the displacement $W_{-}(x,t)$ and $U_{-}(x,t)$ are denoted by suffix minus symbol. As for the transmitting side of the bend, $W_{+}(x,t)$ and $U_{+}(x,t)$ were denoted with suffix plus symbol, with the relationship of $x = \psi\ cos\theta$ for the relative displacement of the incident and transmitted side.

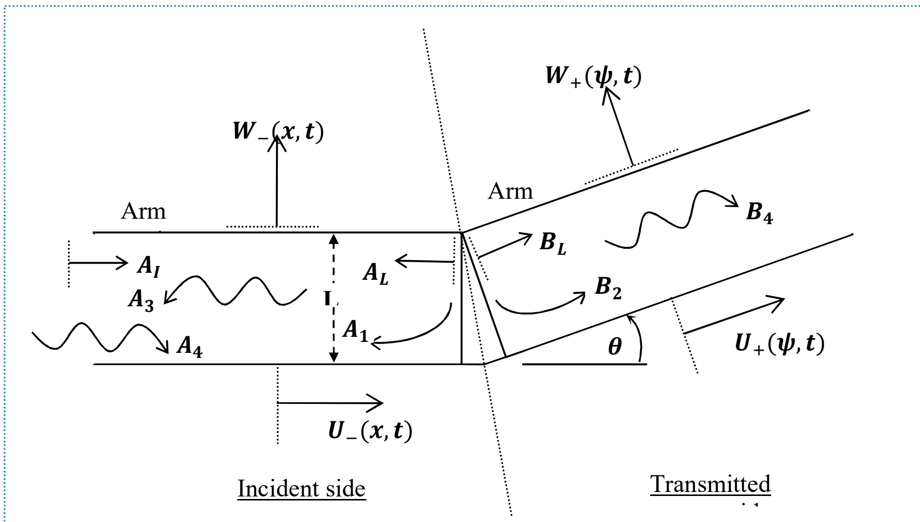

Figure 3-4: Wave motion for the lumped mass of rigid joint in a non-collinear beam

The length 'L' is the thickness or height, and 'w_j' is the width of joint characterising its fixed size for a rigid mass (unit of kg) and inertia (unit of kgm^2) of;

$$m_j = \rho_j \pi L^2 w_j / 4$$

Equation 3-35

$$I_j = m_j L^2 / 8$$

Equation 3-36

Referring to Figure 3-5, this arrangement of joint model illustrates that the joint represented a rigid quarter of a cylinder which remains unchanged regardless of decrease or increment of angle θ.

It is for a clear understanding that such fixed size joint could be illustrated as in Figure 3-5 or at a 90° orientation, despite the original diagram analysis (R. J.L.Horner 1991) as shown together. Such an assumption implies that it is not physically representative of large angles as the transmitting side of the beam would effectively be "folded into" the incident side.

This analysis would continue to re-generate results from the literature, and the rigid joint would be examined as of fixed mass for all orientation of angles. Hence, all equation of continuity, force and moments being considered for this non-collinear beam.

To further illustrate the notation, 'A' represents incident side and 'B' for the transmitting side. Each odd number of waves is representing waves travelling to the left and even numbers of waves travelling to the right side.

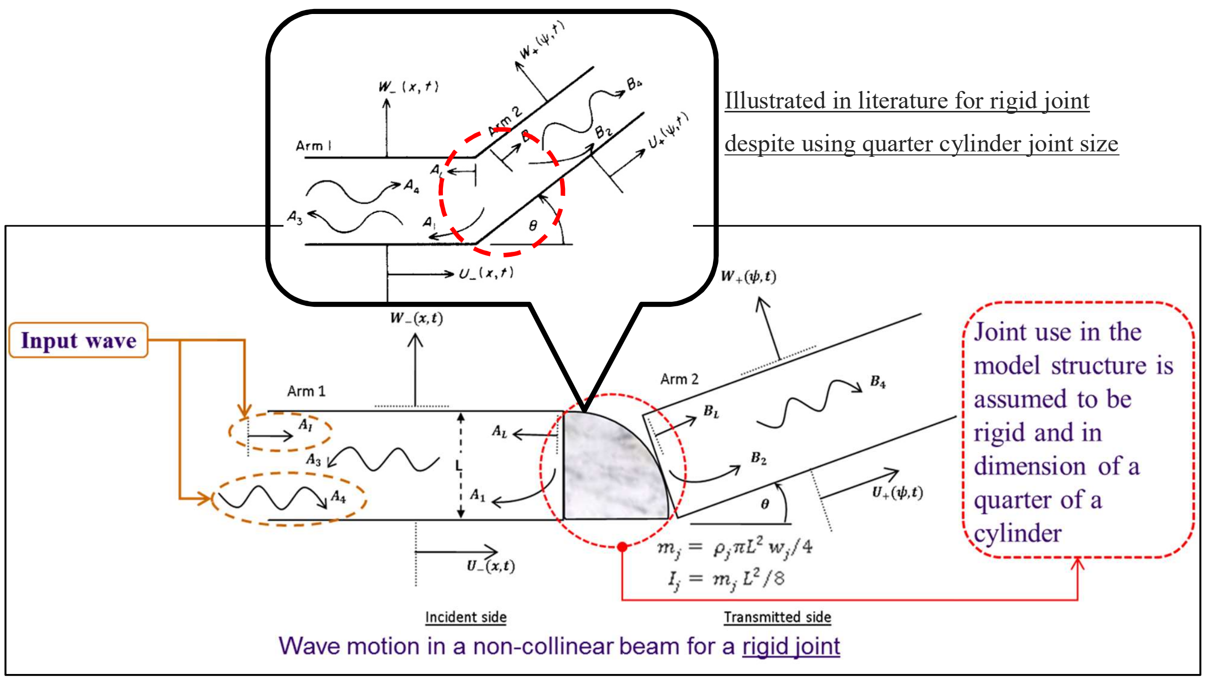

Figure 3-5: Model of rigid joint orientation and notations for analysis

Here, A_3, A_4, B_4 are the flexural travelling wave's amplitudes, A_1, B_2 are the near field flexural wave's amplitudes and A_I, A_L, B_L, are the longitudinal travelling wave's amplitudes. The solution will later consider A_I, A_4 as input waves (both or either one) to the equations. The near field waves carry zero-time averaged power, and their function being to assist the initiation of flexural wave motion. Power is transmitted through the structure by $A_3, A_4, B_4, A_I, A_L, B_L$ of the far field waves only.

On the **incident side** of the bend for flexural displacement, $W_-(x,t)$ and longitudinal displacement, $U_-(x,t)$,

$$\boldsymbol{W_-(x,t) = \{A_1 e^{k_{f1}x} + A_3 e^{ik_{f1}x} + A_4 e^{-ik_{f1}x}\}\ e^{i\omega t}} \quad ;$$

Equation 3-37

$$\boldsymbol{U_-(x,t) = \{A_L e^{ik_{l1}x} + A_I e^{-ik_{l1}x}\}\ e^{i\omega t}};$$

Equation 3-38

For the **transmitting side** of the bend for flexural $W_+(\psi,t)$ and longitudinal $U_+(\psi,t)$, with ψ as a reference of translational displacement from x for the various angle θ.

$$\boldsymbol{W_+(\psi,t) = \{B_2 e^{-k_{f2}\psi} + B_4 e^{-ik_{f2}\psi}\}\ e^{i\omega t}} \quad ;$$

Equation 3-39

$$\boldsymbol{U_+(\psi,t) = \{B_L e^{-ik_{l2}\psi}\}\ e^{i\omega t}} \quad ;$$

Equation 3-40

Applying boundary condition at $x = 0$ and $\psi = 0$, to all equation of continuity, the summation of bending moments, shear forces and compressive forces, yields 6 governing equations as below: -

Continuity of displacement in the axial direction

$$U_- = U_+ \cos\theta - W_+ \sin\theta + \frac{L}{2}\boldsymbol{\sin\theta}\frac{\partial W_+}{\partial\psi}$$

$$\left[\!\left[A_I = -A_L + B_L\cos\theta - B_2\underbrace{\left[\sin\theta + (k_{f2})\frac{L}{2}\boldsymbol{\sin\theta}\right]}_{S1} - B_4\underbrace{\left[i(k_{f2})\frac{L}{2}\boldsymbol{\sin\theta} + \sin\theta\right]}_{S2}\right]\!\right]$$

Equation 3-41

Continuity of displacement in perpendicular direction

$$W_- = U_+ \sin\theta + W_+ \cos\theta - \frac{L}{2}(\mathbf{1} + \mathbf{cos}\,\boldsymbol{\theta})\frac{\partial W_+}{\partial \psi}$$

$$\left[\!\left[A_4 = -A_1 - A_3 + B_L \sin\theta + B_2 \underbrace{\left[\cos\theta + \left[(k_{f2})\frac{L}{2}\,(\mathbf{1} + \mathbf{cos}\,\boldsymbol{\theta})\right]\right]}_{S3} + B_4 \underbrace{\left[\cos\theta + i\left[(k_{f2})\frac{L}{2}\,(\mathbf{1} + \mathbf{cos}\,\boldsymbol{\theta})\right]\right]}_{S4} \right]\!\right]$$

Equation 3-42

Continuity of angular displacement/equal gradient

$$\frac{\partial W_-}{\partial x} = \frac{\partial W_+}{\partial \psi}$$

$$\left[\!\left[A_4 = \underbrace{\left[\frac{A_1}{i}\right]}_{S} + A_3 + \frac{B_2}{i}\underbrace{\left[\frac{k_{f2}}{k_{f1}}\right]}_{S5} + B_4 \underbrace{\left[\frac{k_{f2}}{k_{f1}}\right]}_{S5a} \right]\!\right]$$

Equation 3-43

Equilibrium of bending moment

$$E_1 I_1 \frac{\partial^2 W_-}{\partial x^2} + \frac{L}{2} E_1 I_1 \frac{\partial^3 W_-}{\partial x^3} = E_2 I_2 \frac{\partial^2 W_+}{\partial \psi^2} - \frac{L}{2} E_2 I_2 \frac{\partial^3 W_+}{\partial \psi^3} - I_j \frac{\partial^2 \partial W_-}{\partial t^2 \partial x}$$

$$\left[\!\left[A_4 \underbrace{\left[-\left(E_1 I_1 (k_{f1}^2)\right) + i\left(\frac{L}{2} E_1 I_1 (k_{f1}^3)\right) - i\left(I_j(\omega^2 k_{f1})\right)\right]}_{S6} = -A_1 \underbrace{\left[\left(E_1 I_1 (k_{f1}^2)\right) + \left(\frac{L}{2} E_1 I_1 (k_{f1}^3)\right) + \left(I_j(\omega^2 k_{f1})\right)\right]}_{S7} + A_3 \underbrace{\left[\left(E_1 I_1 (k_{f1}^2)\right) + i\left(\frac{L}{2} E_1 I_1 (k_{f1}^3)\right) - i\left(I_j(\omega^2 k_{f1})\right)\right]}_{S8} + B_2 \underbrace{\left[\left(E_2 I_2 (k_{f2}^2)\right) + \left(\frac{L}{2} E_2 I_2 (k_{f2}^3)\right)\right]}_{S9} - B_4 \underbrace{\left[\left(E_2 I_2 (k_{f2}^2)\right) + i\left(\frac{L}{2} E_2 I_2 (k_{f2}^3)\right)\right]}_{S9a} \right]\!\right]$$

Equation 3-44

Equilibrium of compressive force

$$E_1A_1\frac{\partial U_-}{\partial x} = E_2A_2\frac{\partial U_+}{\partial \psi}\cos\theta + E_2I_2\frac{\partial^3 W_+}{\partial \psi^3}\sin\theta - m_j\frac{\partial^2 U_-}{\partial t^2}$$

$$\left[\!\left[A_I\underbrace{\left[-i\big(E_1A_1(k_{l1})\big)-\left(m_j\omega^2\right)\right]}_{S11} = A_L\underbrace{\left[-i\big(E_1A_1(k_{l1})\big)+\left(m_j\omega^2\right)\right]}_{S12} - B_L\underbrace{\left[i\left(E_2A_2(k_{l2})\cos\theta\right)\right]}_{S13} - B_2\underbrace{\left[E_2I_2\left(k_{f2}^3\right)\sin\theta\right]}_{S14} + B_4\underbrace{\left[i\left(E_2I_2\left(k_{f2}^3\right)\sin\theta\right)\right]}_{S15}\right]\!\right]$$

Equation 3-45

Equilibrium of shear force

$$-E_1I_1\frac{\partial^3 W_-}{\partial x^3} = E_2A_2\frac{\partial U_+}{\partial \psi}\sin\theta - E_2I_2\frac{\partial^3 W_+}{\partial \psi^3}\cos\theta - m_j\frac{\partial^2}{\partial t^2}\left[W_- - \frac{L}{2}\frac{\partial W_-}{\partial x}\right]$$

$$\left[\!\left[A_4\underbrace{\left[\left(-iE_1I_1\left(k_{f1}^3\right)\right)-\left(m_j\omega^2\right)+\left(i\left(m_j\omega^2\right)\frac{L}{2}\left(k_{f1}\right)\right)\right]}_{S1} = A_1\underbrace{\left[\left(E_1I_1\left(k_{f1}^3\right)\right)+\left(m_j\omega^2\right)+\left(\left(m_j\omega^2\right)\frac{L}{2}\left(k_{f1}\right)\right)\right]}_{S17} + A_3\underbrace{\left[\left(-iE_1I_1\left(k_{f1}^3\right)\right)+\left(m_j\omega^2\right)+\left(i\left(m_j\omega^2\right)\frac{L}{2}\left(k_{f1}\right)\right)\right]}_{S1} - B_L\underbrace{\left[iE_2A_2(k_{l2})\sin\theta\right]}_{S19} + B_2\underbrace{\left[E_2I_2\left(k_{f2}^3\right)\cos\theta\right]}_{S20} - B_4\underbrace{\left[iE_2I_2\left(k_{f2}^3\right)\cos\theta\right]}_{S2}\right]\!\right]$$

Equation 3-46

3.5.2 Results and comments

Rearranging all the six equations in the order of $A_1, A_3, A_L, B_L, B_2, B_4$ and the required input from A_I, A_4 yields the matrix below;

$$\underbrace{\begin{bmatrix} 0 & 0 & -1 & \cos\theta & -S1 & -S2 \\ -1 & -1 & 0 & \sin\theta & S3 & S4 \\ S & 1 & 0 & 0 & S5 & S5a \\ -\left(\frac{S7}{S6}\right) & \left(\frac{S8}{S6}\right) & 0 & 0 & \left(\frac{S9}{S6}\right) & -\left(\frac{S9a}{S6}\right) \\ 0 & 0 & \left(\frac{S12}{S1}\right) & -\left(\frac{S13}{S1}\right) & -\left(\frac{S14}{S11}\right) & \left(\frac{S15}{S1}\right) \\ \left(\frac{S1}{S1}\right) & \left(\frac{S18}{S16}\right) & 0 & -\left(\frac{S19}{S16}\right) & \left(\frac{S2}{S1}\right) & -\left(\frac{S21}{S16}\right) \end{bmatrix}}_{[X]} \underbrace{\begin{bmatrix} A_1 \\ A_3 \\ A_L \\ B_L \\ B_2 \\ B_4 \end{bmatrix}}_{[Y]} = \underbrace{\begin{bmatrix} A_I \\ A_4 \\ A_4 \\ A_4 \\ A_I \\ A_4 \end{bmatrix}}_{[Z]}$$

Applying the above derivation and matrix to MATLAB, with the given input for A_I *and* A_4 , the equation becomes;

$[Y] = inv[X].[Z]$, ***(Refer appendix A-1 for derivation and appendix A-2 for the MATLAB coding)***

Result plotted referring to J.L.Horner (1990) & (1991), of cross-section beam dimension 50mm x 6mm using material with *E*= 5.567x10^9 N/m^2. The input frequency of 500Hz (as used in J.L.Horner (1990) & (1991)) was utilised to compare results where both impinging wave of longitudinal (A_I) and flexural (A_4) were given input of unity. This allows a direct matching comparison between this works with literature, for the normalised inputs to the various ratio of power for transmitted and reflected.

The percentage power normalisation is the ratio of reflected and transmitted power to the power of the impinging wave.

For the reflected side, cross-coupling wave of (beam 1) was defined as,

- incident flexural wave with ***reflected*** flexural wave denoted with *FF*
- incident longitudinal wave with ***reflected*** flexural wave denoted with *LF*
- incident flexural wave with ***reflected*** longitudinal wave denoted with *FL*
- incident longitudinal wave with ***reflected*** longitudinal wave denoted with *LL*

For the transmitting side, cross-coupling wave of (beam 2) was defined as,

- incident flexural wave with a ***transmitted*** flexural wave denoted with *FF*
- incident longitudinal wave with a ***transmitted*** flexural wave denoted with *LF*
- incident flexural wave with a ***transmitted*** longitudinal wave denoted with *FL*
- incident longitudinal wave with ***transmitted*** longitudinal wave denoted with *LL*

From Figure 3-6 and Figure 3-7, it is observed that the dominant wave type in each arm is the same type of the impinging wave and other types are related to the bend of the system. Flexural power was shown better transmitted at joints (of various angles) compared to longitudinal power.

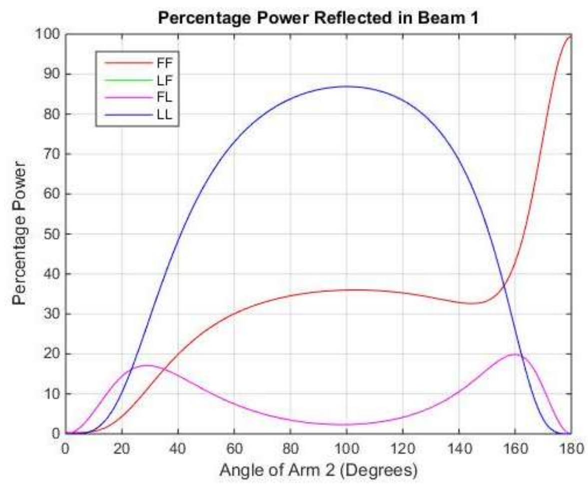

a) Result from analysis

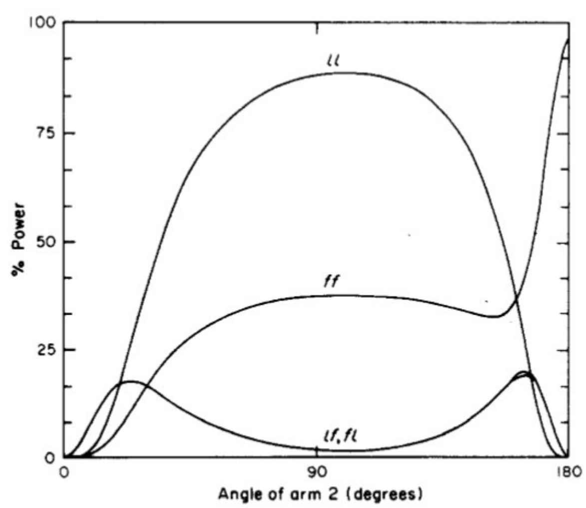

b) Result from JL Horner (1991)

Figure 3-6: a) Percentage of power in beam 1 for all four types of wave, b) Comparison to Literature

Figure 3-6 and Figure 3-7 also presenting this chapter analysis compared to literature and in very good agreement. Both LF and FL for reflected and transmitted were overlaying each other showing equivalent cross-coupling power from flexural and longitudinal.

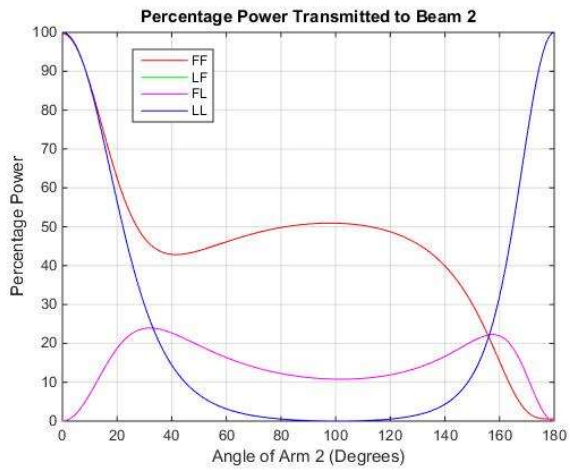

a) Result from analysis

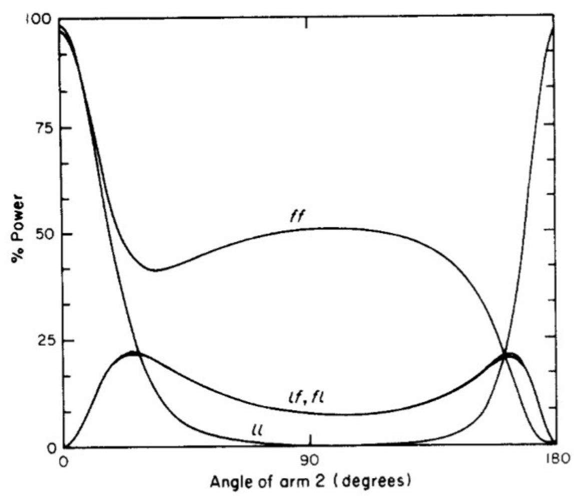

b) Result from JL Horner (1991)

Figure 3-7: a) Percentage of power in beam 2 for all four types of wave, b) Comparison to Literature

Results from the literature were also seen with a power imbalance, for flexural power reflected & transmitted at 180^o angle as well as at the 0^o angle for both flexural and longitudinal power for transmitted. Total power for input wave to output wave can be seen in agreement from both Figure 3-8 and Figure 3-9 of flexural and longitudinal impinging wave. However, for FF1 and FF2, it was observed that there is some power reflected, and less than 100% transmitted at 0^o angle. This observation will be further amplified and commented in Figure 3-10.

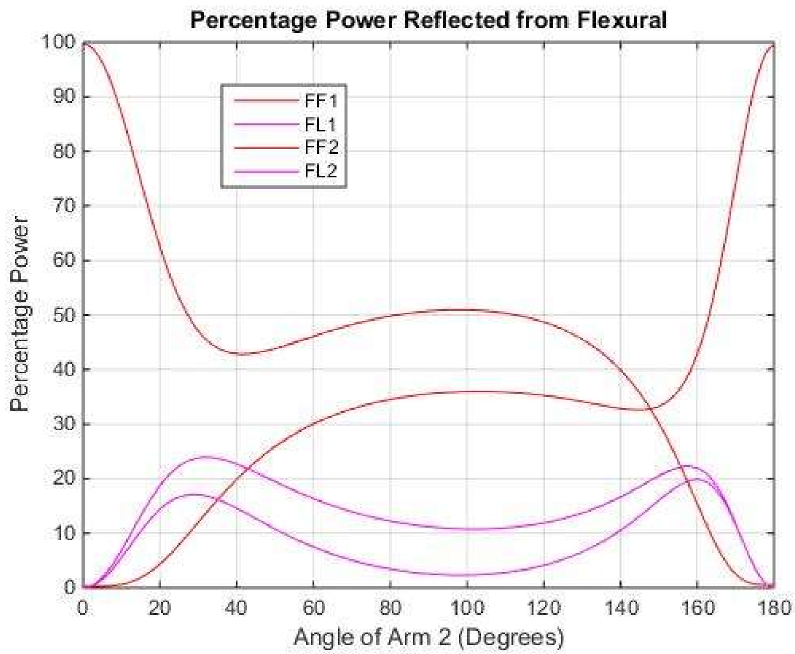

Figure 3-8: Total power of flexural impinging wave for beam 1 & 2

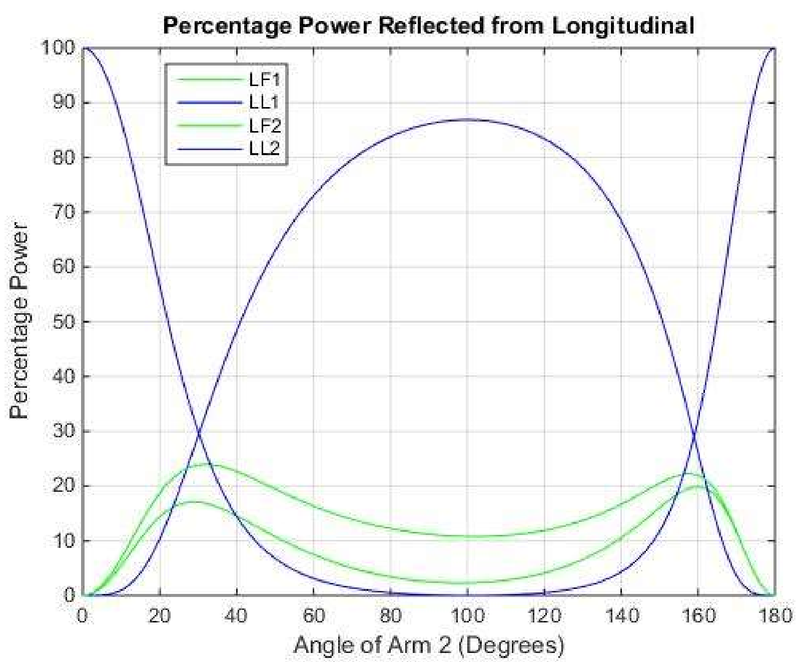

Figure 3-9: Total power of longitudinal impinging wave for beam 1 & 2

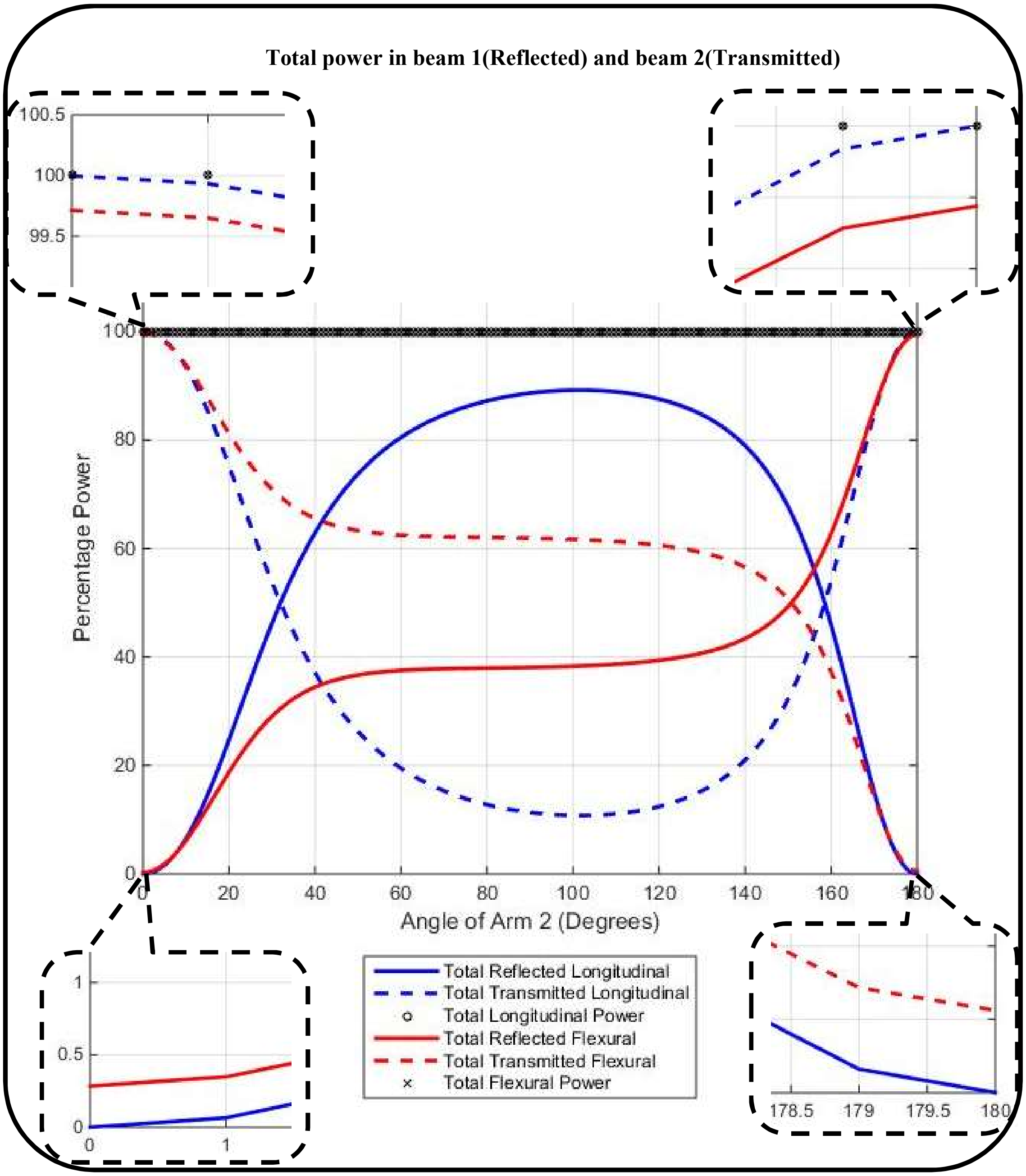

Figure 3-10: Total power of Longitudinal and Flexural in Alpha (beam 1) and Beta (beam 2)

Even that the behaviours obtained are in full agreement with J.L.Horner (1991), but work in this chapter are in better presentation whereby the flexural wave indicates the weakness of previous assumptions of the lumped mass joint. It was noted having a constant physical dimension and orientations of joint, hence causing some reflection during straight beam (0^{o} degree) orientation for power in flexural as in Figure 3-8. Further analysis being elaborated in section 3.6.

3.6 Further analysis

To further relate to the current analysis, the material of Perspex (Plexiglas) used for the experimental work discussed later in chapter 5 with a dimension of 20mm x 100mm and *E*= 1.75×10^9 N/m^2 were being analysed. The other intention was to highlight the weaknesses observed in the previous section of using the same joint dimensions regardless of joint angle. The cross-section ratio used would be 0.2 (20mm thickness / 100mm width) which is thicker beam compared to result in section 3.5.2 of ratio 0.12 (6mm / 50mm).

Figure 3-11 and Figure 3-12 shows the significant behaviour of flexural waves that were directly affected due to the fixed joint or lumped mass joint assumed in the model. Hence at 0^o in Figure 3-11, there are reflected wave power observed and reduced transmitted power at 0^o in Figure 3-12. As for fully bent beam joint at 180^o (both beams lay next to each other), transmitted power occurred despite it was assumed there should be 100% reflection and 0% transmitted previously.

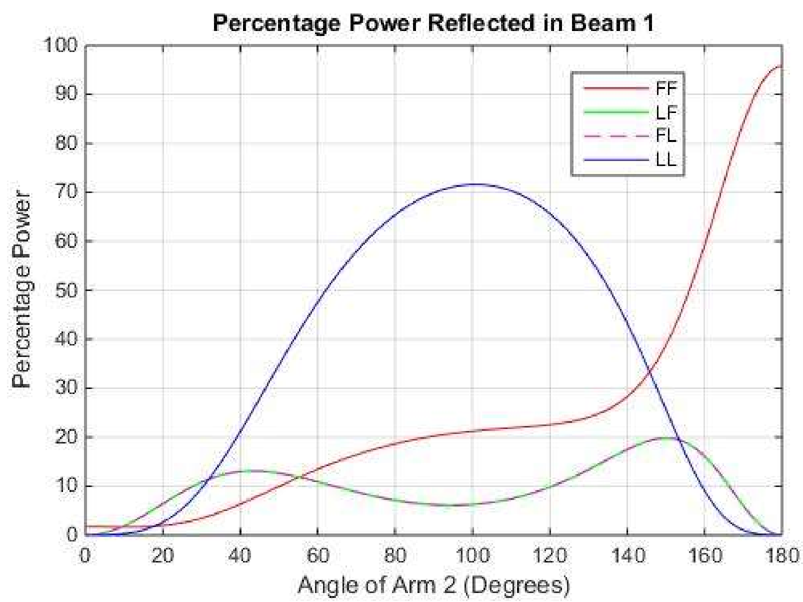

Figure 3-11: Percentage of power in the beam 1 for all four types of wave (cross section ratio 0.2)

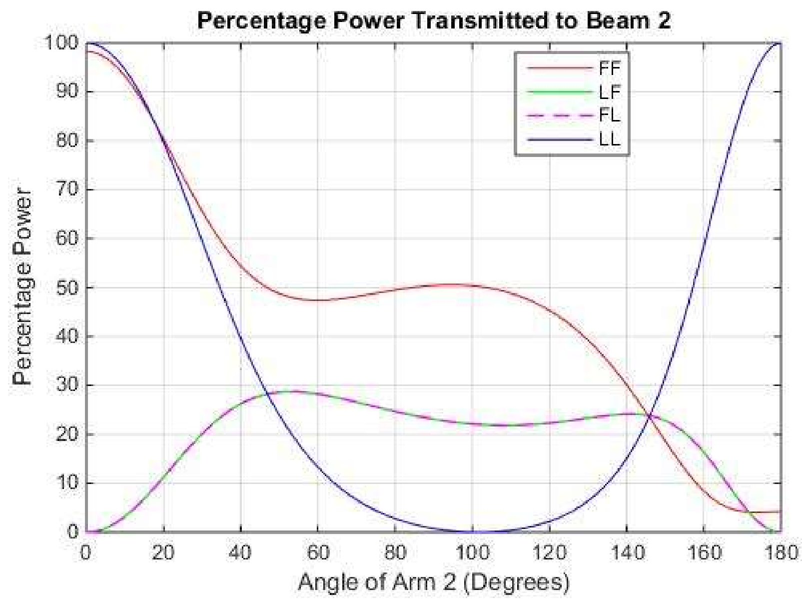

Figure 3-12: Percentage of power in beam 2 for all four types of wave (cross section ratio 0.2)

A closer observation through total power produced by flexural in Figure 3-13 and Figure 3-13, further signifies the main contribution was from only flexure-to-flexure (FF) power which either in reflected or transmitted.

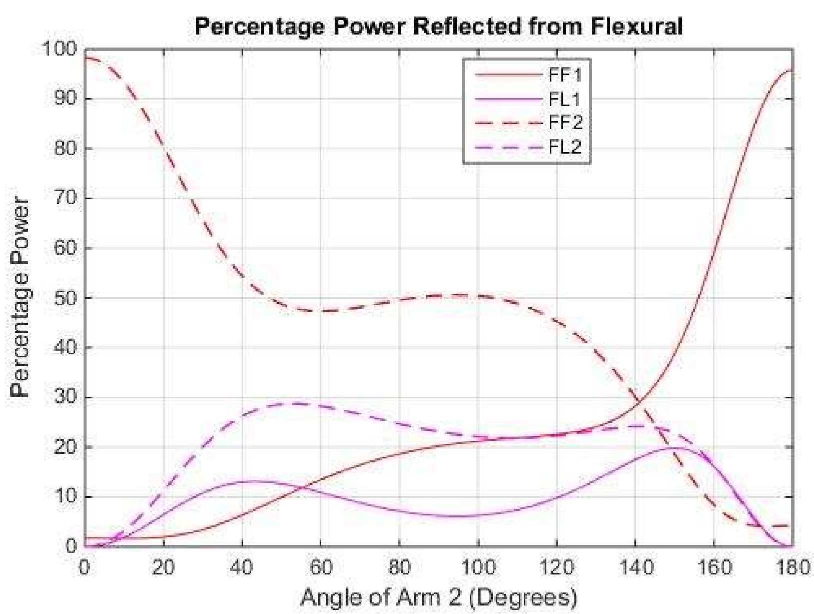

Figure 3-13: Total power of flexural impinging wave for beam 1 & 2 (cross section ratio 0.2)

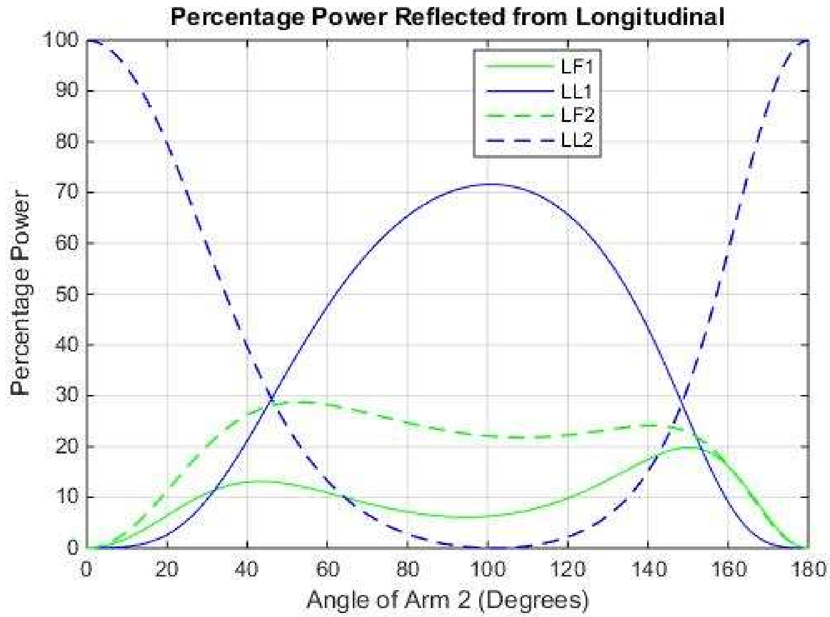

Figure 3-14: Total power of longitudinal impinging wave for beam 1 & 2 (cross section ratio 0.2)

Longitudinal power was plotted balanced as it shows from the power reflected and transmitted in Figure 3-14. The total power from longitudinal and flexural was then equated to the input power which presented in

Figure 3-15. Comparing to Figure 3-10, the flexural power showing higher values for reflected at 0^o and transmitted at 180^o, while reduced power values for transmitted at 0^o and reflected at 180^o. Particularly due to the thicker beam dimension, hence a bigger fixed mass of joint presence throughout the range of beam orientation.

It also shows that the powers were equally distributed for reflected and transmitted at about 145 degrees of beam angle. This will be further commented with a variable joint in next chapter. Mainly, the flexural power caused by the fixed mass joint is obviously a concern with regards to beam cross section ratio and this can be further improved with the introduction of the variable joint method.

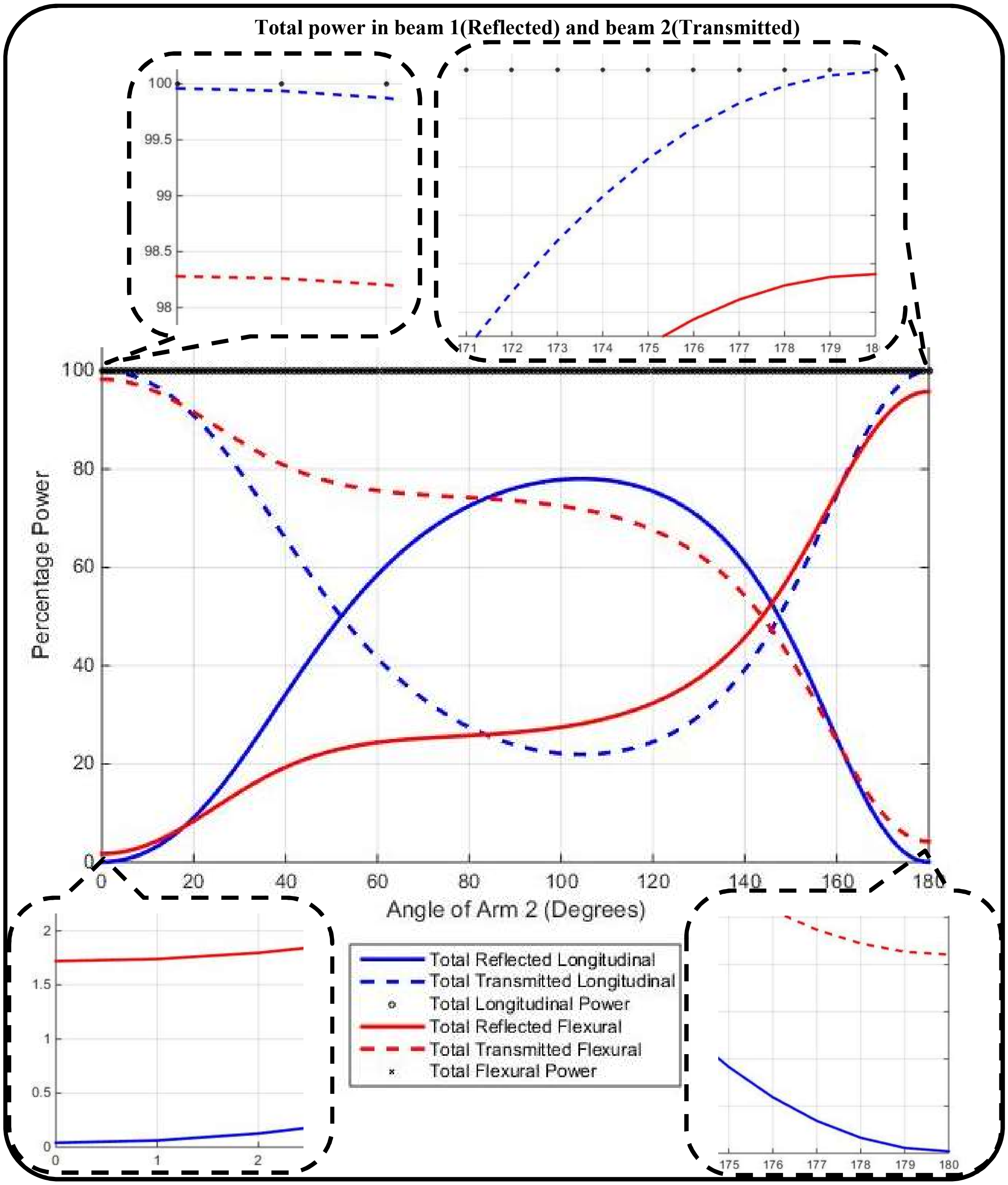

Figure 3-15: Total power of Longitudinal and Flexural in Alpha (beam 1) and Beta (beam 2), (cross section ratio 0.2)

3.7 Concluding remarks

Extended analysis for the previous method of joint analysis shows area of improvements that were required. The flexural power was mainly the concern since the nature of affected wave depends on the cross-sectional area term. Hence, the fixed mass of joint or lumped mass assumed earlier would always be present even at 0^o degree. This allows some flexural power reflecting and less than 100% would be able to be transmitted.

As for longitudinal power, it was observed that the constant mass joint would not obstruct the vibrational wave in the 0^o degree orientation. The lumped joint mass model however would correspond differently for the longitudinal power if the assumed joint size to be in other than the beam cross sectional dimension (smaller or bigger joint in between beam). This is mainly due to the disagreement of displacement continuity (due to fixed joint mass and size) as being considered earlier in the equation.

Assumption for lumped mass have shown various area for improvements. Fixed inertia and absence of moments due to compressive force were noted. Furthermore, a realistic behaviour would be clearly observed missing in the reflected flexure power at 0^o angle (straight beam) and in the transmitted flexure power at 180^o angle. It has been shown significantly when 'L' or thickness of beam increased (joint size increased accordingly), in section 3.6.

Lumped mass could not be a solution representation especially at extremes of angles as this work has shown. The fixed dimensions and weight assumed, has grown significantly irrelevant when beams oriented at 90^o to 180^o of angles, and this has primarily affecting the force and moments equations.

Hence, a better mathematical derivation for the joint is required to eliminate the weakness mentioned above. This will be beneficial for better estimates of vibration power and would improve understanding in especially beams connections or structural assembly configurations.

Chapter 4: Analysis of variable joint modelling

4.1 Variable size of joint

In the previous chapter, it was assumed that the joint between the two beams was the same dimension regardless of the angle of the beams. In this chapter, the joint considered was of variable sizes proportional to the angle acted on by the 2 beams. This would represent more closely a realistic joint, where the mass of the joint increases with the angle of the jointed beam. The constant mass joint discussed previously, would not represent the physical orientation at 0^o (which no joint mathematically exists) and even to the extreme orientation at 180^o where the arm 2 would be physically aligned to arm 1. The comparison between constant mass and variable joint would further aid the simplification as well as establish whether the parameters of the joint would affect the wave behaviour in the angled beam.

4.1.1 Mathematical model of variable joint

The variable joint model is a sector of rigid circular cylinder between the angle beams and rotation of the joint occurs about the centre point of its mid-line as for elements in the beam theory. The physical growth of the joint would then be possible to include into the equation considered.

Let both beam with thickness/depth L, and density of material ρ. Let also the joint rotate through small angle $\emptyset$, and have linear displacement U_M and W_M of its rotational centre *M*. Refer to Figure 4-1.

Similarly, as previous fixed mass joint,

$$\left[\!\left[\frac{\partial W_-}{\partial x} = \frac{\partial W_+}{\partial \psi} = \emptyset\right]\!\right]$$

Equation 4-1

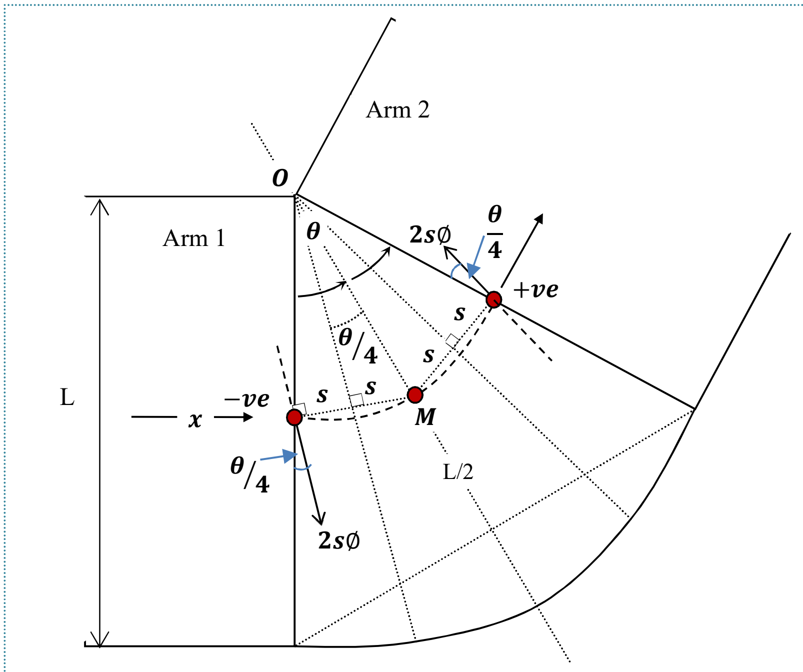

Figure 4-1: Geometry for variable/wedge size of rigid joint in a non-collinear beam

From the Figure 4-1 above,

$$\sin {}^{\theta}\!/_{4} = \frac{s}{{}^{L}\!/_{2}}$$

$$\therefore \quad \mathbf{2s = L \sin {}^{\theta}\!/_{4}}$$

Equation 4-2

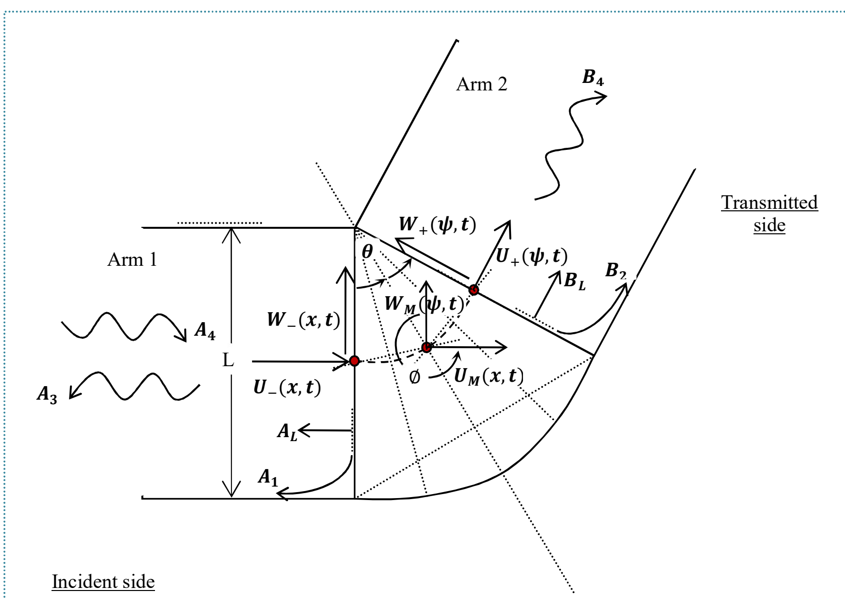

Figure 4-2: Wave motion for variable/wedge size of rigid joint in a non-collinear beam

Then, referring to notation in Figure 4-2:-

$$\boldsymbol{U_{-} = U_M + 2s\emptyset \sin\frac{\theta}{4}}$$

Equation 4-3

$$\boldsymbol{W_{-} = W_M - 2s\emptyset \cos\frac{\theta}{4}}$$

Equation 4-4

$$\boldsymbol{U_{+} = U_M\cos\theta + W_M\sin\theta + 2s\emptyset \sin\frac{\theta}{4}}$$

Equation 4-5

$$\boldsymbol{W_{+} = -U_M\sin\theta + W_M\cos\theta + 2s\emptyset \cos\frac{\theta}{4}}$$

Equation 4-6

Further simplified, ***(refer appendix B-1 for derivation)***

$$\left[\!\left[\boldsymbol{U_{-} = U_{+}\cos\theta - W_{+}\sin\theta + \frac{L\emptyset}{2}[1-\cos\theta]}\right]\!\right]$$

Equation 4-7

$$\left[\!\left[\boldsymbol{W_{-} = U_{+}\sin\theta + W_{+}\cos\theta - \frac{L\emptyset}{2}\sin\theta}\right]\!\right]$$

Equation 4-8

Checking the limit at $\theta = 0,\ \frac{\pi}{2},\ \pi$ for continuity of displacement for the above equation 4-7 & 4-8,

$$\theta = 0, \quad U_{-} = U_{+} \quad , \quad W_{-} = W_{+}$$

$$\theta = \frac{\pi}{2}, \quad U_{-} = -W_{+} + \frac{L\emptyset}{2} \quad , \quad W_{-} = U_{+} - \frac{L\emptyset}{2}$$

$$\theta = \pi, \quad U_{-} = -U_{+} + L\emptyset \quad , \quad W_{-} = -W_{+}$$

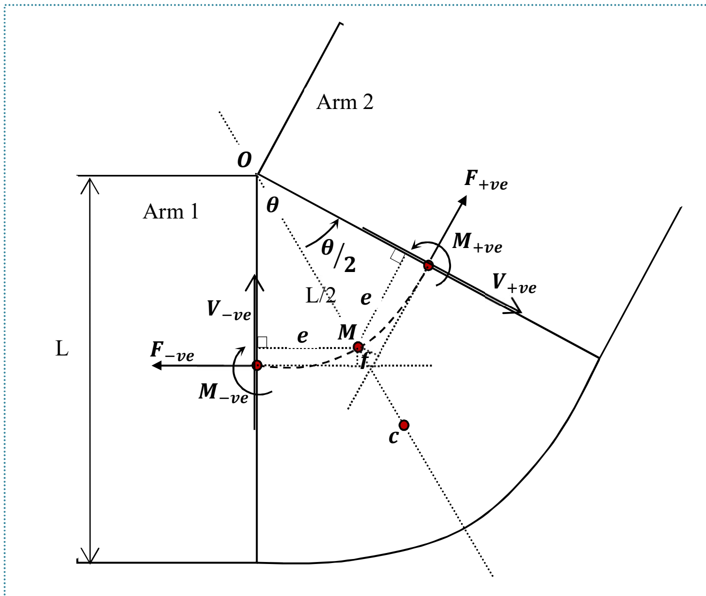

Figure 4-3: Equilibrium of force and moment for <u>variable/wedge size of rigid joint</u> in a non-collinear beam

Using the beam theory where forces act about/ through centre of force, which is point -ve (negative) and +ve (positive), and rotation occurs about point M as in Figure 4-3.

Let joint have mass $\boldsymbol{m}$, inertia $\boldsymbol{I}$, about point $\boldsymbol{M}$.

Then,

$$\llbracket m\ddot{U}_M = F_+ cos\theta + V_+ sin\theta - F_- \rrbracket$$

Equation 4-9

$$\llbracket m\ddot{W}_M = V_- + F_+ sin\theta - V_+ cos\theta \rrbracket$$

Equation 4-10

$$\llbracket I\ddot{\emptyset} = M_+ - M_- - V_+ e - V_- e - F_- f + F_+ f \rrbracket$$

Equation 4-11

From the above equation of forces in flexural & longitudinal as well as the moment around point $\boldsymbol{M}$, notations $\ddot{U}_M$, $\ddot{W}_M$, and $\ddot{\emptyset}$, are the respective translational and rotational acceleration experienced by the variable joint dynamically reacted with the change of angle. To further illustrate the summations of moment, Figure 4-4 defines the distance of both forces from the reference point M with regards to the angle of the joint.

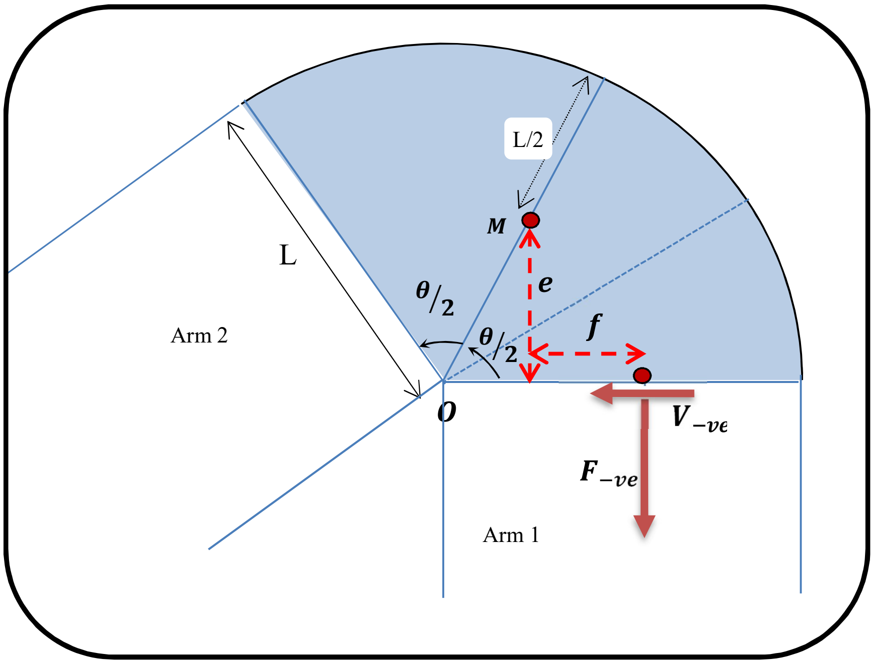

Figure 4-4: Defining moment from the Forces for <u>variable/wedge size of rigid joint</u> in a non-collinear beam

now,

$$\sin {}^{\theta}/_{2} = \frac{e}{{}^{L}/_{2}}$$

$$\boldsymbol{e = {}^{L}/_{2} \sin {}^{\theta}/_{2}}$$

Equation 4-12

and,

$$\boldsymbol{f = {}^{L}/_{2} - {}^{L}/_{2} \cos {}^{\theta}/_{2} = {}^{L}/_{2} \left(1 - \cos {}^{\theta}/_{2}\right)}$$

Equation 4-13

Furthermore,

$$\boldsymbol{m = \frac{\theta}{2\pi}.\pi L^2.w.\rho = \rho w L^2 \frac{\theta}{2}}$$

Equation 4-14

$$I_0 = \int_0^L (\rho w dr.\theta r).r^2$$

$$= \rho w \theta \int_0^L r^3 dr$$

$$= \rho w\theta \frac{L^4}{4}$$

$$\boldsymbol{I_0 = m\frac{L^2}{2}}$$

Equation 4-15

The circular sector considered must acknowledge the change of centroid location as the angle grow. This requires the exact point of reference for the calculation of joint inertia with regards to centre rotation *M*. Hence,

Distance to centroid, $OC \ = \boldsymbol{\frac{2}{3}L \ \mathrm{sinc} \ (\frac{\theta}{2})}$,

So, distance $MC \ = (\boldsymbol{\frac{2}{3}L \ \mathrm{sinc}} \ (\frac{\theta}{2})) - \frac{1}{2}L$

but,

$$\boldsymbol{I_0 = I_c + m\left(\frac{2}{3}L \ \mathrm{sinc} \ (\frac{\theta}{2})\right)^2}$$

Equation 4-16

and,

$$\boldsymbol{I_M = I_c + m\left((\frac{2}{3}L \ \mathrm{sinc} \ (\frac{\theta}{2})) - \frac{1}{2}L\right)^2}$$

Equation 4-17

$$I_M = I_o + m\left(\left(\frac{2}{3}L \ \mathrm{sinc} \ \left(\frac{\theta}{2}\right)\right)^2 - \left(\left(\frac{2}{3}L \ \mathrm{sinc} \ \left(\frac{\theta}{2}\right)\right) - \frac{1}{2}L\right)^2\right)$$

$$= \frac{mL^2}{2}\left(\frac{\theta}{2\pi}\right) + m\left(\frac{2}{3}L \ \mathrm{sinc} \ (\frac{\theta}{2})\right)^2 + \ mL^2\left(\frac{1}{4} - 2\frac{2}{6}\mathrm{sinc} \ \left(\frac{\theta}{2}\right)\right)$$

$$= \frac{mL^2}{4\pi}\left(\theta + \pi + \frac{16\pi}{9}\frac{\sin^2\left(\frac{\theta}{2}\right)}{\left(\frac{\theta}{2}\right)^2} - \frac{8\pi}{3}\frac{\sin\left(\frac{\theta}{2}\right)}{\left(\frac{\theta}{2}\right)}\right)$$

or,

$$\boldsymbol{I_M = \frac{mL^2}{4\pi}\left[\theta + \pi \left(1 + \left\{\frac{2^4}{3\theta} \sin \langle\frac{\theta}{2}\rangle\right\} \left[\left\{\frac{2^2}{3\theta}\sin\langle\frac{\theta}{2}\rangle\right\} - 1\right]\right)\right]}$$

Equation 4-18

Continuity of displacement in axial direction

$$U_{-} = U_{+}\cos\theta - W_{+}\sin\theta + \frac{L}{2}(\mathbf{1}-\mathbf{cos}\,\boldsymbol{\theta})\frac{\partial W_{+}}{\partial\psi}$$

$$\left[\!\!\left[A_I = -A_L + B_L\cos\theta - B_2\underbrace{\left[\sin\theta + (k_{f2})\frac{L}{2}\,(\mathbf{1}-\mathbf{cos}\,\boldsymbol{\theta})\right]}_{S1B2} - B_4\underbrace{\left[i(k_{f2})\frac{L}{2}\,(\mathbf{1}-\mathbf{cos}\,\boldsymbol{\theta}) + \sin\theta\right]}_{S1B4}\right]\!\!\right]$$

Equation 4-19

Continuity of displacement in perpendicular direction

$$W_{-} = U_{+}\sin\theta + W_{+}\cos\theta - \frac{L}{2}(\mathbf{sin}\,\boldsymbol{\theta})\frac{\partial W_{+}}{\partial\psi}$$

$$\left[\!\!\left[A_4 = -A_1 - A_3 + B_L\sin\theta + B_2\underbrace{\left[\cos\theta + \left[(k_{f2})\frac{L}{2}\,(\mathbf{sin}\,\boldsymbol{\theta})\right]\right]}_{S2B2} + B_4\underbrace{\left[\cos\theta + i\left[(k_{f2})\frac{L}{2}\,(\mathbf{sin}\,\boldsymbol{\theta})\right]\right]}_{S2B4}\right]\!\!\right]$$

Equation 4-20

Continuity of angular displacement/equal gradient

$$\frac{\partial W_{-}}{\partial x} = \frac{\partial W_{+}}{\partial\psi}$$

$$\left[\!\!\left[A_4 = A_1\underbrace{\left[\frac{1}{i}\right]}_{S3A1} + A_3 + B_2\underbrace{\left[\frac{k_{f2}}{k_{f1}}.\frac{1}{i}\right]}_{S3B2} + B_4\underbrace{\left[\frac{k_{f2}}{k_{f1}}\right]}_{S3B4}\right]\!\!\right]$$

Equilibrium of bending moment

$$E_1I_1\frac{\partial^2 W_{-}}{\partial x^2} + \frac{L}{2}\left(\mathbf{sin}\,\tfrac{\theta}{2}\right)E_1I_1\frac{\partial^3 W_{-}}{\partial x^3} = E_2I_2\frac{\partial^2 W_{+}}{\partial\psi^2} - \frac{L}{2}\left(\mathbf{sin}\,\tfrac{\theta}{2}\right)E_2I_2\frac{\partial^3 W_{+}}{\partial\psi^3} - I_j\frac{\partial^2\partial W_{-}}{\partial t^2\partial x} - \boldsymbol{E_1A_1}\frac{\boldsymbol{\partial U_{-}}}{\boldsymbol{\partial x}}\left[\frac{\boldsymbol{L}}{\mathbf{2}}\left(\mathbf{1}-\mathbf{cos}\,\tfrac{\theta}{2}\right)\right] + \boldsymbol{E_2A_2}\frac{\boldsymbol{\partial U_{+}}}{\boldsymbol{\partial\psi}}\left[\frac{\boldsymbol{L}}{\mathbf{2}}\left(\mathbf{1}-\mathbf{cos}\,\tfrac{\theta}{2}\right)\right]$$

$$\left[\!\!\left[A_4 \underbrace{\left[-\left(E_1 I_1\left(k_{f1}^2\right)\right)+\ i\left(\frac{L}{2}\left(\sin\tfrac{\theta}{2}\right)E_1 I_1\left(k_{f1}^3\right)\right)+i\left(I_j\omega^2 k_{f1}\right)\right]}_{S4a} \right.\right.$$

$$+ A_I \underbrace{\boldsymbol{i}\left[\frac{\boldsymbol{L}}{\boldsymbol{2}}\left(\boldsymbol{1}-\boldsymbol{\cos}\tfrac{\theta}{2}\right)\right]\boldsymbol{E_1 A_1 (k_{l1})}}_{S4b}$$

$$= -A_1 \underbrace{\left[\left(E_1 I_1\left(k_{f1}^2\right)\right)+\left(\frac{L}{2}\left(\sin\tfrac{\theta}{2}\right)E_1 I_1\left(k_{f1}^3\right)\right)-\left(I_j\left(\omega^2 k_{f1}\right)\right)\right]}_{S41}$$

$$+ A_3 \underbrace{\left[\left(E_1 I_1\left(k_{f1}^2\right)\right)+i\left(\frac{L}{2}\left(\sin\tfrac{\theta}{2}\right)E_1 I_1\left(k_{f1}^3\right)\right)+i\left(I_j\left(\omega^2 k_{f1}\right)\right)\right]}_{S4}$$

$$- A_L \left[\underbrace{\boldsymbol{i}\left(\frac{\boldsymbol{L}}{\boldsymbol{2}}\left(\boldsymbol{1}-\boldsymbol{\cos}\tfrac{\theta}{2}\right)\right)\boldsymbol{E_1 A_1 (k_{l1})}}_{\boldsymbol{S43}}\right] - B_L \left[\underbrace{\boldsymbol{i}\left(\frac{\boldsymbol{L}}{\boldsymbol{2}}\left(\boldsymbol{1}-\boldsymbol{\cos}\tfrac{\theta}{2}\right)\right)\boldsymbol{E_2 A_2 (k_{l2})}}_{\boldsymbol{S44}}\right]$$

$$+ B_2 \underbrace{\left[\left(E_2 I_2\left(k_{f2}^2\right)\right)+\left(\frac{L}{2}\left(\sin\tfrac{\theta}{2}\right)E_2 I_2\left(k_{f2}^3\right)\right)\right]}_{S4}$$

$$\left.\left. - B_4 \underbrace{\left[\left(E_2 I_2\left(k_{f2}^2\right)\right)+i\left(\frac{L}{2}\left(\sin\tfrac{\theta}{2}\right)E_2 I_2\left(k_{f2}^3\right)\right)\right]}_{S46} \right]\!\!\right]$$

Equation 4-21

Equilibrium of compressive force

$$E_1 A_1 \frac{\partial U_-}{\partial x} = E_2 A_2 \frac{\partial U_+}{\partial \psi}\cos\theta + E_2 I_2 \frac{\partial^3 W_+}{\partial \psi^3}\sin\theta - m_j \frac{\partial^2}{\partial t^2}\left[U_- - \boldsymbol{L}\left(\boldsymbol{\sin}\tfrac{\theta}{4}\right)^{\boldsymbol{2}}\frac{\boldsymbol{\partial W_-}}{\boldsymbol{\partial x}}\right]$$

$$\left[\!\!\left[A_I \underbrace{\left[-i\left(E_1 A_1 (k_{l1})\right)-\left(m_j\omega^2\right)\right]}_{S5b} - A_4 \underbrace{\left[\left(m_j\omega^2\right)\boldsymbol{iL}\left(\boldsymbol{\sin}\tfrac{\theta}{4}\right)^{\boldsymbol{2}}\left(\boldsymbol{k_{f1}}\right)\right]}_{S5a} \right.\right.$$

$$= -A_1 \underbrace{\left[\left(m_j\omega^2\right)\boldsymbol{L}\left(\boldsymbol{\sin}\tfrac{\theta}{4}\right)^{\boldsymbol{2}}\left(\boldsymbol{k_{f1}}\right)\right]}_{S5} - A_3 \underbrace{\left[\left(m_j\omega^2\right)\boldsymbol{iL}\left(\boldsymbol{\sin}\tfrac{\theta}{4}\right)^{\boldsymbol{2}}\left(\boldsymbol{k_{f1}}\right)\right]}_{S52}$$

$$+ A_L \underbrace{\left[-i\left(E_1 A_1 (k_{l1})\right)+\left(m_j\omega^2\right)\right]}_{S53} - B_L \underbrace{\left[i\left(E_2 A_2 (k_{l2})\cos\theta\right)\right]}_{S54}$$

$$\left.\left. - B_2 \underbrace{\left[E_2 I_2\left(k_{f2}^3\right)\sin\theta\right]}_{S55} + B_4 \underbrace{\left[i\left(E_2 I_2\left(k_{f2}^3\right)\sin\theta\right)\right]}_{S56} \right]\!\!\right]$$

Equation 4-22

Note:

Equation for bending moment and compressive forces above were having both A_1 and A_4 as the input wave, to further simplify the equation for matrix arrangement, both equation need to be solve simultaneously.

The equation below being derived to simplify the matrix and being verified by balanced power: -

$$5S = (S5a.S4b) + (S5b.S4a)$$

$$S5A1 = \frac{[(S41.S5a) + (S51.S4a)]}{S5}, \quad S5A3 = \frac{[(S42.S5a) - (S52.S4a)]}{S5},$$
$$S5AL = \frac{[-(S43.S5a) + (S53.S4a)]}{S5}$$

$$S5BL = \frac{[(S44.S5a) + (S54.S4a)]}{S5}, \quad S5B2 = \frac{[(S45.S5a) - (S55.S4a)]}{S5},$$
$$S5AL = \frac{[-(S46.S5a) + (S56.S4a)]}{S5}$$

$$S4A1 = -\left(^{S41}/_{S4a}\right) + \left[S5A1.\left(^{S4b}/_{S4a}\right)\right], \quad S4A3 = \left(^{S42}/_{S4a}\right) + \left[S5A3.\left(^{S4b}/_{S4a}\right)\right],$$
$$S4AL = -\left(^{S43}/_{S4a}\right) - \left[S5AL.\left(^{S4b}/_{S4a}\right)\right]$$

$$S4BL = -\left(^{S44}/_{S4a}\right) + \left[S5BL.\left(^{S4b}/_{S4a}\right)\right], \quad S4B2 = \left(^{S45}/_{S4a}\right) + \left[S5B2.\left(^{S4b}/_{S4a}\right)\right],$$
$$S4B4 = -\left(^{S46}/_{S4a}\right) - \left[S5B4.\left(^{S4b}/_{S4a}\right)\right]$$

Equilibrium of shear force

$$-E_1 I_1 \frac{\partial^3 W_-}{\partial x^3} = E_2 A_2 \frac{\partial U_+}{\partial \psi}\sin\theta - E_2 I_2 \frac{\partial^3 W_+}{\partial \psi^3}\cos\theta$$
$$- m_j \frac{\partial^2}{\partial t^2}\left[W_- + \boldsymbol{L}\left(\mathbf{sin}\tfrac{\theta}{4}\right)\left(\mathbf{cos}\tfrac{\theta}{4}\right)\frac{\partial W_-}{\partial x}\right]$$

$$\left[\!\left[A_4 \underbrace{\left[\left(-iE_1 I_1\left(k_{f1}^3\right)\right) - \left(m_j\omega^2\right) - \left(i\left(m_j\omega^2\right)\boldsymbol{L}\left(\mathbf{sin}\tfrac{\theta}{4}\right)\left(\mathbf{cos}\tfrac{\theta}{4}\right)\left(k_{f1}\right)\right)\right]}_{S6} \right.\right.$$
$$= A_1 \underbrace{\left[\left(E_1 I_1\left(k_{f1}^3\right)\right) + \left(m_j\omega^2\right) - \left(\left(m_j\omega^2\right)\boldsymbol{L}\left(\mathbf{sin}\tfrac{\theta}{4}\right)\left(\mathbf{cos}\tfrac{\theta}{4}\right)\left(k_{f1}\right)\right)\right]}_{S6A1}$$
$$+ A_3 \underbrace{\left[\left(-iE_1 I_1\left(k_{f1}^3\right)\right) + \left(m_j\omega^2\right) - \left(i\left(m_j\omega^2\right)\boldsymbol{L}\left(\mathbf{sin}\tfrac{\theta}{4}\right)\left(\mathbf{cos}\tfrac{\theta}{4}\right)\left(k_{f1}\right)\right)\right]}_{S6A3}$$
$$\left.\left. - B_L \underbrace{\left[iE_2 A_2\left(k_{l2}\right)\sin\theta\right]}_{S6B} + B_2 \underbrace{\left[E_2 I_2\left(k_{f2}^3\right)\cos\theta\right]}_{S6B2} - B_4 \underbrace{\left[iE_2 I_2\left(k_{f2}^3\right)\cos\theta\right]}_{S6B4} \right]\!\right]$$

Equation 4-23

4.1.2 Results and comments

Rearranging all the 6 equations in the order of $A_1, A_3, A_L, B_L, B_2, B_4$ and the required input from A_I, A_4 yields the matrix below;

$$\underbrace{\begin{bmatrix} 0 & 0 & -1 & \cos\theta & -S1B2 & -S2B4 \\ -1 & -1 & 0 & \sin\theta & S2B2 & S2B4 \\ S3A1 & 1 & 0 & 0 & S3B2 & S3B4 \\ S4A1 & S4A3 & S4AL & S4BL & S4B2 & S4B4 \\ -S5A1 & S5A3 & S5AL & -S5BL & S5B2 & S5B4 \\ \left(\frac{S6A1}{S6}\right) & \left(\frac{S6A3}{S6}\right) & 0 & -\left(\frac{S6BL}{S6}\right) & \left(\frac{S6B2}{S6}\right) & -\left(\frac{S6B4}{S6}\right) \end{bmatrix}}_{[X]} \underbrace{\begin{bmatrix} A_1 \\ A_3 \\ A_L \\ B_L \\ B_2 \\ B_4 \end{bmatrix}}_{[Y]} = \underbrace{\begin{bmatrix} A_I \\ A_4 \\ A_4 \\ A_4 \\ A_I \\ A_4 \end{bmatrix}}_{[Z]}$$

Applying the above derivation and matrix to MATLAB, with the given input for $A_I \; and \; A_4$, the equation becomes;

$[Y] = inv[X].[Z]$, ***(Refer appendix B-2 for derivation and appendix B-3 for the MATLAB coding)***

Result plotted with input frequency of 500Hz and similar material type & geometry (for comparison with results in chapter 3) and both impinging wave $A_I \; and \; A_4$, representing input amplitude of longitudinal and flexural respectively, were given input of unity. It can be seen from Figure 4-5 of beam 1 that variable joint reflected lower power for FF-flexural waves at extreme angles and LL-longitudinal power shows similarity with fixed joint until 140^o angle, while the cross-coupling power have taken the remaining power balance compared to rigid joint results. This shows that the realistic geometry of variable joint has considered angle, inertia and the mass of joint effectively. Flexural power for both reflected and transmitted has full agreement at 90^o of angle for fixed joint and variable joint where at this point both model considers the same size, mass and inertia of joint.

As derived earlier for Equation 4-9, Equation 4-10 and Equation 4-11, the variables of $\ddot{\boldsymbol{U}}_{\boldsymbol{M}}$, $\ddot{\boldsymbol{W}}_{\boldsymbol{M}}$, $F_{-}f$, and $F_{+}f$ were the other added improvement to this findings as the displacement in the joints in both directions being explicitly considered, the moments created by the compressive force were as well explicitly calculated. This can be significantly seen from the longitudinal power in both reflected and transmitted power (Figure 4-5 and Figure 4-6) for the extreme of angles (more than 90^o of joint angle) compared to the lumped mass joint result.

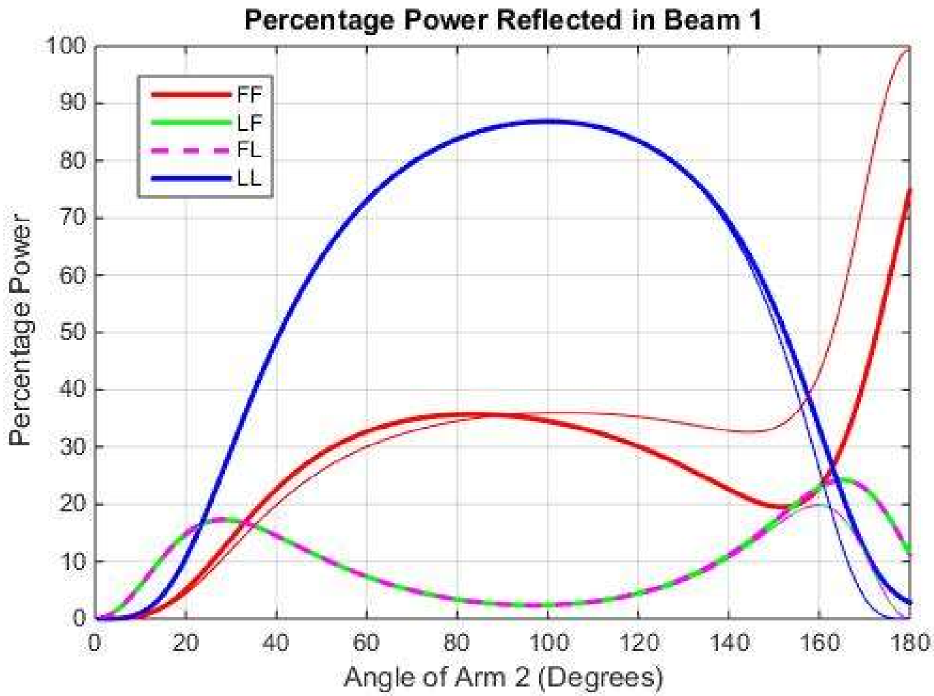

Figure 4-5: % of power in beam 1 for all four types of wave for variable joint (thick lines) comparing to lumped mass joint (thin lines)

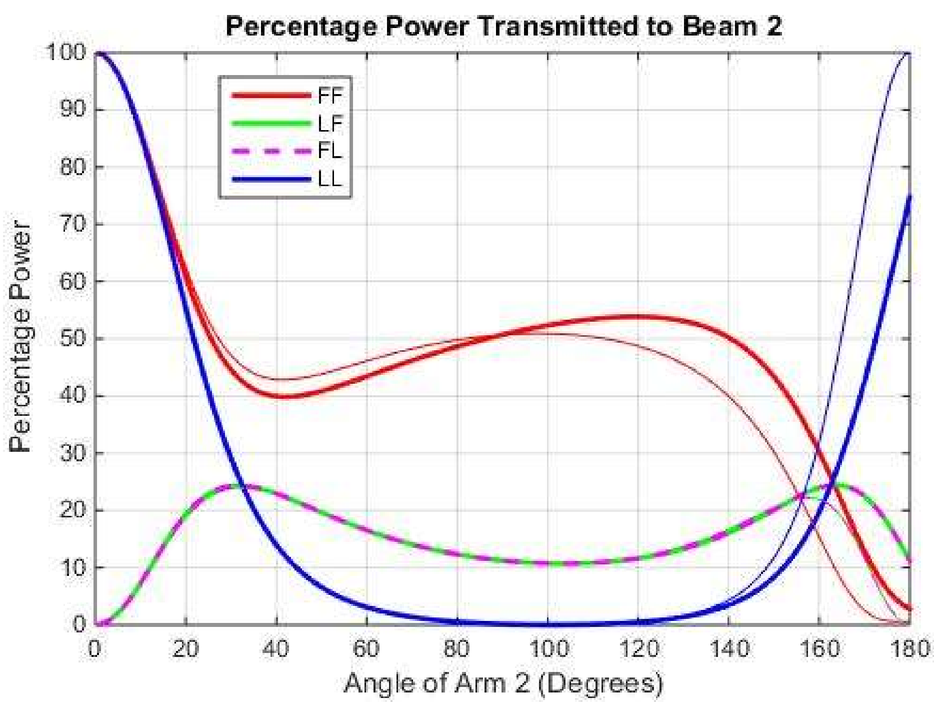

Figure 4-6: % of power in beam 2 for all four types of wave for variable joint (thick lines) comparing to lumped mass joint (thin lines)

Figure 4-6 for the transmitted power shows higher power for variable joint of flexural power after the 90^{o} of angle, but lower power from 140^{o} of angle for longitudinal power transmitted. Power percentage results for variable joint is clearly behaving proportionally to the increase of geometry, mass and inertia where less power reflected for beam1 and higher power transmitted for beam 2, especially from 90^{o} of angle for the flexural power (red lines) in both Figure 4-5 and Figure 4-6 (due to the variably joint increment). Referring to the same figure, cross-coupling of FL and LF were higher for variable joint compared to the fixed mass joint model, where both FL and LF overlay each other for its joint type.

Figure 4-7 and Figure 4-8 shows total power by each flexural and longitudinal of both joint types. Thick lines indicating the variable joint model while the thin lines referring to the fixed or rigid mass joint. Dotted lines representing the transmitted side which is beam 2, so as an example if one need to interpret for transmitted power of FL for variable joint method in Figure 4-7, it would be FL2 as the legend or the thick dotted line. FL2 and FL1 (thin lines) for rigid joint method could be seen overlaying with variable joint up until about 145^{o} of angle, before reducing to 0 percentage of power at 180^{o}. Variable joint cross-coupling for FL1 and FL2 (thick lines) merges at about 165^{o} of angle and reduced to about 10% power at 180^{o} of angle.

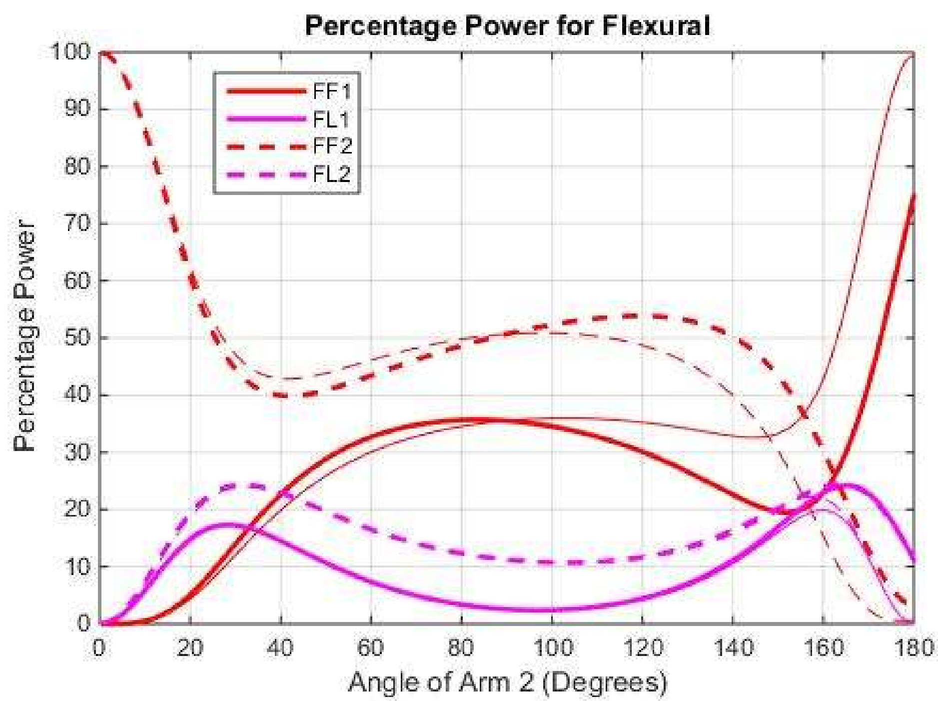

Figure 4-7: Total power of flexural impinging wave for beam 1 & 2 for variable joint (thick lines) comparing to lumped mass joint (thin lines), for reflected (continuous lines) and transmitted (dotted lines)

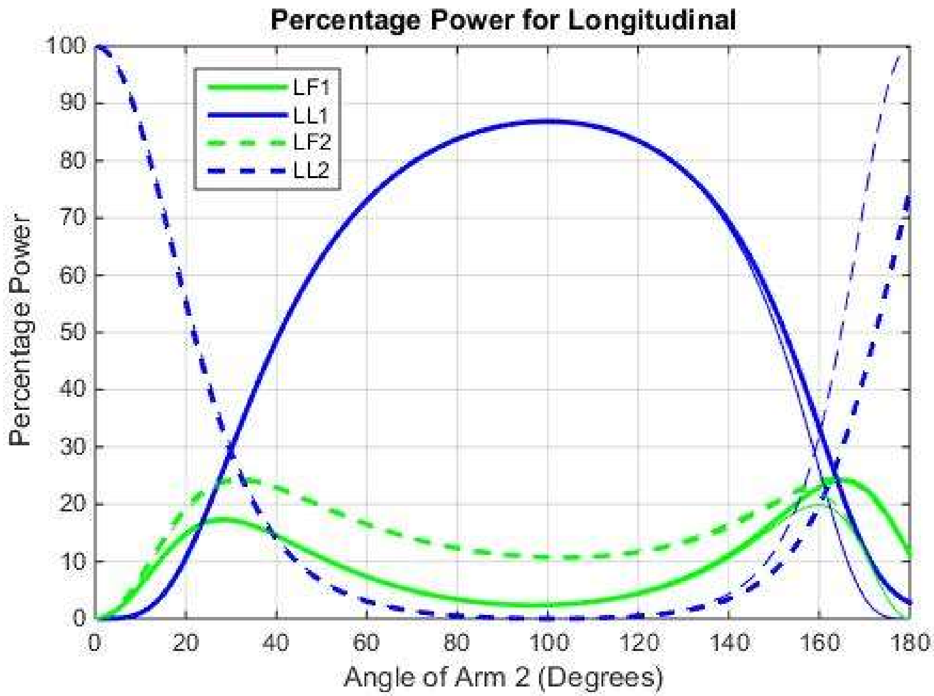

Figure 4-8: Total power of longitudinal impinging wave for beam 1 & 2 for variable joint (thick lines) comparing to lumped mass joint (thin lines), for reflected (continuous lines) and transmitted (dotted lines)

Power for longitudinal can be reviewed in Figure 4-8, where it shows close similarity until 140° of angle between rigid mass joint and variable joint. Longitudinal power for reflected in beam 1 were higher as the angle increased from 140° of angle and reduced in transmitted side of the beam 2. Cross-coupling power were in similar behaviour for LF1 and LF2 of both rigid and variable joint, comparing to the FLs results in Figure 4-7.

This result also shows that from angle 0° to 140° would be best comparable between the two types of joint assumption. The experimentation reported on chapter 5 later, would be taking the angle limitation to ensure measurement result and the modelling appropriately investigated. Interestingly, as the variable joint increase in angle and approaching about 145°, cross-couple differences starts to be seen in power of FL and LF. From the derivation earlier in Equation 4-17, $\boldsymbol{I_C}$ would coincide with $\boldsymbol{I_M}$ as in Figure 4-3 at a particular angle when at *L/2* of joint which is the centre of rotation and force. Solving for Equation 4-17,

$$\left(\frac{2}{3}L\ \text{sinc}\left(\frac{\theta}{2}\right)\right) - \frac{1}{2}L = 0\ or\ ,$$

yield that, (cardinal sin) sinc $\left(\frac{\theta}{2}\right) = 3/4$, where $\theta \approx \pm 2.5514$ or at angle of $\pm 146.126°$, which is around the angle of 145° when the cross-couple of variable joint affecting both FF and LL power compared to fixed mass joint method.

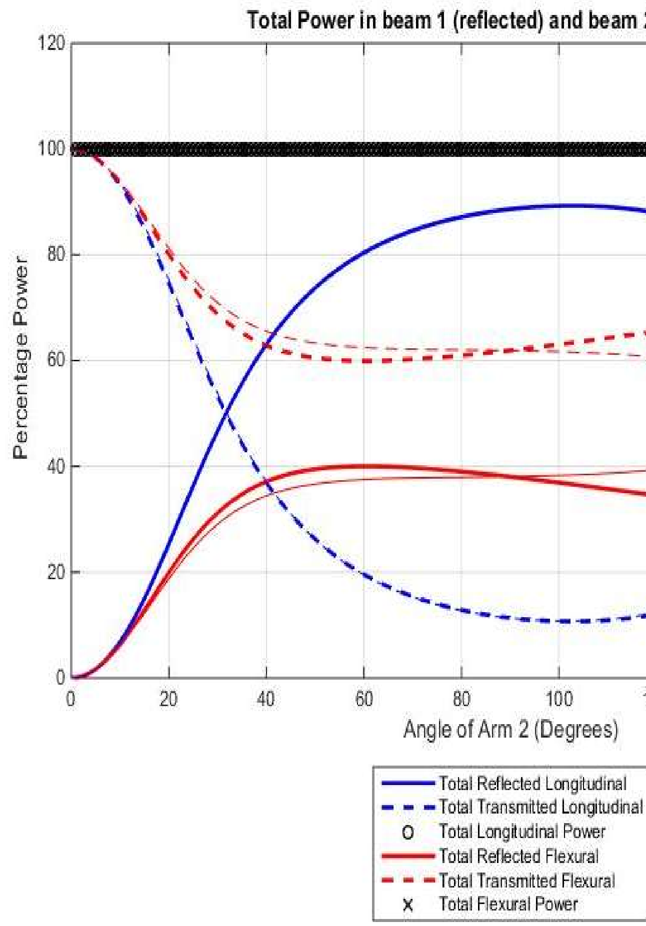

Figure 4-9: Total power of variable joint (thick lines) and rigid joint (thin lines), in beam 1 (reflected-continuous lines) and beam 2 (transmitted-dotted lines) for both Flexural (red) and Longitudinal (blue).

Power balance being checked for both flexural and longitudinal as in Figure 4-9. Total power for each flexural & longitudinal of transmitted & reflected means addition of each power type to equalize the input power. Both joint model was at 100% throughout angle orientation of beam as shown in the figure above. Total power reflected and transmitted for flexural were noted equal at 90^{o} of angle, for both rigid mass joint and variable joint method. Power percentage behaviour were also seen dissimilarity between both method after the extreme angles (above 100^{o}), where variable joint added the advantage for its dynamic change in geometry, mass and inertia. Very interesting to note that at this 500Hz analysis, power of flexural and longitudinal for reflected and transmitted were equally distributed at 50% each during 163^{o} of angle. This can be translated to coefficient of reflection and transmission equal to 1 for each power.

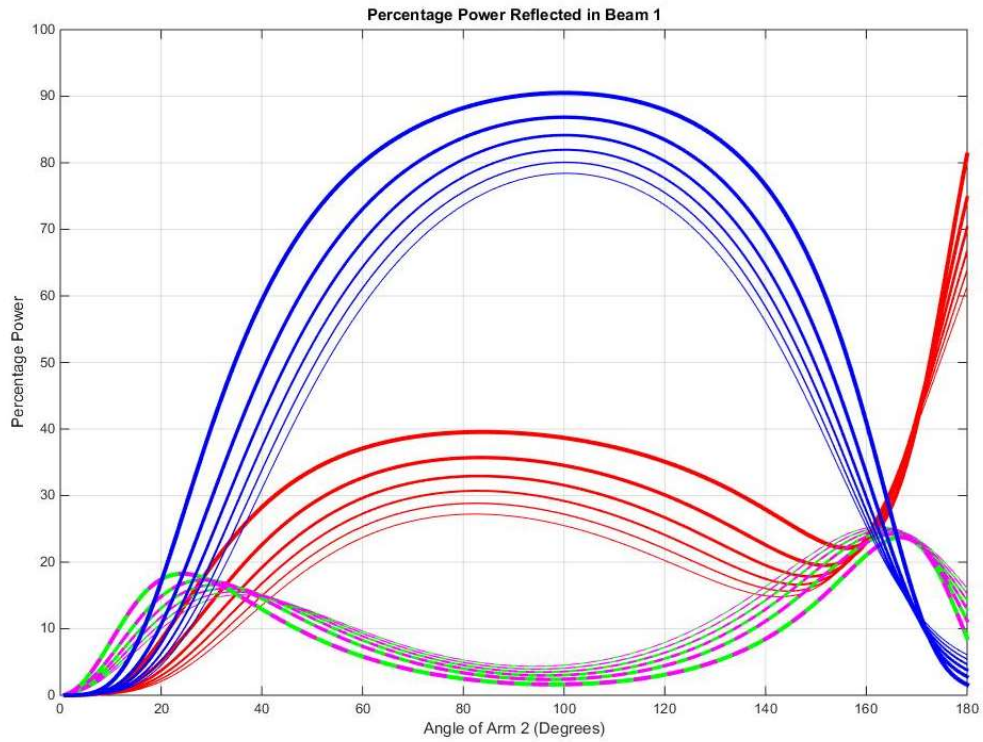

Figure 4-10: **Various frequency input for beam 1, from 250Hz (thickest line) with interval of 250Hz, to 1500Hz (thinnest line)**

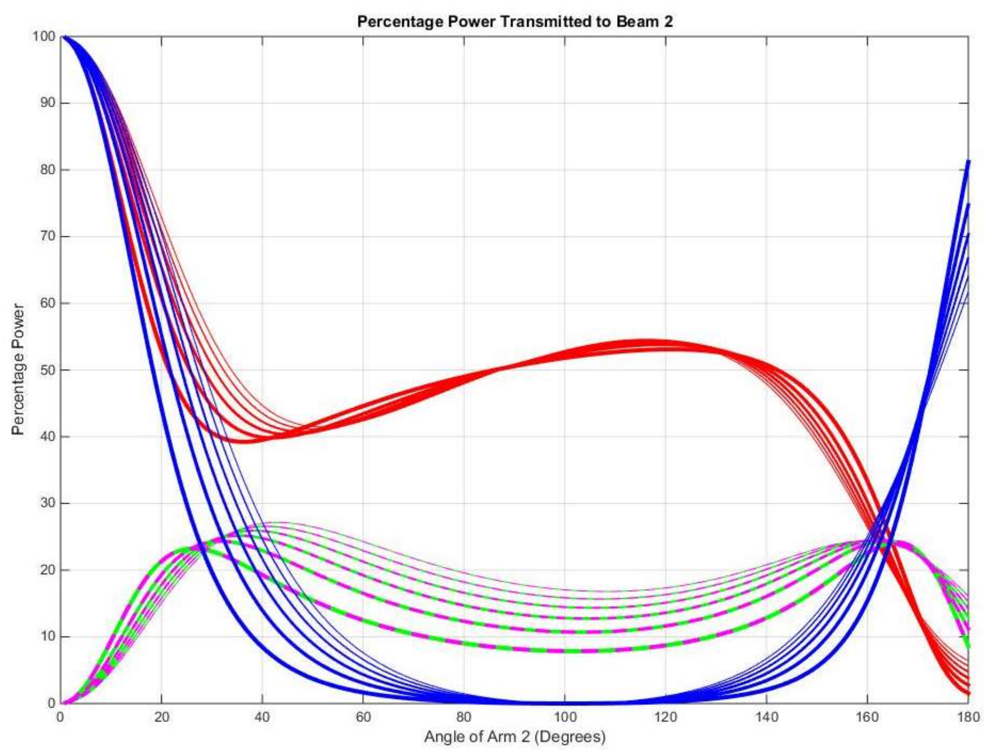

Figure 4-11: **Various frequency input for beam 2, from 250Hz (thickest line) with interval of 250Hz, to 1500Hz (thinnest line)**

Figure 4-10, Figure 4-11 and Figure 4-12 would now examine the various frequency change to the percentage of power for the variable joint. The increase in frequency will reduce total travelling power for both waves at each angle measured in the reflected power for beam 1 of Figure 4-10. Higher power in the cross coupling were observed compensating power reduction in above statement for the increase in frequency. At extreme of angle (170^o), frequency change has minimal effect of power difference for both longitudinal and flexural. It is also observed in Figure 4-11, at about 90^o to 110^o and 170^o of angle of arm 2, the power transmitted by 'flexure to flexure' (FF - red graphs) of incident flexural wave with flexural reflected wave, are similar for all frequency range. When the frequency decreases, the power curve for longitudinal to longitudinal (LL - blue lines) of incident longitudinal wave with longitudinal reflected wave, were broader or flattened. This shows exponential power reduced against angle of joint at before 90^o and increased at after 100^o of angle of arm 2. Cross-coupling power for transmitted side were higher compared to reflected side and increased with frequency from angle 40^o to 140^o. Total power were balanced for all frequency range and having coefficient ratio of 1 at about 160^o angle as in Figure 4-12.

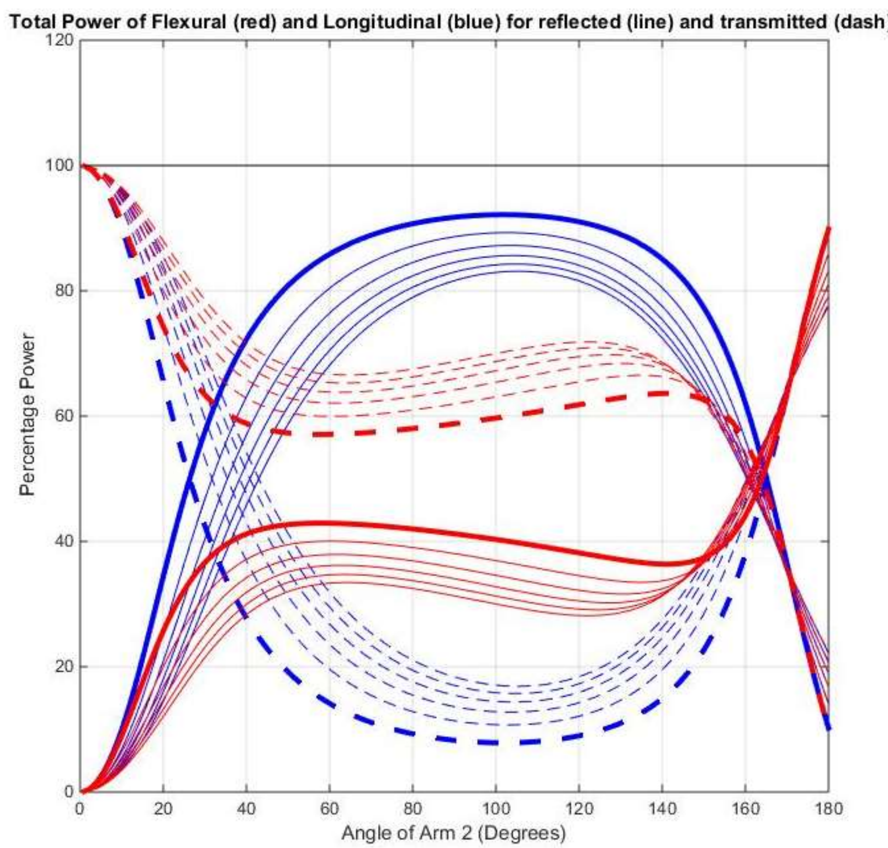

Figure 4-12: Total power for Flexural and Longitudinal, with each frequency equated to 100%, from 250Hz (thickest line) with interval of 250Hz, to 1500Hz (thinnest line)

4.2 Analysis of wave reflected and transmitted

Further analysis for the variable joint were conducted for the various other frequencies. In this section, the dimension and material type were fixed to be 20mm x 100mm cross section with Perspex material as in section 3.6. The variable joint model was tested for power conservation where the output must be equivalent with given input. Alpha is the input wave section and the beta is the output wave section (identified with beam/arm 1 and beam/arm 2). Analysis this time considering frequency at 2500Hz, to further illustrate the behaviour of variable joint.

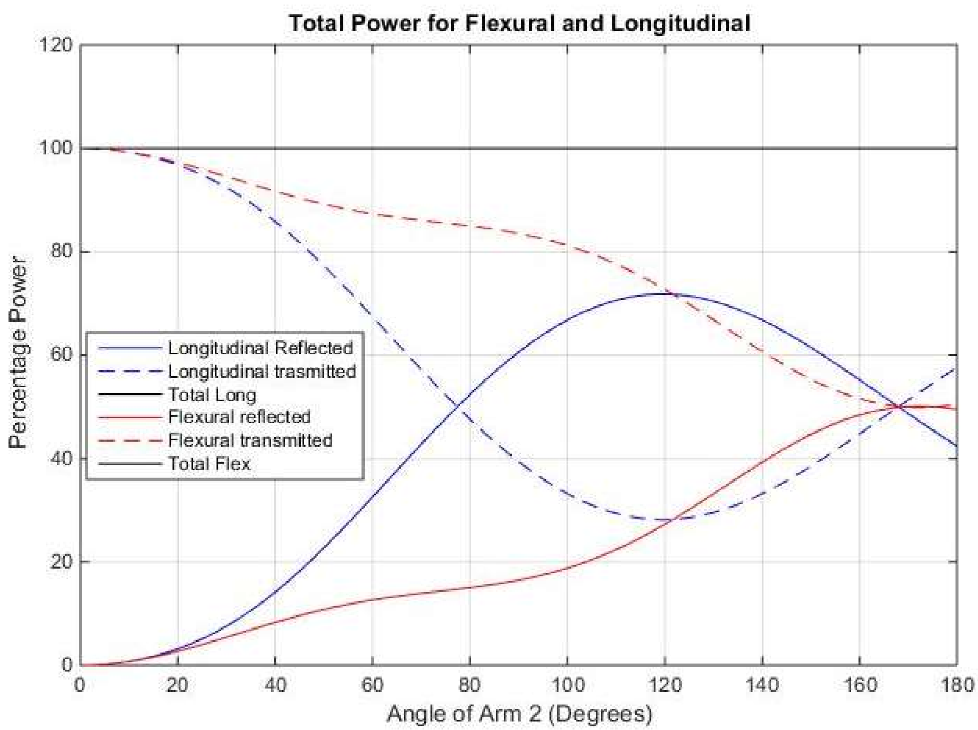

Figure 4-13: Total power of Longitudinal and Flexural for variable joint at 2500Hz

From the Figure 4-13 above, it was agreeable for power conservation of input and output were in balanced. Further verifications on various frequencies at various angles were also conducted. It is to determine at what angles and frequencies the models would give similar power and when do the results start to diverge. Longitudinal power for reflected and transmitted were equalized at 50% for angle 77° and 167°, while flexural power also equalized at 167°.

In Figure 4-14, the maximum power for longitudinal power (blue lines) reflected (beam 1) were at about 105^o of angle with 50% power and the minimum (almost zero) power of longitudinal in Figure 4-15 observed at beam 2 at this angle position. Reflection of flexural power (red lines) was only significant after this angle of 105^o. Cross couple power of LF & FL was noted significant for reflection (beam 1) after this angle as well, but at its maximum in Figure 4-15 during transmitted (beam 2) at orientation of about 75^o.

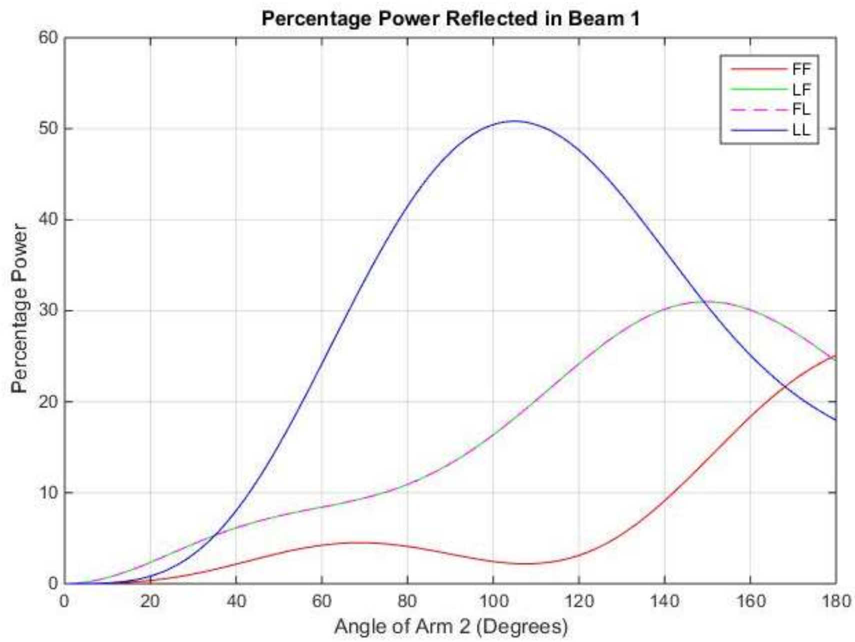

Figure 4-14: Percentage power in beam 1 (alpha) at 2500Hz

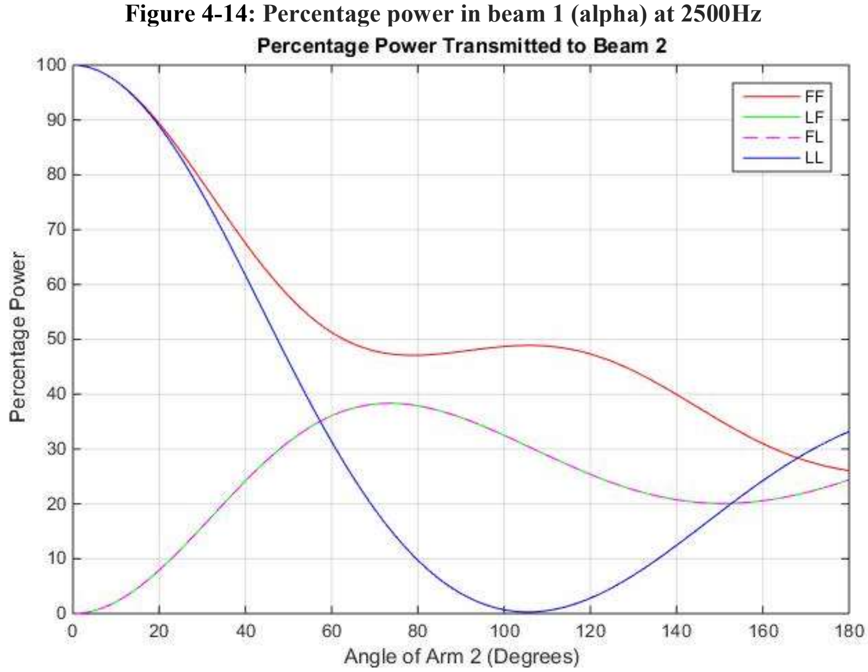

Figure 4-15: Percentage power in beam 2 (beta) at 2500Hz

Analysis for various frequencies at all angles were within range of 500Hz to 3000Hz as shown in Figure 4-16 and Figure 4-17 of beam 1 and beam 2. Observation to the various waves i.e. FF, LL, LF and FL were particularly to understand the characteristics. Reflected power in Figure 4-16 shows that flexural power reduced with the increase of cross-couple power (pink & green lines) at about 145^{o} of angle. Longitudinal power in other hand increase in power when cross-coupling increase with the frequency.

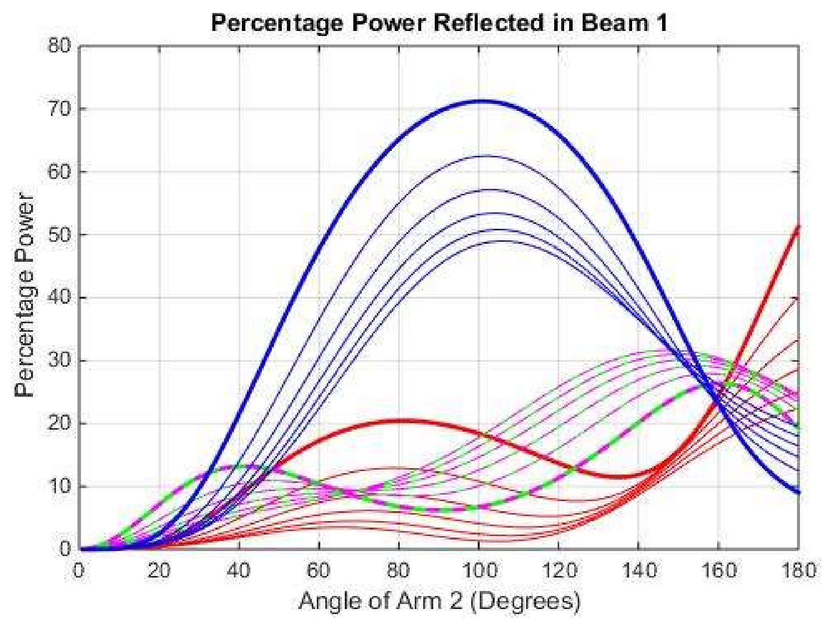

Figure 4-16: **Percentage power in beam 1 (alpha) for 500Hz to 3000Hz with interval of every 500Hz**

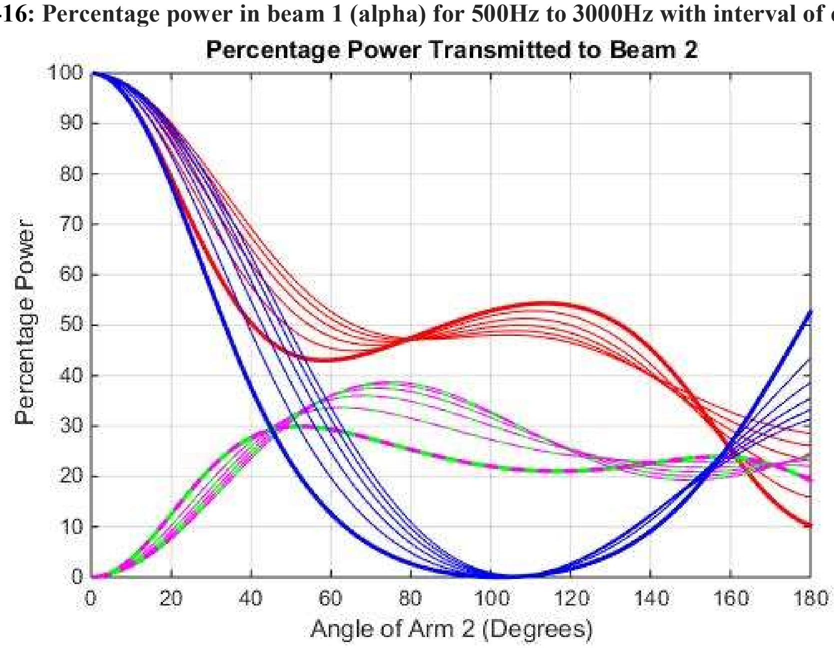

Figure 4-17: **Percentage power in beam 2 (beta) for 500Hz to 3000Hz with interval of every 500Hz**

It is understood to compare the normalised power in both side of the beam with the 3rd axis, hence surf plot was produced at various waves type results as well the total for each flexural and longitudinal power.

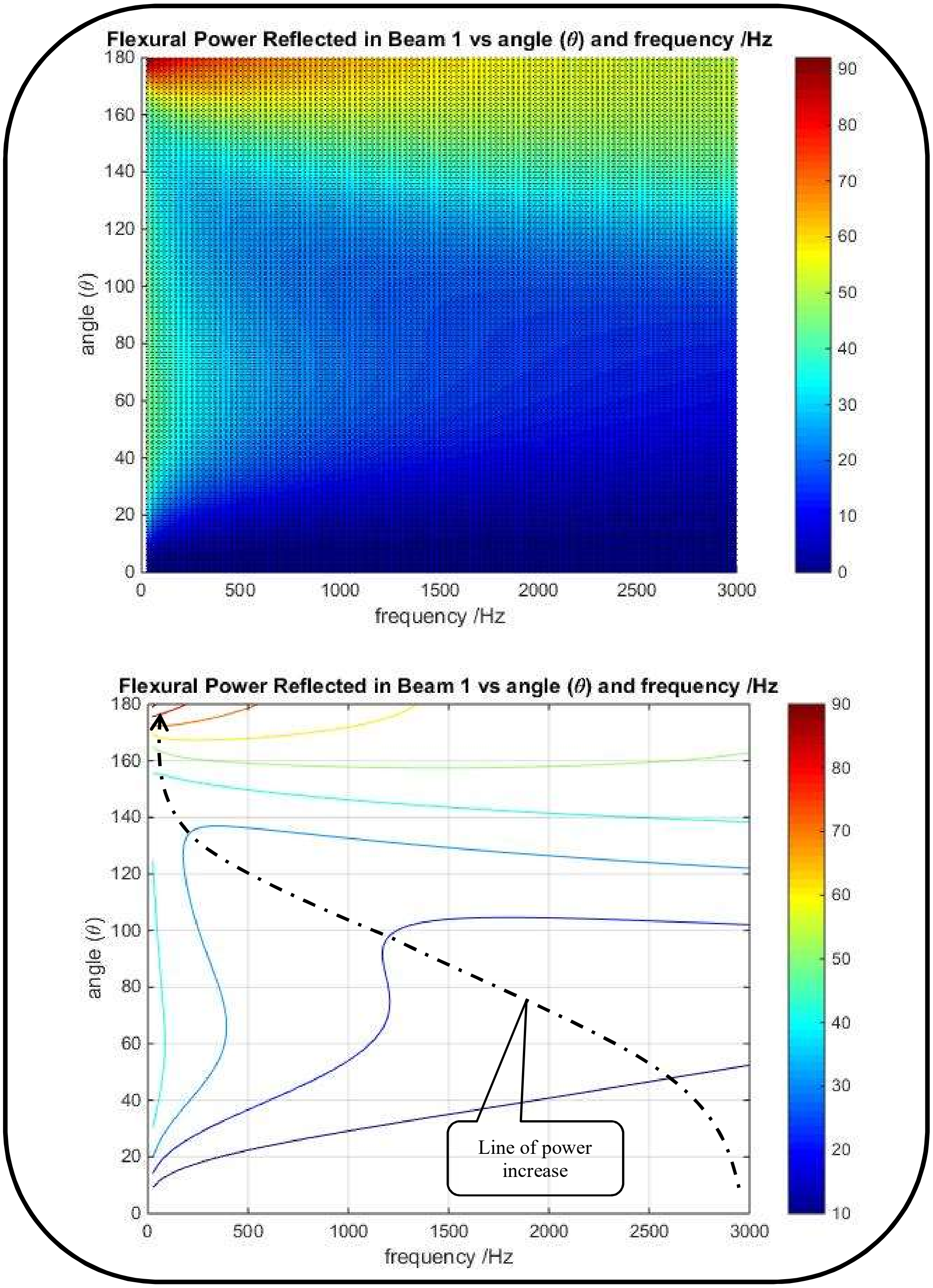

Figure 4-18: Flexural Power reflected in beam 1

Figure 4-18 clearly agreed that the flexural power reflected in beam 1 were at maximum during 180^{o} within low range of frequency (100Hz-200Hz). The reflected power reduces with the increase of frequency at angle 180^{o}. Obviously, the least power (zero) were at orientation of straight beam (0^{o} angle) for highest frequency.

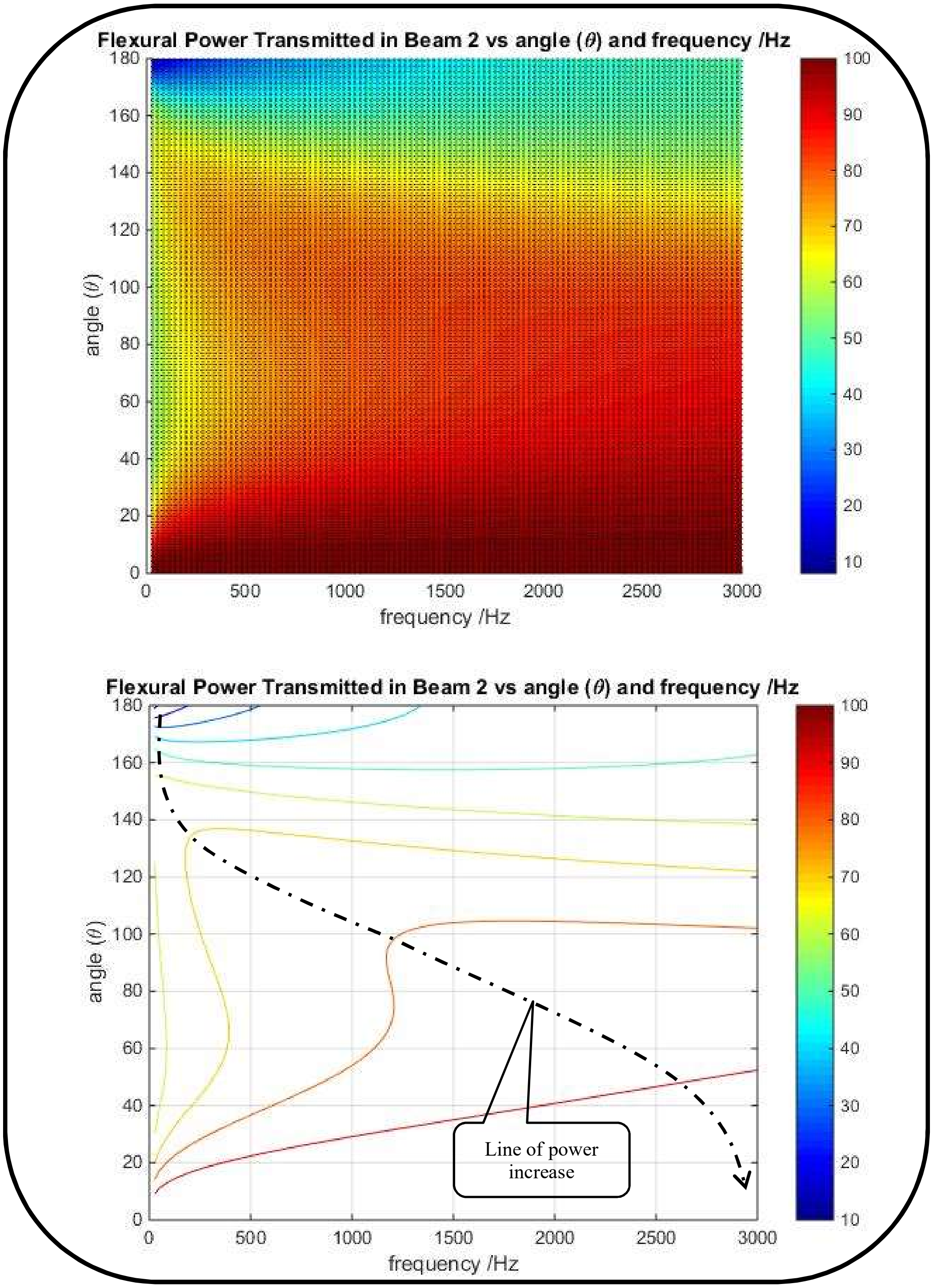

Figure 4-19: Flexural Power transmitted in beam 2

The reversed behaviour in Figure 4-19 is the direct agreement that transmitted waves and power were at maximum during straight beam orientation and impeded at 180^o angle.

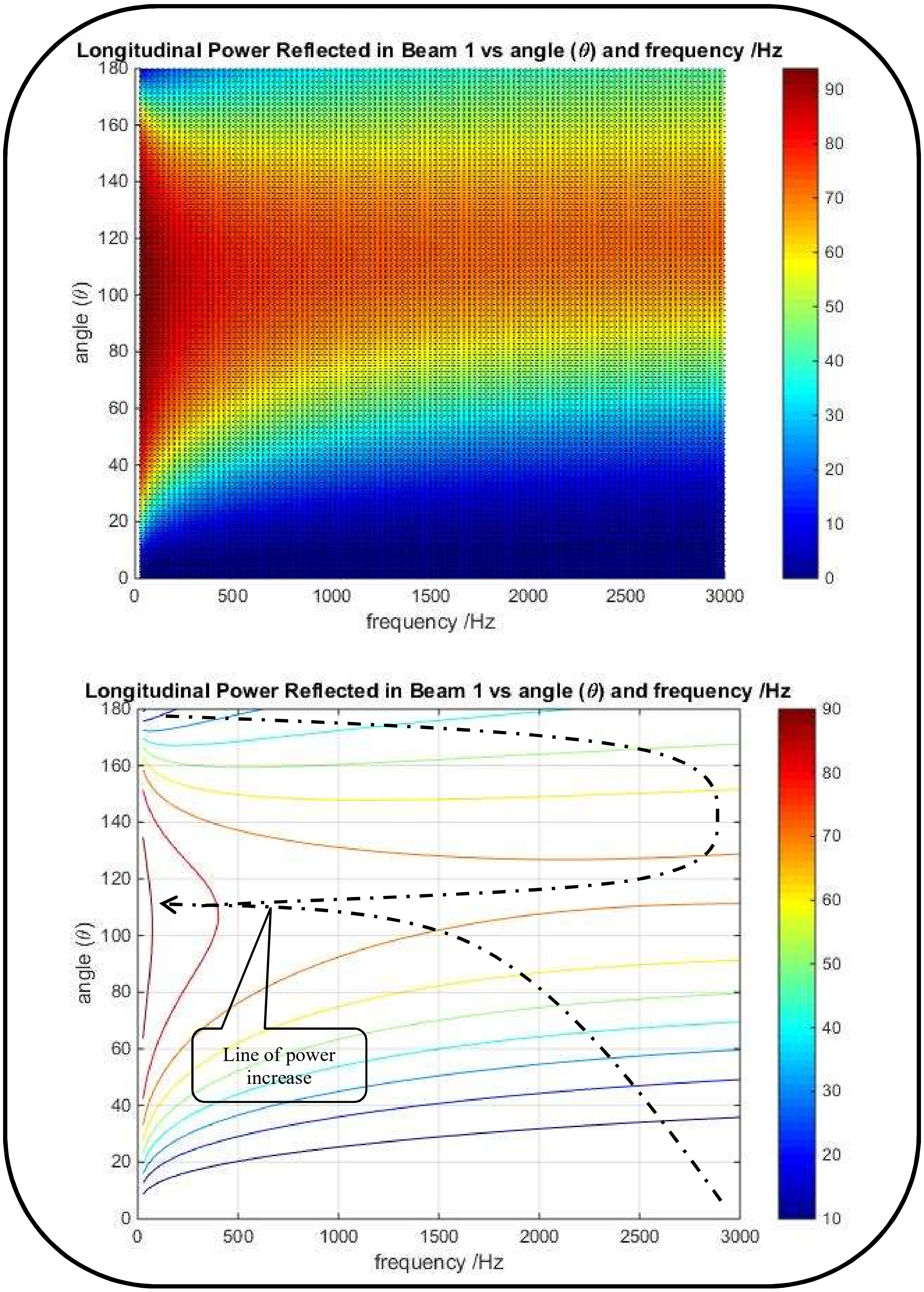

Figure 4-20: Longitudinal Power reflected in beam 1

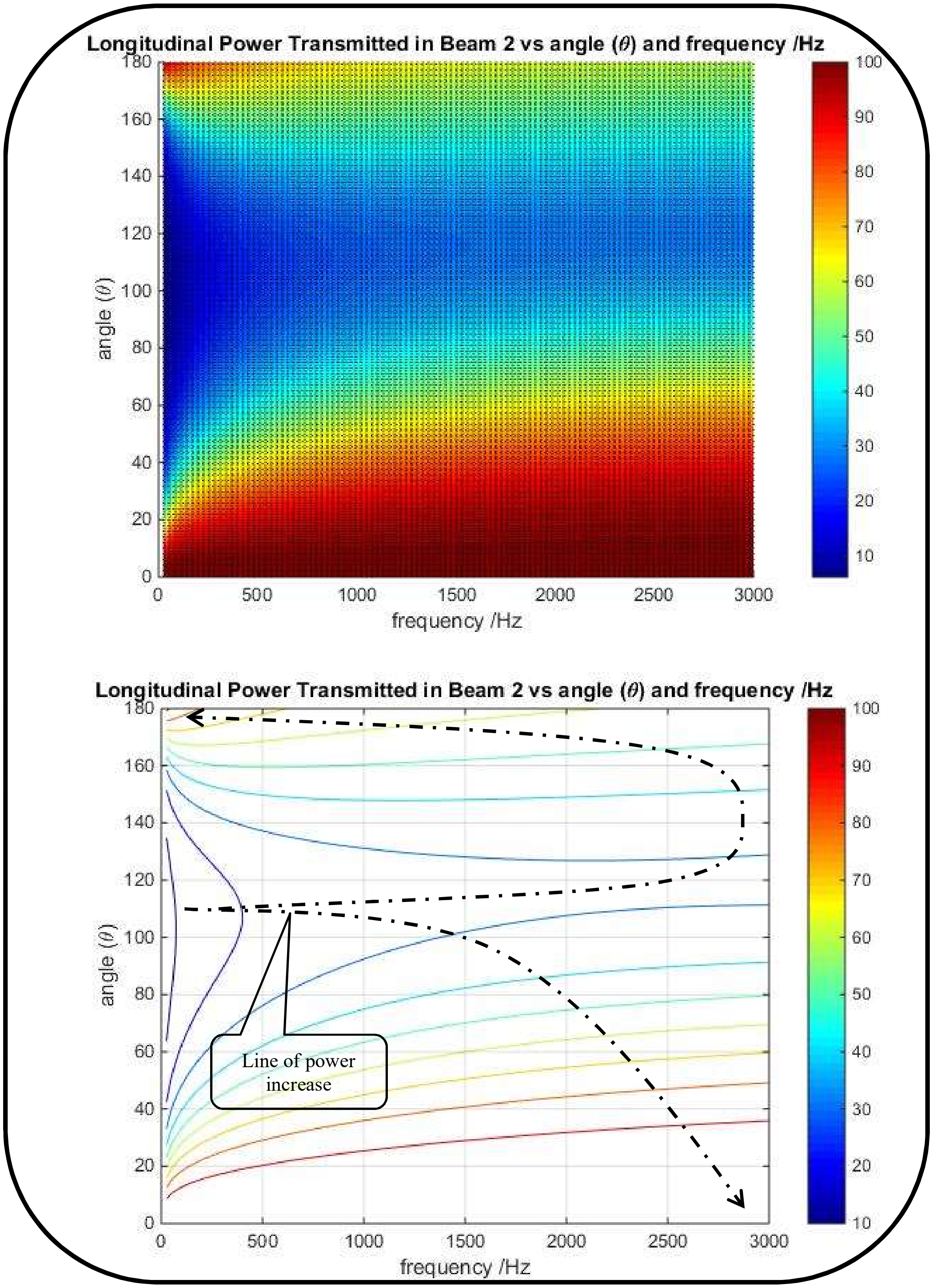

Figure 4-21: Longitudinal Power transmitted in beam 2

Total longitudinal power reflected in beam 1 as Figure 4-20 particularly indicates the maximum is at 110º of beam angle for lowest frequency. The minimum power during low frequency at 180°, while at all range frequency for straight beam (0°) up to around 20° of beam angle. Similarly, for the transmitted side in Figure 4-21 of beam 2, would behaves oppositely.

Further observation in Figure 4-22 to Figure 4-25, are to trace the waves types and its cross-coupling effect to the total power discussed in earlier paragraph. Figure 4-22 to Figure 4-23 are looking at all range of FF, FL, LF and LL power in beam 1 (reflected side), while Figure 4-24 to Figure 4-25 would discussing the pattern in beam 2 (transmitted side).

Total flexural power reflected in beam 1 as in Figure 4-18 could be separated into Figure 4-22, where 'flexure to flexure' and 'longitudinal to flexure' power calculated. The increase in power reflected at higher angles were dominated by cross coupling of LF. At higher frequency as in the figure discussed, the power increases with the dominant angle skewed from around 165° for lower frequency to 150° at higher frequency.

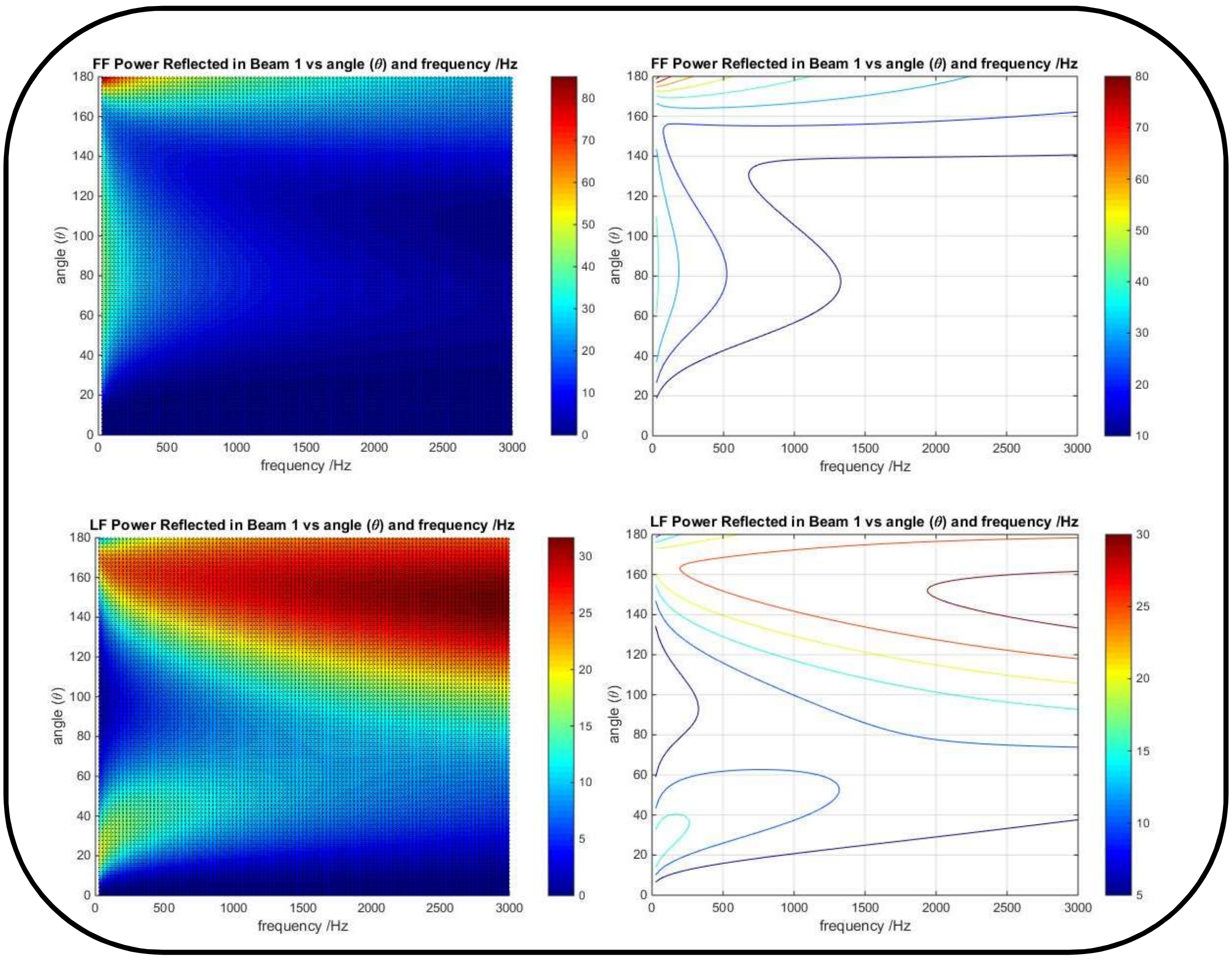

Figure 4-22: FF power (left) and LF power (right) for flexural power in beam 1

Total longitudinal power reflected in beam 1 as in Figure 4-20 were also being examined form its pure LL and cross coupling FL. LF power in the Figure 4-22 and FL power in Figure 4-23 were producing similar behaviour. LL power in Figure 4-23 which produces maximum power at about 105° angle for all frequency would skewed towards 120° angle due to the FL cross coupling power.

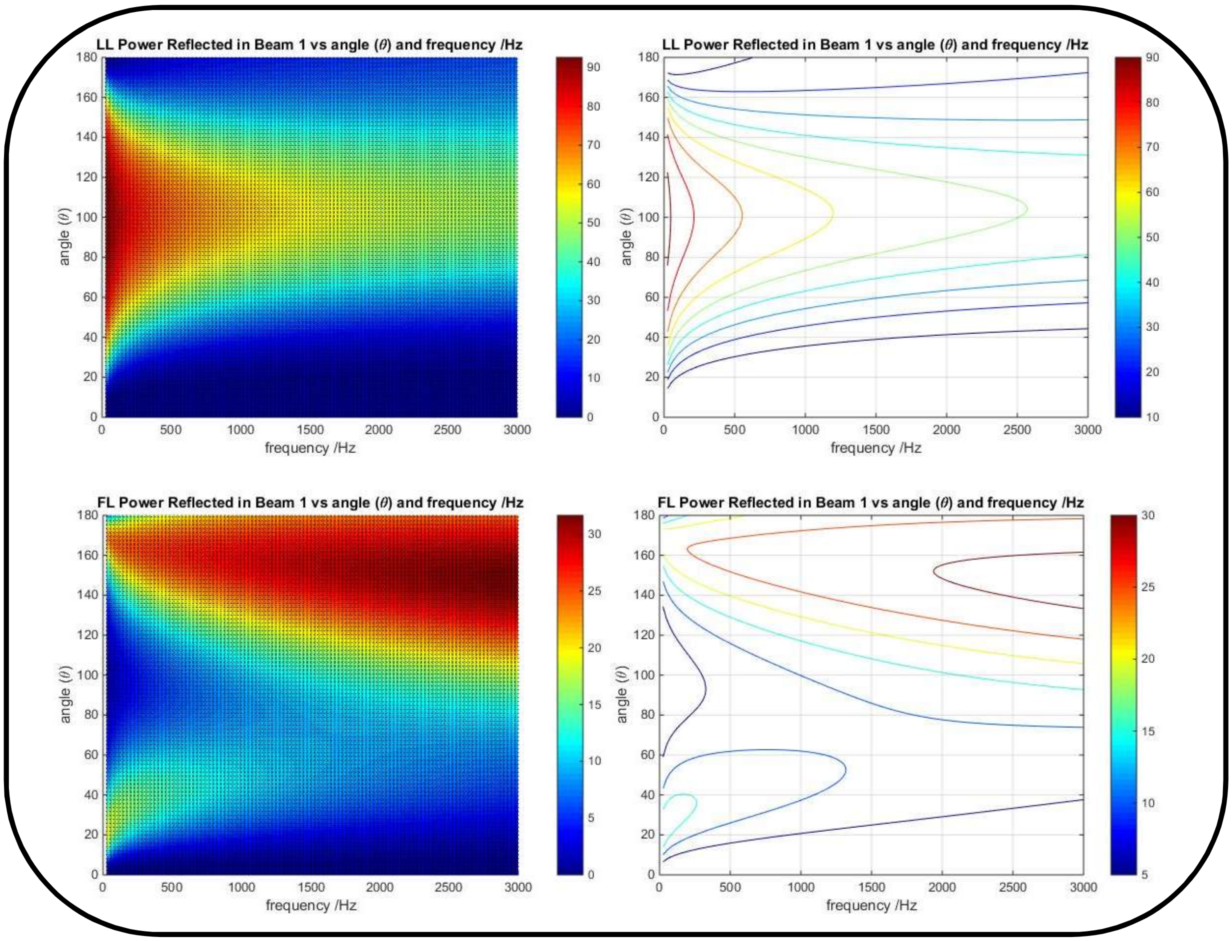

Figure 4-23: LL power (left) and FL power (right) for longitudinal power in beam 1

Total flexural power transmitted in beam 2 as shown in Figure 4-19 is being examined. The dominance of power transmitted at lower angles (region near to straight beam) in Figure 4-24 was widened by the LF cross coupling power in the right figure, which produces maximum power at higher frequency.

Total longitudinal power transmitted in beam 2 as in Figure 4-21 would show the minimum power in left Figure 4-25 skewed from about 105° angle for all frequency towards 120° angle due to the FL cross coupling power in the right figure.

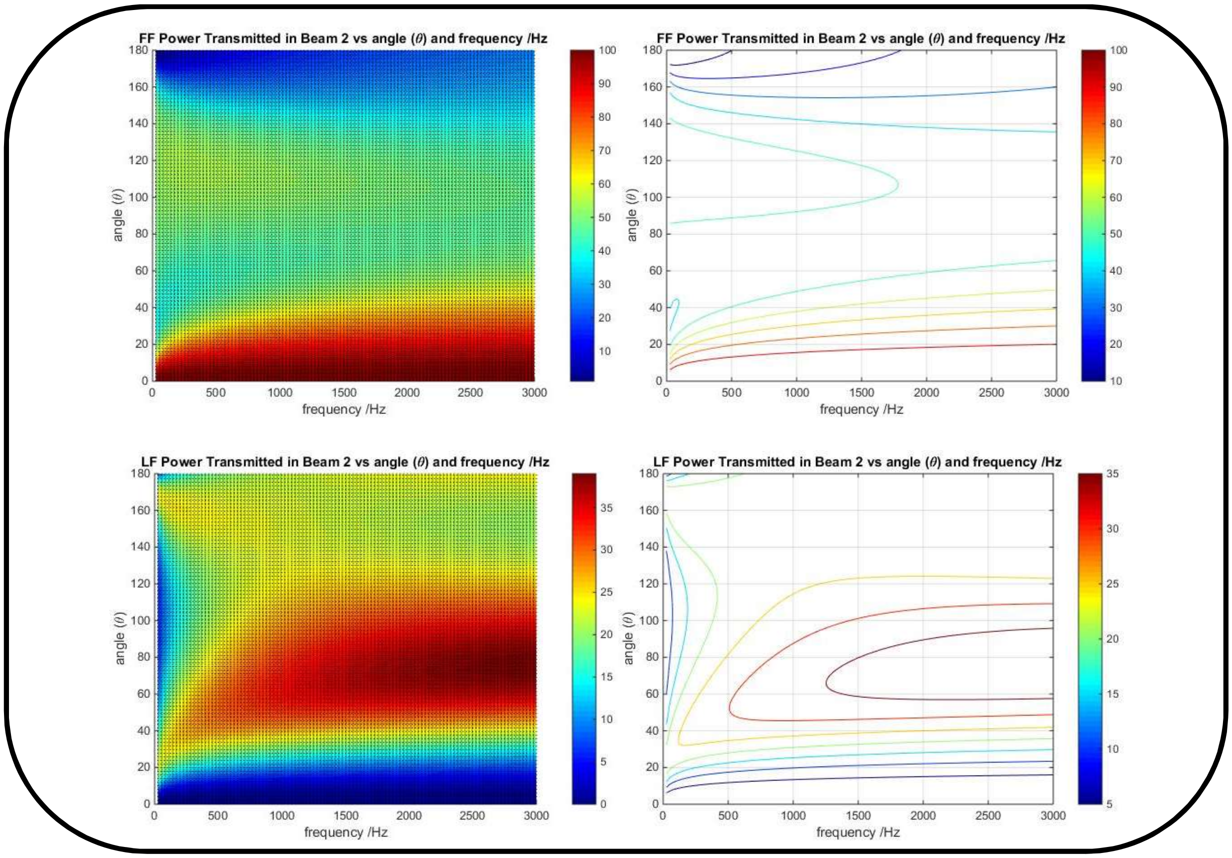

Figure 4-24: FF power (left) and LF power (right) for flexural power in beam 2

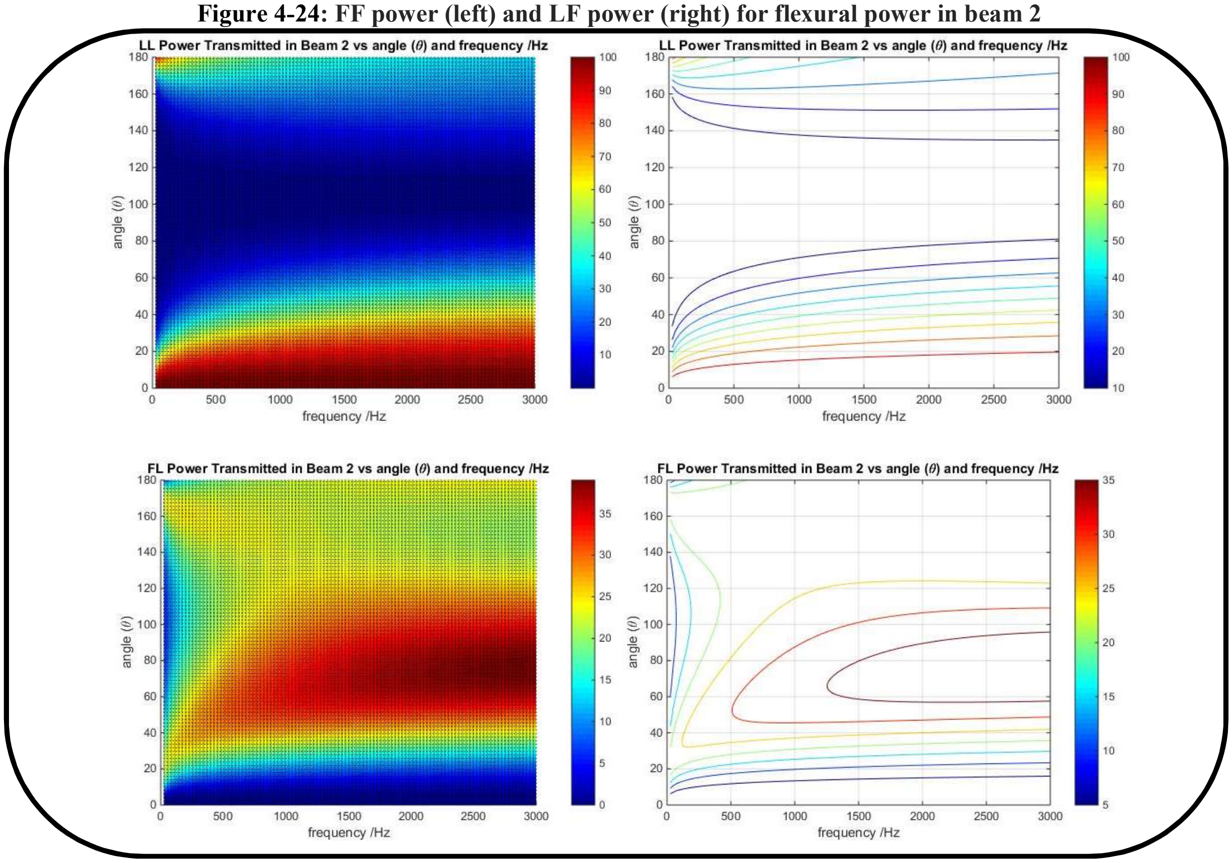

Figure 4-25: LL power (left) and FL power (right) for longitudinal power in beam 2

4.3 Concluding remarks

There have been various comparisons being made to demonstrate the advantage of this variable joint model to the fixed mass joint by Horner. Behaviours were frequency dependent and several angles were noted contributing the obvious changes. Joint model was initially analysed for the effect of angular change, have include a detail consideration of geometry, mass, and rotational inertia of circular sector as it increased in angle. Hence, the result was in good agreement with literature of using 90^o fixed mass joint especially at the lower angles.

Furthermore, the result has shown new observations particularly at the extreme of angle (more than 90^o), as the previous rigid mass joint were unable to relate to the change of angle that would have increase in joint mass and inertia. Several locations of angle were identified for power balance of reflected and transmitted either for flexural or longitudinal power. This would contribute to the additional knowledge on handling vibration power reflected and transmitted in structural system.

The derivation of variable joint model has particularly introduced added considerations realistically with displacement in the joint as well as the for the moments, considered especially due to compressive force and the gradual change of distance to centre of rotation for both shear force and compressive force. Results discussed have elaborated the behaviours and the variable model shown were noted reliable throughout angle examined. However, the lumped mass joint would be said reliable or comparable with the variable angle joint for small range of angles (less than 90^o) and for thinner beam (less influence of joint mass size).

Although it may be argued that various other analyses could be conducted, this work needs to proceed to next level of verifications through physical analysis by a comparable experimentation. Formulation of the joint itself being further explored with the consideration of other cross section such as circular segment of jointed rods, where factors from moment of inertia would be particularly different. Combinations of material types and various cross sections could also be suggested for other researcher's activities.

Chapter 5: Force application for beam joint

5.1 Force input into the beam

Based on the understanding of the amplitude input for the angled beam, a further analysis for the system with force input (which will later be compared to the data from measurements) is important to show correlation with real system. Any real system of structural would always be exposed to various inputs such as the compressive force and flexural force.

To predict a closer behaviour of the beam joint, various fundamental verifications are essential to proceed into the next level of complex modelling of the joint. In this chapter, modelling of semi-infinite beam and eventually the novel variable joint will be elaborated and analysed. This chapter is enhancing the model from previous chapter with the consideration of damping of material. Such analysis is essential to ensure comparative behaviour of the model with the real beam with specific material types.

5.1.1 Infinite continuous beam

An initial mathematical model for a continuous beam is required to give a correct relationship between wave responses due to the force input. Figure 5-1 is considering both flexural and longitudinal force input according to the force direction illustrated.

Both ends were assumed infinite for the beam and having similar notation as previous chapter. The beam is subjected to both directional force (U and W displacement), the jointed part will be modelled as the absence of joint by stating angle equals to zero (0^o). This eliminates the physical joint out from the equations. Waves of B_1, B_3 and B_L in the illustration were as well to be zero (0) since no reflection should be expected from the analysis. As a better clarity, the equations prepared for comparison were from the Figure 5-1 as derived in following pages.

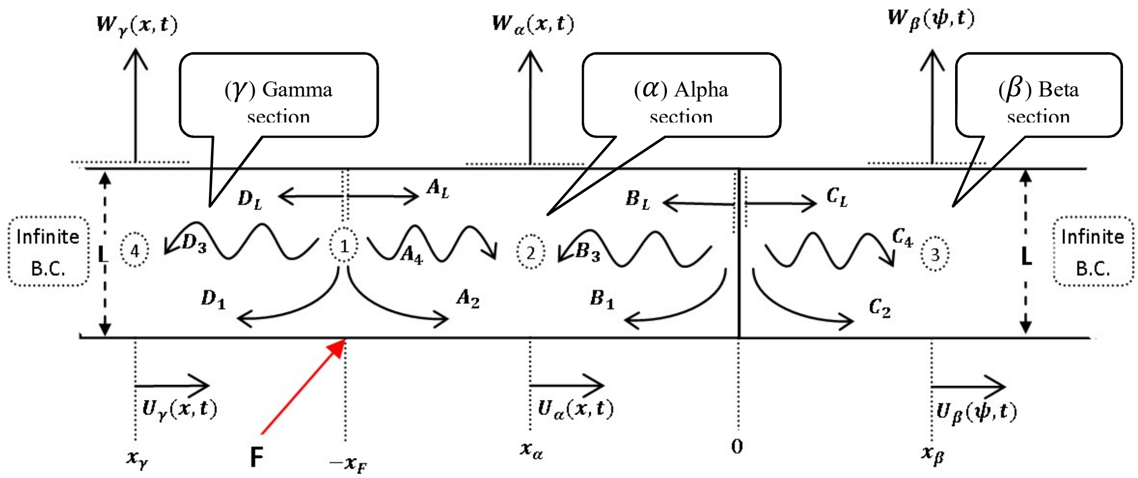

Figure 5-1: Continuous beam with Force input

Assuming force applied at $x = -x_F = m$, and joint at $x = 0 = n$. On the **force input side** of the beam, the flexural displacement was indicated as $W_\alpha(x,t)$ & $W_\gamma(x,t)$and longitudinal displacement as $U_\alpha(x,t)$ & $U_\gamma(x,t)$. Where $\alpha\,(alpha)$,$\beta\,(beta)$ and $\gamma\,(gamma)$ are the section named for the ease of reference. Alpha section located from force $(-x_F)$ to point reference $(x = 0)$, which includes waves for *A* and *B* as in Figure 5-1. Beta section starts from point of reference $(x = 0)$ to the right infinite, which considers waves for *C*. Lastly, gamma section starts from force $(-x_F)$ to the left infinite beam, which account for waves *D*.

U and W direction displacement at $\alpha, \beta\; and\; \gamma$ section was equated to prepare for numerical investigation.

$\boldsymbol{U_\alpha}(x,t) = \left\{A_L e^{-ik_{l\alpha*}|x-m|} + B_L e^{ik_{l\alpha*}|x-m|}\right\}\; e^{i\omega t};$

$at\; x = n\,;\;\; \left\{A_L e^{-ik_{l\alpha*}|n-m|} +\; B_L e^{ik_{l\alpha*}|n-m|}\right\};$

$at\; x = m\;\;;\;\; \{A_L +\; B_L\};$

$\dfrac{\partial \boldsymbol{U_\alpha}}{\partial x} = k_{l\alpha*}\left\{-iA_L e^{-ik_{l\alpha*}|x-m|} + iB_L e^{ik_{l\alpha*}|x-m|}\right\}\;;$

$at\; x = n\,;\;\; k_{l\alpha*}\left\{-iA_L e^{-ik_{l\alpha*}|n-m|} +\; iB_L e^{ik_{l\alpha*}|n-m|}\right\};$

$at\; x = m\;\;;\;\; k_{l\alpha*}\{-iA_L +\; iB_L\};$

$$\boldsymbol{W_\alpha}(x,t) = \left\{A_2 e^{-k_{f\alpha}|x-m|} + A_4 e^{-ik_{f\alpha*}|x-m|} + B_1 e^{k_{f\alpha}|x-m|} + B_3 e^{ik_{f\alpha*}|x-m|}\right\} e^{i\omega t} ;$$

$$at\ x = n\ ;\ \left\{A_2 e^{-k_{f\alpha}|n-m|} + B_1 e^{k_{f\alpha}|n-m|}\right\} + \left\{A_4 e^{-ik_{f\alpha*}|n-m|} + B_3 e^{ik_{f\alpha*}|n-m|}\right\} ;$$

$$at\ x = m\ ;\ \{A_2 + B_1\} + \{A_4 + B_3\} ;$$

$$\frac{\partial \boldsymbol{W_\alpha}}{\partial x} = k_{f\alpha}\left\{-A_2 e^{-k_{f\alpha}|x-m|} + B_1 e^{k_{f\alpha}|x-m|}\right\} + k_{f\alpha*}\left\{-iA_4 e^{-ik_{f\alpha*}|x-m|} + iB_3 e^{ik_{f\alpha*}|x-m|}\right\} ;$$

$$at\ x = n\ ;\ k_{f\alpha}\left\{-A_2 e^{-k_{f\alpha}|n-m|} + B_1 e^{k_{f\alpha}|n-m|}\right\}$$
$$+ k_{f\alpha*}\left\{-iA_4 e^{-ik_{f\alpha*}|n-m|} + iB_3 e^{ik_{f\alpha*}|n-m|}\right\} ;$$

$$at\ x = m\ ;\ k_{f\alpha}\{-A_2 + B_1\} + k_{f\alpha*}\{-iA_4 + iB_3\} ;$$

$$\frac{\partial^2 \boldsymbol{W_\alpha}}{\partial x^2} = {k_{f\alpha}}^2\left\{A_2 e^{-k_{f\alpha}|x-m|} + B_1 e^{k_{f\alpha}|x-m|}\right\} + {k_{f\alpha*}}^2\left\{-A_4 e^{-ik_{f\alpha*}|x-m|} - B_3 e^{ik_{f\alpha*}|x-m|}\right\} ;$$

$$at\ x = n\ ;\ {k_{f\alpha}}^2\left\{A_2 e^{-k_{f\alpha}|n-m|} + B_1 e^{k_{f\alpha}|n-m|}\right\}$$
$$+ {k_{f\alpha*}}^2\left\{-A_4 e^{-ik_{f\alpha*}|n-m|} - B_3 e^{ik_{f\alpha*}|n-m|}\right\} ;$$

$$at\ x = m\ ;\ {k_{f\alpha}}^2\{A_2 + B_1\} + {k_{f\alpha*}}^2\{-A_4 - B_3\} ;$$

$$\frac{\partial^3 \boldsymbol{W_\alpha}}{\partial x^3} = {k_{f\alpha}}^3\left\{-A_2 e^{-k_{f\alpha}|x-m|} + B_1 e^{k_{f\alpha}|x-m|}\right\}$$
$$+ {k_{f\alpha*}}^3\left\{iA_4 e^{-ik_{f\alpha*}|x-m|} - iB_3 e^{ik_{f\alpha*}|x-m|}\right\} ;$$

$$at\ x = n\ ;\ {k_{f\alpha}}^3\left\{-A_2 e^{-k_{f\alpha}|n-m|} + B_1 e^{k_{f\alpha}|n-m|}\right\}$$
$$+ {k_{f\alpha*}}^3\left\{iA_4 e^{-ik_{f\alpha*}|n-m|} - iB_3 e^{ik_{f\alpha*}|n-m|}\right\} ;$$

$$at\ x = m\ ;\ {k_{f\alpha}}^3\{-A_2 + B_1\} + {k_{f\alpha*}}^3\{iA_4 - iB_3\} ;$$

$$\boldsymbol{W_\gamma}(x,t) = \left\{D_1 e^{k_{f\gamma}|x-m|} + D_3 e^{ik_{f\gamma}|x-m|}\right\} e^{i\omega t} ;$$

$$at\ x = m\ ;\ \{D_1 + D_3\} ;$$

$$\frac{\partial W_\gamma}{\partial x} = k_{f\gamma}\left\{D_1 e^{k_{f\gamma}|x-m|} + iD_3 e^{ik_{f\gamma}|x-m|}\right\} ;$$

$$at\ x = m\ ;\ k_{f\gamma}\{D_1 + iD_3\} ;$$

$$\frac{\partial^2 W_\gamma}{\partial x^2} = {k_{f\gamma}}^2\left\{D_1 e^{k_{f\gamma}|x-m|} - D_3 e^{ik_{f\gamma}|x-m|}\right\} ;$$

$$at\ x = m\ ;\ {k_{f\gamma}}^2\{D_1 - D_3\} ;$$

$$\frac{\partial^3 W_\gamma}{\partial x^3} = {k_{f\gamma}}^3\left\{D_1 e^{k_{f\gamma}|x-m|} - iD_3 e^{ik_{f\gamma}|x-m|}\right\} ;$$

$$at\ x = m\ ;\quad k_{f\gamma}{}^3\{D_1 - \ iD_3\ \};$$

$$\boldsymbol{U_\gamma}(x,t) = \left\{D_L e^{ik_{l\gamma}|x-m|}\right\}\ e^{i\omega t}\ \ ;$$

$$at\ x = m\ ;\ \{\ D_L\ \};$$

$$\frac{\partial U_\gamma}{\partial x} = k_{l\gamma}\left\{iD_L e^{ik_{l\gamma}|x-m|}\right\};$$

$$at\ x = m\ ;\ k_{l\gamma}\{\ iD_L\ \};$$

For the **transmitting side** of the bend for flexural $W_\beta(x,t)$ and longitudinal $U_\beta(x,t)$,

$$\boldsymbol{W_\beta}(x,t) = \left\{C_2 e^{-k_{f\beta}|x-n|} + \ C_4 e^{-ik_{f\beta}|x-n|}\right\}\ e^{i\omega t}\ \ ;$$

$$at\ x = n\ ;\quad \{C_2 + \ C_4\ \};$$

$$\frac{\partial W_\beta}{\partial x} = k_{f\beta}\left\{-C_2 e^{-k_{f\beta}|x-n|} - \ iC_4 e^{-ik_{f\beta}|x-n|}\right\};$$

$$at\ x = n\ ;\quad k_{f\beta}\{-C_2 - iC_4\ \};$$

$$\frac{\partial^2 W_\beta}{\partial x^2} = k_{f\beta}{}^2\left\{C_2 e^{-k_{f\beta}|x-n|} - \ C_4 e^{-ik_{f\beta}|x-n|}\right\};$$

$$at\ x = n\ ;\quad k_{f\beta}{}^2\{C_2 - C_4\ \};$$

$$\frac{\partial^3 W_\beta}{\partial x^3} = k_{f\beta}{}^3\left\{-C_2 e^{-k_{f\beta}|x-n|} + \ iC_4 e^{-ik_{f\beta}|x-n|}\right\};$$

$$at\ x = n\ ;\quad k_{f\beta}{}^3\{-C_2 + iC_4\ \};$$

$$\boldsymbol{U_\beta}(x,t) = \left\{C_L e^{-i\ \ _{l\beta}|x-n|}\right\}\ e^{i\omega t}\ \ ;$$

$$at\ x = n\ ;\quad \{C_L\};$$

$$\frac{\partial U_\beta}{\partial x} = k_{l\beta}\left\{-iC_L e^{-ik_{l\beta}|x-n|}\right\};$$

$$at\ x = n\ ;\quad k_{l\beta}\{-iC_L\};$$

Applying boundary condition at $x = m$, and $x = n$, to all equation of continuity, summation of bending moments, shear forces and compressive forces, yields 12 governing equations as below: -

I. Continuity of displacement in axial direction, at $\boldsymbol{x = n}$

$$U_\alpha \quad = \quad U_\beta$$

$$\left[\!\left[0 \quad = A_L e^{-ik_{l\alpha*}|n-m|} + B_L e^{ik_{l\alpha*}|n-m|} - C_L \right]\!\right]$$

Equation 5-1

II. Continuity of displacement in axial direction, at $\boldsymbol{x = m}$

$$U_\gamma \quad = \quad U_\alpha$$

$$\left[\!\left[0 \quad = \quad A_L + B_L - D_L \right]\!\right]$$

Equation 5-2

III. Continuity of displacement in perpendicular direction, at $\boldsymbol{x = n}$

$$W_\alpha \quad = \quad W_\beta$$

$$\left[\!\left[0 \quad = A_2 e^{-k_{f\alpha}|n-m|} + B_1 e^{k_{f\alpha}|n-m|} + A_4 e^{-ik_{f\alpha*}|n-m|} + B_3 e^{ik_{f\alpha*}|n-m|} - C_2 - C_4 \right]\!\right]$$

Equation 5-3

IV. Continuity of displacement in perpendicular direction, at $\boldsymbol{x = m}$

$$W_\alpha \quad = \quad W_\gamma$$

$$\left[\!\left[0 \quad = A_2 + A_4 + B_1 + B_3 - D_1 - D_3 \right]\!\right]$$

Equation 5-4

V. Continuity of angular displacement/equal gradient (joint), at $\boldsymbol{x = n}$

$$\frac{\partial W_\alpha}{\partial x} \quad = \quad \frac{\partial W_\beta}{\partial x}$$

$$k_{f\alpha}\left\{-A_2 e^{-k_{f\alpha}|n-m|} + B_1 e^{k_{f\alpha}|n-m|}\right\} + k_{f\alpha*}\left\{- iA_4 e^{-ik_{f\alpha*}|n-m|} + iB_3 e^{ik_{f\alpha*}|n-m|}\right\}$$
$$= -k_{f\beta}(C_2 + iC_4)$$

$$\left[\!\left[0 \;=\; -A_2 \underbrace{k_{f\alpha}}_{5a} e^{-k_{f\alpha}|n-m|} - iA_4 \underbrace{k_{f\alpha*}}_{5b} e^{-ik_{f\alpha*}|n-m|} + B_1 \underbrace{k_{f\alpha}}_{5d} e^{k_{f\alpha}|n-m|} + iB_3 \underbrace{k_{f\alpha*}}_{5e} e^{ik_{f\alpha*}|n-m|} + C_2 \underbrace{k_{f\beta}}_{5g} + iC_4 \underbrace{k_{f\beta*}}_{5h} \right]\!\right]$$

Equation 5-5

VI. Continuity of angular displacement/equal gradient, at $\boldsymbol{x = m}$

$$\frac{\partial W_\alpha}{\partial x} \quad = \quad \frac{\partial W_\gamma}{\partial x}$$

$$k_{f\alpha}\{-A_2 + B_1\} + k_{f\alpha*}\{-\,iA_4 + iB_3\} \quad = \quad k_{f\gamma}(D_1 + \,iD_3)$$

$$0 \;=\; -A_2 \underbrace{k_{f\alpha}}_{6a} - \;iA_4 \underbrace{k_{f\alpha*}}_{6b} + B_1 \underbrace{k_{f\alpha}}_{6d} + \;iB_3 \underbrace{k_{f\alpha*}}_{6e} - D_1 \underbrace{k_{f\gamma}}_{6j} - iD_3 \underbrace{k_{f\gamma*}}_{6k}$$

Equation 5-6

VII. Equilibrium of bending moment (joint), at $\boldsymbol{x = n}$

$$E_1 I_1 \frac{\partial^2 W_\alpha}{\partial x^2} \quad = \quad E_2 I_2 \frac{\partial^2 W_\beta}{\partial x^2}$$

$$\left(k_{f\alpha}^2\right)\left(\,B_1 e^{k_{f\alpha}|n-m|} - \;B_3 e^{ik_{f\alpha*}|n-m|} - A_4 e^{-ik_{f\alpha*}|n-m|} + \;A_2 e^{-k_{f\alpha}|n-m|}\right)$$

$$= \quad \left(k_{f\beta}^2\right)(C_2 - \,C_4)$$

$$0 \;=\; A_2 \underbrace{\left(k_{f\alpha}^2\right)}_{7a} e^{-k_{f\alpha}|n-m|} + A_4 \underbrace{\left(-k_{f\alpha*}^2\right)}_{7b} e^{-ik_{f\alpha*}|n-m|} + B_1 \underbrace{\left(k_{f\alpha}^2\right)}_{7d} e^{k_{f\alpha}|n-m|}$$

$$+ B_3 \underbrace{\left(-k_{f\alpha*}^2\right)}_{7e} e^{ik_{f\alpha*}|n-m|} + C_2 \underbrace{\left(-k_{f\beta}^2\right)}_{7g} + C_4 \underbrace{\left(k_{f\beta*}^2\right)}_{7h}$$

Equation 5-7

VIII. Equilibrium of bending moment, at $\boldsymbol{x = m}$

$$E_1 I_1 \frac{\partial^2 W_\alpha}{\partial x^2} \quad = \quad E_1 I_1 \frac{\partial^2 W_\gamma}{\partial x^2}$$

$$\left(k_{f\alpha}^2\right)(\,B_1 - \,B_3 - A_4 + \,A_2) \quad = \quad \left(k_{f\gamma}^2\right)(D_1 - \,D_3)$$

$$0 \;=\; A_2 \underbrace{\left(k_{f\alpha}^2\right)}_{8a} + A_4 \underbrace{\left(-k_{f\alpha*}^2\right)}_{8b} + B_1 \underbrace{\left(k_{f\alpha}^2\right)}_{8d} + B_3 \underbrace{\left(-k_{f\alpha*}^2\right)}_{8e} + D_1 \underbrace{\left(-k_{f\gamma}^2\right)}_{8j} + D_3 \underbrace{\left(k_{f\gamma*}^2\right)}_{8k}$$

Equation 5-8

IX. Equilibrium of compressive force (joint), at $\boldsymbol{x = n}$

$$-E_2 A_2 \frac{\partial U_\beta}{\partial x} + \;E_1 A_1 \frac{\partial U_\alpha}{\partial x} \quad = 0$$

$$\left(k_{l\beta}\right)(iC_L) \;+ (k_{l\alpha})\left(\,iB_L e^{ik_{l\alpha*}|n-m|} - \;iA_L e^{-ik_{l\alpha*}|n-m|}\right) \quad = 0$$

$$0 \quad = A_L \underbrace{\left[-i\left(k_{l\alpha*}\right)\right]}_{9c} e^{-ik_{l\alpha*}|n-m|} + B_L \underbrace{\left[i\left(k_{l\alpha*}\right)\right]}_{9f} e^{ik_{l\alpha*}|n-m|} + C_L \underbrace{\left[i\left(k_{l\beta*}\right)\right]}_{9i}$$

Equation 5-9

X. Equilibrium of compressive force, at $\boldsymbol{x = m}$

$$E_1 A_1 \frac{\partial U_\gamma}{\partial x} - \;E_1 A_1 \frac{\partial U_\alpha}{\partial x} \quad = \;F_l$$

$$\left(k_{l\gamma}\right)(iD_L) \;\; - (k_{l\alpha})(\,iB_L - \;iA_L) \;\; = \frac{F_l}{E_1 A_1}$$

$$\frac{F_l}{E_1 A_1} = A_L \underbrace{[i(k_{l\alpha *})]}_{10c} + B_L \underbrace{[-i(k_{l\alpha *})]}_{10f} + D_L \underbrace{[i(k_{l\gamma *})]}_{10l}$$

Equation 5-10

XI. Equilibrium of shear force (joint), at $\boldsymbol{x = n}$

$$-E_1 I_1 \frac{\partial^3 W_\alpha}{\partial x^3} + E_2 I_2 \frac{\partial^3 W_\beta}{\partial x^3} = 0$$

$$-(k_{f\alpha}^3)\left(B_1 e^{k_{f\alpha}|n-m|} - iB_3 e^{ik_{f\alpha *}|n-m|} + iA_4 e^{-ik_{f\alpha *}|n-m|} - A_2 e^{-k_{f\alpha}|n-m|}\right)$$

$$+ (k_{f\beta}^3)(-C_2 + iC_4) = 0$$

$$0 = A_2 \underbrace{(k_{f\alpha}^3)}_{11a} e^{-k_{f\alpha}|n-m|} + A_4 \underbrace{[-i(k_{f\alpha *}^3)]}_{11} e^{-ik_{f\alpha *}|n-m|} + B_1 \underbrace{(-k_{f\alpha}^3)}_{11d} e^{k_{f\alpha}|n-m|}$$

$$+ B_3 \underbrace{[i(k_{f\alpha *}^3)]}_{11} e^{ik_{f\alpha *}|n-m|} + C_2 \underbrace{(-k_{f\beta}^3)}_{11} + C_4 \underbrace{[i(k_{f\beta *}^3)]}_{11h}$$

Equation 5-11

XII. Equilibrium of shear force, at $\boldsymbol{x = m}$

$$E_1 I_1 \frac{\partial^3 W_\alpha}{\partial x^3} - E_1 I_1 \frac{\partial^3 W_\gamma}{\partial x^3} = F_f$$

$$(k_{f\alpha}^3)(B_1 - iB_3 + iA_4 - A_2) - (k_{f\gamma}^3)(D_1 - iD_3) = \frac{F_f}{E_1 I_1}$$

$$\frac{F_f}{E_1 I_1} = A_2 \underbrace{(-k_{f\alpha}^3)}_{12} + A_4 \underbrace{[i(k_{f\alpha *}^3)]}_{12} + B_1 \underbrace{(k_{f\alpha}^3)}_{12d} + B_3 \underbrace{[-i(k_{f\alpha *}^3)]}_{12} + D_1 \underbrace{(-k_{f\gamma}^3)}_{12j}$$

$$+ D_3 \underbrace{[i(k_{f\gamma *}^3)]}_{12}$$

Equation 5-12

5.1.1.1 Results and comments

Rearranging all the 12 equations above as previous preparation, applying the derivation and matrix to MATLAB, with the given input for $F_f = 1N \; and \; F_l = 1N$, the results can be obtained as below. This time, the model need to be derived for additional six (6) governing equation for the force point location of its continuity, force and moments. Hence, justifying the necessity of detail analysis from continuous straight beam and later for the variable angle beam method.

$$\underbrace{\begin{bmatrix} 0 & 0 & \mathbf{1c} & 0 & 0 & \mathbf{1f} & \mathbf{1g} & \mathbf{1h} & \mathbf{1i} & 0 & 0 & 0 \\ 0 & 0 & \mathbf{2c} & 0 & 0 & \mathbf{2f} & 0 & 0 & 0 & 0 & 0 & \mathbf{2l} \\ \mathbf{3a} & \mathbf{3b} & 0 & \mathbf{3d} & \mathbf{3e} & 0 & \mathbf{3g} & \mathbf{3h} & \mathbf{3i} & 0 & 0 & 0 \\ \mathbf{4a} & \mathbf{4b} & 0 & \mathbf{4d} & \mathbf{4e} & 0 & 0 & 0 & 0 & \mathbf{4j} & \mathbf{4k} & 0 \\ \mathbf{5a} & \mathbf{5b} & 0 & \mathbf{5d} & \mathbf{5e} & 0 & \mathbf{5g} & \mathbf{5h} & 0 & 0 & 0 & 0 \\ \mathbf{6a} & \mathbf{6b} & 0 & \mathbf{6d} & \mathbf{6e} & 0 & 0 & 0 & 0 & \mathbf{6j} & \mathbf{6k} & 0 \\ \mathbf{7a} & \mathbf{7b} & \mathbf{7c} & \mathbf{7d} & \mathbf{7e} & \mathbf{7f} & \mathbf{7g} & \mathbf{7h} & \mathbf{7i} & 0 & 0 & 0 \\ \mathbf{8a} & \mathbf{8b} & 0 & \mathbf{8d} & \mathbf{8e} & 0 & 0 & 0 & 0 & \mathbf{8j} & \mathbf{8k} & 0 \\ \mathbf{9a} & \mathbf{9b} & \mathbf{9c} & \mathbf{9d} & \mathbf{9e} & \mathbf{9f} & \mathbf{9g} & \mathbf{9h} & \mathbf{9i} & 0 & 0 & 0 \\ 0 & 0 & \mathbf{10c} & 0 & 0 & \mathbf{10f} & 0 & 0 & 0 & 0 & 0 & \mathbf{10l} \\ \mathbf{11a} & \mathbf{11b} & 0 & \mathbf{11d} & \mathbf{11e} & 0 & \mathbf{11g} & \mathbf{11h} & \mathbf{11i} & 0 & 0 & 0 \\ \mathbf{12a} & \mathbf{12b} & 0 & \mathbf{12d} & \mathbf{12e} & 0 & 0 & 0 & 0 & \mathbf{12j} & \mathbf{12k} & 0 \end{bmatrix}}_{[X]} \underbrace{\begin{bmatrix} A_2 \\ A_4 \\ A_L \\ B_1 \\ B_3 \\ B_L \\ C_2 \\ C_4 \\ C_L \\ D_1 \\ D_3 \\ D_L \end{bmatrix}}_{[Y]} = \underbrace{\begin{bmatrix} 0 \\ 0 \\ 0 \\ 0 \\ 0 \\ 0 \\ 0 \\ 0 \\ 0 \\ \left(\frac{F_l}{E_1 A_1}\right) \\ 0 \\ \left(\frac{F_f}{E_1 I_1}\right) \end{bmatrix}}_{[Z]}$$

Firstly, the analysis considers zero material damping assumption to equate the output against the input power. Damping value can be introduced using a complex modulus *E*, which results in a complex stiffness for the material.

Figure 5-2 shows balanced power transmitted and <u>no reflection</u> due to its physical orientation as continuous beam. It was observed that 50% of Normalised power which was against input of each flexural and longitudinal unit force recorded at both alpha & gamma section. Continuous 50% power was also transmitted to beta section since no damping included for this initial analysis.

Total flexural power (pink line) in Figure 5-2 were equated from gamma section with beta section, to prove output power equalized to input power. Longitudinal power plot would display the comparable results as all section equally receive the input power. This indicates a good agreement to proceed into consideration of material damping for straight beam analysis. Figure 5-3 shows the flexural true power in each section accordingly.

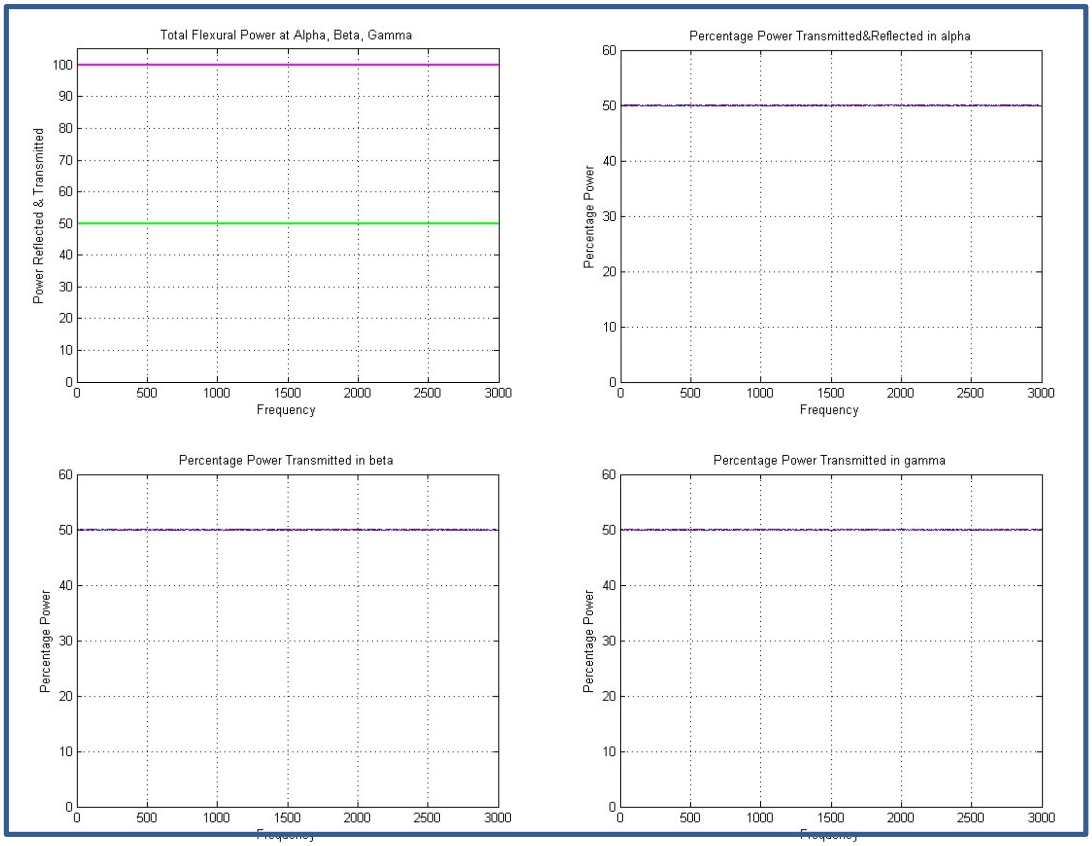

Figure 5-2: **Normalised power for Alpha, Beta and Gamma section of the beam, (top left) Green line – Total power of 50% in Alpha, Beta and Gamma, Pink line – 100% for Beta + Gamma; (top right) Blue and red lines – Power transmitted in Alpha with no reflected (due to no finite section); (bottom left and right) Blue and red lines – Transmitted power for Flexural in Beta and Gamma section.**

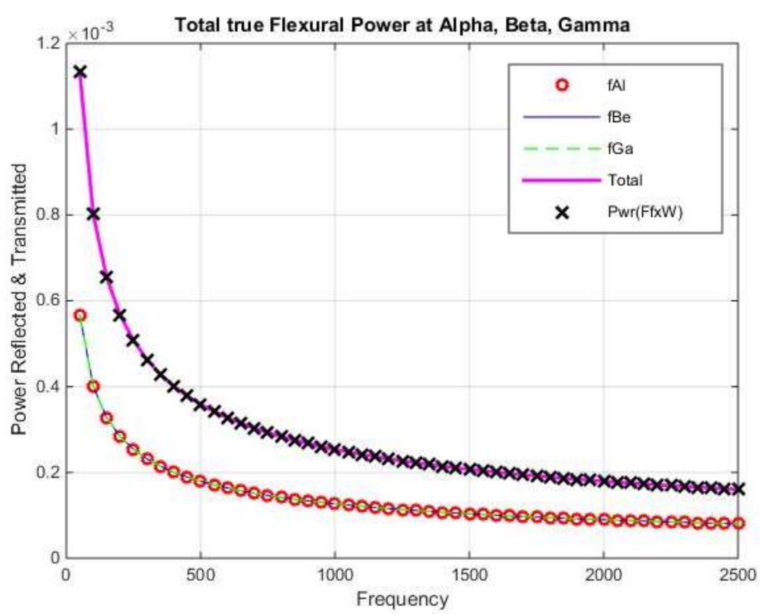

Figure 5-3: **Total true flexural power (Nm/s) in all section, Black 'X' – Input power (force x velocity), Green dotted line – flex power in Gamma, Blue line –Beta power (red 'O' of Alpha power overlapped with blue line), Pink line – Total for Gamma + Beta**

Figure 5-4 shows the longitudinal true power for all section of alpha, beta and gamma. These true power results from initial 1N force initiated for both flexural and longitudinal direction for the unit of Nm/s, as from Equation 3-26 and Equation 3-34, while using material from section 4.2. Power in flexural were noted in 10^{-3} while longitudinal in the range of 10^{-5}, which very insignificant compared to flexural.

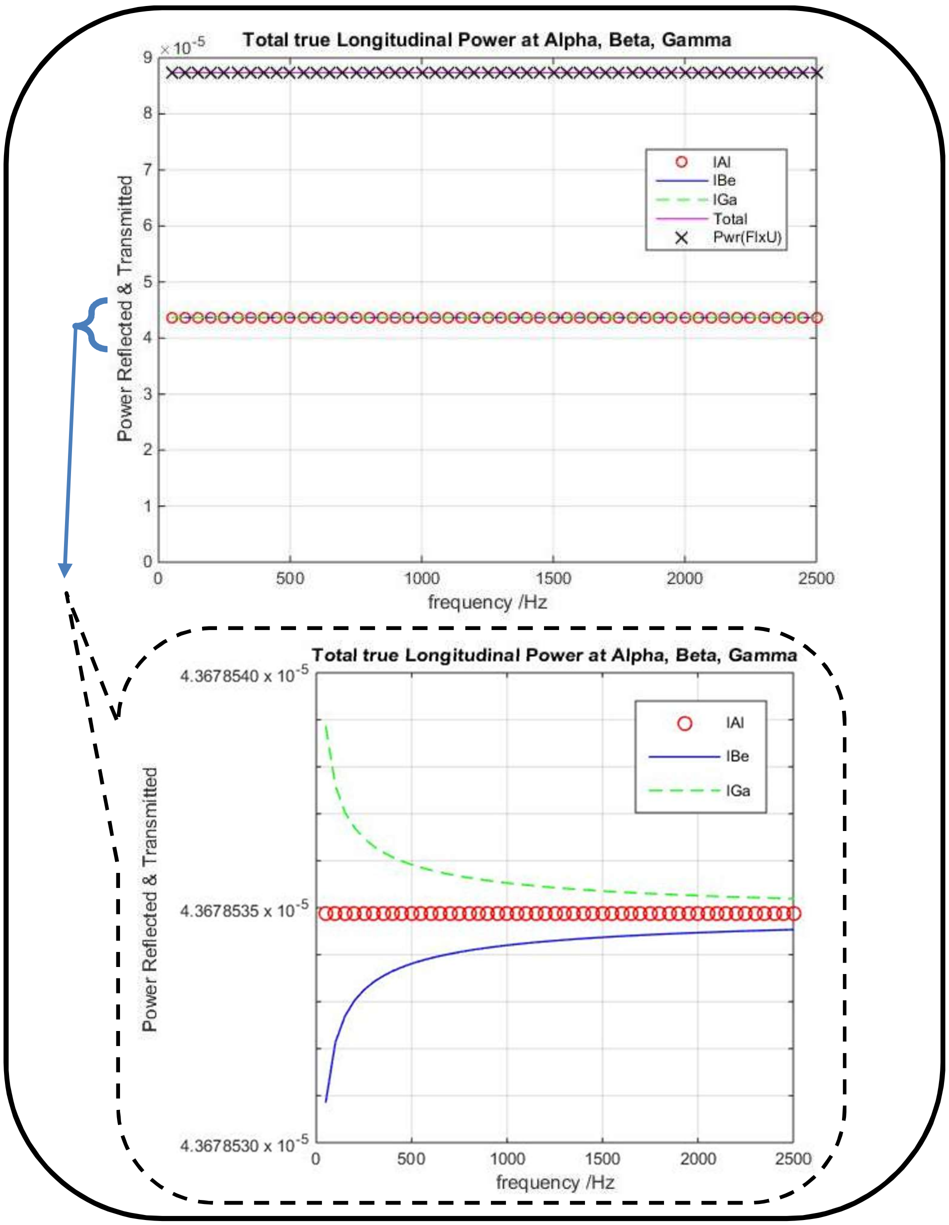

Figure 5-4: Total true longitudinal power (Nm/s) in all section against frequency (with amplified view for power axis), Black 'X' – Input power (force x velocity), Green dotted line – longitudinal power in Gamma, Blue line –Beta power, Red 'O' of Alpha power, Pink line – Total for Gamma + Beta

Secondly referring to Figure 5-5, damping assumes to be in accordance to the Perspex material chosen which around 0.07 (value obtained from measurement) were included into the equation. Transmitted power was observed reduced in alpha and gamma, while the total power would reduce as the frequency increased.

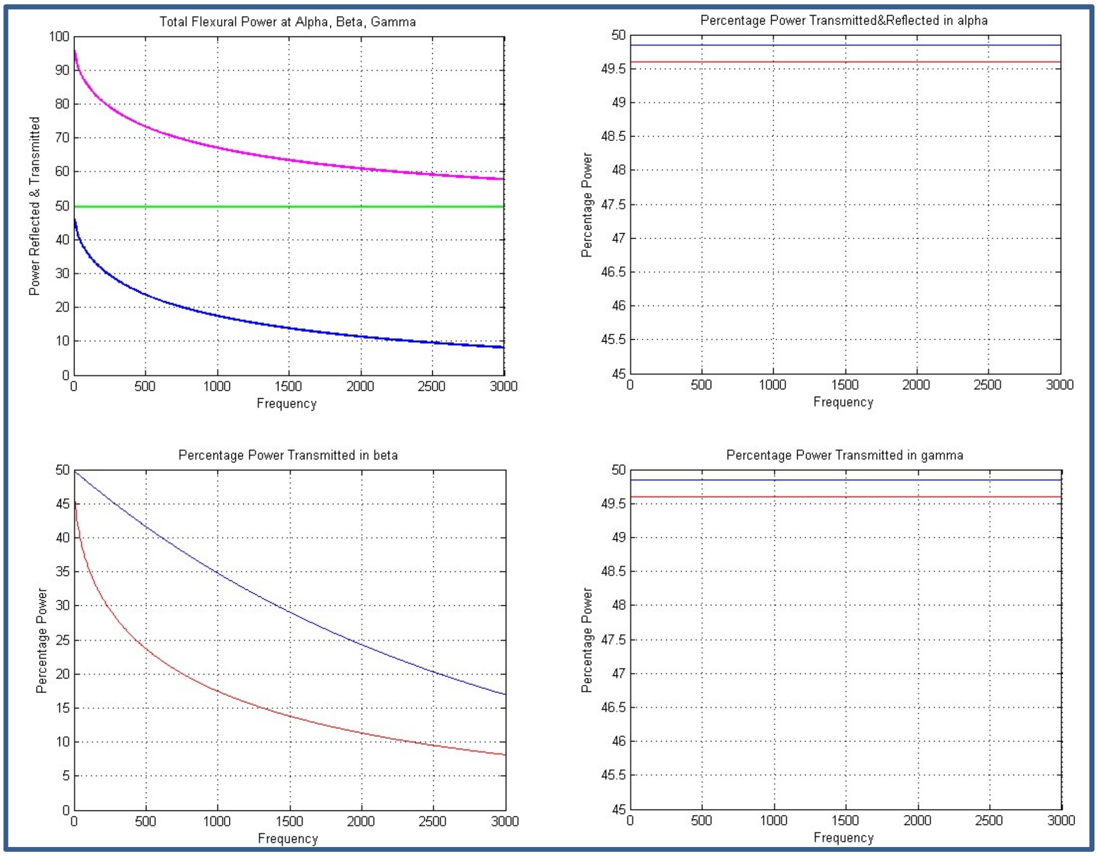

Figure 5-5: Normalised power for Alpha, Beta and Gamma section of the beam, (top left) Green line – Total power of 50% in Alpha and Gamma, Pink line – for Beta + Gamma; Blue line – Power in Beta with reduction due to damping; (top right) Blue and red lines – Reduced power longitudinal (blue) and flexural (red) transmitted in Alpha with no reflected; (bottom left and right) Blue and red lines – Transmitted power longitudinal (blue) and flexural (red) in Beta (due to alpha finite section) and Gamma section.

Figure 5-5 shows the effect of material damping to reduction of power with increase in frequency in beta section. This was due to the finite section of alpha which a length specified. Figure 5-6 indicates the reduced power level for alpha and gamma section (red line overlay green line of gamma) and exponentially decayed power in beta with increase of frequency due to material damping from finite section alpha, for total of flexural and longitudinal power. Damping was agreed affecting flexural power more than the longitudinal power.

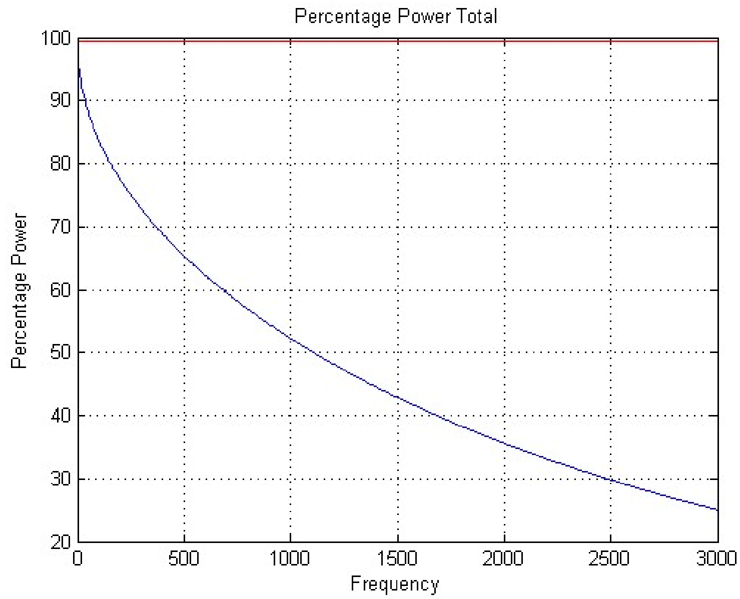

Figure 5-6: Normalised power at Alpha and Gamma (red line overlapped with green line) with reduced power at Beta (blue line) section due to material damping.

It was agreed that the numerical findings were in good agreement for both damped and non-damped analysis. The power values obtained for alpha and gamma sections were from force location of right and left of the beam while beta section considered in a distance away to the right of the straight beam.

5.1.2 Semi-infinite Jointed beam with various angle (Variable Joints)

Further analysis is required to examine the model with load or force which represents a real application in engineering as in Figure 5-7. Work in this section would now consider the variable joint to be included at the point of reference ($x = 0$). The solution was derived for 12x12 matrixes where 6 additional terms of continuity, forces and moment equations are considered at the excitation position, x_F.

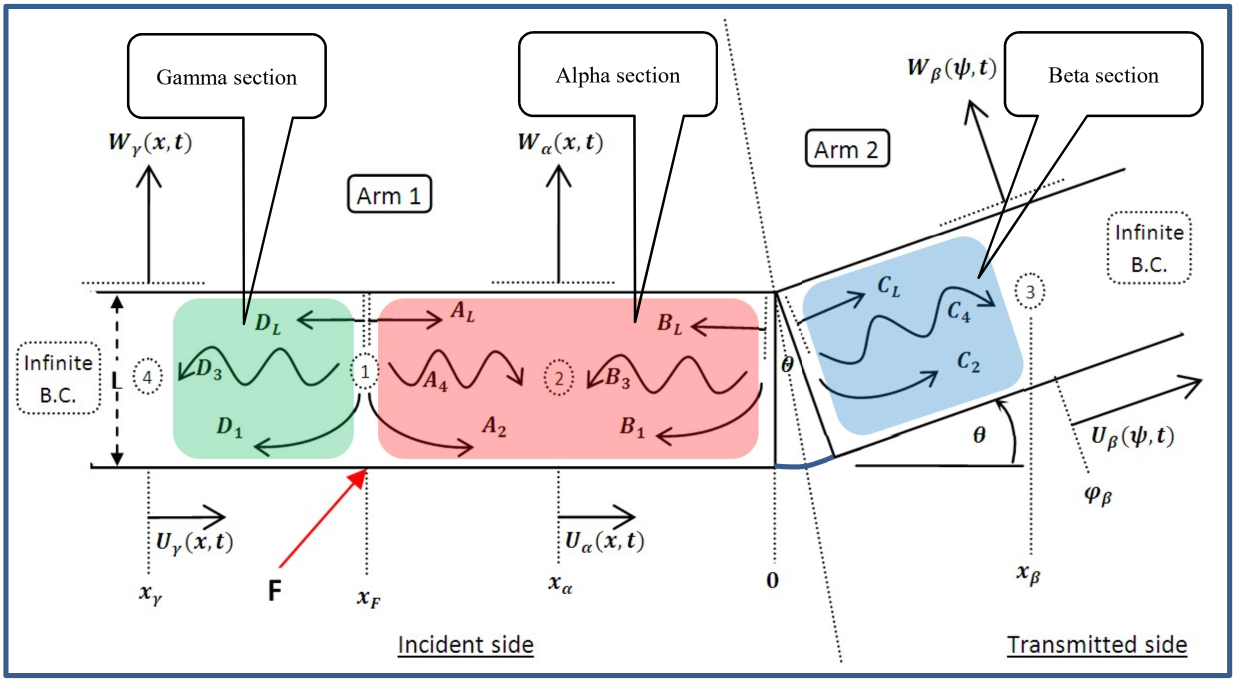

Figure 5-7: Force input to non-collinear beam with various angle joint; for assuming, $x_F = m$, and $0\ (joint) = n$

Result from the continuous beam in previous section shows plausible relationship which agreed with the theoretical behaviour of power transmission and vibration characteristics. This advanced model for non-collinear beam was derived to prepare a closer behaviour between the model, and the experimentation in chapter 6.

The algorithm in this analysis is ultimately to obtain the numerical relationship of forced input to non-collinear beam with various angle joint (variable angle). The joint model form chapter 4 was being included into this derivation to complete the analysis. Finite section of the beam (alpha section) is governed by the distance from force location, (noted as *m* and *n* which refers to x_F and 0 in Figure 5-7) in the positioning set-up.

Rearranging all the 12 equations above as previous preparation, applying the derivation and matrix to MATLAB, with again the given input for $F_f = 1N\ and\ F_l = 1N$, for unity values. Yields the matrix obtaining all 12 waves amplitudes,

$[Y] = inv[X].[Z]$, ***Refer Appendix C-1 and C-2 for equation derivation and MATLAB coding.***

$$
\underbrace{\begin{bmatrix}
0 & 0 & 1c & 0 & 0 & 1f & 1g & 1h & 1i & 0 & 0 & 0 \\
0 & 0 & 2c & 0 & 0 & 2f & 0 & 0 & 0 & 0 & 0 & 2l \\
3a & 3b & 0 & 3d & 3e & 0 & 3g & 3h & 3i & 0 & 0 & 0 \\
4a & 4b & 0 & 4d & 4e & 0 & 0 & 0 & 0 & 4j & 4k & 0 \\
5a & 5b & 0 & 5d & 5e & 0 & 5g & 5h & 0 & 0 & 0 & 0 \\
6a & 6b & 0 & 6d & 6e & 0 & 0 & 0 & 0 & 6j & 6k & 0 \\
7a & 7b & 7c & 7d & 7e & 7f & 7g & 7h & 7i & 0 & 0 & 0 \\
8a & 8b & 0 & 8d & 8e & 0 & 0 & 0 & 0 & 8j & 8k & 0 \\
9a & 9b & 9c & 9d & 9e & 9f & 9g & 9h & 9i & 0 & 0 & 0 \\
0 & 0 & 10c & 0 & 0 & 10f & 0 & 0 & 0 & 0 & 0 & 10l \\
11a & 11b & 0 & 11d & 11e & 0 & 11g & 11h & 11i & 0 & 0 & 0 \\
12a & 12b & 0 & 12d & 12e & 0 & 0 & 0 & 0 & 12j & 12k & 0
\end{bmatrix}}_{[X]}
\underbrace{\begin{bmatrix} A_2 \\ A_4 \\ A_L \\ B_1 \\ B_3 \\ B_L \\ C_2 \\ C_4 \\ C_L \\ D_1 \\ D_3 \\ D_L \end{bmatrix}}_{[Y]}
=
\underbrace{\begin{bmatrix} 0 \\ 0 \\ 0 \\ 0 \\ 0 \\ 0 \\ 0 \\ 0 \\ 0 \\ \frac{F_l}{E_1 A_1} \\ 0 \\ \frac{F_f}{E_1 I_1} \end{bmatrix}}_{[Z]}
$$

The results were plotted for the range of angle and frequency. A check need to be made to ensure the algorithm behaves exactly as previous chapter which earlier only includes impinging waves as input.

5.2 Analysis of results for variable joints

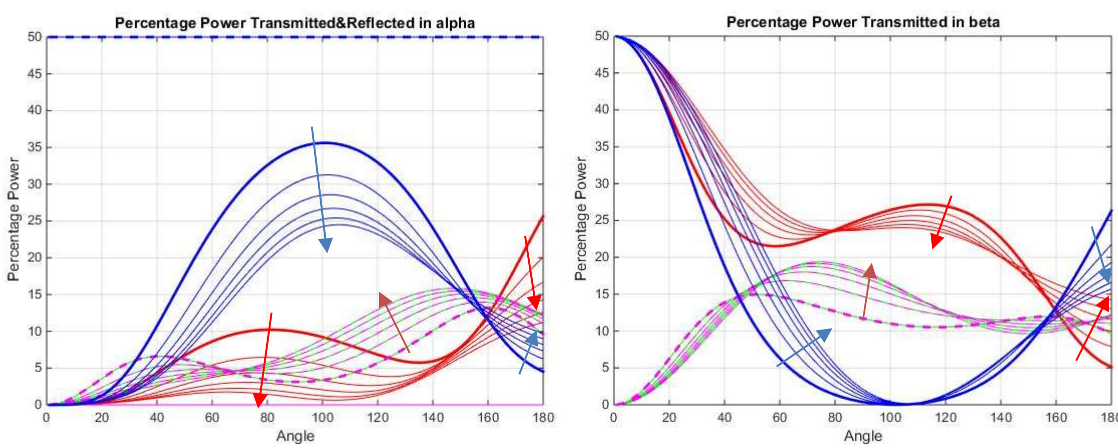

Figure 5-8: Normalised power 500 (thicker lines) to 3000Hz (thinnest lines) from forced input for flexural and longitudinal power (arrows towards increase of frequency).

Similar material properties used as in section 3.6 and 4.2 for the above analysis. Result in Figure 5-8 shows exact power curve which agrees on the algorithm derived for the 12x12 matrix with power balanced being checked. Thicker lines are the lowest frequency (500Hz) and thinner lines are the higher frequency (until 3000Hz). Power in reflected side for longitudinal and flexural were lower as increase of frequency, but the cross-coupling power were increased with the increment of frequency. Transmitted power in alpha were from the input force of waves A_L and A_4. Transmitted power in beta shows the opposite behaviours, except at 80° to 145° of angle for flexure power (also decreased with increase of frequency), 155° to 180° of angle for longitudinal power (also decreased with increase of frequency), and 50° to 130° for cross-coupling power (increased with higher frequency).

Further analysis of particularly at 2500Hz frequency waves plotted as the following figures.

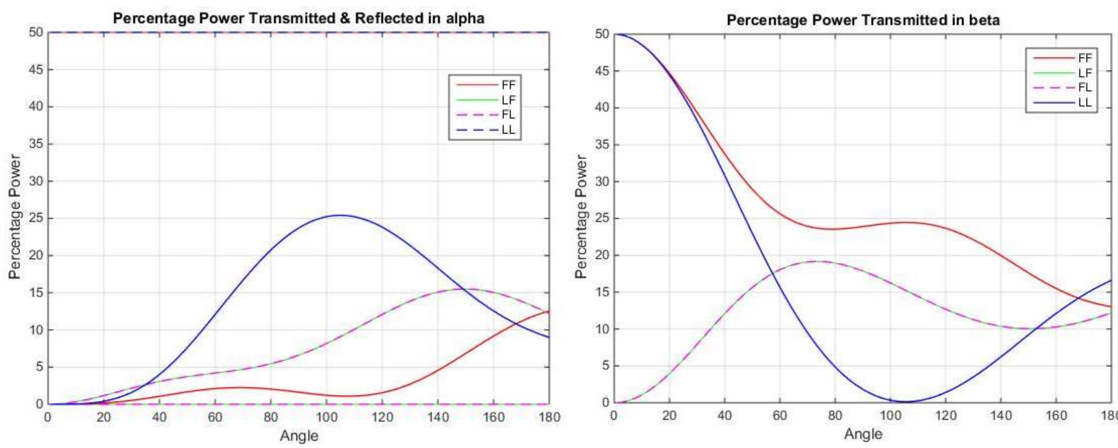

Figure 5-9: Normalised power in Alpha and Beta at 2500Hz from forced input for flexural (red lines), longitudinal power (blue lines) and cross coupling power (pink lines).

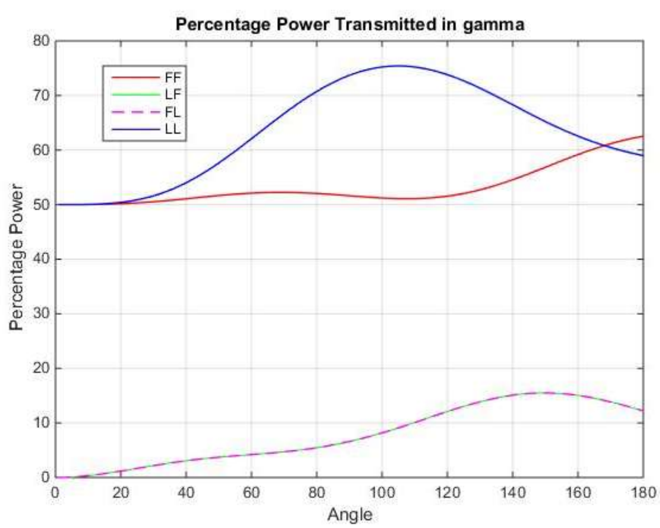

Figure 5-10: Normalised power in Gamma at 2500Hz from forced input for flexural (red lines), longitudinal power (blue lines) and cross coupling power (pink lines).

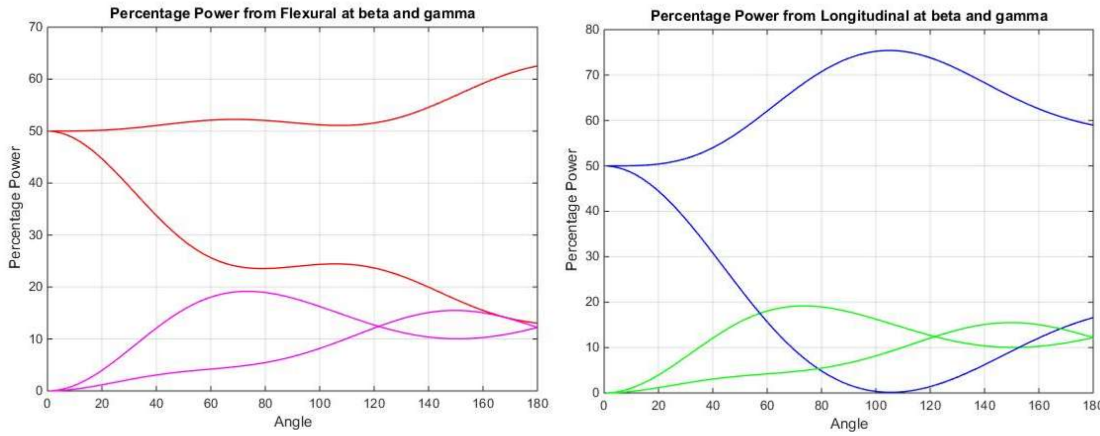

Figure 5-11: Normalised power at 2500Hz from forced input for flexural (red lines), longitudinal power (blue lines) and cross coupling power (pink lines and green lines).

Figure 5-9, Figure 5-10 and Figure 5-11 show agreement of results from amplitude input of joint model in chapter 4 of section 4.2, which was analysed at 2500Hz using the similar Perspex material and dimensions. It was observed that the results agreed with 6x6 matrixes from earlier chapter. This concludes that the equation derivation was successful and authentic results were achieved. The results in this section is with the advantage of examining power in the gamma section as well as the finite section of alpha that have been carefully introduced.

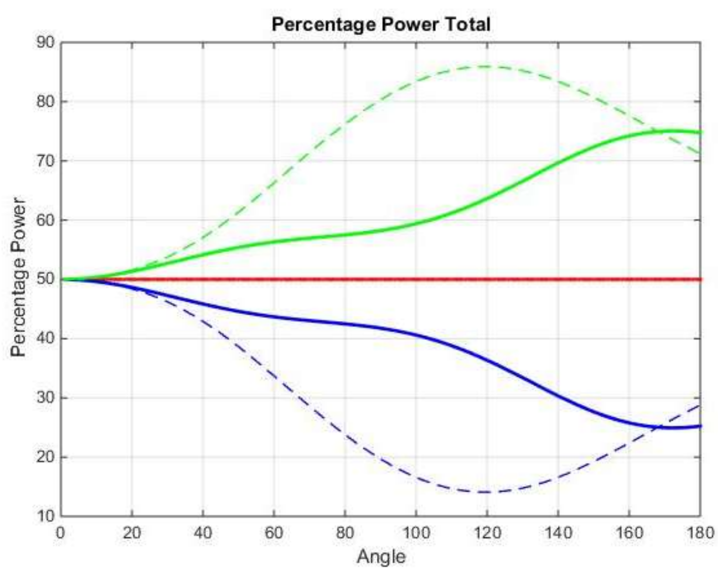

Figure 5-12: Normalised total power at 2500Hz for flexural (thick lines) and longitudinal (dotted lines) of alpha (red), beta (blue) & gamma (green)

Figure 5-12 were the total power for each flexural & longitudinal in all three sections (alpha, beta, gamma) Flexural power in gamma was observed increased at all angle before settled at 75%, while the opposite was observed in alpha and beta. Longitudinal power achieved peak level at about 120^o and reduced to 70% at 180^o angle. Oppositely, the longitudinal power in alpha and beta reduce to about 5% with regards to beam angle until 120^o and regain power up to 30% at 180^o.

Figure 5-13 shows total power trend line by each 3 sections (flexural+longitudinal for each alpha, beta and gamma) and the power balance (black line at 200%). Both Flexural and longitudinal power were given input of 1 Newton in the analysis.

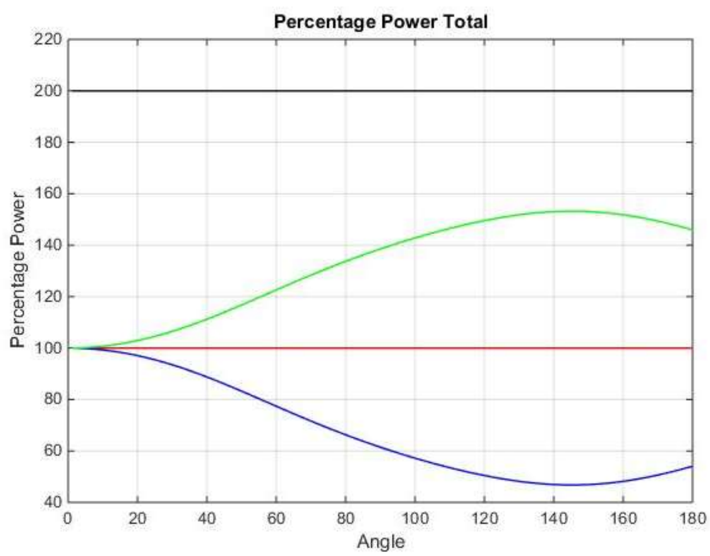

Figure 5-13: Normalised total power at 2500Hz for alpha (red), beta (blue) & gamma (green)

The comparison between the beam with damping and without damping is also essential to understand the true material behaviour as well as to confirm the output obtained for the analysis. Transmitted power in alpha in Figure 5-14 refers to straight lines (thin lines - no damping, and dotted lines -material damping included), shows higher reduction affects for the flexural waves compared to longitudinal (amplified figure in Figure 5-14).

Longitudinal power at 100^o angle were reduced 50% comparing to beam without material damping. Flexure power were also significantly reduced at extreme angles, and the cross-couple power being seen separated (was overlaying each other) with the introducing of material damping.

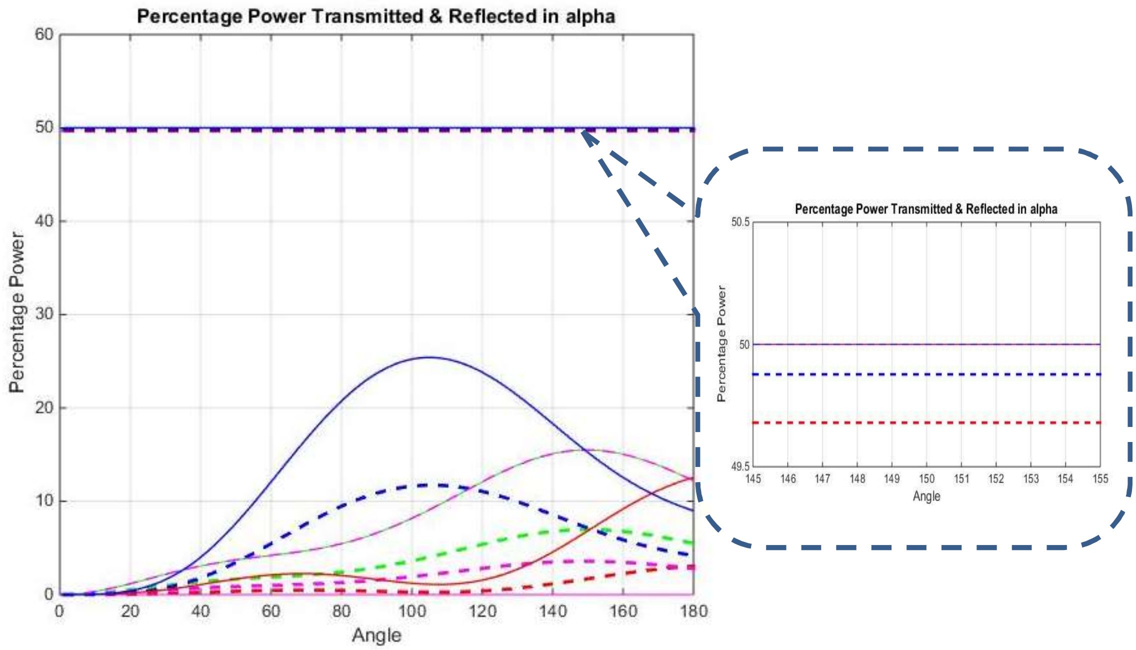

Figure 5-14: Normalised total power transmitted & reflected at 2500Hz in alpha section: Comparison of material with damping (dotted lines) and without damping (thin lines) for flexural (red), longitudinal (blue), flexural to longitudinal-FL (pink) & longitudinal to flexural-LF (green). Close-up of transmitted power in alpha (smaller figure on the right)

Figure 5-15 and Figure 5-16 shows the comparison of the effect with and without damping material considered for beta and gamma section in the numerical analysis. Remaining of 23% and 12% of power seen at straight beam (0^{o} angle) for longitudinal and flexural in beta section. Cross coupling of LF and FL were also seen separated compared to without damping as the damping values suppress each wave types to the respective wavelengths.

In both figures, FL (dotted pink lines) were seen higher than LF (dotted green lines) where maintaining the maximum peak level at about 150^{o} for reflected side (alpha) and at about 70^{o} for transmitted side (beta). The material damping effects were not being examined from previous literature, hence this work has paved a much clearer and detail behaviour to be observed form the reflected and transmitted power.

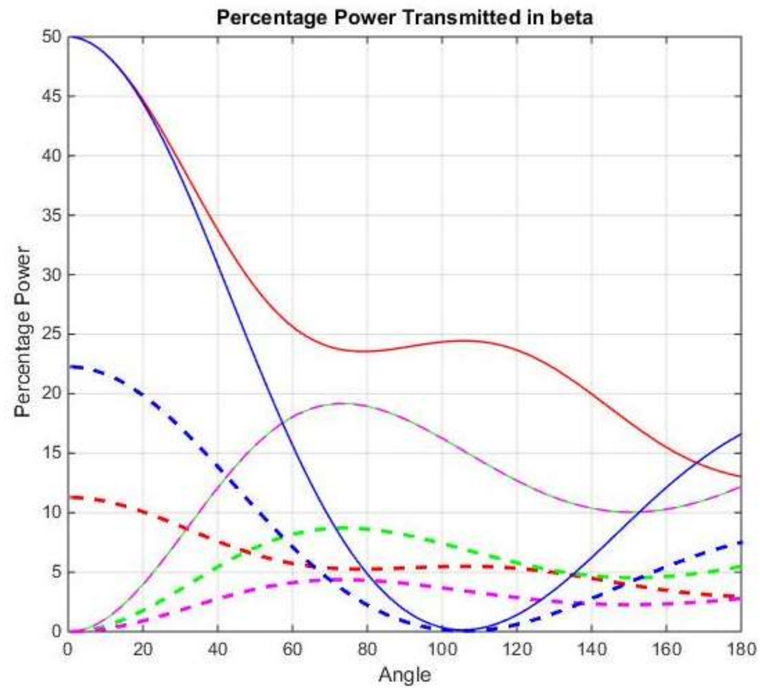

Figure 5-15: Normalised total power transmitted at 2500Hz in beta section: Comparison of material with damping (dotted lines) and without damping (thin lines) for flexural (red), longitudinal (blue), flexural to longitudinal-FL (pink) & longitudinal to flexural-LF (green)

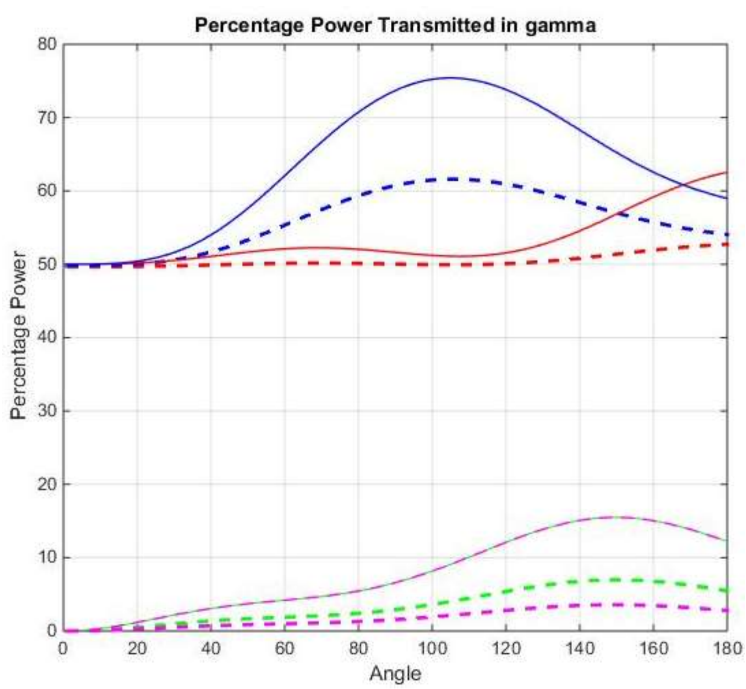

Figure 5-16: Normalised total power transmitted at 2500Hz in gamma section: Comparison of material with damping (dotted lines) and without damping (thin lines) for flexural (red), longitudinal (blue), flexural to longitudinal-FL (pink) & longitudinal to flexural-LF (green)

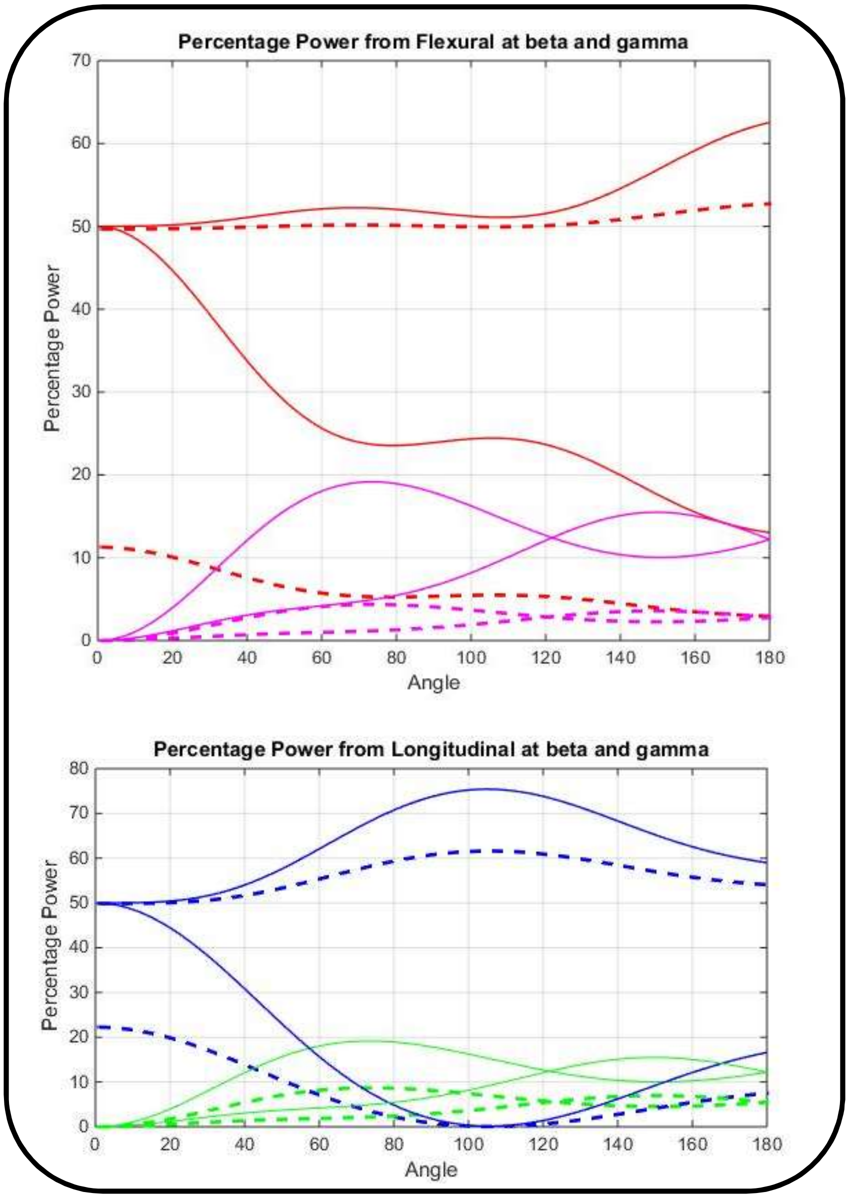

Figure 5-17: Normalised total power reflected & transmitted at 2500Hz in beta & gamma section: Comparison of material with damping (dotted lines) and without damping (thin lines) for flexural (red), longitudinal (blue), flexural to longitudinal-FL (pink) & longitudinal to flexural-LF (green)

Figure 5-17 shows separately of flexural power and longitudinal power in respective section of beta and gamma. Dotted lines represent the beam with material damping and continuous lines represents the beam without material damping being considered.

Figure 5-18 shows total power of flexural and longitudinal with regards to damping values. Reduced power transmitted in gamma section as well in beta section, while alpha section shows higher power (less power reflected) with the effect of damping considered.

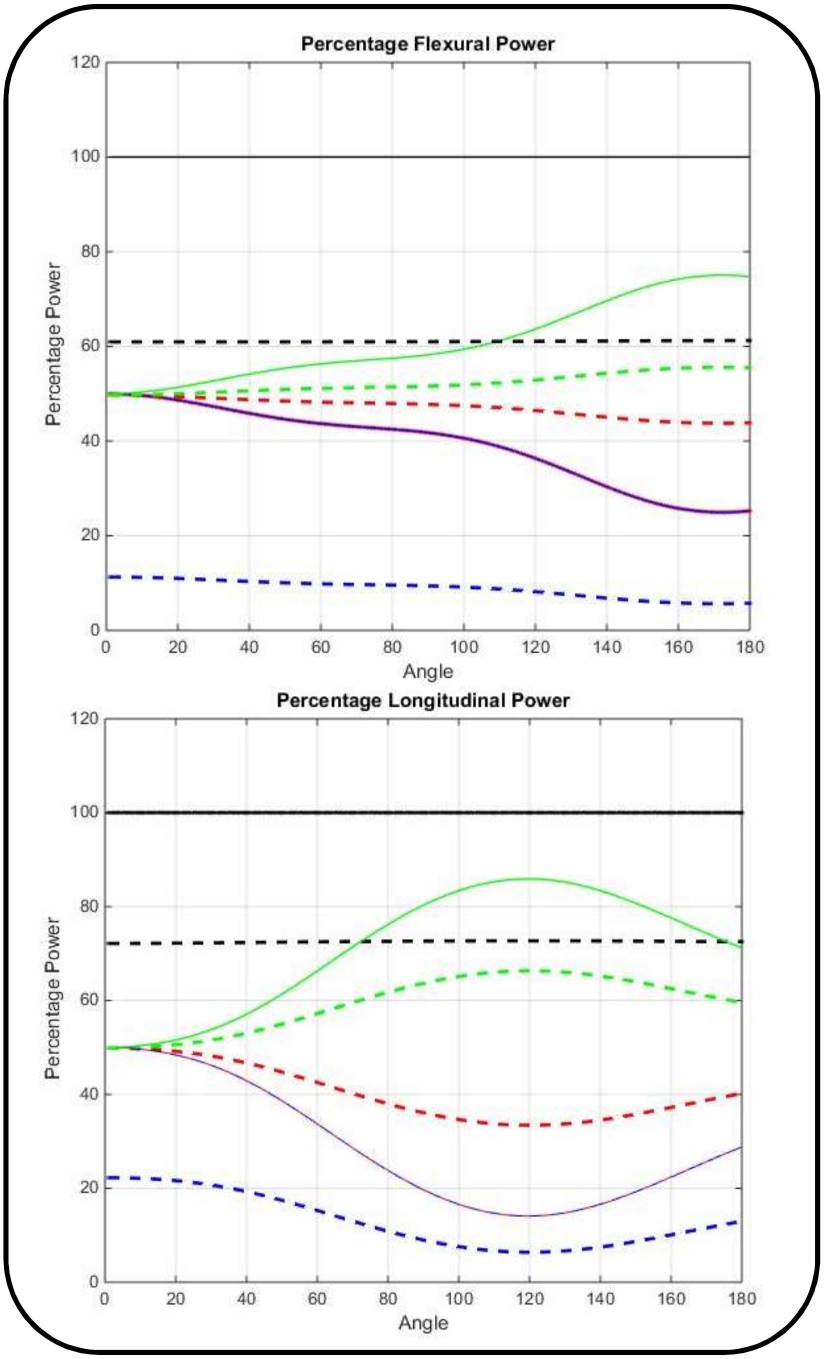

Figure 5-18: Normalised total power transmitted at 2500Hz for flexural and longitudinal: Comparison of material with damping (dotted lines) and without damping (thin lines) for alpha (red), beta (blue) & gamma (green)

Total power was equated for beta+gamma where flexural power obtained about 60% and longitudinal power at about 72% as in Figure 5-18. This indicates that flexural power reduces higher compared to longitudinal power with the material damping included.

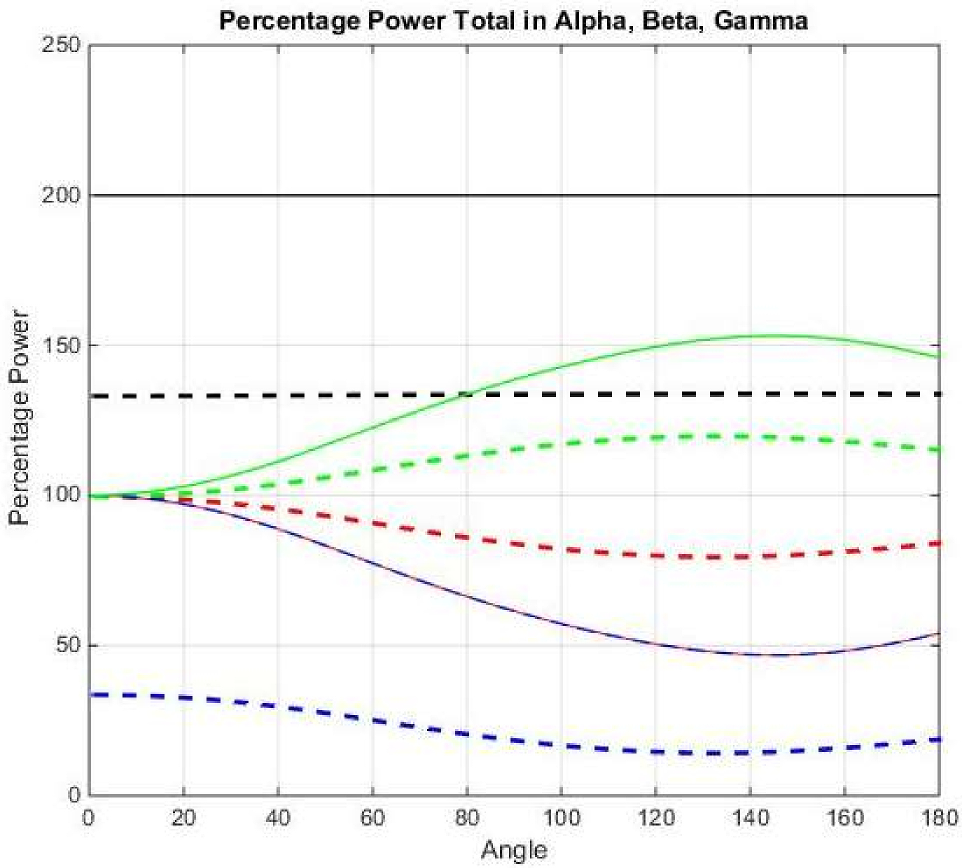

Figure 5-19: Normalised total power transmitted at 2500Hz for Alpha, Beta & Gamma: Comparison of material with damping (dotted lines) and without damping (thin lines) for alpha (red), beta (blue) & gamma (green)

Figure 5-19 concluded the total power from both flexural and longitudinal which in agreement of damping value included in the beam analysis. Total power from both wave types (Figure 5-18 and in Figure 5-19) being equate to the black lines and dotted-black lines representing balanced power measured from the input.

5.3 Concluding remarks

The study of vibration transmission through structural connections have concluded several mathematical results and is moving towards considering agreement in modelling through observation in the experimentation activities. Damping behaviour were observed corresponds to the value chosen for Perspex material which was around 0.07. The results obtained were plotted against the damping value and will be used for the other analysis in this work.

Algorithm for the variable joint have been proven authentic with the initial straight beam analysis, followed by the power balanced analysis for variable joint included. Material damping that have been introduced also have shown realistic behaviours with respect to each wave types for the range of angles examined.

In the finite section Alpha, flexural power (FF) reflected with material damping were marginally increase after 140^o of joint angle, and longitudinal power (LL) reflected were at its maximum for 100^o of joint angle. While higher power transmitted by LF than FL and reaches maximum at 150^o of joint angle. In Beta section for transmitted power, LL would be at 0% for 100^o joint angle, while FF reduces 50% at 60^o of joint angle and continues to drop as the joint angle increases. LF power would be transmitted higher than FL, and both reaches maximum at 70^o of angle. Those were some observation in examining the behaviour of power reflected and transmitted with material damping of Perspex beam. With given other specific material properties and cross-section, behaviours of power reflected and transmitted could be elaborated for the benefits of design and construction requirements.

It is important to take steps of examining areas to be improved for the lumped mass joint as in chapter 3, into the derivation of variable joint which considers realistic angle change for the connected beam in chapter 4, and finally validating beam arrangements of the variable joint with force applications and the inclusion of material damping value of the beam. This chapter moved closer to real application in engineering with all the consideration above before embarking into validation through measurement in following chapter.

Chapter 6: Experimental apparatus and measurement method

6.1 Experiment Set-up

The earlier model of the fixed mass joint which constant parameters of geometry irrespective of angle was inappropriate to be measured physically, hence the developed variable joint mass thus making the measurements directly comparable to theory. This chapter looks at the behaviour of vibration power transmitted and reflected from an angled junction between two beams and the measured data will be compared in subsequent chapters to the estimates of power from the mathematical model derived earlier in chapters 4 and 5.

When considering the joint mass modelled in previous chapters, the possibilities and limitations for the physical model were carefully considered for the measurements. For the rectangular cross section of the beam, the dimension ratio 1:10 were preferred to adhere with Euler-Bernoulli limitations. Several pairs of beam (consisting of left and right of the joint) were prepared. A Perspex type of material was chosen due to the inherent material damping and the speed of the waves in the material. Angled joints have been fabricated as illustrated below in Figure 6-1. The 2-beam system will be used for measurement in the vibration lab for each measurement of angle 0^o, 10^o, 40^o, 60^o, 90^o, 120^o, 140^o, 160^o and 175^o.

Figure 6-1: (from left) sample of an angled joint, 2-beam system for measurement joint at 120^o, Close-up of the angle joint fixed between 2 beams.

Consideration for the support of the structure under test is also an important part of the test set-up. The support conditions should be well defined and experimentally repeatable if the results of the dynamic measurements are to reflect the properties of the structure without undue influence from the support.

Usually either the grounded or free boundary conditions are the two extremes that are most frequently employed. As the nature of this research requires observation of transmission and reflection of vibration power, it is understood that the best applied support would be free boundary condition. It was decided that the two-beam jointed structure of test set-up would be suspended using rubber bands or flexible strings (example as shown in-Figure 6-2).

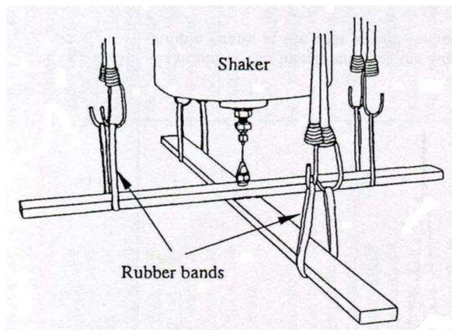

Figure 6-2: Example of rubber band mounting for free boundary condition (McConnell 2008)

However, due to the constraint of work space in the laboratory, test set-up for this work was simplified to 2 flexible strings from 'A' shape metal tube structure. Whole test set-up would be done on floor level as to account repetition and shifting sand boxes for various angle beam orientation.

Both ends of the beam system were buried in box contained dried sand to simulate the measurement assumption of semi-infinite condition, where both end are treated infinite and only waves around the joint will be considered for analysis. The sand boxes also contained tapered foam wedges which were sized on the effective wavelength in the beams as shown in Figure 6-3.

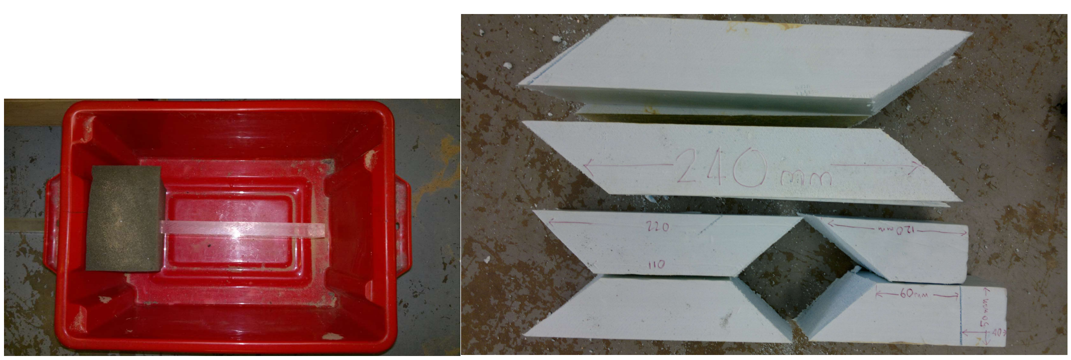

Figure 6-3: Foam wedges sizes used in the sandbox

The method of attachment for accelerometer to the test system was using wax as shown in Figure 6-4 where it is considered as the best option from the frequency response result compared to other type of attachments.

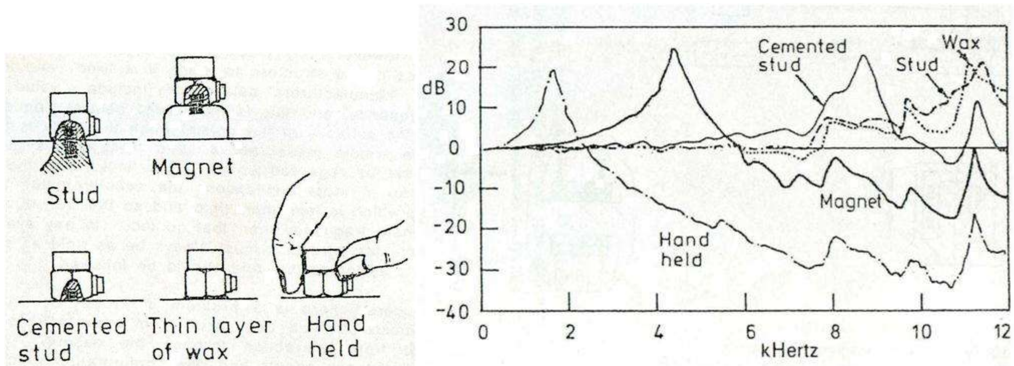

Figure 6-4: Method of attachment and frequency response (McConnell 2008)

6.2 Calibration

The initial condition of all equipment being used for experiments must always be good to avoid unreliable response data and time waste. Equipment such as amplifier, shaker, computer and analyser were easily defined for its condition by calibration date or maintenance schedule. Transducers or any signal sensors' reliability can only be determined by testing them. Calibration is required so that the values measured by the equipment which represent electrical voltage can be correctly translated into units of output interest such as acceleration or force.

Transducer or accelerometer's quoted sensitivities by manufacturers might not be reliable since the sensor may have suffered damage, while still working but have lost the response linearity. Calibration set-up and measurement would be the solution, using a simple rigid structure, such as the steel block and measurements equipment as shown in the Appendix F section.

6.3 Measuring input power to a structure, the reflected & transmitted power

Using Power flow (watts) measurement technique from (J.L.Horner, R.G.White 1990), the calculation will further define best possible input power and transmitted power for the experimentation.

$$\text{Power flow (watts)} = Im\,(G_{a,b}) \times \frac{1}{GDX1\ x\ GDX2\ x\ GS1\ x\ GS2} \times \frac{\sqrt{m_b EI}}{\Delta\omega^2} \times \frac{1}{GCA\ x\ GCB} \times \frac{k\Delta}{\sin(k\Delta)}$$

Where,

$Im\,(G_{a,b})$	=	Imaginary part of cross-spectral density
$GDX/GS/GC$	=	gains for power, display & charge amplifier
k	=	wavenumber
Δ	=	accelerometer spacing
m_b	=	ρA (mass per length)
EI	=	bending stiffness
$\frac{k\Delta}{\sin(k\Delta)}$	=	correction due to finite difference approximation to obtain true power

To measure the input power, from (R. R.J.Pinnington 1981), (C.J.Wu 1995),

$$\langle P \rangle = \frac{1}{2}|F|^2 \frac{Im\{I_{11}\}}{\omega}$$

Equation 6-1

Where the point accelerance of an equivalent infinite structure from the following expression,

$$I_{11} = \frac{\sqrt{\omega}(1+i)}{4\rho A}\sqrt[4]{\frac{\rho A}{EI}}$$

Equation 6-2

Material properties of the beam were as follows: -

E=1.75 x 10^9 N/m^2, length = 1.8m, thickness/depth (d) = 0.02m, breadth (b) = 0.1m, ρ = 1170 kg/m^3

Beam set-up for experimentation with 0.03m depth in sand box for both ends, so each beam was exposed for 1.5m, while force to accelerometer distance and accelerometer distance to termination were 0.3m.

Lower frequency limit due to termination is then calculated from length of beam in sand box and due to force to acceleration midpoint (which are 0.3m x 2). Upper frequency limit was calculated from 5 times of the accelerometer spacing (which is 30mm x 5).

Equation from chapter 3 for flexural wavenumber (Equation 3-19) and wavelength (Equation 3-20) being utilised for the algorithm. Input of white noise were used in the experimentation.

6.4 Set-up and measurements for experiment of 10^o to 175^o angle beam

The beams, each with 1.8 meters in length were jointed together with various angle shapes. Both ends were embedded in a sand box to achieve an anechoic termination for infinite boundary condition as Figure 6-5.

Sets of joints were fabricated ranging from 10^o to 175^o as to ensure enough comparable data to the numerical analysis. Joints were then attached using strong glue and left to dry for every set-up for the measurements. After each measurement, the joints would be cut and clean-up for the next joint to be tested. This cycle of activity often repeated due to issues such as poor adhesive, misaligned beams jointed, cracked at the joints and mishandling of beam causing detachment of the assembly. The work is as summarized in Figure 6-6.

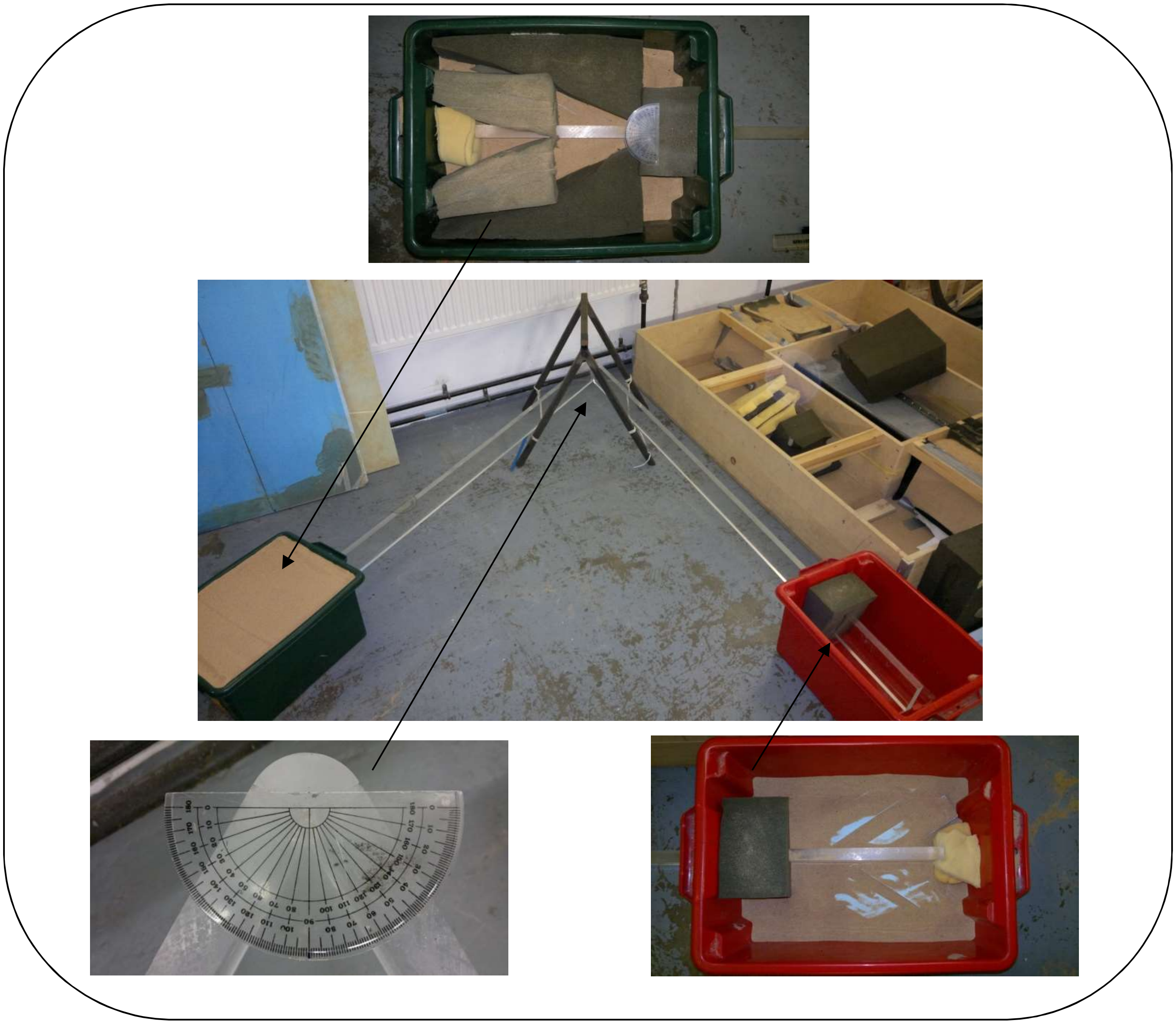

Figure 6-5: Angle beam set-up for infinite boundary condition and free boundary condition at the joint

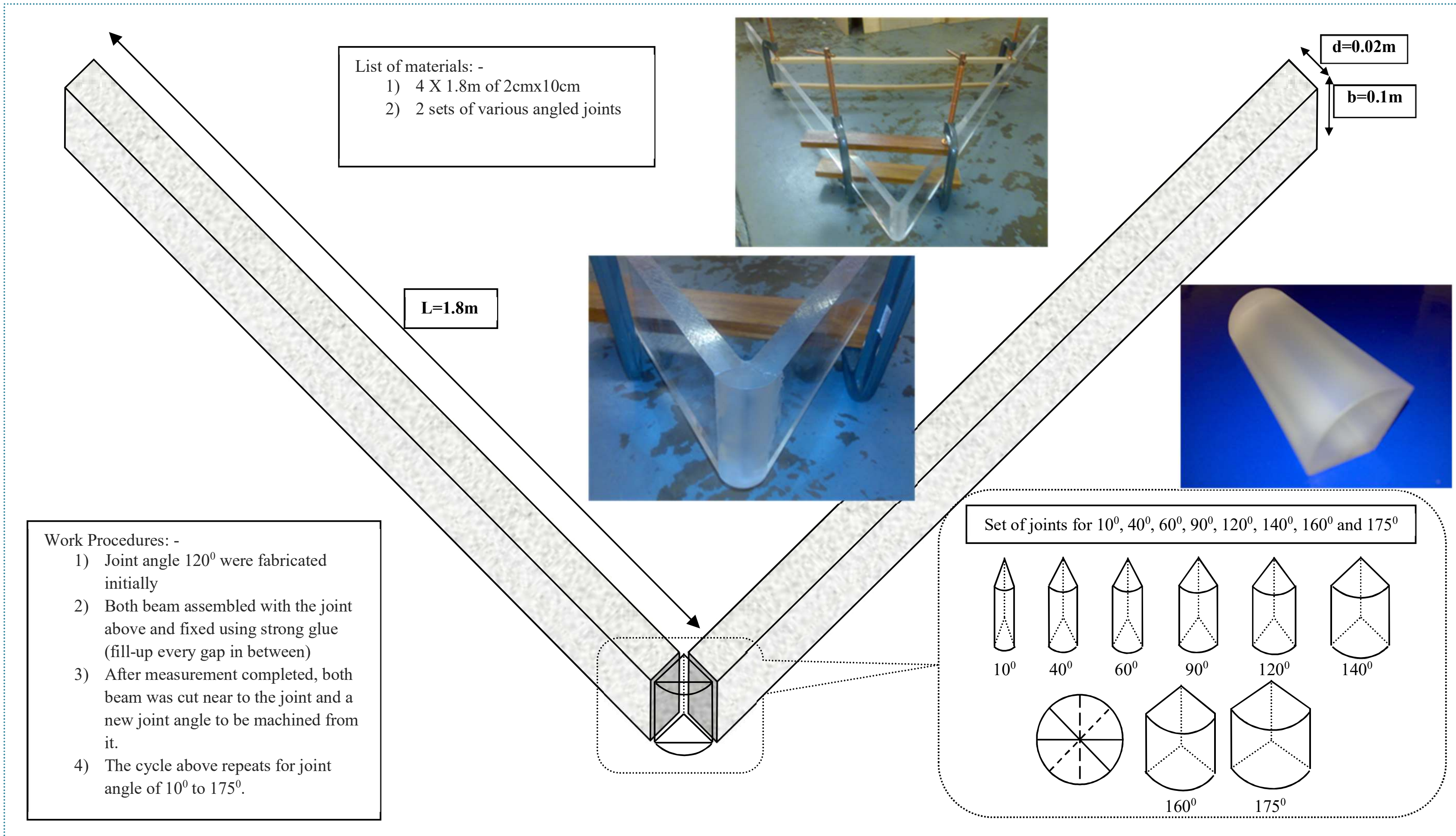

Figure 6-6: Perspex material – joint set-up and dimension

Measurement activities have an initial data confirmation of mobility values (Figure 6-7) that correspond fairly with the modelling characteristic. This will be further improved with consideration of damping and some correction value for the Young modulus and density of the Perspex material.

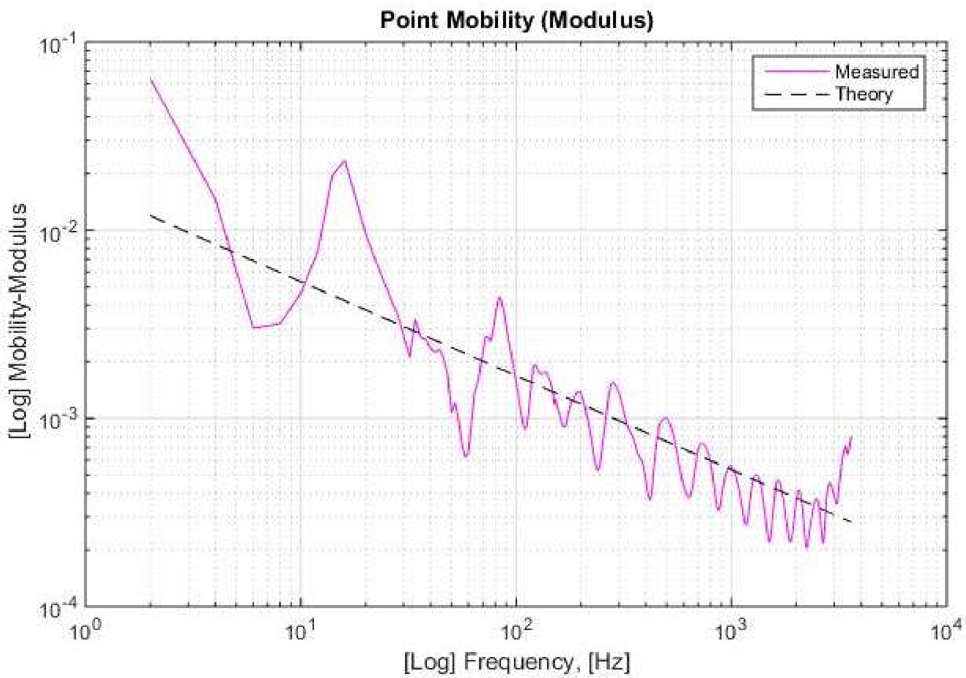

Figure 6-7: Log Mobility-modulus against log frequency

Initially, the wavelength of flexural and longitudinal were calculated for the Perspex beam chosen, to understand the limitations and set-up range required for the measurements. It can be seen from Figure 6-8 that the longitudinal measurements were not possible for the set-up and hence the focus would then be for the flexural wave that ranges from 200Hz to 2000Hz, which having about 17mm down to 7mm wavelength. Frequency limitations will be described in the measurements results section.

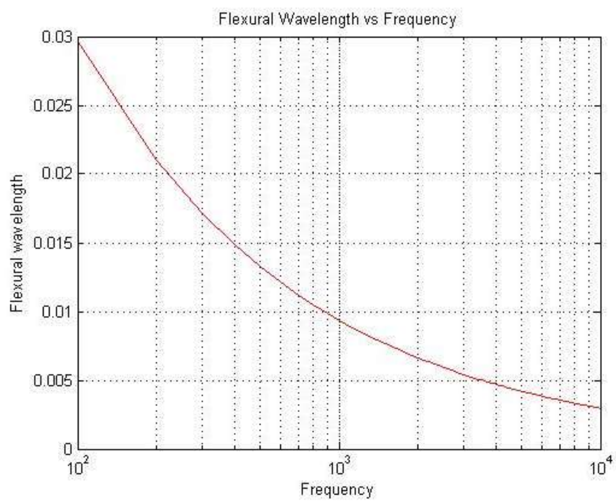

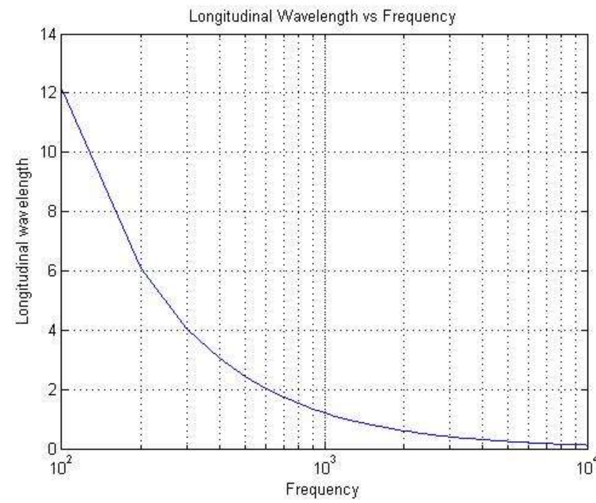

Figure 6-8: Flexural wavelength and longitudinal wavelength for the Perspex beam used

Measurements were performed for the various set-ups of the joint described earlier. Coherence, spectral density and cross spectral were obtained in order to quantify the power transmitted and reflected in the beam. The shaker was placed in location 1 and an accelerometer at location 2 which was 600mm from the joint, as in Figure 6-9. All the sections of alpha, beta and gamma were identified (similar to beam figures in chapter 5) and allocated each for a pair of accelerometers of 5&6 (alpha), 7&8 (beta) and 3&4 (gamma). Beams and variable joints were jointed using regular epoxy glue and left to dry, at least a day before measurements takes place.

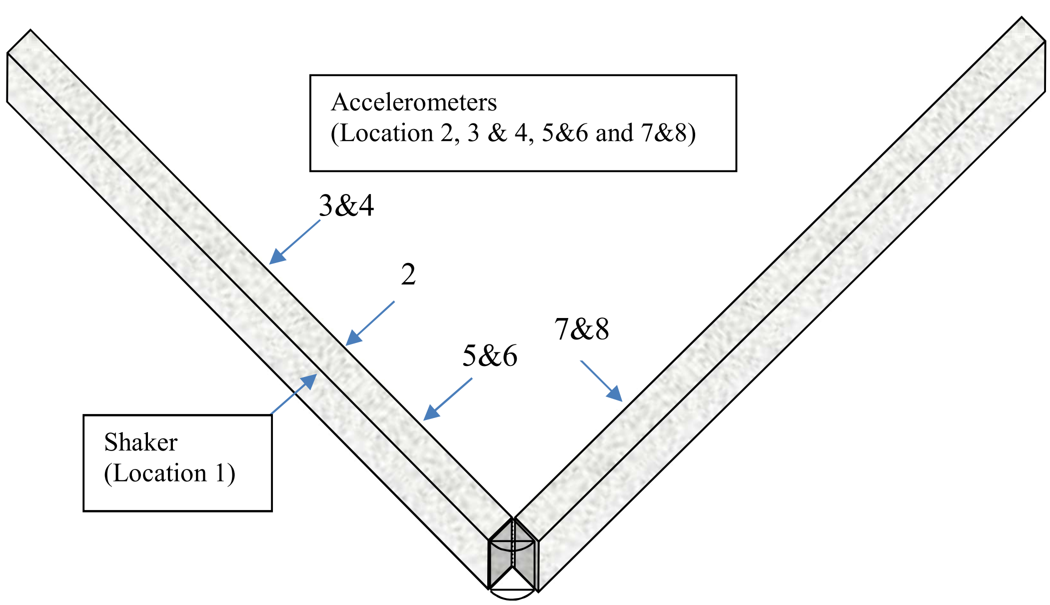

Figure 6-9: Measurement set-up for shaker and accelerometer locations

Pairs of accelerometers were located at locations 5 & 6 which is 300mm away from the joint for alpha section (finite length of reflected section), 7 & 8 for beta section is also 300mm away from the joint (transmitted section of infinite length) and, 3 & 4 for the gamma section (transmitted section of infinite length) is located 300mm away from the shaker. Each of these pairs were placed with 30mm separated distance of accelerometers as shown in Figure 6-10. H_{1_21} of the frequency response for input force at 1 and displacement at 2, as well as other parameters such as spectral density, G_{21} and coherence, Coh_{21} were systematically stored for each setup measurements at each locations of accelerometers

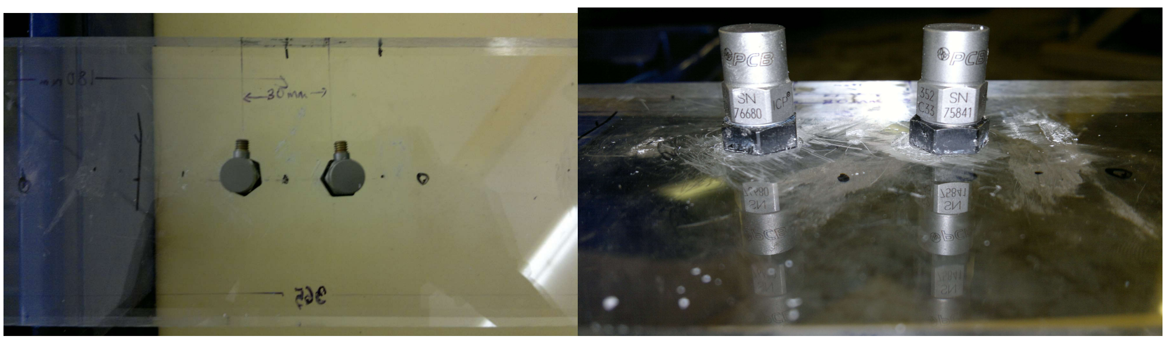

Figure 6-10: Accelerometer spacing for all three pairs in the measurement

6.5 Measurements results

Results from measurements for all the set-up were considered between 250Hz and 2000Hz which considers the lower limits due to half wave length for the sand box and upper limit of the pairing accelerometer 30mm spacing. Shaker excitation was using white noise, coherence between shaker and accelerometers as well as between each pairs of accelerometers, were observed very well achieved in all arrangements of joints and hence all the other data obtained would be agreeable to be analysed (sample of display as in Appendix F). The measurements however had gone through several repetitions and stages of rectifications as well as refinements to achieve the final data collected.

Data display was provided in the appendix section for verifications as well as the MATLAB coding for the measurements in appendix C-3. The measurements results were repeated in various occasions due to issues such as ensuring repeatability, suspected poor calibration initial set-ups, and poor adhesions of joints as well as adhesion of accelerometers which uses bee wax that's affected by ambience temperature and humidity change.

6.6 Comparison with numerical plots

Results from measurements were plotted against the numerical in each display as to compare directly for every joint angle measured experimentally. Lower limit and upper limit of frequency explained before were noted as range observed. Unit for power reflected and transmitted is in N.m/s for all results, or in N.mm/s x 10^{-3}.

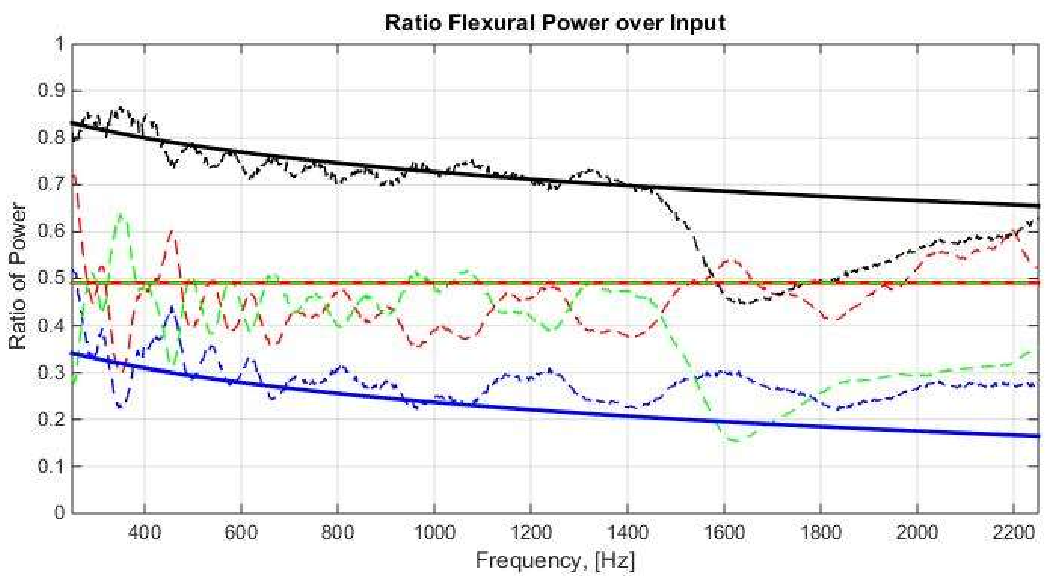

Figure 6-11: Ratio each power over input power against Frequency (*250Hz to 2250Hz*) of Measurement (thin dotted lines) vs. **Numerical** (**bold lines**) for **0°** set-up of beam angle.
Beta (blue), Alpha (red), Gamma (green) and **Total Power**=Gamma+Beta (**black**)

Comparison of result as in Figure 6-11 were from the straight beam or 2-beam jointed to behave as a continuous beam. This is also marked as 0° angle joint arrangement in the analysis. Good agreement observed in the figure for the measurements as well as for the numerical work.

Due to the ‘noise’ in the measurements lines, ratio of power was adopted to monitor a better characteristic of all flexural waves in the respective sections of alpha, beta and gamma. Fluctuations in the power flow quantities were observed increased as the angle of beams expanded. This was due to the finite section of ‘Alpha’ which is in-between the force and the joint. The model is considering the dimension of Alpha section in the programming as exactly in the experimental distance of force to the joint, hence produces the fluctuations in the results.

Figure 6-12 shows a log scale for frequency which starts from 250Hz where lower limit due to half-wavelength for the sand box being removed from the display. Power ratio at alpha and gamma were at 0.5 while it is around 0.4 for the measured result. Result for beta section (blue line) were observed corresponds to the power transmitted with effect of the material damping.

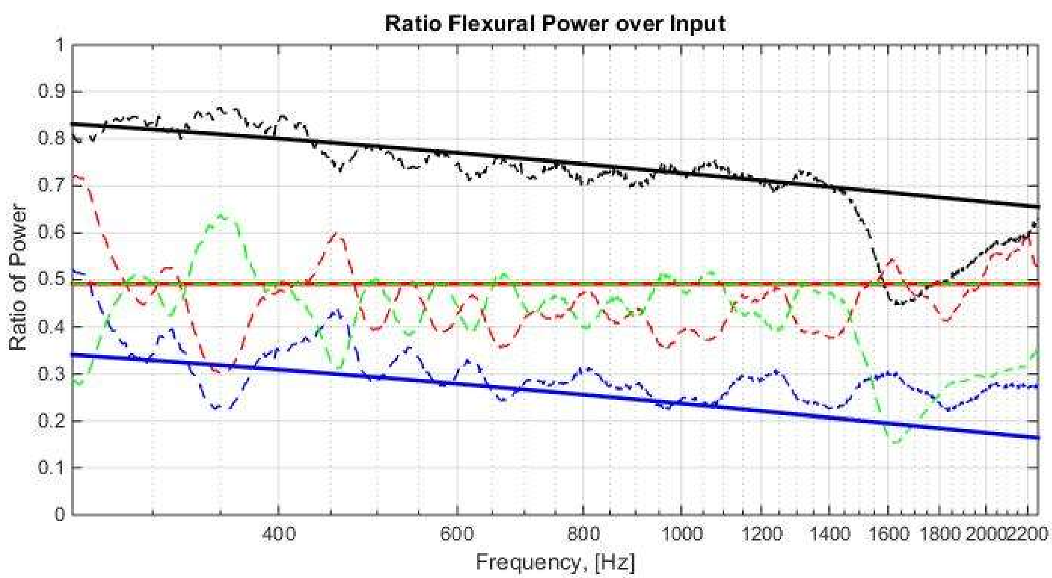

Figure 6-12: Ratio each power over input power against ***Log*** Frequency (*250Hz to 2250Hz*) of Measurement (thin dotted lines) vs. **Numerical** (**bold lines**) for **0º** set-up of beam angle.
Beta (blue), Alpha (red), Gamma (green) and **Total Power**=Gamma+Beta (**black**)

Total power was equated from gamma+beta of the beam for both measurements and the modelling algorithm. The straight beam results for measurement also shows significant noises which suspected from the sandbox anechoic termination. This is noted as weaknesses of this measurement activity as measurement form a 1.8-meter beam (without jointed section) would produce the similar data noises.

Joint angle of 10º as in Figure 6-13 and Figure 6-14 also shows similar relationship especially for transmitted power in beta (blue lines). Transmitted power was reduced to nearly 0.1 ratio at highest frequency compared to the straight beam results.

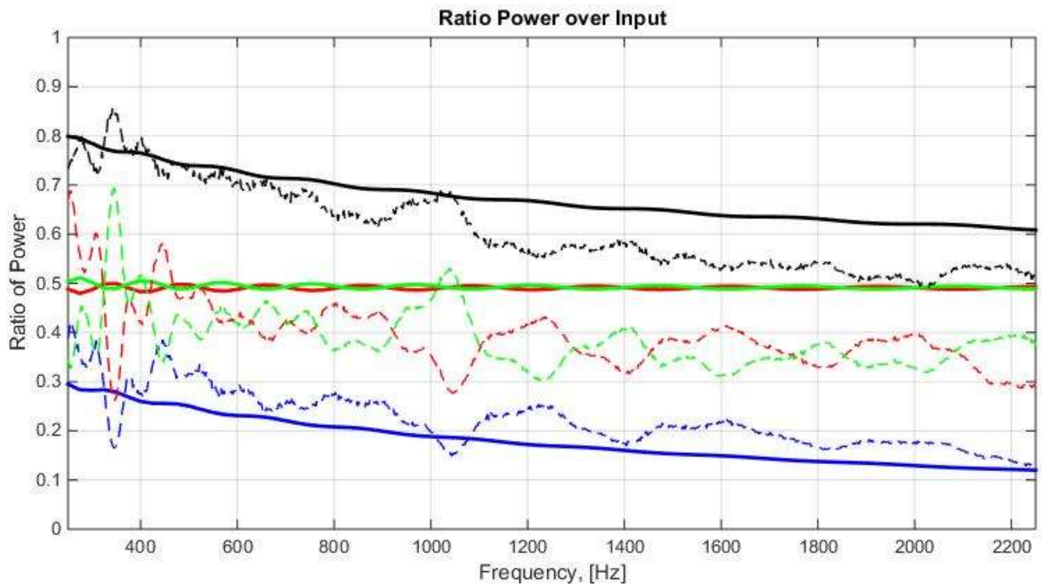

Figure 6-13: Ratio each power over input power against Frequency (*250Hz to 2250Hz*) of Measurement (thin dotted lines) vs. **Numerical** (**bold lines**) for **10º** set-up of beam angle.
Beta (blue), Alpha (red), Gamma (green) and **Total Power**=Gamma+Beta (**black**)

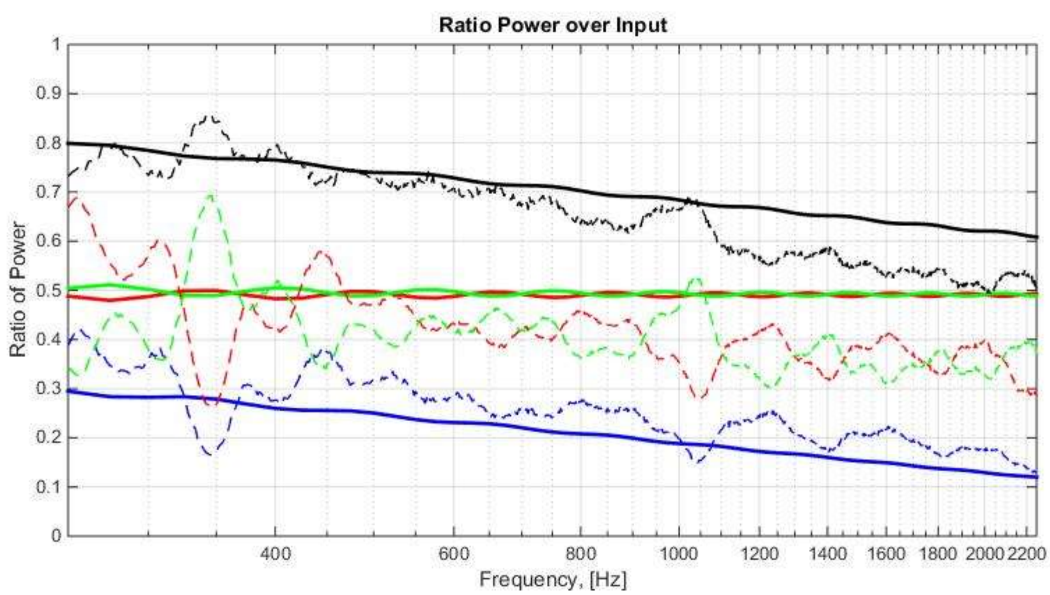

Figure 6-14: Ratio each power over input power against ***Log*** Frequency (*250Hz to 2250Hz*) of Measurement (thin dotted lines) vs. **Numerical** (**bold lines**) for **10º** set-up of beam angle.
Beta (blue), Alpha (red), Gamma (green) and **Total Power**=Gamma+Beta (**black**)

Figure 6-15 and Figure 6-16 for angle of 40° as displayed were in better agreement where resonance from finite section (between force and joint) of alpha starts to be in effect with the angle of joint increased. Numerically for alpha and gamma is around 0.5 power ratio, while in beta section reduces comparing to the 0° angle displayed before.

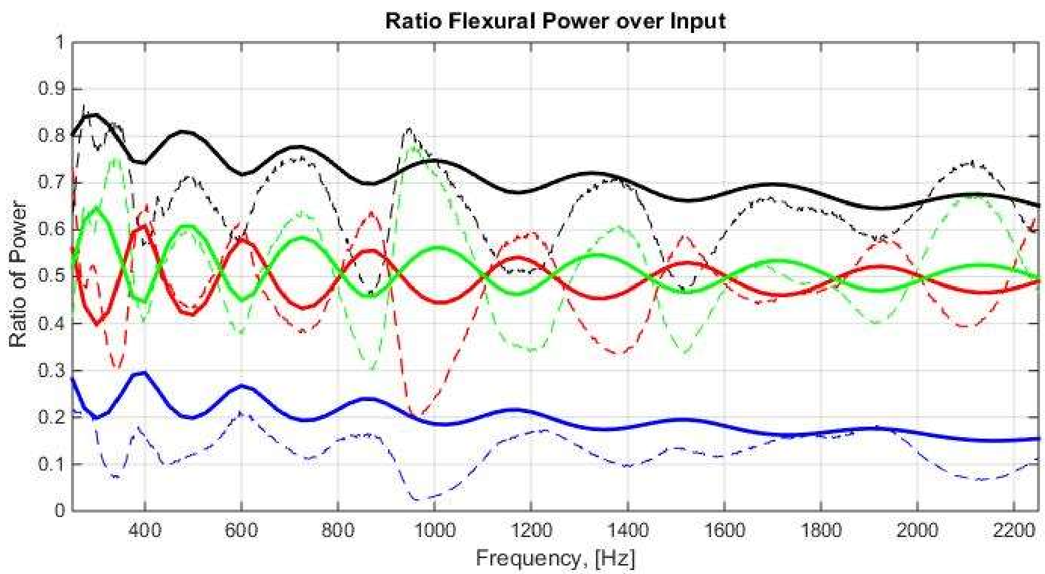

Figure 6-15: Ratio each power over input power against Frequency (*250Hz to 2250Hz*) of Measurement (thin dotted lines) vs. **Numerical** (**bold lines**) for **40°** set-up of beam angle.
Beta (blue), Alpha (red), Gamma (green) and **Total Power**=Gamma+Beta (**black**)

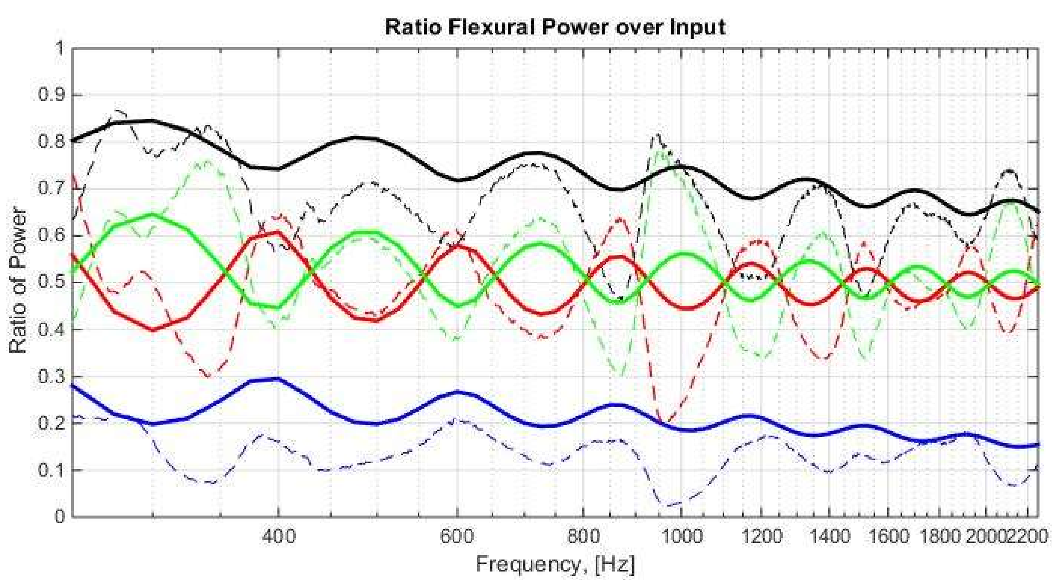

Figure 6-16: Ratio each power over input power against ***Log*** Frequency (*250Hz to 2250Hz*) of Measurement (thin dotted lines) vs. **Numerical** (**bold lines**) for **40°** set-up of beam angle.
Beta (blue), Alpha (red), Gamma (green) and **Total Power**=Gamma+Beta (**black**)

Figure 6-17 and Figure 6-18 and discussed for joint angle of 60°. A close resemblance for the resonance within the frequency range measured to the numerical results. Beta section power were seen lower ratio but with increased amplitudes in this 60° angle joint analysis.

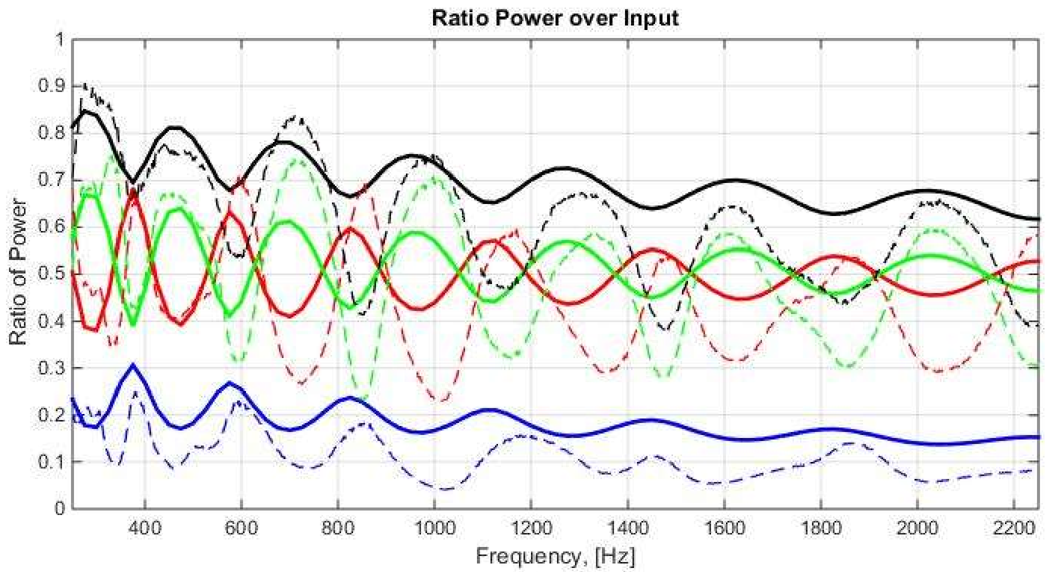

Figure 6-17: Ratio each power over input power against Frequency (*250Hz to 2250Hz*) of Measurement (thin dotted lines) vs. **Numerical** (**bold lines**) for **60°** set-up of beam angle.
Beta (blue), Alpha (red), Gamma (green) and **Total Power**=Gamma+Beta (**black**)

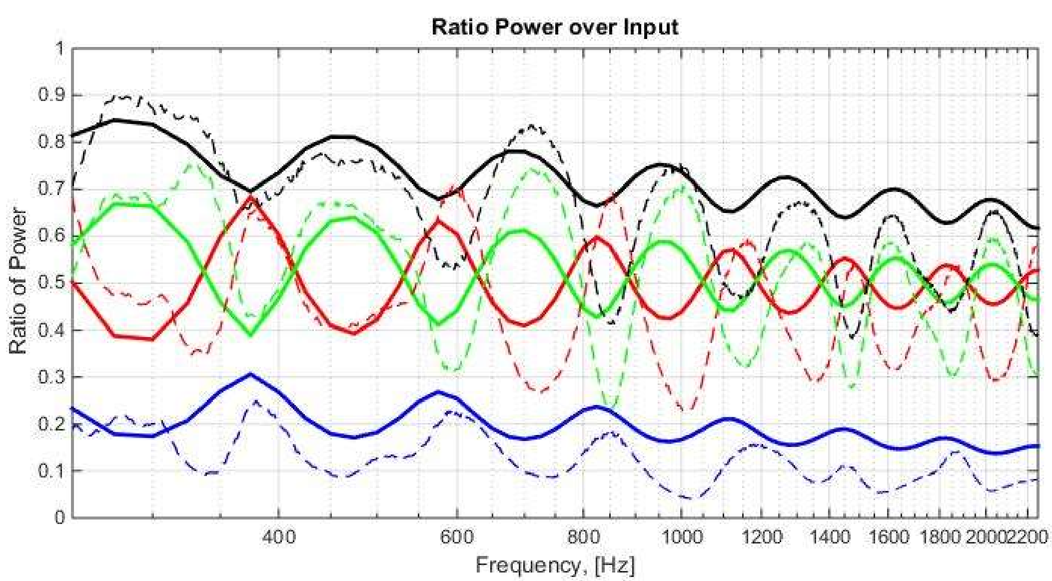

Figure 6-18: Ratio each power over input power against ***Log*** Frequency (*250Hz to 2250Hz*) of Measurement (thin dotted lines) vs. **Numerical** (**bold lines**) for **60°** set-up of beam angle.
Beta (blue), Alpha (red), Gamma (green) and **Total Power**=Gamma+Beta (**black**)

Figure 6-19 and Figure 6-20 shows result of 90º joint angle analysis. Unit of power is at Nm/s as stated earlier and result from ratio of power were observed in fair agreement as well for the interested frequency range.

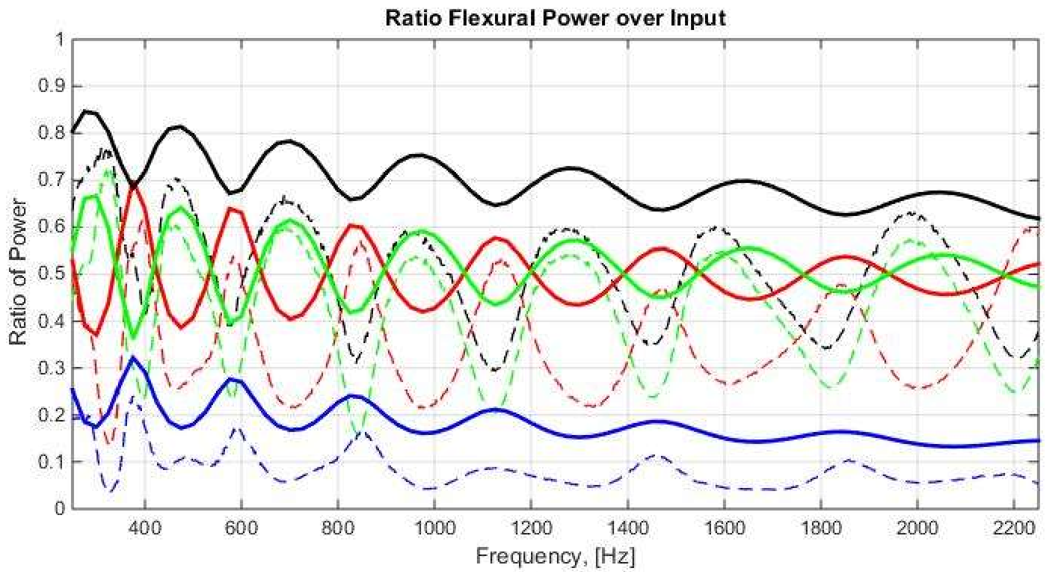

Figure 6-19: Ratio each power over input power against Frequency (*250Hz to 2250Hz*) of Measurement (thin dotted lines) vs. **Numerical** (**bold lines**) for **90º** set-up of beam angle.
Beta (blue), Alpha (red), Gamma (green) and **Total Power**=Gamma+Beta (**black**)

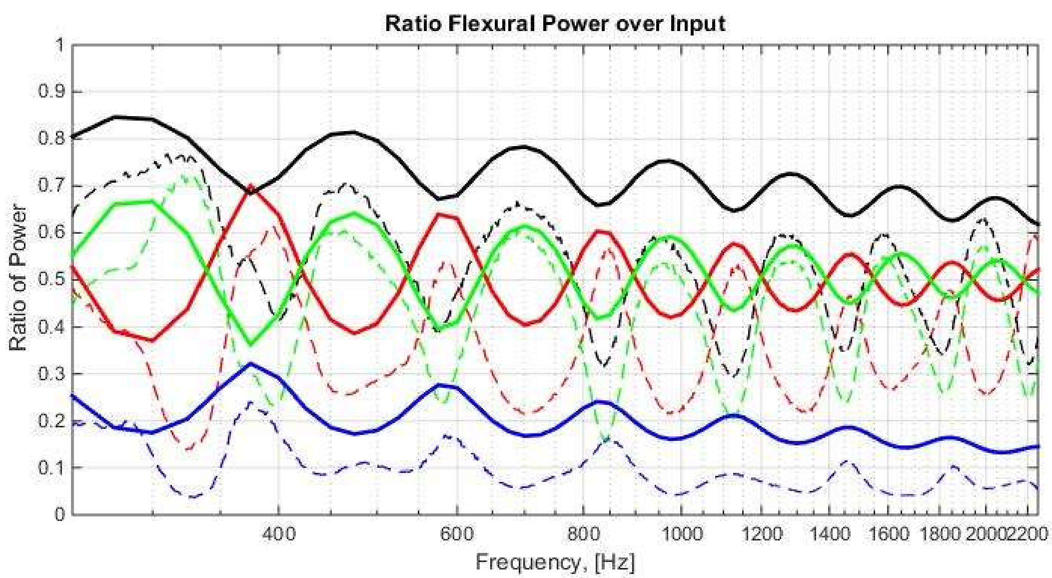

Figure 6-20: Ratio each power over input power against ***Log*** Frequency (*250Hz to 2250Hz*) of Measurement (thin dotted lines) vs. **Numerical** (**bold lines**) for **90º** set-up of beam angle.
Beta (blue), Alpha (red), Gamma (green) and **Total Power**=Gamma+Beta (**black**)

Figure 6-21 and Figure 6-22 displays the result for angle 120º. Amplitudes at lower frequencies were noted higher and this corresponds to the increased angle of joint for the analysis.

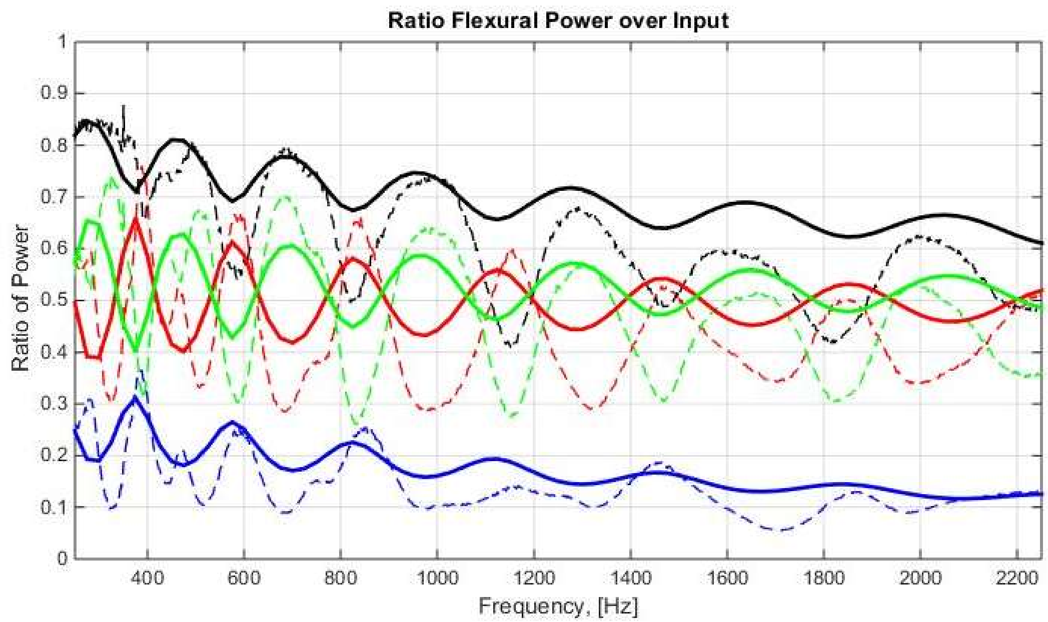

Figure 6-21: Ratio each power over input power against Frequency (*250Hz to 2250Hz*) of Measurement (thin dotted lines) vs. **Numerical** (**bold lines**) for **120º** set-up of beam angle.
Beta (blue), Alpha (red), Gamma (green) and **Total Power**=Gamma+Beta (**black**)

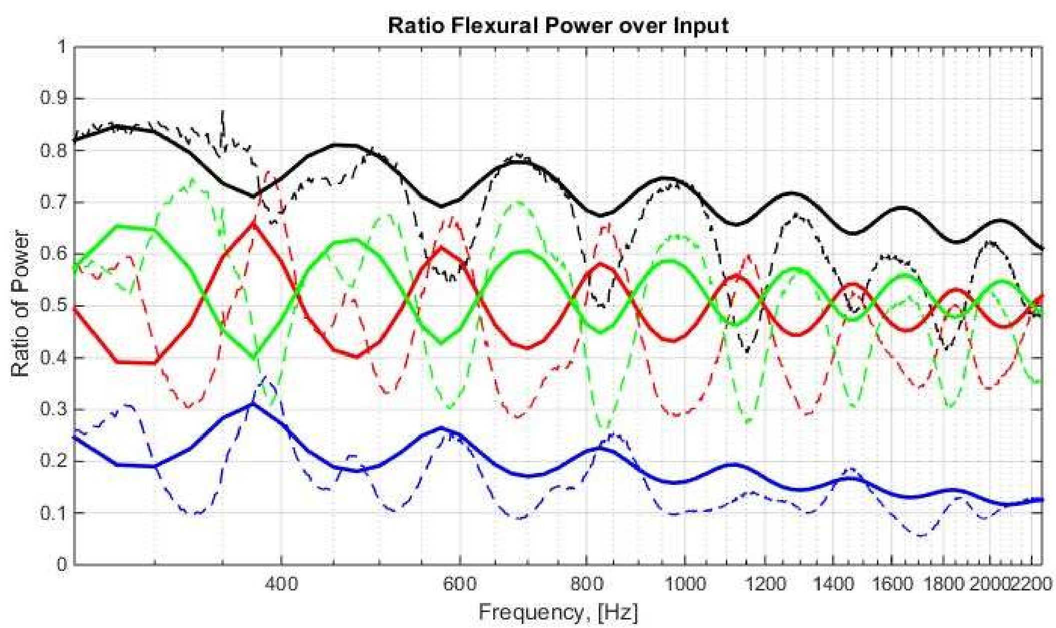

Figure 6-22: Ratio each power over input power against ***Log*** Frequency (*250Hz to 2250Hz*) of Measurement (thin dotted lines) vs. **Numerical** (**bold lines**) for **120º** set-up of beam angle.
Beta (blue), Alpha (red), Gamma (green) and **Total Power**=Gamma+Beta (**black**)

Figure 6-23 and Figure 6-24 successfully compare the measured and numerical results for joint at angle 140º. Power ratio were observed lower than 0.1 at higher frequencies and amplitudes were noted reduced at this angle of joint.

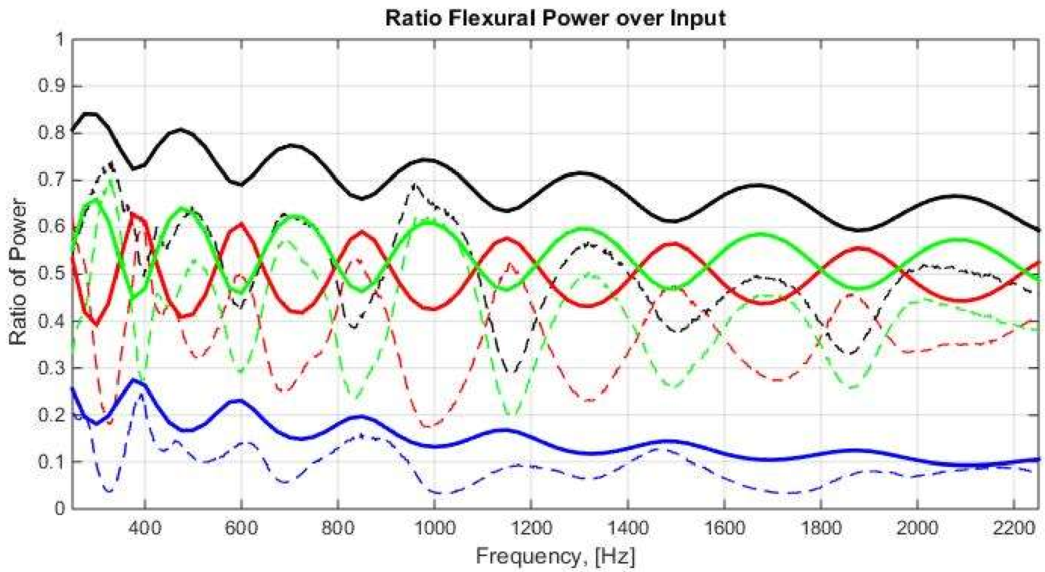

Figure 6-23: Ratio each power over input power against Frequency (*250Hz to 2250Hz*) of Measurement (thin dotted lines) vs. **Numerical** (**bold lines**) for **140º** set-up of beam angle.
Beta (blue), Alpha (red), Gamma (green) and **Total Power**=Gamma+Beta (**black**)

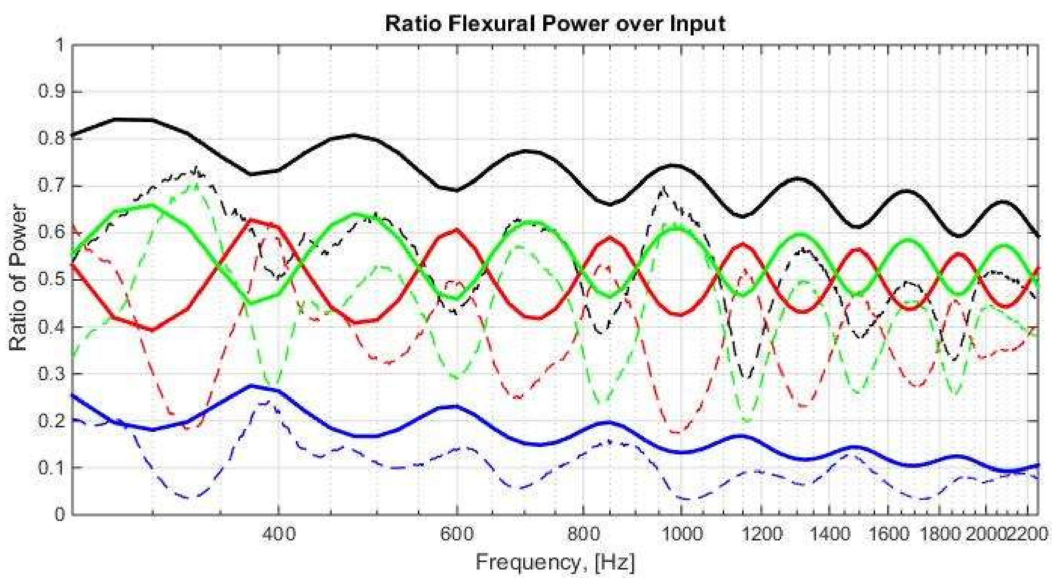

Figure 6-24: Ratio each power over input power against ***Log*** Frequency (*250Hz to 2250Hz*) of Measurement (thin dotted lines) vs. **Numerical** (**bold lines**) for **140º** set-up of beam angle.
Beta (blue), Alpha (red), Gamma (green) and **Total Power**=Gamma+Beta (**black**)

Figure 6-25 and Figure 6-26 also successfully compares results obtained for angle of 160° of joint in the beam.

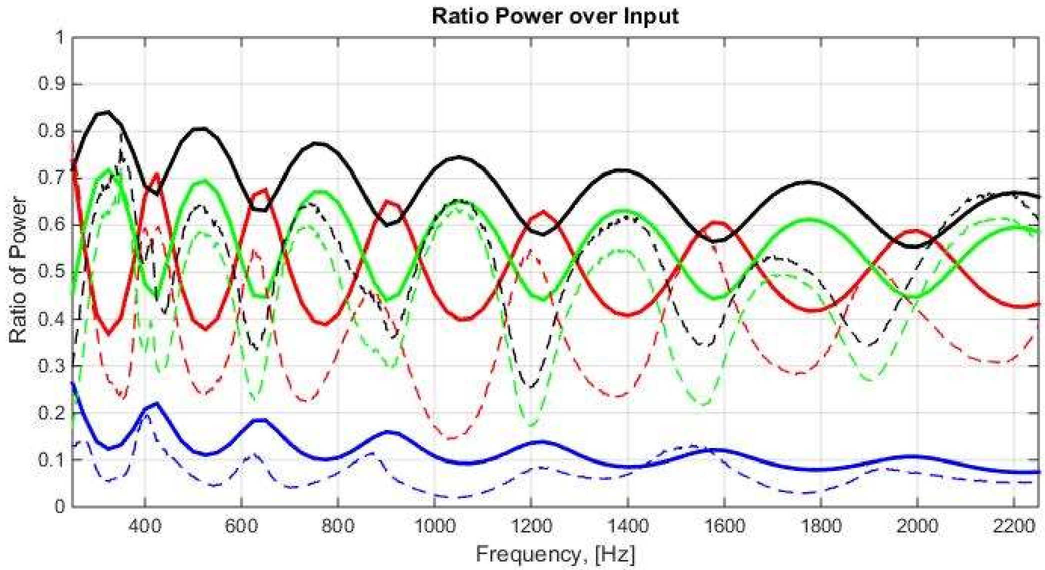

Figure 6-25: Ratio each power over input power against Frequency (*250Hz to 2250Hz*) of Measurement (thin dotted lines) vs. **Numerical** (**bold lines**) for **160°** set-up of beam angle.
Beta (blue), Alpha (red), Gamma (green) and **Total Power**=Gamma+Beta (**black**)

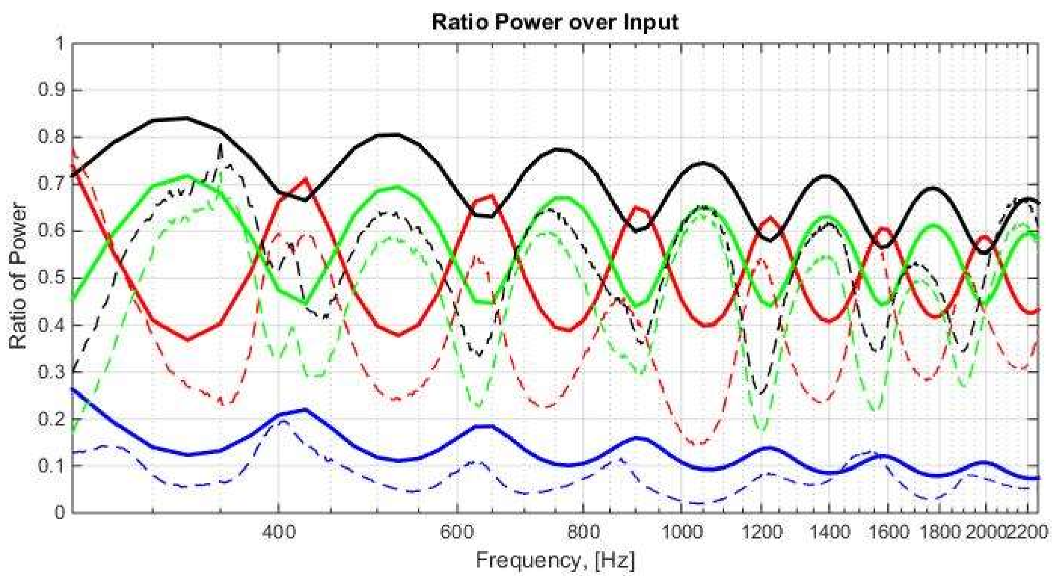

Figure 6-26: Ratio each power over input power against ***Log*** Frequency (*250Hz to 2250Hz*) of Measurement (thin dotted lines) vs. **Numerical** (**bold lines**) for **160°** set-up of beam angle.
Beta (blue), Alpha (red), Gamma (green) and **Total Power**=Gamma+Beta (**black**)

Figure 6-27 and Figure 6-28 would finally discussed the result obtained for angle 175°, which was the most extreme angle that could physically being measured. This was due to the positioning of accelerometer would not be possible for angle closer to 180° as the beam will collapse to each other and forming a 'thicker beam' assembly.

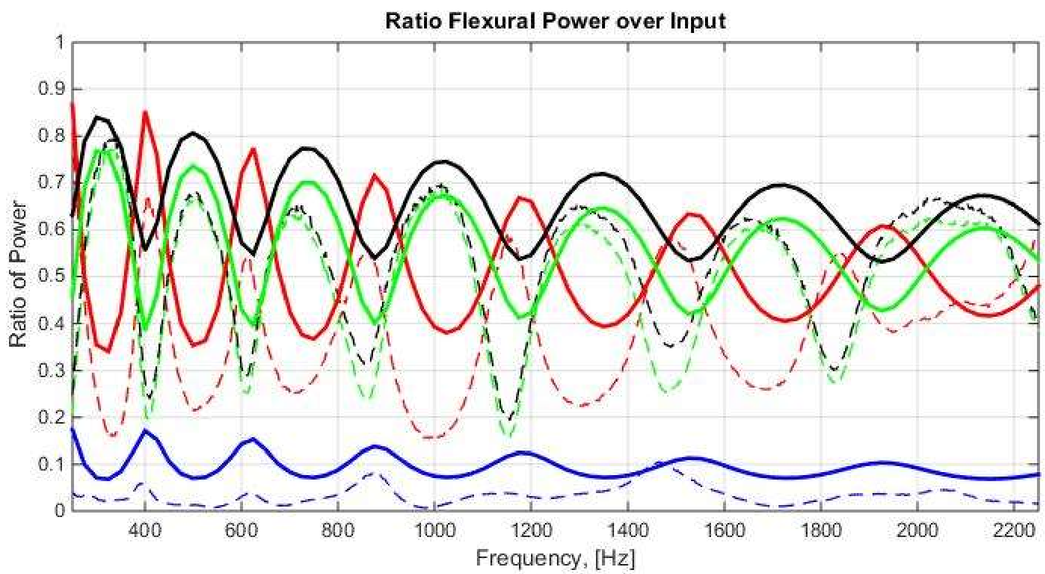

Figure 6-27: Ratio each power over input power against Frequency (*250Hz to 2250Hz*) of Measurement (thin dotted lines) vs. **Numerical** (**bold lines**) for **175°** set-up of beam angle.
Beta (blue), Alpha (red), Gamma (green) and **Total Power**=Gamma+Beta (**black**)

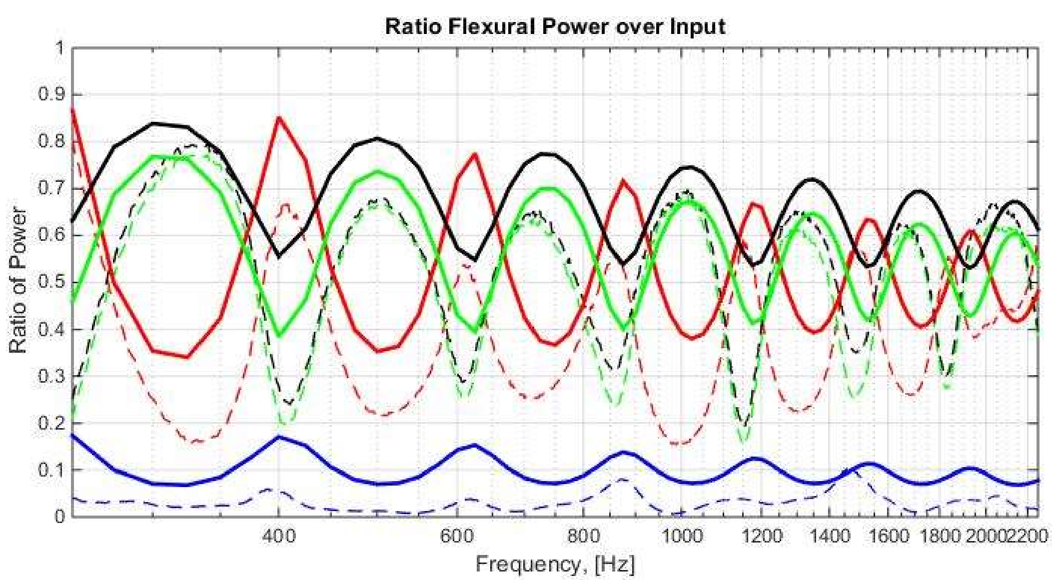

Figure 6-28: Ratio each power over input power against ***Log*** Frequency (*250Hz to 2250Hz*) of Measurement (thin dotted lines) vs. **Numerical** (**bold lines**) for **175°** set-up of beam angle.
Beta (blue), Alpha (red), Gamma (green) and **Total Power**=Gamma+Beta (**black**)

It is observed that at this extreme angle power transmitted in beta section were lower in numerical investigation but much lower for the measurement findings. However, both results were noted in great comparisons in terms of its power reflected and transmitted.

6.7 Concluding remarks

A procedure for the measurement of vibrational power for two beams connected with an angle joint for force excitation have been established and shows good agreement in almost all the results. Angle of interest was based on initial result from the variable joint model which concerning at 40 and 160 degrees. Results between measurements and numerical results were found to be corresponding to the expected power level of reflected and transmitted. Comparisons were done only for flexural power, due to accelerometer set-up distance for wavelength limitations, and above all due to the beam length limitations. Longitudinal power behaviour could be predicted numerically with the agreement concluded for flexural power relationship.

Phase matching were seen in acceptable similarity as consideration of phase error which includes the accelerometer distance as well as the manual adjustment of accelerometer locations in the experimentation. This model and experimentation validation is important to further analyse and determine the vibration power characteristic concerning the reflected & transmitted in the beam. Full spectrum of power for all angles against frequency being elaborated in chapter 7 while comparing with the effect of added rubber layer as additional stiffness and damping at the joint of set-up. Results provided in this chapter have successfully concur to the mathematical derivation and modelling of variable joint which outlined in the earlier objective of this work.

Appendix F would further illustrate the measurement data obtained from the various joint configurations. This would support the consistency and assurance that the measurement activity was done with stated limitations and weaknesses declared.

Chapter 7: Comparison of modelling and measurement due to rubber sheet hysteresis damping effect

7.1 Introduction

As an extended research towards the variable joints achieved in previous chapters, the beam will now be investigated for its behaviour with rubber layer adhered in-between the joints as in Figure 7-1. The rubber layer is to add both stiffness and increased damping to the joint. Similar arrangements were prepared relating to the variable angles of joints but are limited to 0º, 40º, 90º, 140º and 175º angles of joints.

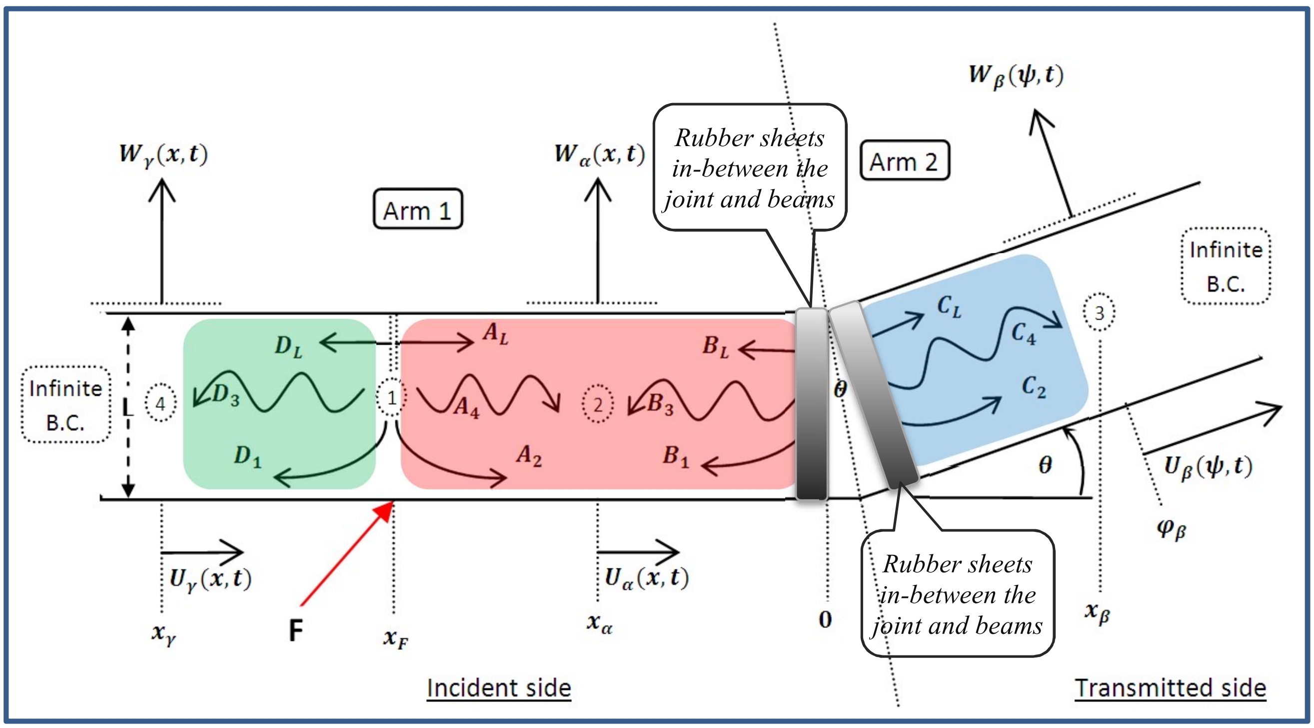

Figure 7-1: Force input to non-collinear beam with rubber layer at various angle joint; for assuming, $x_F = m$, and $0\ (joint) = n$

The simple joint for a straight continuous beam (0º angle) was formed by just using one rubber sheet, and the remaining four angle orientations with the respective joints are as illustrated in Figure 7-1. A special mixing of strong glue was used to hold the assembly together (requires adhesion capability for rubber with Perspex) with a very delicate handling procedure (could easily be detached due to length of beam and twisting motion).

Theoretically, with the added rubber means additional damping material into the system of this variable joint angle. The solution was again derived for 12X12 matrixes where the similar 6 additional terms of continuity, forces and moment equations were considered at the excitation position, X_F. Section of alpha, beta and gamma will be further investigated with regards to the additional damping.

7.2 Measurements for rubber layer in-between joints

Similar set-up being arrange for the measurement whereby mainly affecting the joint layer of the variable angle. Equation from previous matrix in displacement, force and moment application in beam of chapter 5 being utilized. However only parameters of equation bending moment, compressive force and shear force being modified to accommodate the presence of rubber layer at the joint area.

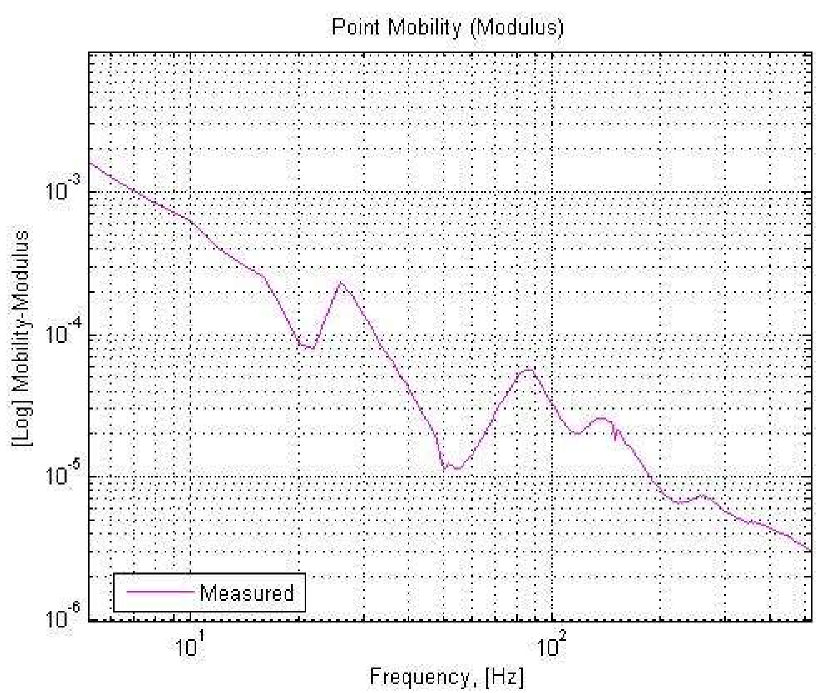

Figure 7-2: Point mobility for rubber sheet

The rubber material used were measured for its point mobility to obtain the hysteretic material damping or the complex stiffness value as in Figure 7-2.

It was proven that from the equation of motion,

$$[-m\omega^2 + k^*]X = F_o$$

Equation 7-1

And

$$X = {F_o}/{[-m\omega^2 + k^*]}$$

Equation 7-2

Where X is now being refer to the displacement considered in the earlier chapter as U and W directions with regards to flexural and longitudinal.

Hysteresis (or solid or structural) damping of rubber represented in form of: -

$$k^* = h_s(1 + i\omega h)$$

Equation 7-3

is called the complex stiffness of the system and $\boldsymbol{h}$ is a constant indicating dimensionless measurement of damping caused by the friction between the internal planes that slip or slide as the material deforms. It was agreed that the energy loss per cycle due to internal friction is independent of the frequency but approximately proportional to the square of the amplitude.

Effect of material damping force at the joint by the rubber layer were calculated for both sides at alpha and beta section. It is then acted to gradually dissipate energy produced and all the results being collected in the figures for experiment measurements in appendix F, as earlier activity in chapter 6.

7.3 *Numerical parameters*

Model of the joint with rubber is then being developed focusing at the 3 contributing equations of moment and two forces of compressive & shear. Similar numerical coding of MATLAB was used and forces contributing to the viscoelastic dissipation of energy by the rubber being included in the equations.

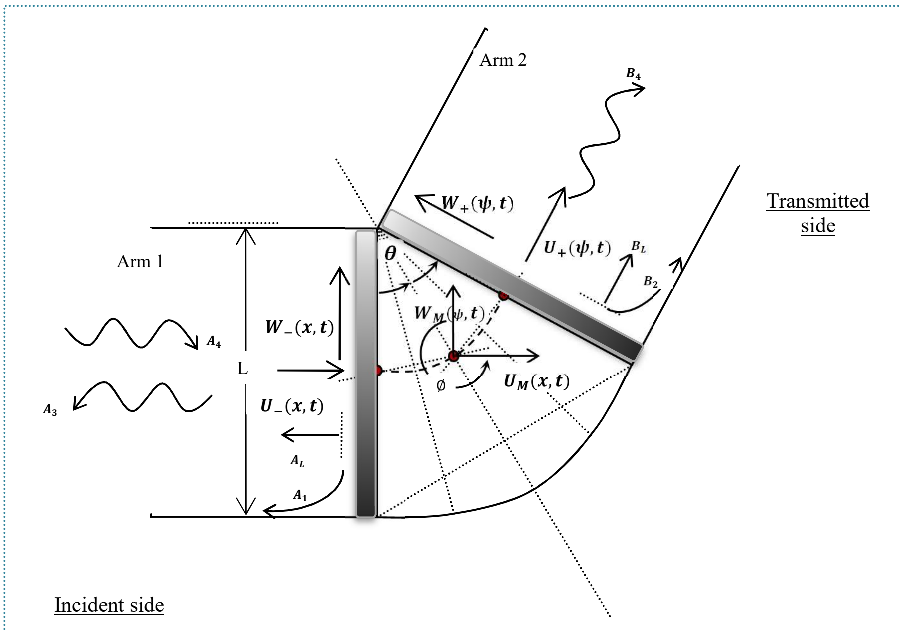

Figure 7-3: Wave motion for variable/wedge size of rigid joint in a non-collinear beam with rubber layer

Then, referring to notation in Figure 7-3 and deriving similarly from chapter 4, displacement equation was used and being prepared for the analysis.

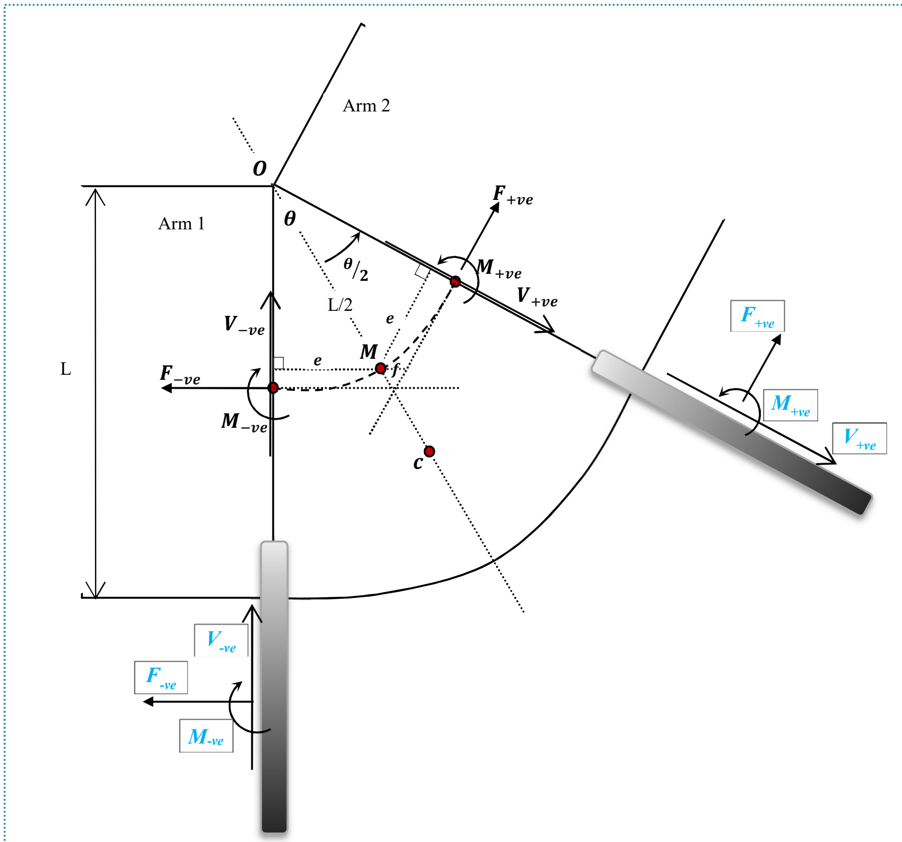

Figure 7-4: Equilibrium of force and moment for <u>variable/wedge size of rigid joint</u> in a non-collinear beam with rubber layer

Again, using the beam theory where forces act about/ through centre of force, which is point -ve and +ve, and rotation occurs about point M as in Figure 7-4.

Let joint have mass *m*, inertia *I*, about point M, and now all the V, shear force, F, compressive force and M, moment would include the rubber layer.

Then, from equation of compressible force: -

$$\left[\!\left[m\ddot{U}_M = F_+ cos\theta + V_+ sin\theta - F_- \right]\!\right]$$

and include the rubber mass, stiffness and damping, yield: -

$$[(F_-) - (D_{rL})(-U_-)] = [(F_+)(cos\theta) - (D_{rL})(U_+)(cos\theta)]$$
$$+[(V_+)(sin\theta) - (D_{rF})(-W_+)(sin\theta)] - M_j\ddot{U}$$

Equation 7-4

From equation of shear force: -

$$\left[\!\left[\boldsymbol{m\ddot{W}_M = V_- + F_+sin\theta - V_+cos\theta} \right]\!\right]$$

and include the rubber mass, stiffness and damping, yield: -

$$[-(V_-) + (D_{rF})(W_-)] = [(F_+)(sin\theta) - (D_{rL})(U_+)(sin\theta)]$$
$$-[(V_+)(cos\theta) - (D_{rF})(-W_+)(cos\theta)] - M_j\ddot{W}$$

Equation 7-5

From equation of moment: -

$$\left[\!\left[\boldsymbol{I\ddot{\emptyset} = M_+ - M_- - V_+e - V_-e - F_-f + F_+f} \right]\!\right]$$

and include the rubber inertial mass, stiffness and damping, yield: -

$$[(M_-) - (D_{rM-})(\theta)] + [(V_-)(e) - (D_{rF})(W_-)(e)]$$
$$= [(M_+) - (D_{rM+})(\theta)] - [(V_+)(e) - (D_{rF})(-W_+)(e)] - I_j\ddot{\theta}$$
$$- [(F_-)(f) - (D_{rL})(-U_-)(f)] + [(F_+)(f) - (D_{rL})(U_+)(f)]$$

Equation 7-6

Where: -

$$D_{rL} = (-M_r\omega^2) + h_{sl}(1 + i\omega h_l) \text{ in unit of kg/s}^2$$
$$D_{rF} = (-M_r\omega^2) + h_{sf}(1 + i\omega h_f) \text{ in unit of kg/s}^2$$
$$D_{rM} = (-I_r\omega^2) + h_{sm}(1 + i\omega h_m) \text{ in unit of kgm}^2\text{/s}^2$$

are all the mass, inertia and hysteresis for respective directions of compressive, shear and moment.

As being derived in earlier chapter, the force of shear and compression as well the moment with the inclusion of the rubber layer were summarised for the model. Characters used were also similarly obtained from displacement relationship described in earlier chapter. Equation of bending moment, compressive force and shear force were further manipulated for the matrix with the rubber layer in analysis as in appendix D-1.

7.4 Results

Similar approach was used to compare the results obtained which plotted together both numerical and measurement in the figures below. Figure 7-5 and Figure 7-6 displays the straight beam of 0° angle jointed beam. Obviously, a layer of rubber used to join the 2-beam system. Due to the section of the rubber, resonance behaviour was noted and agreed in the power ratio results. Unit for power reflected and transmitted is in N.m/s for all results, or in N.mm/s x 10^{-3}.

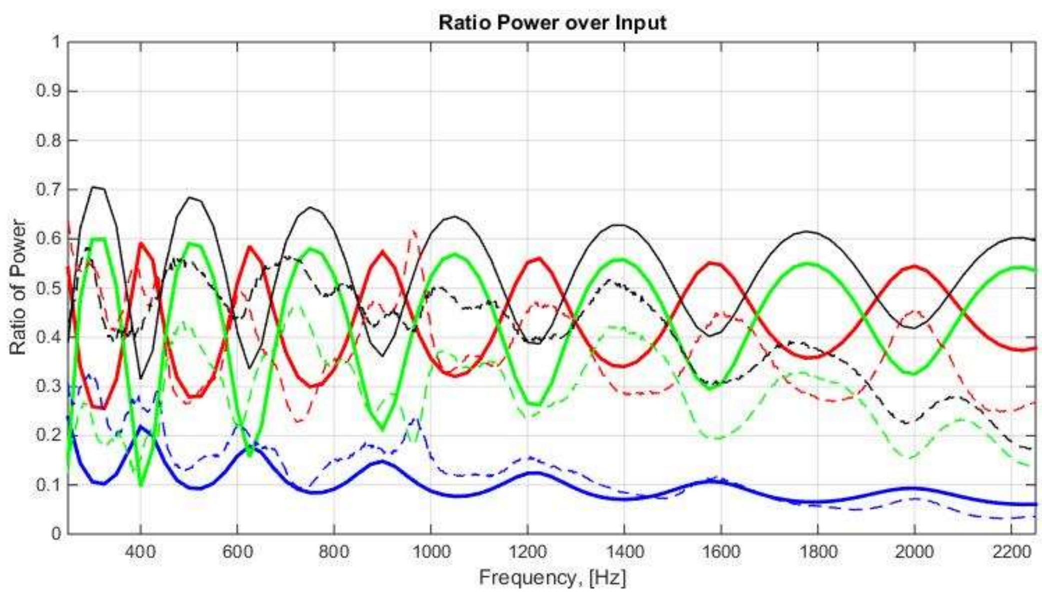

Figure 7-5: Ratio each power over input power against Frequency (*250Hz to 2250Hz*) of Measurement (thin dotted lines) vs. **Numerical** (**bold lines**) for **0°** set-up of beam angle with rubber
Beta (blue), Alpha (red), Gamma (green) and **Total Power**=Gamma+Beta (**black**)

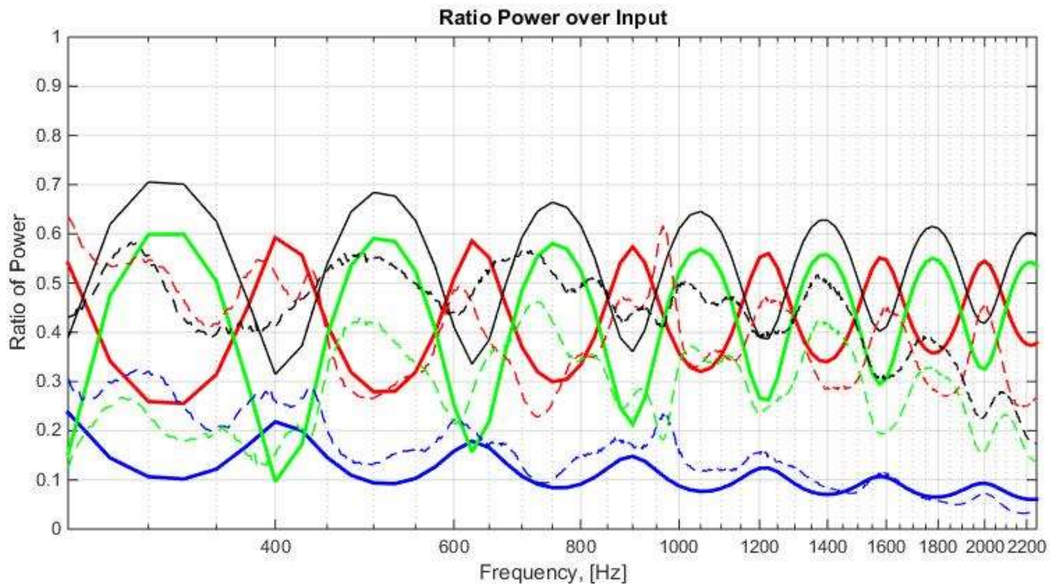

Figure 7-6: Ratio each power over input power against ***Log*** Frequency (*250Hz to 2250Hz*) of Measurement (thin dotted lines) vs. **Numerical** (**bold lines**) for **0º** set-up of beam angle <u>with rubber</u>
Beta (blue), Alpha (red), Gamma (green) and **Total Power**=Gamma+Beta (**black**)

Figure 7-7 and Figure 7-8 shows results obtained from 40º angle joint with the rubber layer at both sides of the joint. Numerical and measurement noted in agreement of the vibrational power reflected and transmitted.

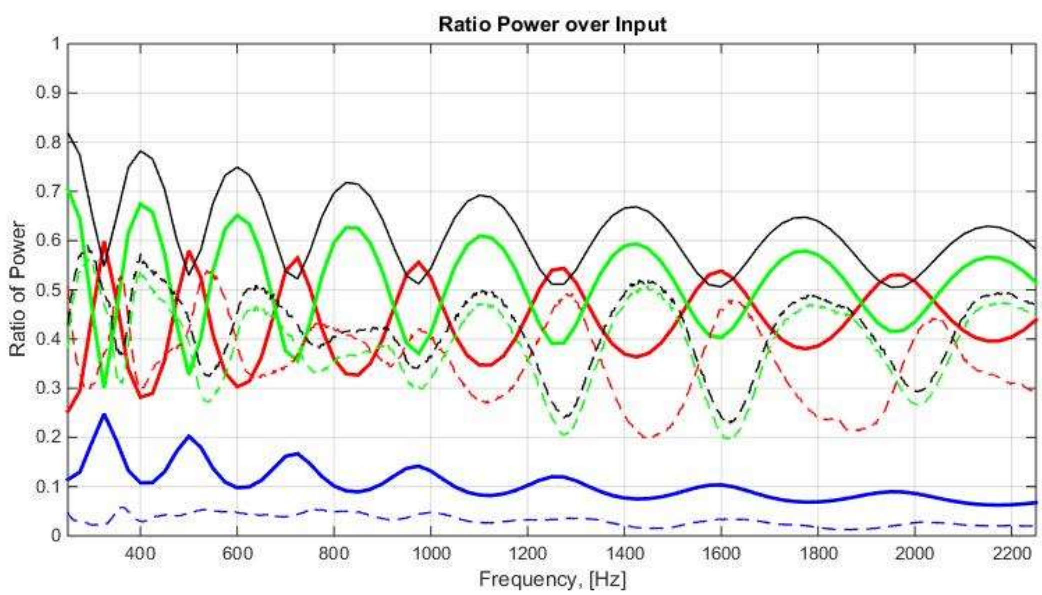

Figure 7-7: Ratio each power over input power against Frequency (*250Hz to 2250Hz*) of Measurement (thin dotted lines) vs. **Numerical** (**bold lines**) for **40º** set-up of beam angle <u>with rubber</u>
Beta (blue), Alpha (red), Gamma (green) and **Total Power**=Gamma+Beta (**black**)

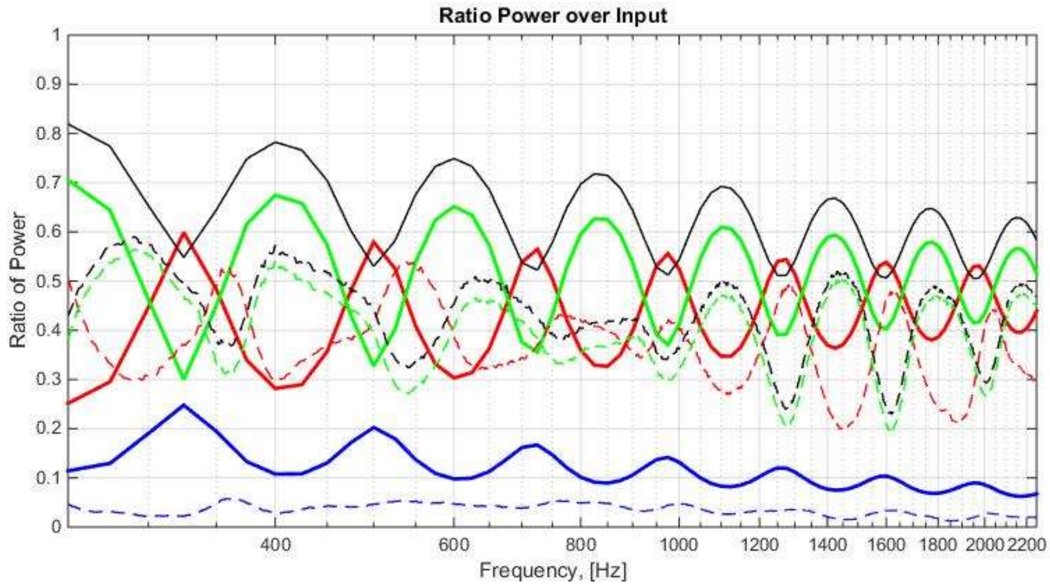

Figure 7-8: Ratio each power over input power against ***Log*** Frequency (*250Hz to 2250Hz*) of Measurement (thin dotted lines) vs. **Numerical** (**bold lines**) for **40º** set-up of beam angle with rubber
Beta (blue), Alpha (red), Gamma (green) and **Total Power**=Gamma+Beta (**black**)

Figure 7-9 and Figure 7-10 shows the ratio of power at 90º of joint which also in good agreement of phase angle and the power result. Power in beta were noted dissipated at high frequency despite numerical shows gradual change. This were suspected from adhesion of rubber layer in the measurements due to handling and delicate preparation.

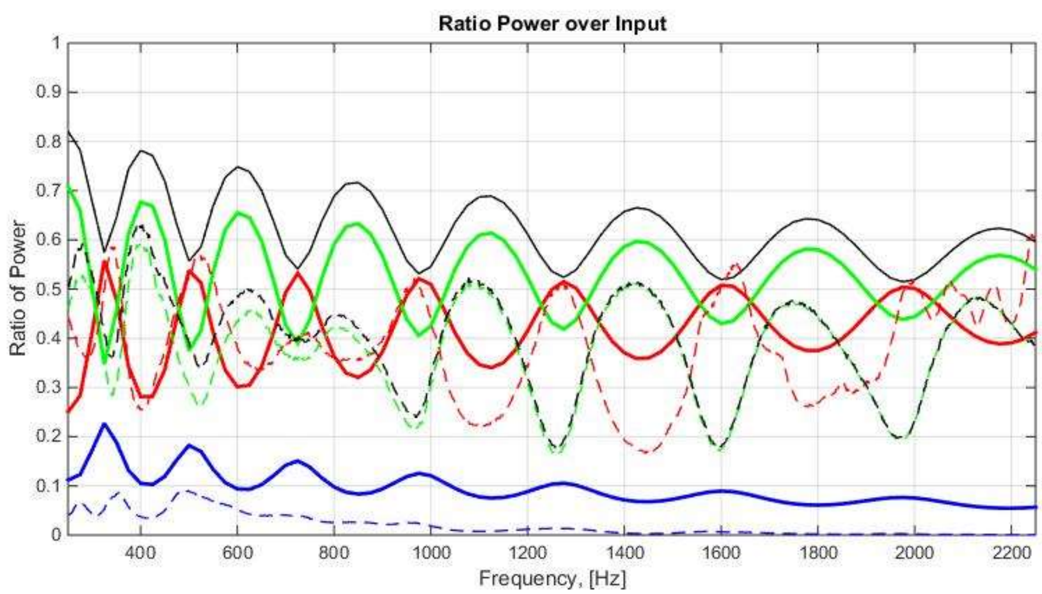

Figure 7-9: Ratio each power over input power against Frequency (*250Hz to 2250Hz*) of Measurement (thin dotted lines) vs. **Numerical** (**bold lines**) for **90º** set-up of beam angle with rubber
Beta (blue), Alpha (red), Gamma (green) and **Total Power**=Gamma+Beta (**black**)

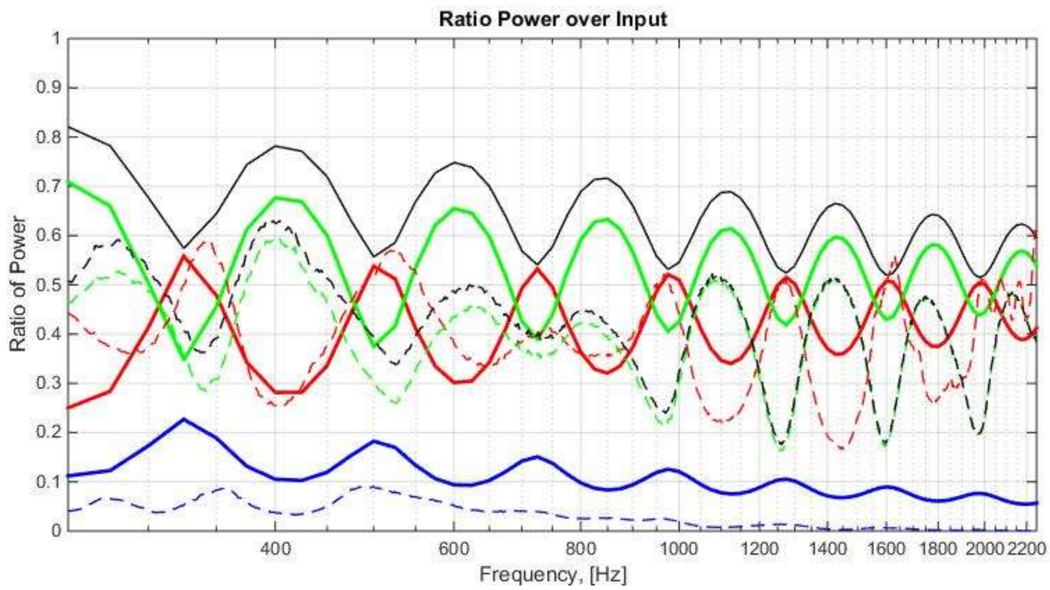

Figure 7-10: Ratio each power over input power against ***Log*** Frequency (*250Hz to 2250Hz*) of Measurement (thin dotted lines) vs. **Numerical** (**bold lines**) for **90º** set-up of beam angle <u>with rubber</u>
Beta (blue), Alpha (red), Gamma (green) and **Total Power**=Gamma+Beta (**black**)

Figure 7-11 and Figure 7-12 for the 140º set-up however shows again a good agreement of results obtained from both numerical and measurements work.

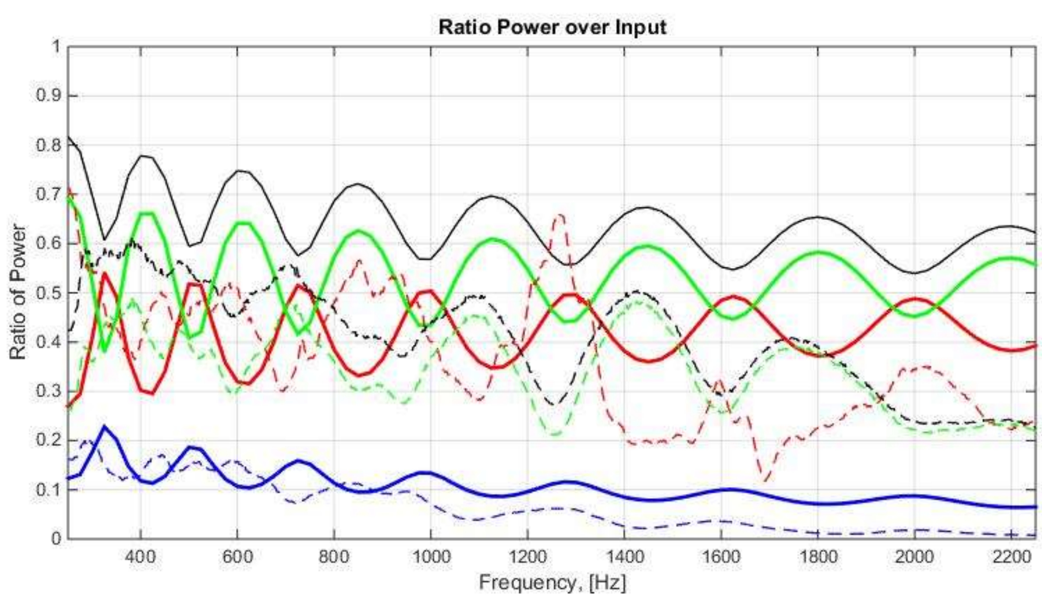

Figure 7-11: Ratio each power over input power against Frequency (*250Hz to 2250Hz*) of Measurement (thin dotted lines) vs. **Numerical** (**bold lines**) for **140º** set-up of beam angle <u>with rubber</u>
Beta (blue), Alpha (red), Gamma (green) and **Total Power**=Gamma+Beta (**black**)

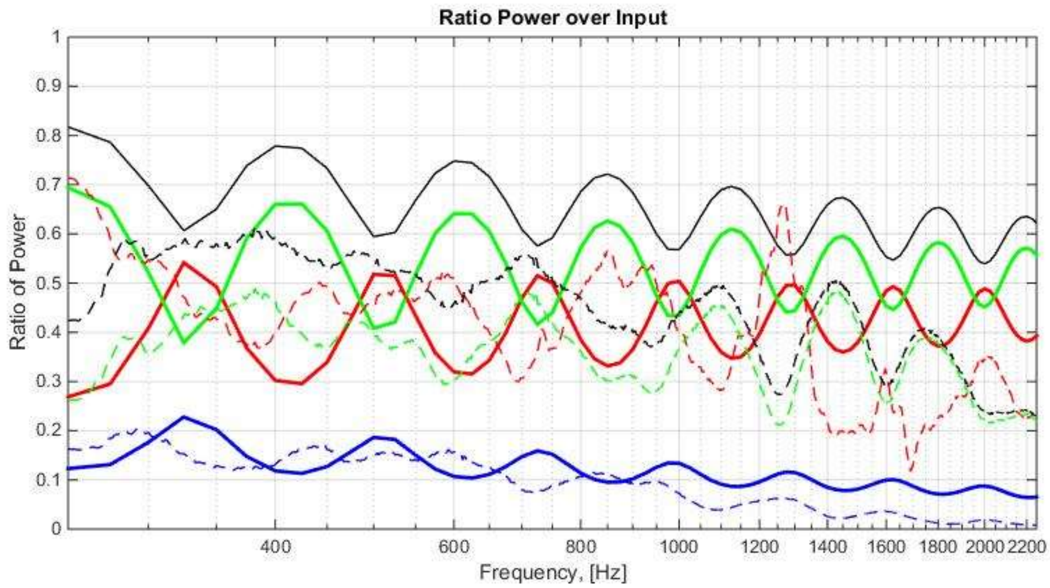

Figure 7-12: Ratio each power over input power against ***Log*** Frequency (*250Hz to 2250Hz*) of Measurement (thin dotted lines) vs. **Numerical** (**bold lines**) for **140º** set-up of beam angle with rubber
Beta (blue), Alpha (red), Gamma (green) and **Total Power**=Gamma+Beta (**black**)

Figure 7-13 and Figure 7-14 were finally concurs the numerical and measurement analysis upon the power input, transmitted and reflected in the 2-beam system with rubber layer. This result from 175º angle were noted shows the best comparisons as well as from the same angle in analysis of chapter 6 (without rubber layer). This assembly of joint were the best adhered during preparation as it is close together and could be clamped neatly hence minimizing the damage at the joint area.

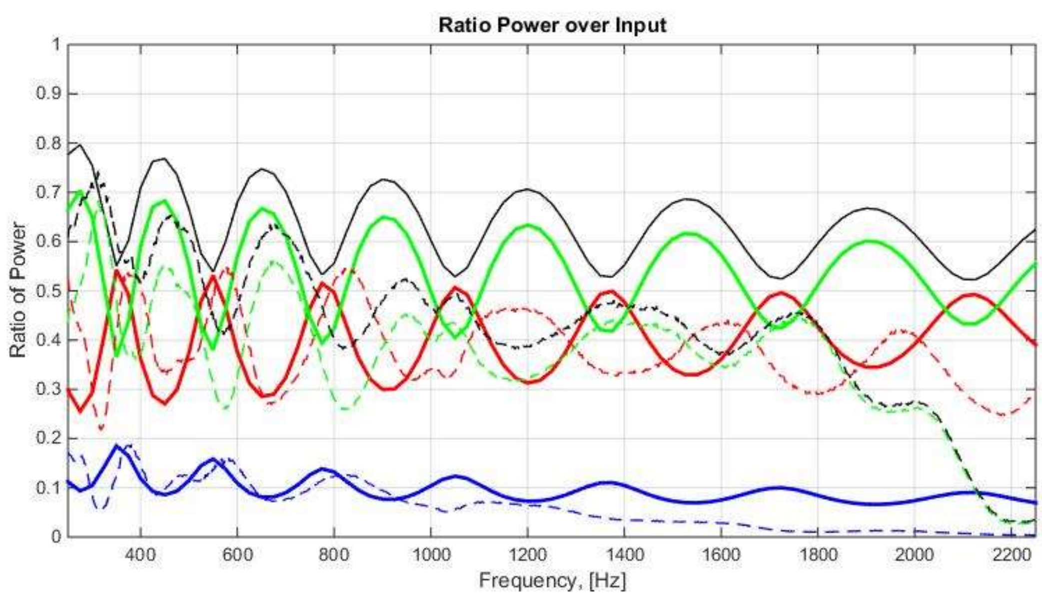

Figure 7-13: Ratio each power over input power against Frequency (*250Hz to 2250Hz*) of Measurement (thin dotted lines) vs. **Numerical** (**bold lines**) for **175º** set-up of beam angle with rubber
Beta (blue), Alpha (red), Gamma (green) and **Total Power**=Gamma+Beta (**black**)

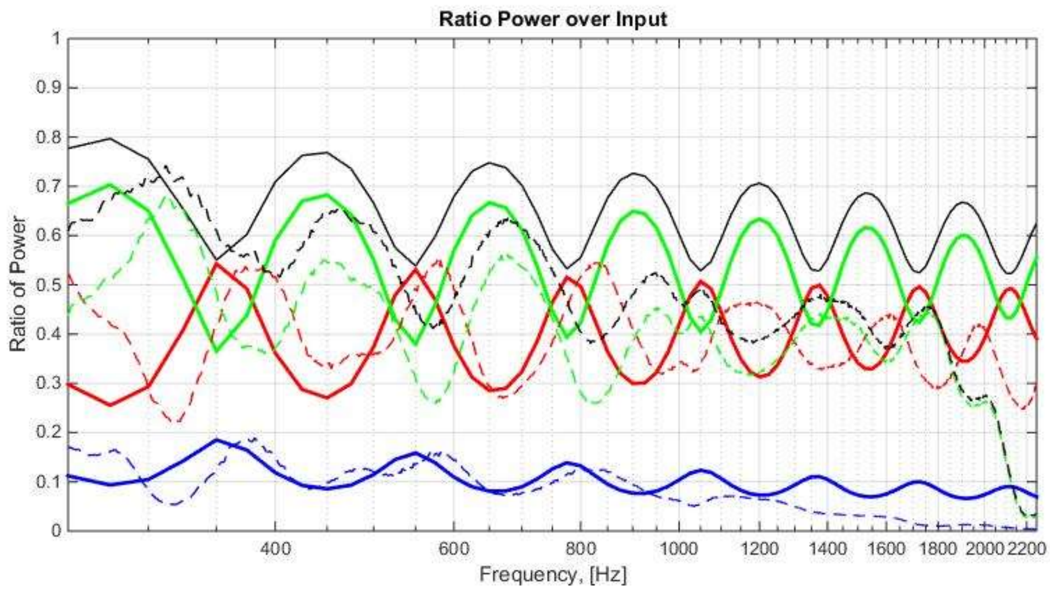

Figure 7-14: Ratio each power over input power against ***Log*** Frequency (*250Hz to 2250Hz*) of Measurement (thin dotted lines) vs. **Numerical** (**bold lines**) for **175º** set-up of beam angle with rubber
Beta (blue), Alpha (red), Gamma (green) and **Total Power**=Gamma+Beta (**black**)

It is fair to declare that the measurement results concurred to the numerical method established for the analysis of variable joint of 2-beam system with rubber layer. Results obtained were seen slightly poor on 90º of angle but it agrees fairly at the low frequency from above 200Hz to 600Hz of frequency before the measurement shows power dissipated. Over all the method and technique established were concluded plausible within the range of lower limit and upper limit of measurement frequency of the 2-beam set-up.

Higher power reflected can be seen from the results as the angle increase for this measurements by comparing results from chapter 6 which was without addition of rubber layer. Next step is to establish relationship of the rubber layer in between the variable joint system for the range of 0º to 180º numerically against frequency. Measurement result were noted could be improved for better preparation of beam joints as well as technique of handling.

7.5 *Further analysis with range of angles at 500Hz frequency*

This section considers a further analysis on examining the modelling of the rubber layer in the joint for 500Hz frequency at all range of angles. This is to understand the reflected and transmitted power with additional damping material added to the system. The numerical coding of the previous chapter has been used for the estimates of reflected and transmitted power.

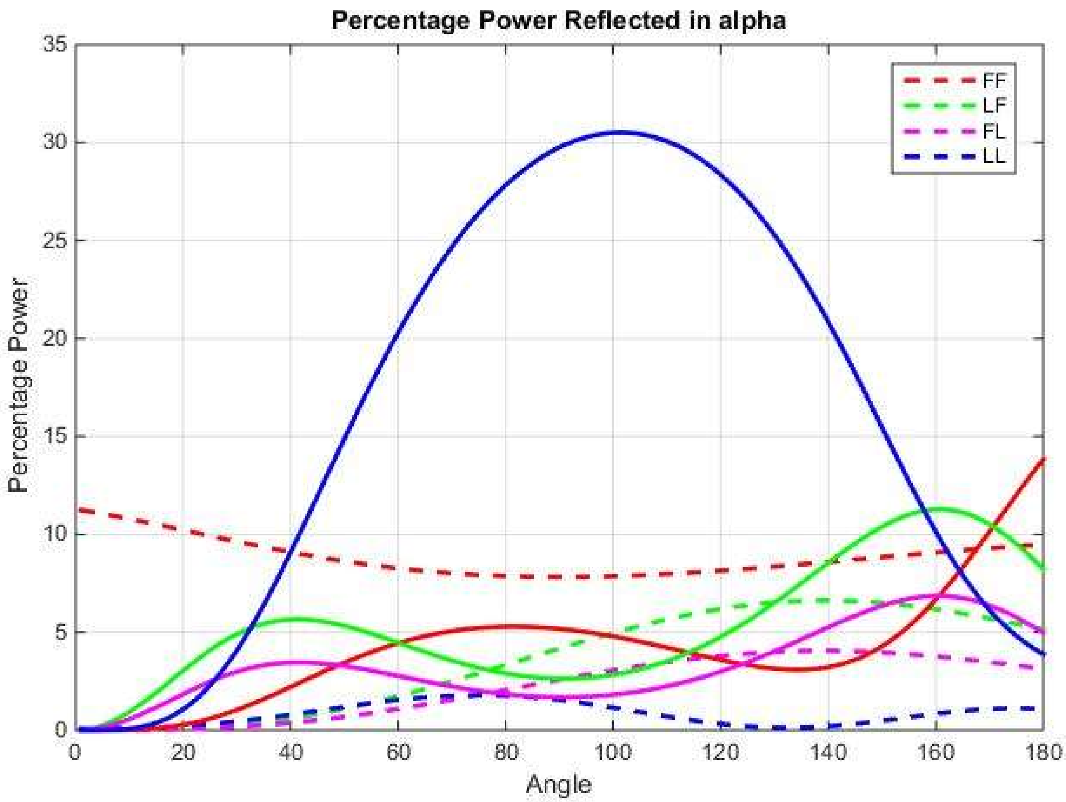

Figure 7-15: Normalised reflected power in Alpha (with rubber) **of 500 Hz, original joint (bold lines) and with rubber (dotted lines) for 0º to 180º beam angle.**
Longitudinal (blue), Flexural (red), Long-Flex (green) and Flex-Long (pink)

In Figure 7-15, longitudinal power reflected were dampened to about 3% at 80º of angle compared to about 27% for without rubber layer. Flexural power reflected at 0º angle from 0% to about 11% and reduces to around 8% from 40º to the extreme of angle. This shows increase of power reflected compared to joint without rubber. Cross-coupling power of LF and FL were seen lower as well except at angle between 80º to about 130º of angle of joint.

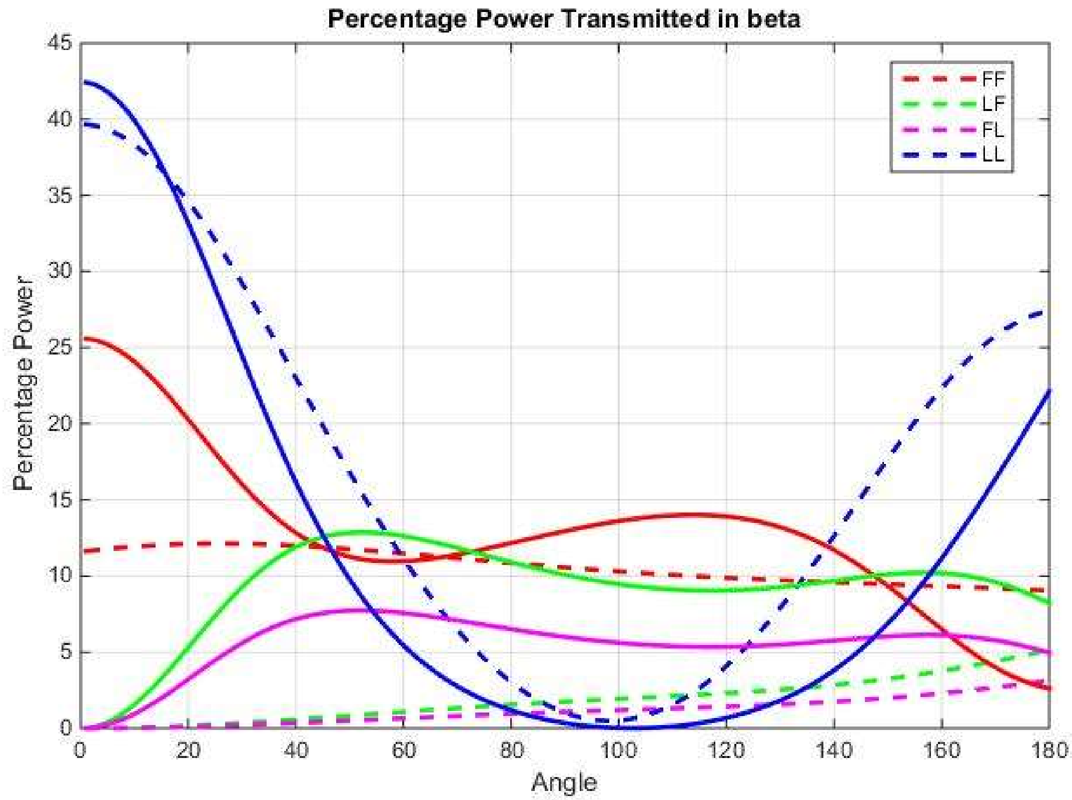

Figure 7-16: Normalised reflected power in Beta (with rubber) **of 500 Hz, original joint (bold lines) and with rubber (dotted lines) for 0º to 180º beam angle.**
Longitudinal (blue), Flexural (red), Long-Flex (green) and Flex-Long (pink)

In Figure 7-16, longitudinal power transmitted slightly higher for joint with rubber layer but minimised at about 100º of angle, the same as joint without rubber layer. Flexural power for 500Hz frequency averagely at 10% of power throughout all joint angle orientation with rubber layer, and the lowest at the extreme of angle 180º. Cross-coupling power were 0% at straight beam orientation and slightly increase to around 4% and 5% at 180º for FL and LF respectively.

7.6 Power in beam 1 and 2 for flexural and longitudinal

Figure 7-17 and Figure 7-18 shows the power distribution for reflected and transmitted beam without material damping in alpha and beta respectively. This will be compared to the

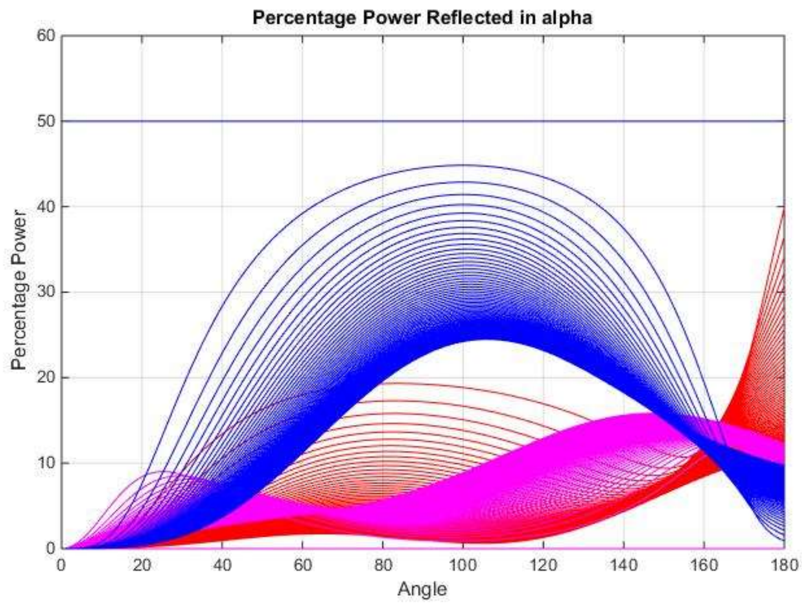

Figure 7-17: Reflected power in Alpha **of 0 to 3000 Hz for 0º to 180º beam angle. Longitudinal (blue), Flexural (red), and Flex-Long & Long-Flex (pink)**

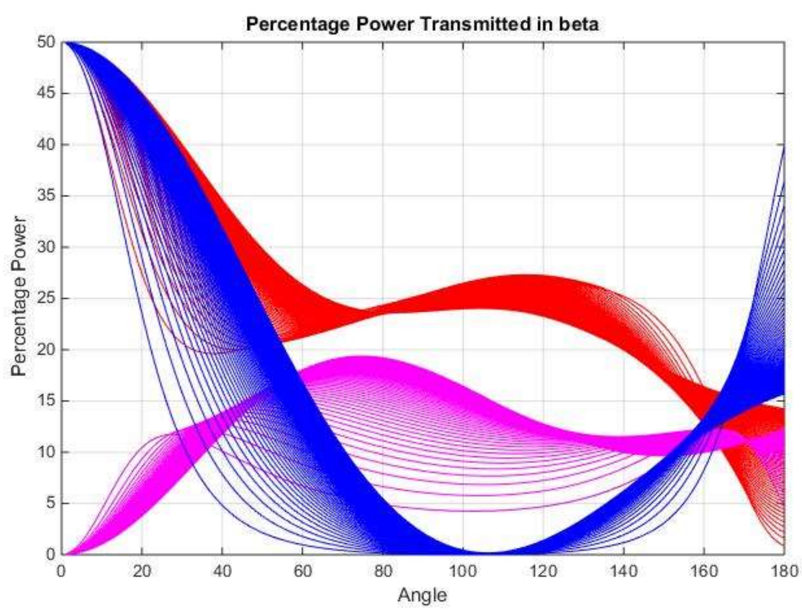

Figure 7-18: Transmitted power in Beta **of 0 to 3000 Hz for 0º to 180º beam angle. Longitudinal (blue), Flexural (red), and Flex-Long & Long-Flex (pink)**

Figure 7-19 and Figure 7-20, which shows the reduction of power for both impinging wave types of FF and LL. Generally, it is difficult to review the power behaviour in this presentation especially with result of rubber layer included. Hence, the following sub-section (contour plot) would present the changes observed from the sequence of without material damping, adaptation material damping and finally with the rubber layer included.

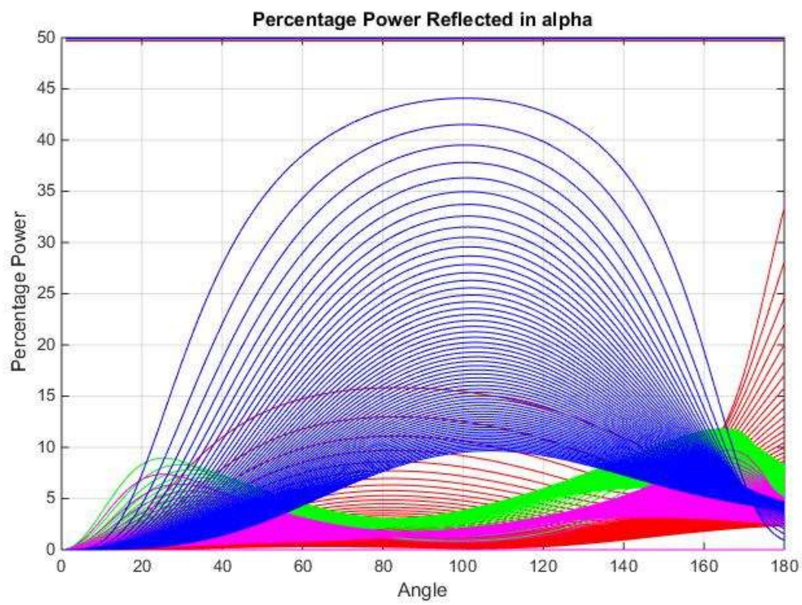

Figure 7-19: Reflected power in Alpha **of 0 to 3000 Hz for 0° to 180° beam angle with material damping 0.07 Longitudinal (blue), Flexural (red), and Flex-Long (pink) & Long-Flex (green)**

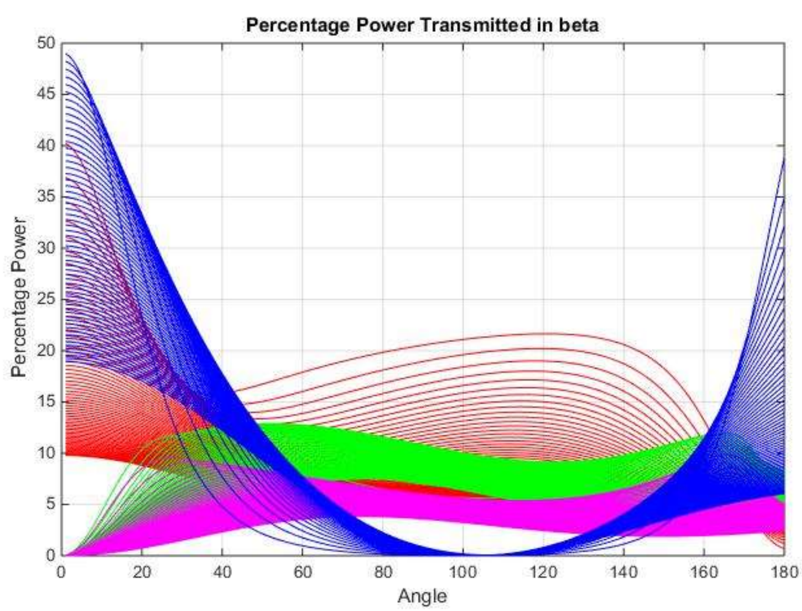

Figure 7-20: Transmitted power in Beta **of 0 to 3000 Hz for 0° to 180° beam angle with material damping 0.07 Longitudinal (blue), Flexural (red), and Flex-Long (pink) & Long-Flex (green)**

7.6.1 Flexural power-reflected (beam1-alpha) and transmitted (beam2-beta)

It is essential to understand the overall behaviour of reflected and transmitted power for flexural due to the changes adapted from the beginning of this work. Results plotted in contour of power for all beam variable joint angles vs the frequency range (0 – 3000Hz).

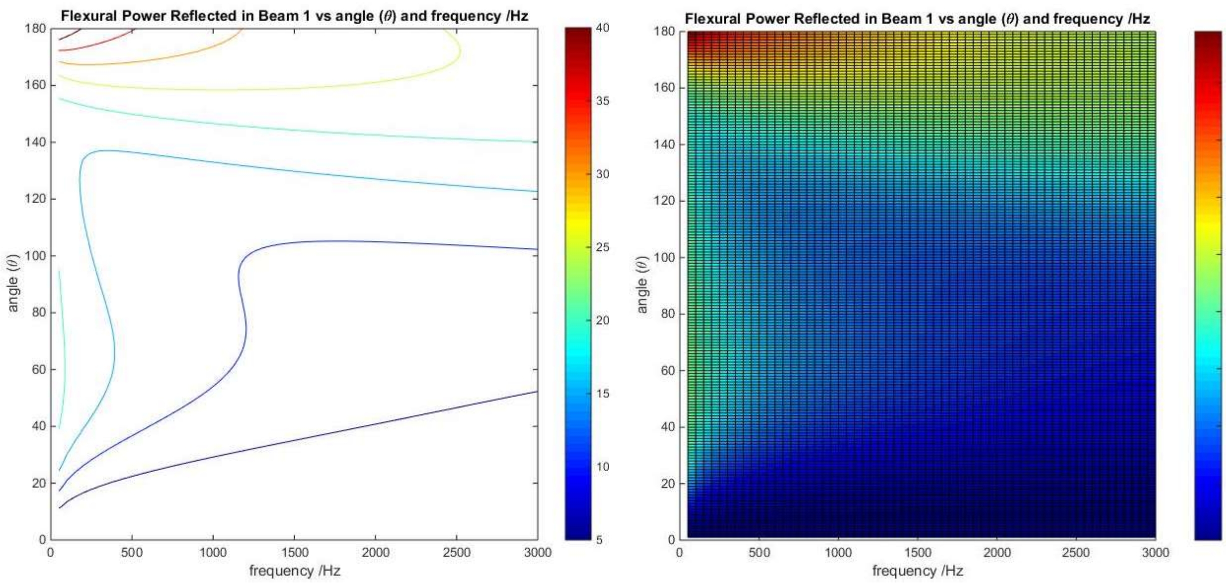

a) **Flexural** power reflected for beam 1 without beam material damping

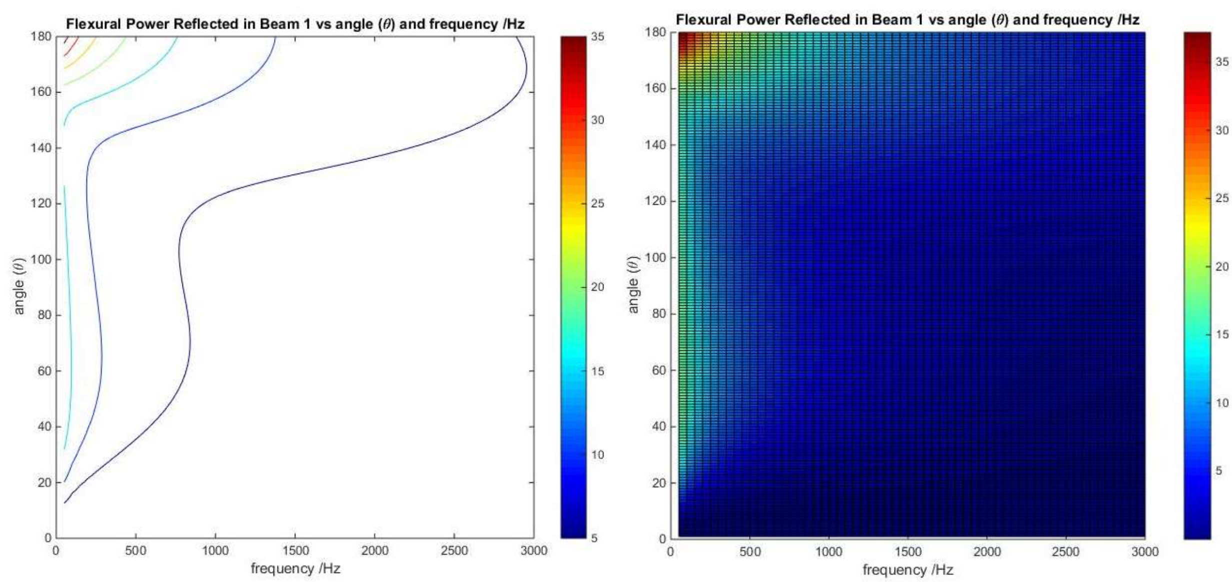

b) **Flexural** power reflected for beam 1 with beam material damping of 0.07

Figure 7-21: Flexural power reflected in beam 1 (alpha) with and without beam material damping

Figure 7-21 shows the reflected flexural power which in alpha section of the beam. Maximum power reflected (at 45%) can be observed occurred at just before 180° angle for up to 500Hz of frequency. As the material damping included into the beam joint analysis, the maximum power reduces to around 37% and squeezed to the corner of plot b) for the lowest frequency at 180° angle joint. This strictly shows flexural power reflected maximum at the extreme angle for only low frequency. Power of about 15% can be obtained from 30° of angle up to 120°, and from 150° for low frequency to 180° of 750Hz of frequency.

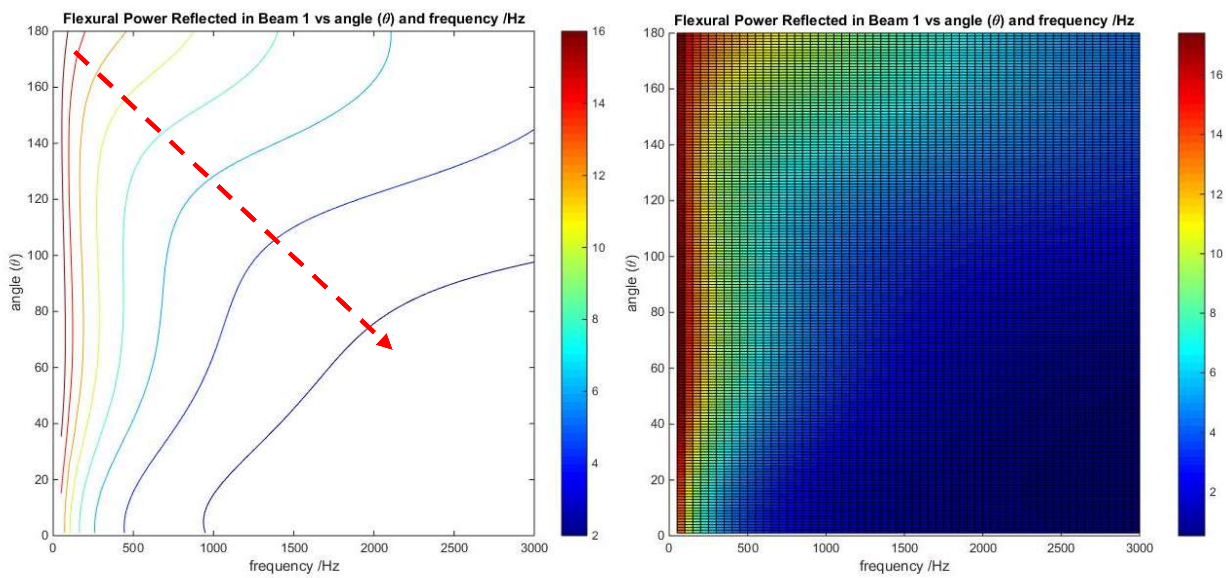

Figure 7-22: Flexural power reflected in beam 1 (alpha) with beam material damping and rubber layer in-between beams and joints

With the added rubber layer, as in Figure 7-22, maximum power reflected of about 17% occurs at all angle orientation of the beam. Power reflected reduced gradually at 180° angle and rapidly at straight beam, with increase of frequency. For example, to obtain 8% power reflected, is at about 250Hz of 0° angle, at 750Hz of 120° angle and at 2000Hz of 180° angle of joint.

Flexural power transmitted in Figure 7-23a) shows maximum power during straight beam (0^o angle) for all range frequency and minimum power at lowest frequency during 180^o angle of beam. With material damping included in Figure 7-23b), the maximum power focuses at lowest frequency for straight beam orientation. The power dissipates with the increase of frequency due to complex Young's modulus of the material.

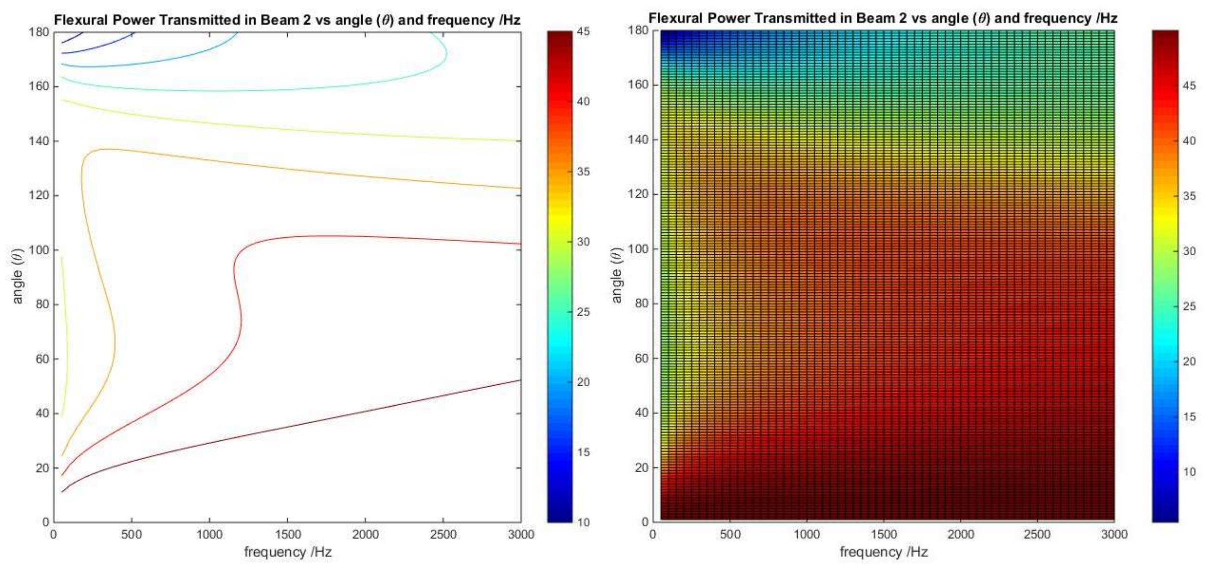

a) **Flexural** power transmitted for beam 2 without beam material damping

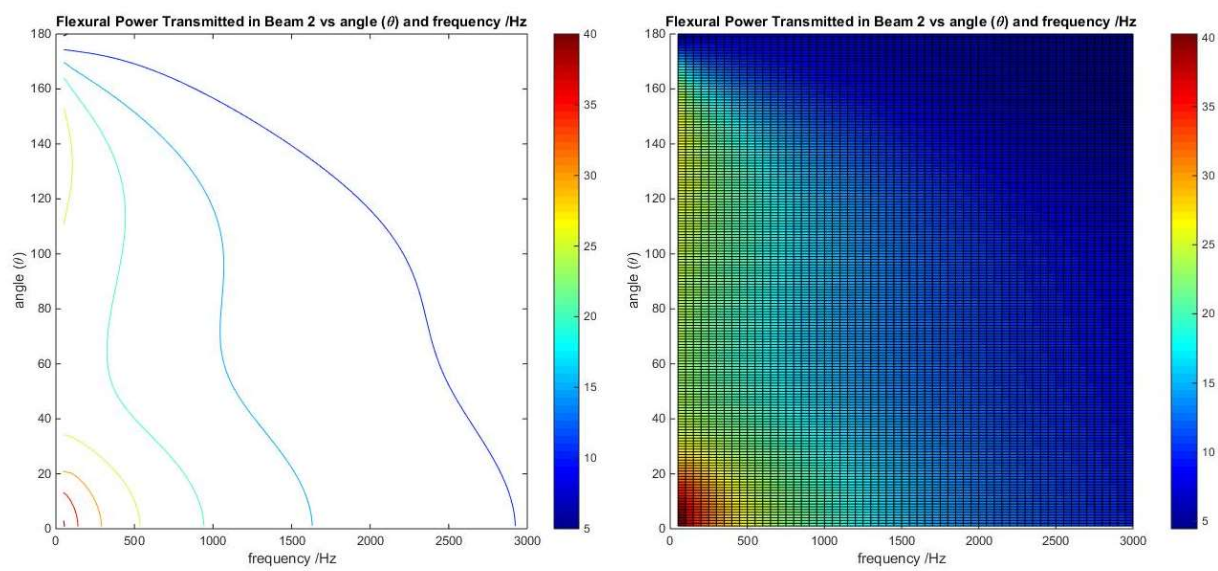

b) **Flexural** power transmitted for beam 2 with beam material damping of 0.07

Figure 7-23: Flexural power transmitted in beam 2 (beta) with and without beam material damping

Figure 7-24 shows that with the added rubber layer into the joint arrangement, maximum power transmitted for flexural can be reduced 50%, from 40% in Figure 7-23b) to around 22% especially during lowest frequency between 40º to 160º of angle. Gradual reduction of power transmitted can be obtained following the dotted line marked in the contour, which from 100º to 60º angle with the increase of frequency.

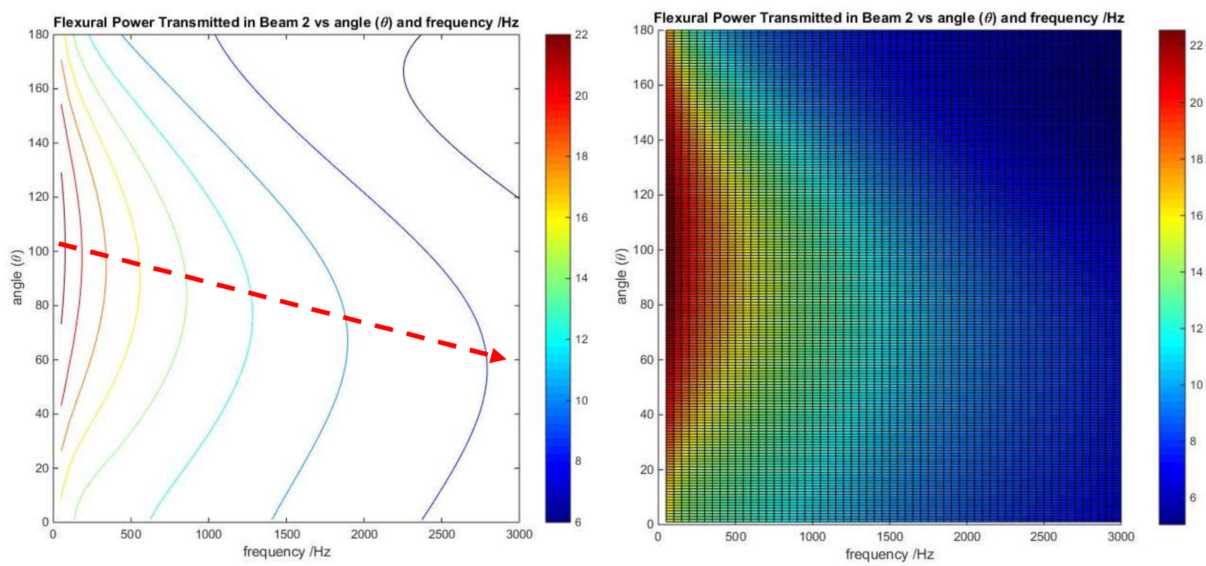

Figure 7-24: Flexural power transmitted in beam 2 (beta) with beam material damping and rubber layer in-between beams and joints

7.6.2 Longitudinal power-reflected (beam1-alpha) and transmitted (beam2-beta)

Longitudinal power was known to have longer wavelength, for this analysis using Perspex beam it can be seen in Figure 7-25a) that maximum power reflected occurs at around 100º of angle for up to 500Hz. With consideration of material damping in Figure 7-25b), the power can be gradually reduced along 100º angle to 120º joint angle with the increase of frequency.

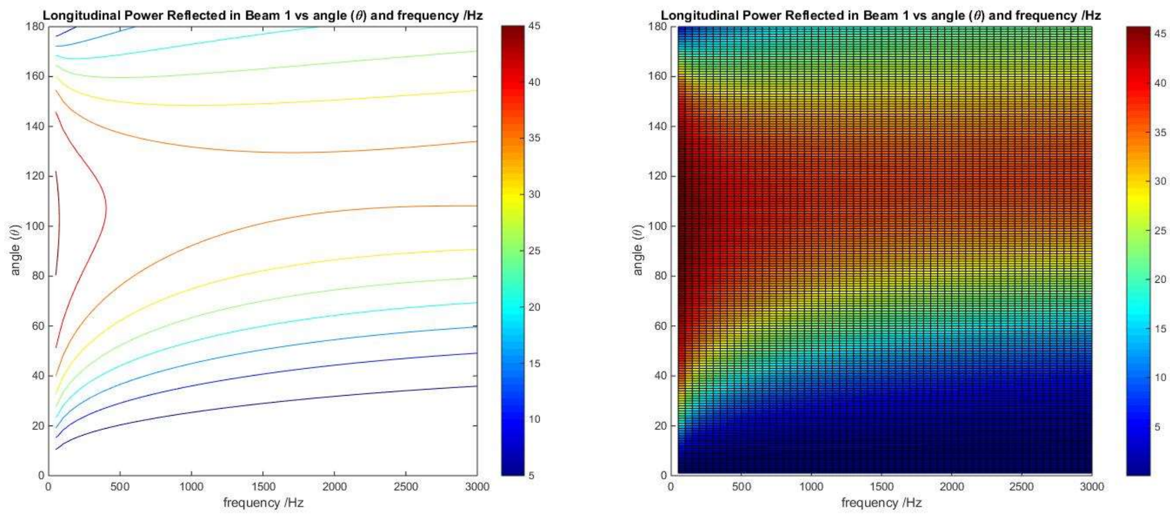

a) **Longitudinal** power reflected for beam 1 without material damping

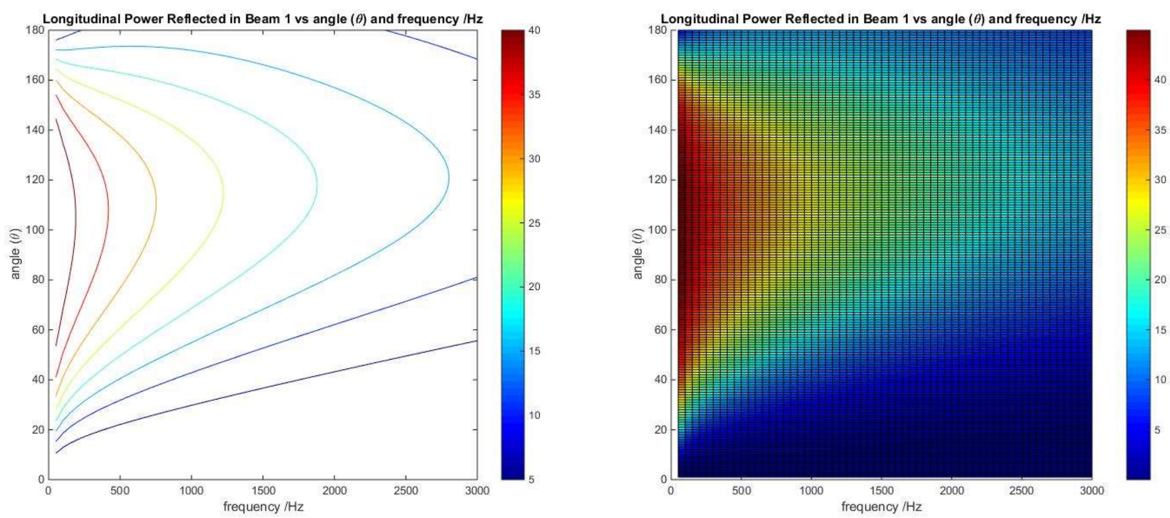

b) **Longitudinal** power reflected for beam 1 with material damping of 0.07

Figure 7-25: Longitudinal power reflected in beam 1 (alpha) with and without beam material damping

Added rubber layer as in Figure 7-26 shows that the maximum power can be reduced to 20%, while minimum power region at 2% for all frequency can be achieved by 20^{o} angle of joint orientation.

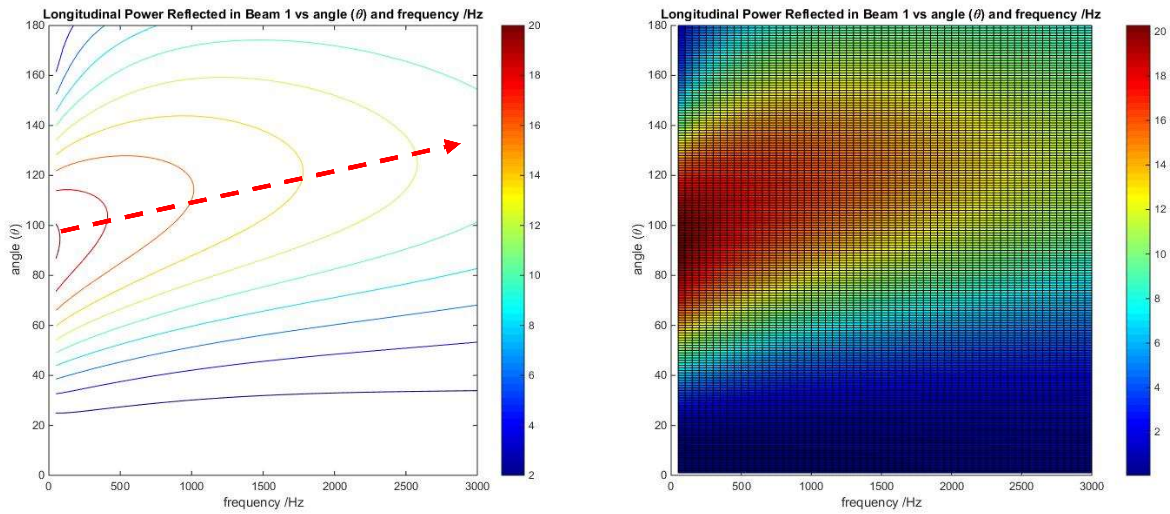

Figure 7-26: Longitudinal power reflected in beam 1 (alpha) with beam material damping and rubber layer in-between beams and joints

Figure 7-27 for longitudinal transmitted power shows that minimum power was during 100° to 120° angle for all range frequency. Maximum power could be isolated to low frequency at low angle joint with the added material damping into the analysis.

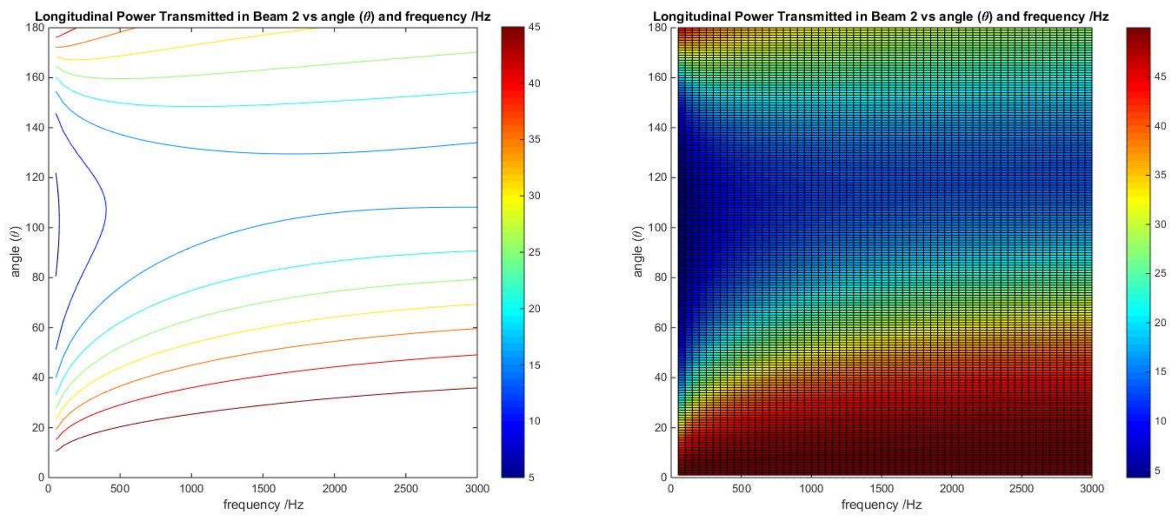

a) **Longitudinal** power transmitted for beam 2 without material damping

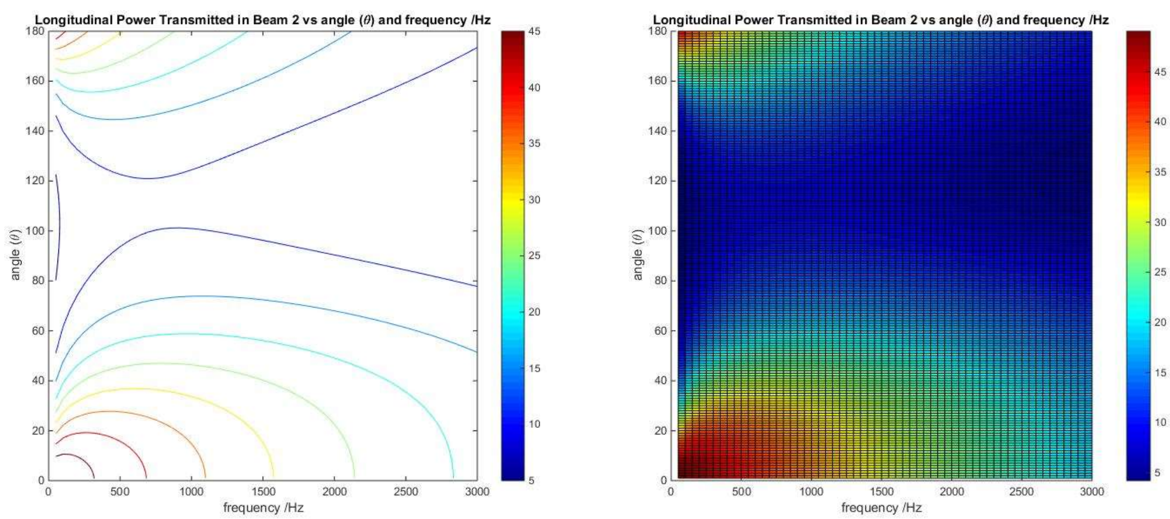

b) **Longitudinal** power transmitted for beam 2 with material damping of 0.07

Figure 7-27: Longitudinal power transmitted in beam 2 (beta) with and without beam material damping

Figure 7-28 of the added rubber layer into the joint assembly shows minimal action can be taken to achieve low power transmitted, unless to always be at low frequency (100Hz) during 100º of angle, or at 2500Hz frequency during 120º angle joint.

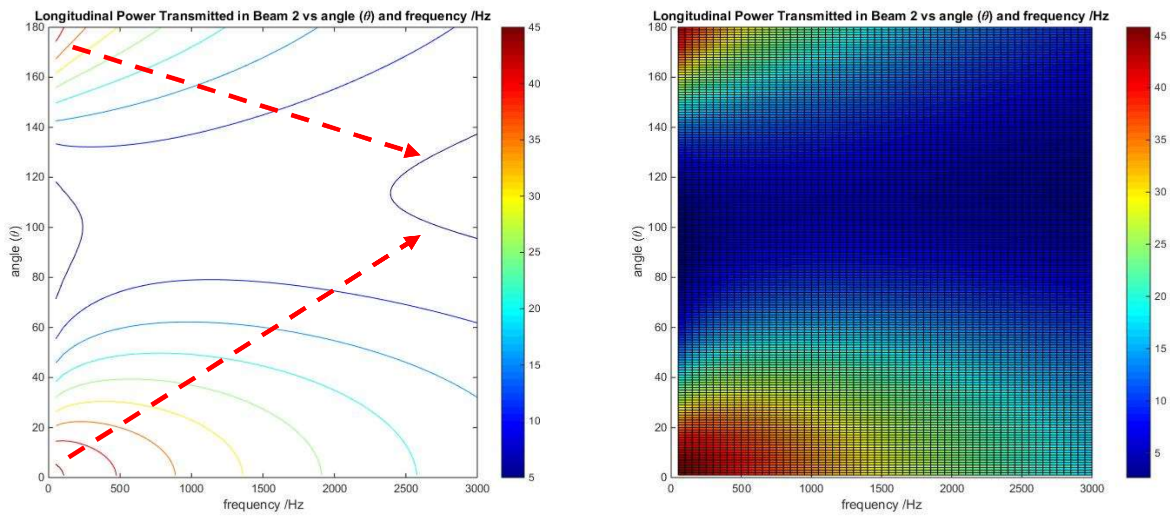

Figure 7-28: Longitudinal power transmitted in beam 2 (beta) with beam material damping and rubber layer in-between beams and joints

7.7 Concluding remarks

Various analysis relating to the development of joint type, consideration of material damping and finally to include rubber layer at the novel variable joint, have obtained considerable result. Material examined were mainly on Perspex beam of the particular size and Young's modulus. The behaviour observed would definitely able to assist various other area of research pertaining the reflection and transmission of vibration power in jointed beams.

This chapter have considered additional damping which is the hysteresis damping for the benefit of analysis with the variable joint. Measurement results were plotted in comparison to the numerical results which were derived and carefully programmed in the MATLAB code. Rubber material used were noted to be an effective medium to mitigate and manipulate the vibrational power of reflection and transmission for flexural and longitudinal.

In the finite section Alpha, total flexural power reflected with consideration of material damping and rubber layer, were suppressed for lower frequency and only at its maximum for 180^o of angle. Whereas the total reflected longitudinal power at its maximum for 100^o of joint angle during lower frequency, and as the frequency increased, maximum power observed to be at around 125^o of joint angle. In Beta section of transmitted power, flexural would be maximum at 100^o of angle and longitudinal power peaks at 180^o and 0^o for lower frequency range. The results could be further interpreted for several types of cross-sections or different rubber layer properties for the purpose of design and configurations.

Overall, analysis of the variable joint was agreed successful in predicting the vibration power behaviour of reflected and transmitted, as well as elaborating on the contrast between different sections of alpha, beta, gamma and as well as between flexural and longitudinal power of the results.

Chapter 8: Conclusion

Vibration power for transmission and reflection have been investigated in this work. Method of using SEA as well as the WFE elaborated in early chapter, could be assisted by the understanding of power reflected and transmitted obtained in this thesis work. The knowledge of vibration in this area could be said have extended onwards. Contributions in terms of precise joint modelling have been successful and validated with the previous works, numerical validation as well as measurement outcomes.

Novelty of the said work have been verified through several measurements, checked for power balanced as well as analysed in particular frequency to ensure its validity. Set-up of measurements were also reflected successful as results obtained were plausible in terms of corresponding power at frequency and angle investigated. Method used were following the parameters and technique suggested in literatures. Free-free boundary condition of the 2-beam set-up have been complied with the best effort possible.

8.1 Variable joint

Chapter 4 have concluded the effects of variable joints, while Chapter 5 successfully models the analysis in representation of real systems. Chapter 6 and 7 deals with the experimentations while comparing with the models and summarises several design rules and design perspectives. It is important to highlight that the effect of considering material damping has given clearer insight of how the reflected and transmitted vibration power dominates or suppressed in certain angles.

Starting from consideration of joint increments, mass of joint affecting the centre of mass location, and to finally equate the continuity, force and moments, the variable joint has successfully shows the advantages and substantial results. Incorporation of force input in the numerical model for comparison to experimental work relates real applications to the beam.

The variable joint was derived from a physical mathematical model hence the corresponding response could be calculated with the Euler Bernoulli theory. Points have been highlighted for the dynamic changes for the novel variable joint model which at about 145° of angle, the centre of rotation for beam analysis would coincide with the geometric centre. This have provided a new highlight for the power reflected and transmitted especially relating to cross-coupling power.

Change in material type for the joint, could as well be an area of further understanding the power reflected and transmitted. The consideration of other theory such as Timoshenko beam could also be incorporated into the comparison for the optimum method.

8.2 Numerical Investigations

An analysis at 90° joint angle would be best to be elaborated in the success of this work. Result plotted from previous analysis in section 7.6.1and section 7.6.2 for reflected and transmitted of flexural and longitudinal power were further examined.

Figure 8-1 shows the power in beam 1 & beam 2 for flexural reflected and transmitted at 90° of joint angle. Power for beams without material damping would not considers the loss factor and be equated to 50% (as another 50% of power flexural were transmitted to opposite direction of beam). Once material damping being considered, the loss factor effect could be clearly observed especially on transmitted side in beam2. Rubber layer provides additional power loss at beam 2, but however in beam 1 the reflected power slightly increases in between 0 to 1500Hz.

Figure 8-2 examines the longitudinal power behaviour for its reflection and transmission at 90° angle of joint. Total of 50% power would be equated for beams without material damping due the same comments as flexure power. With the use of complex Young’s modulus, which considering the loss factor, the power reflected seen drastically drops especially for reflection in beam 1, as the increase of frequency. Rubber layer addition into the beam-joint arrangements causes further drop in power in both sides. This analysis could be expanded to various other joint angles of particular interest.

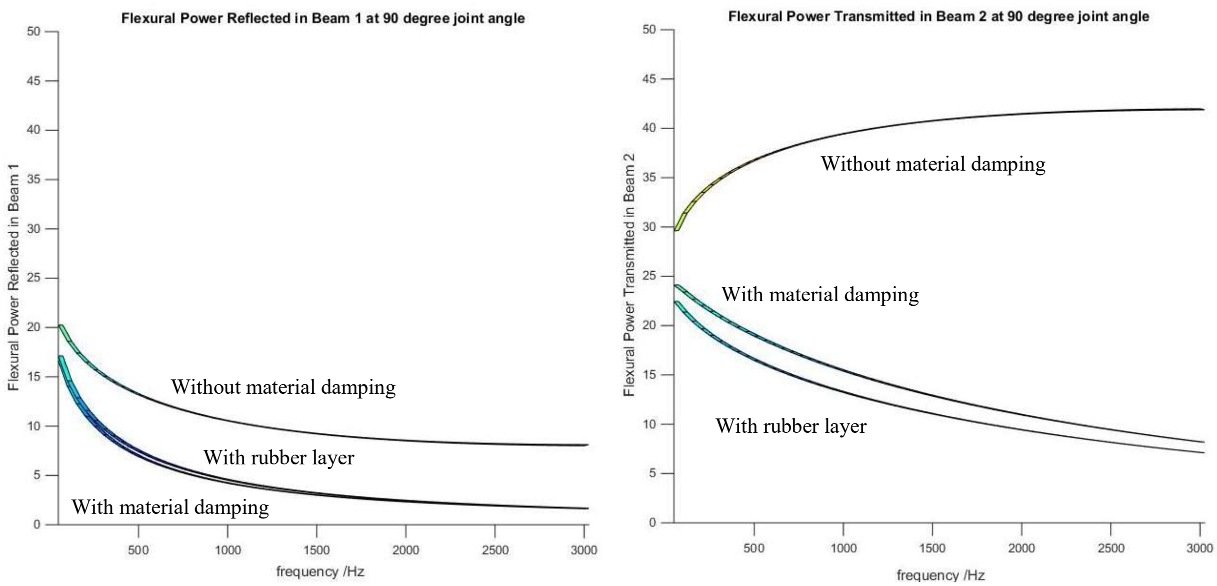

Figure 8-1: Flexural power reflected in beam 1 (alpha) & transmitted in beam 2 (beta) at 90º of joint angle beam with & without material damping, and rubber layer in-between beams and joints

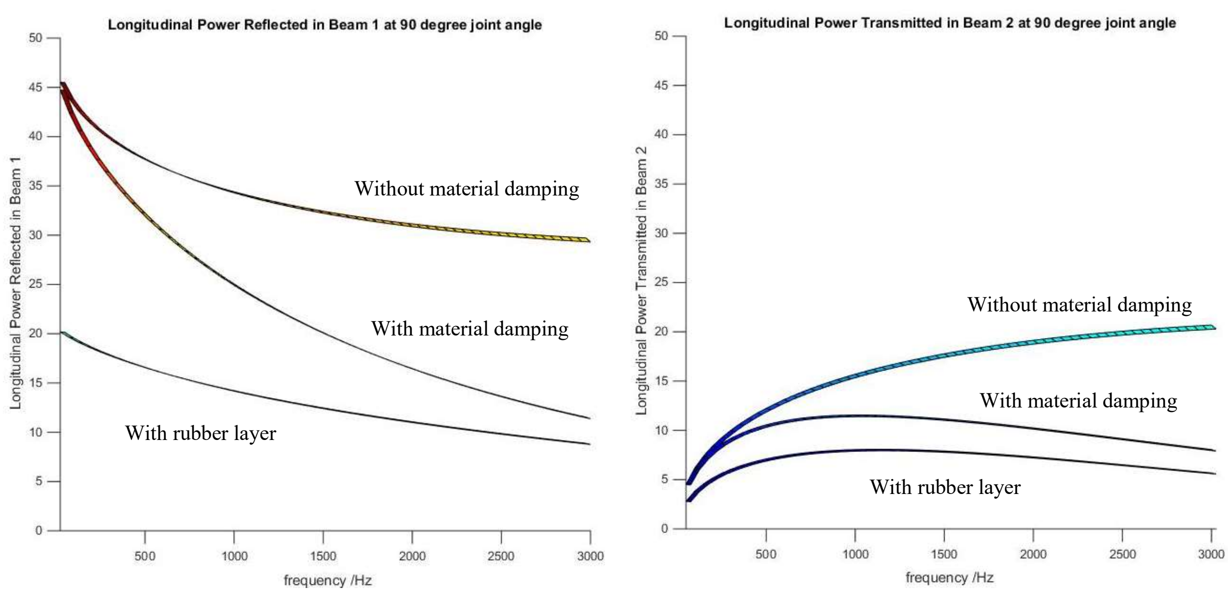

Figure 8-2: Longitudinal power reflected in beam 1 (alpha) & transmitted in beam 2 (beta) at 90º of joint angle beam with & without material damping, and rubber layer in-between beams and joints

Vast numerical investigation could be performed using the model achieved. Variable angle joint model was agreed as novel approach to understand the reflection and transmitted vibration power in the beam. This can be adopted for other types of joint with regards to the physical types of joint. Effects on range of the joint density change or beam cross section change could also be analysed using the codes developed. The work done have considered both region of frequency and angle against vibration power. Limitation of experimentation especially at 180° angle could be concluded as well from relationship obtained in previous chapters.

8.3 Future works: hybrid of cross sections, beam & joint materials

Further consideration will include the effect of damping and stiffness of other real joint which using bolts, welding and other types of structural fixtures. Development of a good relationship between the experiment and model will take this research to further in-depth knowledge for handling the real and more complicated joints.

Angle change in the joint could be further manipulated mathematically by considering various other beam cross section. This will extend another area of analysis of the variable joint. As highlighted earlier, the joint material properties could be further manipulated to consider material damping as well to obtain vibration power characteristics for reflected and transmitted vibration in beams.

Cross section of beam from shapes of square, wider rectangular (lower height to width ratio), or hollow beams could be further analysed and investigated for the vibration transmission power. These examples of various areas of further works would complement the current work, acknowledge the past and of course improving the future, on vibration power reflection and transmission.

Bibliography

Albert.L.Stiehl. "Power flow analysis of beam members with multiple wave types." *Finite Element in analysis and design (21).* 1996. 253-264.

B.Kang. "Transfer function of one dimensional distributed parameter systems by wave approach." *Journal of Vibration and Acoustics* 129 (,April 2007): 193-291.

B.M.Gibbs, & J.D.Tattersal. "Vibrational energy transmission and mode conversion of a corner junction of square section rods." *Journal of Vibration, Acoustics, Stress and Reliability in Design* 109 (Oct 1987): 348-355.

B.R.Mace. "Active control of flexural vibrations." *Journal of Sound and Vibration, 114(2)* 114(2) (1987): 253-270.

B.R.Mace. "Wave reflection and transmission in beams." *Journal of Sound and Vibration* 97(2) (1984): 237-246.

C.J.Wu, R.G.White. "Reduction of vibrational power in periodically supported beams by use of neutralizer." *Journal of Sound and Vibration* 187(2) (1995): 329-338.

C.Mei. "Effect of material coupling on wave vibration of composite Euler-Bernoulli beam structures." *Journal of Sound and Vibration* 288 (2005): 177-193.

C.Mei. "The Analysis and control of longitudinal vibrations from wave viewpoint." *Journal of Vibration and Acoustic* 124 (October 2002): 645-649.

C.Mei. "Wave analysis of In-Plane vibrations of H-and T-shaped planar frame structures." *Journal of Vibration and Acoustics, vol 130, 061004* 130 (Dec 2008): 1-10.

C.Mei, B.R.Mace. "Wave reflection and transmission in Timoshenko beams and wave analysis of Timoshenko beam structures." *Transaction of ASME, vol 127* 127 (August 2005): 382-394.

Chun-Chuan Liu, Feng-Ming Li, Bo Fang, Yang Zhao, Wen-Hu Huang. "Active control of power flow transmission in finite connected plate." *Journal of Sound and Vibration (329)* 329 (2010): 4124-4135.

Cremer, Heckl, Petersson. *Structure-borne sound : Structural Vibrations and Sound Radiation at Radio Frequency, 3rd Edition.* Springer-Verlag, 2005.

Dossing, Ole. *Structural testing Part 1&2.* Naerum Denmark: Bruel&Kjaer, 1988.

E.Viola, P.Ricci, M.H.Aliabadi. "Free vibration analysis of axially loaded cracked Timishenko beam structures using the dynamic stiffness method." *Journal of Sound and Vibration (304)* 304 (2007): 124-153.

F.Fariborzi, M.F.Golnaraghi, G.R.Heppler. "Experimental control of free and forced structural vibration using a linear coupling strategy." *Smart material structure*, June (1997): 540-548.

H.Tongue, Benson. *Principle of Vibration 2nd Edition.* New York: Oxford University Press Inc, 2002.

Hyungmi Oh, Usik-Lee, Dong-Hynn Park. "Dynamics of an axially moving Bernoulli-Euler Beam: Spectral Element Modelling and analysis." *KSME International Journal, volume 18* 18 (2004), no. 3 (2004): no.3, 395-406.

J.Dai, J.C.S.Lai, H.M.Williamson, Y.J.Li. "Investigation of vibration power transmission over a rectangular excitation area using effective point mobility." *Journal of Sound and Vibration (225)5* 225(5) (1999): 831-844.

J.F. Doyle, S.Kamle. "An experimental study of the reflection and transmission of flexural waves at an arbitrary T-joint." *Journal of Applied Mechanics* 54 (1987): 136–140.

J.L.Horner. “Vibration Power Transmission through Beam-Like structures.” *PhD Thesis University of Southampton.* UK, 1990.

J.L.Horner, R.G.White. “Prediction of vibrational power transmission through bends and joints in beam like structures.” *Journal of sound and vibration, volume 147, Issue 1*, 1991: 87-103.

J.L.Horner, R.G.White. “Prediction of vibrational power transmission through jointed beams.” *International Journal of the Mechanical Sciences* 32, no. 3 (1990).

J.M. Muggleton, T.P. Waters, B.R. Mace, B. Zhang. “Approaches to estimating the reflection and transmission coefficients of discontinuities in waveguides from measured data.” *Journal of Sound and Vibration* 307, no. Issues 1-2 (2007): 280-294.

J.W.Verheij. “Cross spectral density methods for measuring structure borne power flow on beam and pipes.” *Journal of Sound and Vibration* 70(1) (1980): 133-139.

Jonas L.Svensson, Patrick B.U.Andersson, Joachim Scheuren, Wolfgang Kropp. “Active scattering control of Flexural Waves at beam junctions: The influence of beam properties on Power flow and control effort.” *Journal of Sound and Vibration* 313 (2008).

K.Renji, M.Mahalakshmi. “High frequency vibration energy transfer in a system of three plates connected at discrete points using statistical energy analysis.” *Journal of Sound and Vibration (296)* 296 (2006): 539-553.

K.Shankar, A.J.Keane. “Vibrational Energy flow analysis using a substructure approach : The application of receptance theory to FEA and SEA.” *Journal of Sound and Vibration (201)4* 201(4) (1997): 491-513.

L.C.Chow, R.J.Pinnington. “Practical industrial method of increasing structural damping in machinery, I:Squeeze film damping with air.” *Journal of Sound and Vibration (118)1* 118(1) (1987): 123-139.

L.Gaul. “Wave transmission and energy dissipation at structural and machine joints.” *Journal of Vibration, Acoustic, Stress, and Reliability in Design* 105 (October 1983): 489-496.

M.Meo, G.Zumpano, M.Piggott, G.Marengo. “Impact Identification on a sandwich plate from wave propagation responses.” *Composite structures 71*, 2005: 302-306.

M.O.Kaya, O.Ozdemir Ozgumus. “Flexural-torsional-coupled vibration analysis of axially loaded closed-section composite Timoshenko beam using DTM.” *Journal of Sound and Vibration (306)* 306 (Sept 2007): 495-506.

M.Petyt, G.H.Koopmann and R.J.Pinnington. “The acoustic modes of a rectangular cavity containing a rigid incomplete partition.” *Journal of Sound and Vibration* 53(1) (1977): 71-82.

McConnell, Kenneth G, and Paul S.Varoto. *Vibration Testing Theory and Practice, 2nd Edition.* New Jersey: John Wiley and Sons, 2008.

R.J.Pinnington. “Vibrational power transmission from a finite source beam to an infinite receiver beam via a continuous complaint mount.” *Journal of Sound and Vibration (137)1* 137 (1) (1990): 117-129.

R.J.Pinnington. “Vibrational power transmission to a seating of a vibration isolated motor.” *Journal of Sound and Vibration (118)3* 118(3) (1987): 515-530.

R.J.Pinnington, R.G.White. “Power flow through machine isolators to resonant and non-resonant beams.” *Journal of Sound and Vibration* 75(2) (1981): 179-197.

R.Martinez-Val, E.Perez. “Aeronautics and Astronautics: recent progress and future trends.” *Journal Mechanical Engineering Science* (Proc IMechE : Journal Mechanical Engineering Science) 223, no. Part C (n.d.): Proc IMechE vol 223 Part C.

R.S.Langley. “A variational principle for periodic structures.” *Journal of Sound and Vibration* 135(1) (1989): 135-142.

R.S.Langley. “Analysis of beam and plate vibrations by using the wave equation.” *Journal of Sound and Vibration* 150 (1) (1991): 47-65.

R.S.Langley. “Elastic wave transmission coefficients and coupling loss factors for structural junctions between curved panels.” *Journal of Sound and Vibration* 69(3) (1994): 297-317.

R.S.Langley. “Power transmission in a one-dimensional periodic structure subjected to single-point excitation.” *Journal of Sound and Vibration (185)3* 185(3) (1995): 552-558.

R.S.Langley. “The statistics of wave transmission through disordered periodic waveguides.” *Journal of Sound and Vibration* 189 (4) (1996): 421-441.

—. “Wave motion and SEA.” *Seminar of High Frequency vibration prediction .* Madingley Hall, Cambridge University, U.K, 2010.

R.S.Langley, K.H.Heron. “Elastic wave transmission through plate/beam junction.” *Journal of Sound and Vibration, 143 (2)*, 1990: 241-253.

R.Whalley, M.Ebrahimi. *Vibration and control of aircraft wings.* Proc IMechE, 1998.

Renno, Jamil M, and Brian R Mace. “Calculation of reflection and transmission coefficients of joints using a hybrid finite element/wave and finite element approach.” *Journal of Sound and Vibration 332*, 2013: 2149-2164.

S.J.Walsh, R.G.White. “Measuring of vibrational power transmission in curved beams.” *Journal of Sound and Vibration (241)2* 241(2) (2001): 157-183.

S.J.Walsh, R.G.White. “Vibrational power transmission in curved beams.” *Journal of Sound and Vibration (233)3* 233 (3) (2000): 455-488.

S.K.Lee. “Identification of a vibration transmission path in a vehicle by measuring vibrational power flow.” *IMechE Journal Automobile Engineering, vol 218* Vol 218 (2004): Part D.

S.K.Lee, B.R.Mace, M.J.Brennan. “Wave propogation reflection and transmission in curved beams.” *Journal of Sound and Vibration (306)* 306 (2007): 636-656.

T.Eck, S.J.Walsh, J.L.Horner. “Measurement of vibrational energy and point mobility of a beam subjected to moment excitation using a finite difference approximation.” *Journal Mechanical Engineering Science Proc IMechE, vol 220, Part C*, 2000: 795-806.

T.N.Farris, J.F.Doyle. “Wave propogation in a split Timoshenko-beam.” *Journal of Sound and Vibration, 130(1)* 130(1) (1989): 137-147.

T.Y.Li, W.H.Zhang, T.G.Liu,. “Vibrational power flow analysis of damaged beam structures.” *Journal of Sound and Vibration* 242, no. 1 (2001): 59-68.

W.T.Thomson. *Theory of Vibration with application 3rd Edition.* New Delhi: CBS Publishers & Distributors, 2002.

Wan-Chun Yuan, Li Zhou, Fuh-Gwo Yuan. “Wave reflection and transmission in composite beams containing semi-infinite delamination.” *Journal of Sound and Vibration, 313* 313 (2008): 676-695.

Y.P.Guo. “Flexural wave transmission through angled structural joints.” *Journal Acoustic Society of America* 97(1) (1995): 289-297.

Appendix Section

Appendix: $\boxed{\text{A-1}}$ Lumped mass Joint equation derivation: -

On the **incident side** of the bend for flexural displacement $W_{-}(x,t)$ and longitudinal displacement $U_{-}(x,t)$,

$$W_{-}(x,t) = \left\{A_1 e^{k_{f1}x} + A_3 e^{ik_{f1}x} + A_4 e^{-ik_{f1}x}\right\} e^{i\omega t} \;;$$

$$at\ \ x = 0 \quad \xrightarrow{yields} \quad \{A_1 + A_3 + A_4\}$$

$$\frac{\partial W_{-}}{\partial x} = k_{f1}\left\{A_1 e^{k_{f1}x} + iA_3 e^{ik_{f1}x} - iA_4 e^{-ik_{f1}x}\right\} \;;$$

$$at\ x = 0 \quad \xrightarrow{yields} \quad k_{f1}\{A_1 + iA_3 - iA_4\}$$

$$\frac{\partial^2 W_{-}}{\partial x^2} = {k_{f1}}^2\left\{A_1 e^{k_{f1}x} - A_3 e^{ik_{f1}x} - A_4 e^{-ik_{f1}x}\right\} \;;$$

$$at\ x = 0 \quad \xrightarrow{yields} \quad {k_{f1}}^2\{A_1 - A_3 - A_4\}$$

$$\frac{\partial^3 W_{-}}{\partial x^3} = {k_{f1}}^3\left\{A_1 e^{k_{f1}x} - iA_3 e^{ik_{f1}x} + iA_4 e^{-ik_{f1}x}\right\} \;;$$

$$at\ x = 0 \quad \xrightarrow{yields} \quad {k_{f1}}^3\{A_1 - iA_3 + iA_4\}$$

$$U_{-}(x,t) = \left\{A_L e^{ik_{l1}x} + A_I e^{-ik_{l1}x}\right\} e^{i\omega t} \;;$$

$$at\ \ x = 0 \quad \xrightarrow{yields} \quad \{A_L + A_I\}$$

$$\frac{\partial U_{-}}{\partial x} = k_{l1}\left\{iA_L e^{ik_{l1}x} - iA_I e^{-ik_{l1}x}\right\} \;;$$

$$at\ x = 0 \quad \xrightarrow{yields} \quad k_{l1}\{iA_L - iA_I\}$$

Differentiates $W_{-}$and $U_{-}$with respect to time (t);

$$\frac{\partial U_{-}}{\partial t} = i\omega\left\{A_L e^{ik_{l1}x} + A_I e^{-ik_{l1}x}\right\} e^{i\omega t} \;;$$

$$at\ t = 0, x = 0 \quad \xrightarrow{yields} \quad i\omega\{A_L + A_I\}$$

$$\frac{\partial^2 U_{-}}{\partial t^2} = -\omega^2\left\{A_L e^{ik_{l1}x} + A_I e^{-ik_{l1}x}\right\} e^{i\omega t} \;;$$

$$at\ t = 0, x = 0 \quad \xrightarrow{yields} \quad -\omega^2\{A_L + A_I\}$$

$$\frac{\partial W_{-}}{\partial t} = i\omega\left\{A_1 e^{k_{f1}x} + A_3 e^{ik_{f1}x} + A_4 e^{-ik_{f1}x}\right\} e^{i\omega t} \;;$$

$$at\ t = 0, x = 0 \quad \xrightarrow{yields} \quad i\omega\{A_1 + A_3 + A_4\}$$

$$\frac{\partial^2 W_-}{\partial t^2} = -\omega^2\{A_1 e^{k_{f1}x} + A_3 e^{ik_{f1}x} + A_4 e^{-ik_{f1}x}\}\ e^{i\omega t}\ ;$$

$$at\ t = 0, x = 0 \xrightarrow{yields} -\omega^2\{A_1 + A_3 + A_4\}$$

$$\frac{\partial}{\partial t}\frac{\partial W_-}{\partial x} = i\omega k_{f1}\{A_1 e^{k_{f1}x} + iA_3 e^{ik_{f1}x} - iA_4 e^{-ik_{f1}x}\}\ e^{i\omega t}\ ;$$

$$at\ t = 0, x = 0 \xrightarrow{yields} i\omega k_{f1}\{A_1 + iA_3 - iA_4\}$$

$$\frac{\partial^2}{\partial t^2}\frac{\partial W_-}{\partial x} = -\omega^2 k_{f1}\{A_1 e^{k_{f1}x} + iA_3 e^{ik_{f1}x} - iA_4 e^{-ik_{f1}x}\}\ e^{i\omega t}\ ;$$

$$at\ t = 0, x = 0 \xrightarrow{yields} -\omega^2 k_{f1}\{A_1 + iA_3 - iA_4\}$$

For the **transmitting side** of the bend for flexural $W_+(\psi, t)$ and longitudinal $U_+(\psi, t)$,

$$W_+(\psi, t) = \{B_2 e^{-k_{f2}\psi} + B_4 e^{-ik_{f2}\psi}\}\ e^{i\omega t}\ ;\quad at\ \psi = 0 \xrightarrow{yields} \{B_2 + B_4\}$$

$$\frac{\partial W_+}{\partial \psi} = k_{f2}\{-B_2 e^{-k_{f2}\psi} - iB_4 e^{-ik_{f2}\psi}\};\quad at\ \psi = 0 \xrightarrow{yields} k_{f2}\{-B_2 - iB_4\}$$

$$\frac{\partial^2 W_+}{\partial \psi^2} = k_{f2}{}^2\{B_2 e^{-k_{f2}\varphi} - B_4 e^{-ik_{f2}\varphi}\};\quad at\ \psi = 0 \xrightarrow{yields} k_{f2}{}^2\{B_2 - B_4\}$$

$$\frac{\partial^3 W_+}{\partial \psi^3} = k_{f2}{}^3\{-B_2 e^{-k_{f2}\psi} + iB_4 e^{-ik_{f2}\psi}\};\quad at\ \psi = 0 \xrightarrow{yields} k_{f2}{}^3\{-B_2 + iB_4\}$$

$$U_+(\psi, t) = \{B_L e^{-ik_{l2}\psi}\}\ e^{i\omega t}\ ;\quad at\ \psi = 0 \xrightarrow{yields} \{B_L\}$$

$$\frac{\partial U_+}{\partial \psi} = k_{l2}\{-iB_L e^{-ik_{l2}\psi}\};\quad at\ \psi = 0 \xrightarrow{yields} k_{l2}\{-iB_L\}$$

Applying boundary condition at $x = 0$ and $\psi = 0$, to all equation of continuity, summation of bending moments, shear forces and compressive forces, yields 6 governing equations as below: -

I. Continuity of displacement in axial direction

$$U_- = U_+\cos\theta - W_+\sin\theta + \frac{L}{2}\boldsymbol{\sin\theta}\frac{\partial W_+}{\partial \psi}$$

$$A_I + A_L = B_L\cos\theta - (B_2 + B_4)\sin\theta + \frac{L}{2}\boldsymbol{\sin\theta}\,(-k_{f2})(B_2 + iB_4)$$

$$A_I = -A_L + B_L\cos\theta - B_2\sin\theta - B_4\sin\theta - (k_2)\frac{L}{2}\,B_2\boldsymbol{\sin\theta} - (k_{f2})\frac{L}{2}\,iB_4\,\boldsymbol{\sin\theta}$$

$$\left[\!\left[A_I = -A_L + B_L\cos\theta - B_2 \underbrace{\left[\sin\theta + \left(k_{f2}\right)\frac{L}{2}\ \mathbf{sin}\,\boldsymbol{\theta}\right]}_{S1} - B_4 \underbrace{\left[i\left(k_{f2}\right)\frac{L}{2}\ \mathbf{sin}\,\boldsymbol{\theta} + \sin\theta\right]}_{S2} \right]\!\right]$$

II. Continuity of relative displacement in perpendicular direction

$$W_- = U_+\sin\theta + W_+\cos\theta - \frac{L}{2}(\mathbf{1}+\mathbf{cos\,\theta})\frac{\partial W_+}{\partial\psi}$$

$$A_1 + A_3 + A_4 = B_L\sin\theta + (B_2 + B_4)\cos\theta - \frac{L}{2}\,(\mathbf{1}+\mathbf{cos\,\theta})\left(-k_{f2}\right)(B_2 + iB_4)$$

$$A_4 = -A_1 - A_3 + B_L\sin\theta + B_2\cos\theta + B_4\cos\theta + B_2\left[\left(k_{f2}\right)\frac{L}{2}\,(\mathbf{1}+\mathbf{cos\,\theta})\right] + iB_4\left[\left(k_{f2}\right)\frac{L}{2}\,(\mathbf{1}+\mathbf{cos\,\theta})\right]$$

$$\left[\!\left[A_4 = -A_1 - A_3 + B_L\sin\theta + B_2\underbrace{\left[\cos\theta + \left[\left(k_{f2}\right)\frac{L}{2}\,(\mathbf{1}+\mathbf{cos\,\theta})\right]\right]}_{S3} + B_4\underbrace{\left[\cos\theta + i\left[\left(k_{f2}\right)\frac{L}{2}\,(\mathbf{1}+\mathbf{cos\,\theta})\right]\right]}_{S4} \right]\!\right]$$

III. Continuity of angular displacement/equal gradient

$$\frac{\partial W_-}{\partial x} = \frac{\partial W_+}{\partial\psi}$$

$$k_{f1}(A_1 + iA_3 - iA_4) = -k_{f2}(B_2 + iB_4)$$

$$-A_1 - iA_3 + iA_4 = \frac{k_{f2}}{k_{f1}}(B_2 + iB_4)$$

$$iA_4 = A_1 + iA_3 + B_2\left[\frac{k_{f2}}{k_{f1}}\right] + B_4\left[i\frac{k_{f2}}{k_{f1}}\right]$$

$$\left[\!\left[A_4 = \underbrace{\left[\frac{A_1}{i}\right]}_{S} + A_3 + \frac{B_2}{i}\underbrace{\left[\frac{k_{f2}}{k_{f1}}\right]}_{S5} + B_4\underbrace{\left[\frac{k_{f2}}{k_{f1}}\right]}_{S5a} \right]\!\right]$$

IV. Equilibrium of bending moment

$$E_1 I_1 \frac{\partial^2 W_-}{\partial x^2} + \frac{L}{2} E_1 I_1 \frac{\partial^3 W_-}{\partial x^3} = E_2 I_2 \frac{\partial^2 W_+}{\partial \psi^2} - \frac{L}{2} E_2 I_2 \frac{\partial^3 W_+}{\partial \psi^3} - I_j \frac{\partial^2 \partial W_-}{\partial t^2 \partial x}$$

$$E_1 I_1 (k_{f1}^2)(A_1 - A_3 - A_4) + \frac{L}{2} E_1 I_1 (k_{f1}^3)(A_1 - iA_3 + iA_4) = E_2 I_2 (k_{f2}^2)(B_2 - B_4) - \frac{L}{2} E_2 I_2 (k_{f2}^3)(iB_4 - B_2) - I_j(-\omega^2)(k_{f1})(A_1 + iA_3 - iA_4)$$

$$-A_4 \left(E_1 I_1 (k_{f1}^2)\right) + iA_4 \left(\frac{L}{2} E_1 I_1 (k_{f1}^3)\right) - iA_4 \left(I_j(\omega^2 k_{f1})\right) = B_2 \left(E_2 I_2 (k_{f2}^2)\right) - B_4 \left(E_2 I_2 (k_{f2}^2)\right) + B_2 \left(\frac{L}{2} E_2 I_2 (k_{f2}^3)\right) - iB_4 \left(\frac{L}{2} E_2 I_2 (k_{f2}^3)\right) - A_1 \left(\left(E_1 I_1 (k_{f1}^2)\right) + \left(\frac{L}{2} E_1 I_1 (k_{f1}^3)\right) + \left(I_j(\omega^2 k_{f1})\right)\right) + A_3 \left(\left(E_1 I_1 (k_{f1}^2)\right) + i\left(\frac{L}{2} E_1 I_1 (k_{f1}^3)\right) - i\left(I_j(\omega^2 k_{f1})\right)\right)$$

$$\left[\!\left[A_4 \underbrace{\left[-\left(E_1 I_1 (k_{f1}^2)\right) + i\left(\frac{L}{2} E_1 I_1 (k_{f1}^3)\right) - i\left(I_j(\omega^2 k_{f1})\right)\right]}_{S6} = -A_1 \underbrace{\left[\left(E_1 I_1 (k_{f1}^2)\right) + \left(\frac{L}{2} E_1 I_1 (k_{f1}^3)\right) + \left(I_j(\omega^2 k_{f1})\right)\right]}_{S7} + A_3 \underbrace{\left[\left(E_1 I_1 (k_{f1}^2)\right) + i\left(\frac{L}{2} E_1 I_1 (k_{f1}^3)\right) - i\left(I_j(\omega^2 k_{f1})\right)\right]}_{S8} + B_2 \underbrace{\left[\left(E_2 I_2 (k_{f2}^2)\right) + \left(\frac{L}{2} E_2 I_2 (k_{f2}^3)\right)\right]}_{S9} - B_4 \underbrace{\left[\left(E_2 I_2 (k_{f2}^2)\right) + i\left(\frac{L}{2} E_2 I_2 (k_{f2}^3)\right)\right]}_{S9a} \right]\!\right]$$

V. Equilibrium of compressive force

$$E_1A_1\frac{\partial U_-}{\partial x} = E_2A_2\frac{\partial U_+}{\partial \psi}\cos\theta + E_2I_2\frac{\partial^3 W_+}{\partial \psi^3}\sin\theta - m_j\frac{\partial^2 U_-}{\partial t^2}$$

$$E_1A_1(k_{l1})(iA_L - iA_I) = E_2A_2(k_{l2})(-iB_L)\cos\theta + E_2I_2\left(-k_{f2}^3\right)(B_2 - iB_4)\sin\theta - m_j(-\omega^2)(A_I + A_L)$$

$$\left[\!\left[A_I\underbrace{\left[-i\left(E_1A_1(k_{l1})\right) - \left(m_j\omega^2\right)\right]}_{S1} = A_L\underbrace{\left[-i\left(E_1A_1(k_{l1})\right) + \left(m_j\omega^2\right)\right]}_{S1} - B_L\underbrace{\left[i(E_2A_2(k_{l2})\cos\theta)\right]}_{S1} - B_2\underbrace{\left[E_2I_2\left(k_{f2}^3\right)\sin\theta\right]}_{S14} + B_4\underbrace{\left[i\left(E_2I_2\left(k_{f2}^3\right)\sin\theta\right)\right]}_{S1} \right]\!\right]$$

VI. Equilibrium of shear force

$$-E_1I_1\frac{\partial^3 W_-}{\partial x^3} = E_2A_2\frac{\partial U_+}{\partial \psi}\sin\theta - E_2I_2\frac{\partial^3 W_+}{\partial \psi^3}\cos\theta - m_j\frac{\partial^2}{\partial t^2}\left[W_- - \frac{L}{2}\frac{\partial W_-}{\partial x}\right]$$

$$-E_1I_1\left(k_{f1}^3\right)(A_1 - iA_3 + iA_4) = E_2A_2(k_{l2})\,(-iB_L)\sin\theta - E_2I_2\left(-k_{f2}^3\right)(B_2 - iB_4)\cos\theta - m_j\omega^2\left[-(A_1 + A_3 + A_4) - \langle\frac{L}{2}(k_{f1})(A_1 + iA_3 - iA_4)\rangle\right]$$

$$iA_4\left(-E_1I_1\left(k_{f1}^3\right)\right) + A_1\left(-E_1I_1\left(k_{f1}^3\right)\right) - iA_3\left(-E_1I_1\left(k_{f1}^3\right)\right) = -iB_L(E_2A_2(k_{l2})\sin\theta) + B_2\left(E_2I_2\left(k_{f2}^3\right)\cos\theta\right) - iB_4\left(E_2I_2\left(k_{f2}^3\right)\cos\theta\right) + A_4\left(m_j\omega^2\right) + {}_1\left(m_j\omega^2\right) + A_3\left(m_j\omega^2\right) - iA_4\left(\left(m_j\omega^2\right)\frac{L}{2}(k_{f1})\right) + A_1\left(\left(m_j\omega^2\right)\frac{L}{2}(k_{f1})\right) + iA_3\left(\left(m_j\omega^2\right)\frac{L}{2}(k_{f1})\right)$$

$$\left[\!\left[A_4 \underbrace{\left[\left(-iE_1I_1\left(k_{f1}^3\right)\right) - \left(m_j\omega^2\right) + \left(i\left(m_j\omega^2\right)\frac{L}{2}\left(k_{f1}\right)\right)\right]}_{S16} \right.\right.$$

$$= A_1 \underbrace{\left[\left(E_1I_1\left(k_{f1}^3\right)\right) + \left(m_j\omega^2\right) + \left(\left(m_j\omega^2\right)\frac{L}{2}\left(k_{f1}\right)\right)\right]}_{S1}$$

$$+ A_3 \underbrace{\left[\left(-iE_1I_1\left(k_{f1}^3\right)\right) + \left(m_j\omega^2\right) + \left(i\left(m_j\omega^2\right)\frac{L}{2}\left(k_{f1}\right)\right)\right]}_{S18} - B_L \underbrace{\left[iE_2A_2\left(k_{l2}\right)\sin\theta\right]}_{S19}$$

$$\left.\left. + B_2 \underbrace{\left[E_2I_2\left(k_{f2}^3\right)\cos\theta\right]}_{S20} - B_4 \underbrace{\left[iE_2I_2\left(k_{f2}^3\right)\cos\theta\right]}_{S21} \right]\!\right]$$

Appendix: A-2 MATLAB coding for Lumped Mass Joint: -

```
%function Coupled_joint_comparex
%% Coupled and joint - (bending<flex> and compressive<long> waves)
clear all
clf
format long e
%Given
b=0.1;%0.05;                    %m
d=0.02;%0.006;                  %m
E1=1.75e9;%5.567e9;%            %N/m^2
I1=(b*(d^3))/12;                %m^4
A1=b*d;                         %m^2
E2=1.75e9;%5.567e9;%            %N/m^2
I2=(b*(d^3))/12;                %m^4
A2=b*d;                         %m^2
RHO=1170;%1165;                 %kg/m^3
RHOj=1170;%1165;                %kg/m^3
Jw=1*b;                         %m
L=1*d;                          %m

%Input
A4=1;%25e-6;                    %m
Ai=1;%25e-6;                    %m

%% Main

tht=zeros;
fqt=zeros;

nP1=zeros;
nP2=zeros;
nP3=zeros;
nP4=zeros;
nP5=zeros;
nP6=zeros;
nP7=zeros;
nP8=zeros;

Kf1=zeros;
Kf1t=zeros;
Kf2=zeros;
Kf2t=zeros;
Kl1=zeros;
Kl1t=zeros;
Kl2=zeros;
Kl2t=zeros;
Mj=zeros;
Mjt=zeros;
Ij=zeros;
Ijt=zeros;
```

```
afFF=zeros;
afFL=zeros;
btFF=zeros;
btFL=zeros;
afLL=zeros;
afLF=zeros;
btLL=zeros;
btLF=zeros;
afLN=zeros;
afFN=zeros;
btLN=zeros;
btFN=zeros;

%% main looping
fqcnt=0;
for fq=1500:500:1500;                                    %1/s
    fqcnt=fqcnt+1;

    thcnt=0;
    for thet=0:1:10;
        thcnt=thcnt+1;

        theta=pi*thet/180;
        Mj=RHOj*pi*(L^2)*Jw/4;                           %kg
        Ij=Mj*(L^2)/8;                                   %kgm^2

        omega=2*pi*fq;                                   %1/s
        Kf1=(omega^0.5)*(((RHO*A1)/(E1*I1))^0.25);       %1/m
        Kf2=(omega^0.5)*(((RHO*A2)/(E2*I2))^0.25);       %1/m
        Kl1=omega*sqrt(RHO/E1);                          %1/m
        Kl2=omega*sqrt(RHO/E2);                          %1/m

        %% matrix

        S=1/1i;

        S1=(sin(theta))*(1+(Kf2*(L/2)));
        S2=(sin(theta))*(1+(1i*Kf2*(L/2)));

        S3=(cos(theta))+(Kf2*L/2)+ (Kf2*L/2*(cos(theta)));
        S4=(cos(theta))+(1i*Kf2*L/2)+ (1i*Kf2*L/2*(cos(theta)));

        S5=(Kf2/Kf1)*(1/1i);
        S5a=Kf2/Kf1;

        S6=-(E1*I1*(Kf1^2))+(1i*(L/2)*E1*I1*(Kf1^3))-(1i*Ij*Kf1);
        S7=(E1*I1*(Kf1^2))+((L/2)*E1*I1*(Kf1^3))+(Ij*Kf1);
        S8=(E1*I1*(Kf1^2))+(1i*(L/2)*E1*I1*(Kf1^3))-(1i*Ij*Kf1);
        S9=(E2*I2*(Kf2^2))+((L/2)*E2*I2*(Kf2^3));
        S9a=(E2*I2*(Kf2^2))+(1i*(L/2)*E2*I2*(Kf2^3));

        S11=-(1i*E1*A1*Kl1)-(Mj*(omega^2));
        S12=-(1i*E1*A1*Kl1)+(Mj*(omega^2));
        S13=1i*E2*A2*Kl2*(cos(theta));
        S14=E2*I2*(Kf2^3)*(sin(theta));
```

```
S15=1i*E2*I2*(Kf2^3)*(sin(theta));

S16=-(1i*E1*I1*(Kf1^3))-((Mj*(omega^2))*(1-(1i*Kf1*(L/2))));
S17=(E1*I1*(Kf1^3))+((Mj*(omega^2))*(1+(Kf1*(L/2))));
S18=-(1i*E1*I1*(Kf1^3))+((Mj*(omega^2))*(1+(1i*Kf1*(L/2))));
S19=1i*E2*A2*Kl2*(sin(theta));
S20=E2*I2*(Kf2^3)*(cos(theta));
S21=1i*E2*I2*(Kf2^3)*(cos(theta));

x(1,1)=0;
x(1,2)=0;
x(1,3)=-1;
x(1,4)=cos(theta);
x(1,5)=-S1;
x(1,6)=-S2;

x(2,1)=-1;
x(2,2)=-1;
x(2,3)=0;
x(2,4)=sin(theta);
x(2,5)=S3;
x(2,6)=S4;

x(3,1)=S;
x(3,2)=1;
x(3,3)=0;
x(3,4)=0;
x(3,5)=S5;
x(3,6)=S5a;

x(4,1)=-(S7/S6);
x(4,2)=(S8/S6);
x(4,3)=0;
x(4,4)=0;
x(4,5)=(S9/S6);
x(4,6)=-(S9a/S6);

x(5,1)=0;
x(5,2)=0;
x(5,3)=(S12/S11);
x(5,4)=-(S13/S11);
x(5,5)=-(S14/S11);
x(5,6)=(S15/S11);

x(6,1)=(S17/S16);
x(6,2)=(S18/S16);
x(6,3)=0;
x(6,4)=-(S19/S16);
x(6,5)=(S20/S16);
x(6,6)=-(S21/S16);

zL=[Ai;0;0;0;Ai;0];
zF=[0;A4;A4;A4;0;A4];

yL=x\zL;
```

```
        yF=x\zF;

        tht(thcnt)=theta;
        fqt(fqcnt)=fq;
        Kf1t(fqcnt)=Kf1;
        Kf2t(fqcnt)=Kf2;
        Kl1t(fqcnt)=Kl1;
        Kl2t(fqcnt)=Kl2;
        Mjt(thcnt)=Mj;
        Ijt(thcnt)=Ij;

        %Note that for the matrix of X;
        %y(1)       %A1 Nm/s  xxxx
        %y(2)       %A3 Nm/s
        %y(3)       %AL Nm/s
        %y(4)       %BL Nm/s
        %y(5)       %B2 Nm/s  xxxx
        %y(6)       %B4 Nm/s

        afFF(thcnt)=(real(yF(2)))^2;
        afLF(thcnt)=(real(yL(2)))^2;
        btFF(thcnt)=(real(yF(6)))^2;
        btLF(thcnt)=(real(yL(6)))^2;

        afLL(thcnt)=(real(yL(3)))^2;
        afFL(thcnt)=(real(yF(3)))^2;
        btLL(thcnt)=(real(yL(4)))^2;
        btFL(thcnt)=(real(yF(4)))^2;

        afLN(thcnt)=(imag(yL(1)))^2;
        afFN(thcnt)=(imag(yF(1)))^2;
        btLN(thcnt)=(imag(yL(5)))^2;
        btFN(thcnt)=(imag(yF(5)))^2;

        Pf1=E1*I1*(Kf1^3)*omega*((yF(2))^2);        %Power in A due to
reflected flexural wave         yF(2)-> A3
        Pf2=E1*I1*(Kf1^3)*omega*((yL(2))^2);        %Power in A due to
reflected flexural wave         yL(2)-> A3
        Pf3=E2*I2*(Kf2^3)*omega*((yF(6))^2);        %Power in B due to
transmitted flexural wave       yF(6)-> B4
        Pf4=E2*I2*(Kf2^3)*omega*((yL(6))^2);        %Power in B due to
transmitted flexural wave       yL(6)-> B4

        Pl1=0.5*E1*A1*omega*Kl1*((yL(3))^2);        %Power in A due to
reflected longitudinal wave     yL(3)-> AL
        Pl2=0.5*E1*A1*omega*Kl1*((yF(3))^2);        %Power in A due to
reflected longitudinal wave     yF(3)-> AL
        Pl3=0.5*E2*A2*omega*Kl2*((yL(4))^2);        %Power in B due to
transmitted longitudinal wave   yL(4)-> BL
        Pl4=0.5*E2*A2*omega*Kl2*((yF(4))^2);        %Power in B due to
transmitted longitudinal wave   yF(4)-> BL

        PFlex=E1*I1*Kf1^3*omega*((abs(A4))^2);
        PLong=0.5*E1*A1*Kl1*omega*((abs(Ai))^2);
```

```
        nP1(thcnt,fqcnt)=(abs(Pf1)/abs(PFlex))*100;       % %power in A -
flexural incidence wave, flexural reflected wave
        nP2(thcnt,fqcnt)=(abs(Pf2)/abs(PLong))*100;       % %power in A -
longitudinal incidence wave, flexural reflected wave
        nP3(thcnt,fqcnt)=(abs(Pl2)/abs(PFlex))*100;       % %power in A -
flexural incidence wave, longitudinal reflected wave
        nP4(thcnt,fqcnt)=(abs(Pl1)/abs(PLong))*100;       % %power in A -
longitudinal incidence wave, longitudinal reflected wave

        nP5(thcnt,fqcnt)=(abs(Pf3)/abs(PFlex))*100;       % %power in B -
flexural incidence wave, flexural transmitted wave
        nP6(thcnt,fqcnt)=(abs(Pf4)/abs(PLong))*100;       % %power in B -
longitudinal incidence wave, flexural transmitted wave
        nP7(thcnt,fqcnt)=(abs(Pl4)/abs(PFlex))*100;       % %power in B -
flexural incidence wave, longitudinal transmitted wave
        nP8(thcnt,fqcnt)=(abs(Pl3)/abs(PLong))*100;       % %power in B -
longitudinal incidence wave, longitudinal transmitted wave


        A=nP2+nP4;
        B=nP6+nP8;
        C=B+A;

        D=nP1+nP3;
        E=nP5+nP7;
        F=D+E;

    end

end

fqt=1000:1000:5000;
tht=0:1:10;

figure(1)
plot(tht,nP1,'r')
hold on
plot(tht,nP2,'g')
hold on
plot(tht,nP3,'m')
hold on
plot(tht,nP4,'b')
hold on
grid on
title 'Percentage Power Reflected in Beam 1'
xlabel 'Angle of Arm 2 (Degrees)'
ylabel 'Percentage Power'
legend('FF','LF','FL','LL','Location','best');

figure(2)
plot(tht,nP5,'r')
hold on
plot(tht,nP6,'g')
hold on
plot(tht,nP7,'m')
```

```
hold on
plot(tht,nP8,'b')
hold on
grid on
title 'Percentage Power Transmitted to Beam 2'
xlabel 'Angle of Arm 2 (Degrees)'
ylabel 'Percentage Power'
legend('FF','LF','FL','LL','Location','best');

figure(3)
plot(tht,nP1,'r')
hold on
plot(tht,nP3,'m')
hold on
plot(tht,nP5,'r')
hold on
plot(tht,nP7,'m')
hold on
grid on
title 'Percentage Power Reflected from Flexural'
xlabel 'Angle of Arm 2 (Degrees)'
ylabel 'Percentage Power'
legend('FF1','FL1','FF2','FL2','Location','best');

figure(4)
plot(tht,nP2,'g')
hold on
plot(tht,nP4,'b')
hold on
plot(tht,nP6,'g')
hold on
plot(tht,nP8,'b')
hold on
grid on
title 'Percentage Power Reflected from Longitudinal'
xlabel 'Angle of Arm 2 (Degrees)'
ylabel 'Percentage Power'
legend('LF1','LL1','LF2','LL2','Location','best');

figure(5)
plot(tht,A,'r')
hold on
plot(tht,B,'b')
hold on
plot(tht,C,'k')
hold on
plot(tht,D,'.r')
hold on
plot(tht,E,'.b')
hold on
plot(tht,F,'.k')
hold on
grid on
title 'Total Power in Alpha and Beta'
xlabel 'Angle of Arm 2 (Degrees)'
ylabel 'Percentage Power'
```

```
legend('A','B','C','D','E','F','Location','best');

figure(6)
plot(tht,afFF,'r')
hold on
plot(tht,afLF,'g')
hold on
plot(tht,afFL,'m')
hold on
plot(tht,afLL,'b')
hold on
grid on
title 'Wave Amplitudes in Alpha'
xlabel 'Angle of Arm 2 (Degrees)'
ylabel 'Wave Amplitudes'
legend('FF','LF','FL','LL');

figure(7)
plot(tht,btFF,'r')
hold on
plot(tht,btLF,'g')
hold on
plot(tht,btFL,'m')
hold on
plot(tht,btLL,'b')
hold on
grid on
title 'Wave Amplitudes in Beta'
xlabel 'Angle of Arm 2 (Degrees)'
ylabel 'Wave Amplitudes'
legend('FF','LF','FL','LL');

figure(8)
plot(tht,afLN,'.b')
hold on
plot(tht,afFN,'.r')
hold on
plot(tht,btLN,'.g')
hold on
plot(tht,btFN,'.m')
hold on
grid on
title 'Near Field Wave Amplitudes in Alpha and Beta'
xlabel 'Angle of Arm 2 (Degrees)'
ylabel 'NF Wave Amplitudes'
legend('afLN','afFN','btLN','btFN');

figure(6)
surf(fqt,tht,nP1);
xlabel('frequency /Hz')
ylabel('angle \theta')
zlabel('FF - NP Reflected in Beam 1')
title('(Figure-5)Power vs angle \theta and frequency/Hz')
grid

figure (6)
```

```
surf(fqt,tht,nP2);
xlabel('frequency /Hz')
ylabel('angle \theta')
zlabel('LF - NP Reflected in Beam 1')
title('(Figure-6)Power vs angle \theta and frequency/Hz')
grid

figure (7)
surf(fqt,tht,nP3);
xlabel('frequency /Hz')
ylabel('angle \theta')
zlabel('FL - NP Reflected in Beam 1')
title('(Figure-7)Power vs angle \theta and frequency/Hz')
grid

figure (8)
surf(fqt,tht,nP4);
xlabel('frequency /Hz')
ylabel('angle \theta')
zlabel('LL - NP Reflected in Beam 1')
title('(Figure-8)Power vs angle \theta and frequency/Hz')
grid

figure (9)
surf(fqt,tht,nP5);
xlabel('frequency /Hz')
ylabel('angle \theta')
zlabel('FF - NP Transmitted to Beam 2')
title('(Figure-9)Power vs angle \theta and frequency/Hz')
grid

figure (10)
surf(fqt,tht,nP6);
xlabel('frequency /Hz')
ylabel('angle \theta')
zlabel('LF - NP Transmitted to Beam 2')
title('(Figure-10)Power vs angle \theta and frequency/Hz')
grid

figure (11)
surf(fqt,tht,nP7);
xlabel('frequency /Hz')
ylabel('angle \theta')
zlabel('FL - NP Transmitted to Beam 2')
title('(Figure-11)Power vs angle \theta and frequency/Hz')
grid

figure (12)
surf(fqt,tht,nP8);
xlabel('frequency /Hz')
ylabel('angle \theta')
zlabel('LL - NP Transmitted to Beam 2')
title('(Figure-12)Power vs angle \theta and frequency/Hz')
grid
```

```
% one joint in semi-infinite beam Feb 2010
% original coding from Dan Baldry
% calculates three different angle configurations

% onejoint.m


clear all

freq=input('Frequency in Hz = ');
w=2*pi*freq;              %Frequency (rad/sec)

b1=50e-3;                 %Breadth of beam A (metres)
d1=6e-3;                  %Depth of beam A (metres)
b2=b1;                    %Breadth of beam B (metres)
d2=d1;                    %Depth of beam B (metres)

A1=b1*d1;
A2=b2*d2;


E1=5.0e9;                 %Youngs Modulus of beam A
E2=5.0e9;                 %Youngs Modulus of beam B

I1=(b1*(d1^3))/12;
I2=(b2*(d2^3))/12;

rho1=1180;                %Density of beam A
rho2=1180;                %Density of beam B


rhoj=1180;                %Density of joint
J=50e-3;                  %Width of joint
L=6e-3;                   %Radius of joint
Mj=rhoj*pi*(L^2)*J/4;
Ij=Mj*L*L/8;

kf1=((rho1*b1*d1*(w^2))/(E1*I1))^(0.25)
kf2=kf1;

kl1=w*((rho1/E1)^(0.5))
kl2=kl1;




for n=1:180
    theta=n*2*pi/360;


B=[
```

```
   kf1 kf2 i*kf1 i*kf2 0 0
   -E1*I1*(kf1^3)-w*w*Mj*(1-kf1*(L/2)) -E2*I2*(kf2^3)*cos(theta)
i*E1*I1*(kf1^3)-w*w*Mj*(1-i*kf1*(L/2)) i*E2*I2*(kf2^3)*cos(theta)
i*E2*A2*kl2*sin(theta) 0
   0 (1+kf2*(L/2))*sin(theta) 0 (1+kf2*i*(L/2))*sin(theta) -cos(theta) 1
      E1*I1*(kf1^2)*(1+kf1*(L/2))-Ij*w*w*kf1 -E2*I2*(kf2^2)*(1+kf2*(L/2)) -
E1*I1*(kf1^2)*(1+kf1*i*(L/2))-Ij*i*w*w*kf1 E2*I2*(kf2^2)*(1+kf2*i*(L/2))    0
0

   1 -cos(theta)-kf2*(L/2)*(1+cos(theta)) 1 -cos(theta)-
kf2*i*(L/2)*(1+cos(theta)) -sin(theta) 0
   0 E2*I2*(kf2^3)*sin(theta) 0 -E2*I2*i*(kf2^3)*sin(theta)
i*E2*A2*kl2*cos(theta) i*E1*A1*kl1-Mj*w*w];

C=[ 0 0 -1  0  0 -i*E1*A1*kl1+Mj*w*w]';
%For longitudinal incident wave
D=[-i*kf1 -i*E1*I1*(kf1^3)+w*w*Mj*(1+kf1*-i*(L/2)) 0  E1*I1*(kf1^2)*(1-kf1*-
i*(L/2))-w*w*-i*kf1*Ij  -1 0]';    %For flexural incident wave

Along=(inv(B))*C;
%Longitudinal amplitudes
Aflex=(inv(B))*D;
%Flexural amplitudes

Along1(n,1)=Along(1,1);
Along2(n,1)=Along(2,1);
Along3(n,1)=Along(3,1);
Along4(n,1)=Along(4,1);

Along5(n,1)=Along(5,1);
Along6(n,1)=Along(6,1);

Aflex1(n,1)=Aflex(1,1);
Aflex2(n,1)=Aflex(2,1);
Aflex3(n,1)=Aflex(3,1);
Aflex4(n,1)=Aflex(4,1);

Aflex5(n,1)=Aflex(5,1);
Aflex6(n,1)=Aflex(6,1);

end

Pflex1=E1*I1*(kf1^3)*w*(Aflex3.^2);        %Power in beam A due to reflected
flexural wave
Pflex2=E1*I1*(kf1^3)*w*(Along3.^2);        %Power in beam A due to reflected
flexural wave
Pflex3=E2*I2*(kf2^3)*w*(Aflex4.^2);        %Power in beam B due to
transmitted flexural wave
Pflex4=E2*I2*(kf2^3)*w*(Along4.^2);        %Power in beam B due to
transmitted flexural wave


Plong1=0.5*E1*A1*w*kl1*(Along5.^2);        %Power in beam A due to reflected
longitudinal wave
```

```
Plong2=0.5*E1*A1*w*kl1*(Aflex5.^2);        %Power in beam A due to reflected
longitudinal wave
Plong3=0.5*E2*A2*w*kl2*(Along6.^2);        %Power in beam B due to
transmitted longitudinal wave
Plong4=0.5*E2*A2*w*kl2*(Aflex6.^2);        %Power in beam B due to
transmitted longitudinal wave


Pflexref=E1*I1*(kf1^3)*w*(1);
Plongref=0.5*E1*A1*w*kl1*(1);

P1=(abs(Pflex1)./Pflexref)*100;      %Percentage power in beam A - flexural
incidence wave, flexural reflected wave
P2=(abs(Pflex2)./Plongref)*100;      %Percentage power in beam A -
longitudinal incidence wave, flexural reflected wave
P3=(abs(Plong2)./Pflexref)*100;      %Percentage power in beam A - flexural
incidence wave, longitudinal reflected wave
P4=(abs(Plong1)./Plongref)*100;      %Percentage power in beam A -
longitudinal incidence wave, longitudinal reflected wave

P5=(abs(Pflex3)./Pflexref)*100;      %Percentage power in beam B - flexural
incidence wave, flexural transmitted wave
P6=(abs(Pflex4)./Plongref)*100;      %Percentage power in beam B -
longitudinal incidence wave, flexural transmitted wave
P7=(abs(Plong4)./Pflexref)*100;      %Percentage power in beam B - flexural
incidence wave, longitudinal transmitted wave
P8=(abs(Plong3)./Plongref)*100;      %Percentage power in beam B -
longitudinal incidence wave, longitudinal transmitted wave




thetaplot=[1:1:180];

figure(1)
plot(thetaplot,P1,'k')
grid on
hold on
plot(thetaplot,P2,'r')
hold on
plot(thetaplot,P3,'b')
hold on
plot(thetaplot,P4,'g')
hold on
title 'Percentage Power Reflected in Beam 1'
xlabel 'Angle of Arm 2 (Degrees)'
ylabel 'Percentage Power'
legend('FF','FL','LF','LL');

figure(2)
plot(thetaplot,P5,'k')
grid on
hold on
plot(thetaplot,P6,'r')
hold on
```

```
plot(thetaplot,P7,'b')
hold on
plot(thetaplot,P8,'g')
hold on
title 'Percentage Power Transmitted to Beam 2'
xlabel 'Angle of Arm 2 (Degrees)'
ylabel 'Percentage Power'
legend('FF','FL','LF','LL');
```

Appendix: $\boxed{\textbf{B-1}}$ U and W displacement for Variable Joint equation derivation: -

$$U_{+}cos\theta - W_{+}sin\theta = U_{M} + 2s\emptyset\left[sin\frac{\theta}{4}cos\theta - cos\frac{\theta}{4}sin\theta\right]$$

$$U_{+}sin\theta + W_{+}cos\theta = W_{M} + 2s\emptyset\left[sin\frac{\theta}{4}sin\theta + cos\frac{\theta}{4}cos\theta\right]$$

$$U_{-} = U_{+}cos\theta - W_{+}sin\theta + 2s\emptyset\left[sin\frac{\theta}{4} + sin\frac{3\theta}{4}\right]$$

$$W_{-} = U_{+}sin\theta + W_{+}cos\theta - 2s\emptyset\left[cos\frac{\theta}{4} + cos\frac{3\theta}{4}\right]$$

$$U_{-} = U_{+}cos\theta - W_{+}sin\theta + L\emptyset sin\frac{\theta}{4}\left[2sin\frac{\theta}{2}cos\frac{\theta}{4}\right]$$

$$W_{-} = U_{+}sin\theta + W_{+}cos\theta - L\emptyset sin\frac{\theta}{4}\left[2cos\frac{\theta}{2}cos\frac{\theta}{4}\right]$$

or

$$U_{-} = U_{+}cos\theta - W_{+}sin\theta + L\emptyset sin^{2}\frac{\theta}{2}$$

$$W_{-} = U_{+}sin\theta + W_{+}cos\theta - L\emptyset sin\frac{\theta}{2}cos\frac{\theta}{2}$$

Appendix: $\boxed{\text{B-2}}$ Variable Joint equation derivation: -

Continuity of displacement in axial direction

$$U_- = U_+ \cos\theta - W_+ \sin\theta + \frac{L}{2}(\mathbf{1-\cos\boldsymbol{\theta}})\frac{\partial W_+}{\partial\psi}$$

$$A_I + A_L = B_L \cos\theta - (B_2 + B_4)\sin\theta + \frac{L}{2}(\mathbf{1-\cos\boldsymbol{\theta}})(-k_{f2})(B_2 + iB_4)$$

$$A_I = -A_L + B_L\cos\theta - B_2\sin\theta - B_4\sin\theta - (k_{f2})\frac{L}{2}B_2(\mathbf{1-\cos\boldsymbol{\theta}}) - (k_{f2})\frac{L}{2}iB_4(\mathbf{1-\cos\boldsymbol{\theta}})$$

$$A_I = -A_L + B_L\cos\theta - B_2\underbrace{\left[\sin\theta + (k_{f2})\frac{L}{2}(\mathbf{1-\cos\boldsymbol{\theta}})\right]}_{S1B2} - B_4\underbrace{\left[i(k_{f2})\frac{L}{2}(\mathbf{1-\cos\boldsymbol{\theta}}) + \sin\theta\right]}_{S1B4}$$

Continuity of relative displacement in perpendicular direction

$$W_- = U_+\sin\theta + W_+\cos\theta - \frac{L}{2}(\mathbf{\sin\theta})\frac{\partial W_+}{\partial\psi}$$

$$A_1 + A_3 + A_4 = B_L\sin\theta + (B_2 + B_4)\cos\theta - \frac{L}{2}(\mathbf{\sin\theta})(-k_{f2})(B_2 + iB_4)$$

$$A_4 = -A_1 - A_3 + B_L\sin\theta + B_2\cos\theta + B_4\cos\theta + B_2\left[(k_{f2})\frac{L}{2}(\mathbf{\sin\theta})\right] + iB_4\left[(k_{f2})\frac{L}{2}(\mathbf{\sin\theta})\right]$$

$$\left[\!\!\left[A_4 = -A_1 - A_3 + B_L \sin\theta + B_2 \underbrace{\left[\cos\theta + \left[\left(k_{f2}\right)\frac{L}{2}\ (\mathbf{sin}\,\boldsymbol{\theta})\right]\right]}_{S2B2} + B_4 \underbrace{\left[\cos\theta + i\left[\left(k_{f2}\right)\frac{L}{2}\ (\mathbf{sin}\,\boldsymbol{\theta})\right]\right]}_{S2B4} \right]\!\!\right]$$

Continuity of angular displacement/equal gradient

$$\frac{\partial W_-}{\partial x} = \frac{\partial W_+}{\partial \psi}$$

$$k_{f1}(A_1 + iA_3 - iA_4) = -k_{f2}(B_2 + iB_4)$$

$$-A_1 - iA_3 + iA_4 = \frac{k_{f2}}{k_{f1}}(B_2 + iB_4)$$

$$iA_4 = A_1 + iA_3 + B_2\left[\frac{k_{f2}}{k_{f1}}\right] + B_4\left[i\frac{k_{f2}}{k_{f1}}\right]$$

$$\left[\!\!\left[A_4 = A_1 \underbrace{\left[\frac{1}{i}\right]}_{S3A1} + A_3 + B_2 \underbrace{\left[\frac{k_{f2}}{k_{f1}}.\frac{1}{i}\right]}_{S3B2} + B_4 \underbrace{\left[\frac{k_{f2}}{k_{f1}}\right]}_{S3B4} \right]\!\!\right]$$

Equilibrium of bending moment

$$E_1I_1\frac{\partial^2 W_-}{\partial x^2} + \frac{L}{2}\left(\mathbf{sin}\,\tfrac{\theta}{2}\right)E_1I_1\frac{\partial^3 W_-}{\partial x^3}$$
$$= E_2I_2\frac{\partial^2 W_+}{\partial \psi^2} - \frac{L}{2}\left(\mathbf{sin}\,\tfrac{\theta}{2}\right)E_2I_2\frac{\partial^3 W_+}{\partial \psi^3} - I_j\frac{\partial^2 \partial W_-}{\partial t^2 \partial x}$$
$$- \boldsymbol{E_1A_1\frac{\partial U_-}{\partial x}\left[\frac{L}{2}\left(1 - \cos\tfrac{\theta}{2}\right)\right]} + \boldsymbol{E_2A_2\frac{\partial U_+}{\partial \psi}\left[\frac{L}{2}\left(1 - \cos\tfrac{\theta}{2}\right)\right]}$$

$$E_1I_1\left(k_{f1}^2\right)(A_1 - A_3 - A_4) + \frac{L}{2}\left(\mathbf{sin}\,\tfrac{\theta}{2}\right)E_1I_1\left(k_{f1}^3\right)(A_1 - iA_3 + iA_4)$$
$$= E_2I_2\left(k_{f2}^2\right)(B_2 - B_4) - \frac{L}{2}\left(\mathbf{sin}\,\tfrac{\theta}{2}\right)E_2I_2\left(k_{f2}^3\right)(iB_4 - B_2)$$
$$- I_j(-\omega^2)\left(k_{f1}\right)(A_1 + iA_3 - iA_4) - \boldsymbol{\left[\frac{L}{2}\left(1 - \cos\tfrac{\theta}{2}\right)\right]E_1A_1(k_{l1})(iA_L - iA_I)}$$
$$+ \boldsymbol{\left[\frac{L}{2}\left(1 - \cos\tfrac{\theta}{2}\right)\right]E_2A_2(k_{l2})(-iB_L)}$$

$$-A_4\left(E_1I_1\left(k_{f1}^2\right)\right)+\ iA_4\left(\frac{L}{2}\left(\mathbf{sin}\,\tfrac{\theta}{2}\right)E_1I_1\left(k_{f1}^3\right)\right)+iA_4\left(I_j\omega^2k_{f1}\right)$$

$$=B_2\left(E_2I_2\left(k_{f2}^2\right)\right)-B_4\left(E_2I_2\left(k_{f2}^2\right)\right)+B_2\left(\frac{L}{2}\left(\mathbf{sin}\,\tfrac{\theta}{2}\right)E_2I_2\left(k_{f2}^3\right)\right)$$

$$-\ iB_4\left(\frac{L}{2}\left(\mathbf{sin}\,\tfrac{\theta}{2}\right)E_2I_2\left(k_{f2}^3\right)\right)$$

$$-\ A_1\left(\left(E_1I_1\left(k_{f1}^2\right)\right)+\left(\frac{L}{2}\left(\mathbf{sin}\,\tfrac{\theta}{2}\right)E_1I_1\left(k_{f1}^3\right)\right)-\left(I_j\left(\omega^2k_{f1}\right)\right)\right)$$

$$+A_3\left(\left(E_1I_1\left(k_{f1}^2\right)\right)+i\left(\frac{L}{2}\left(\mathbf{sin}\,\tfrac{\theta}{2}\right)E_1I_1\left(k_{f1}^3\right)\right)+i\left(I_j\left(\omega^2k_{f1}\right)\right)\right)$$

$$-\boldsymbol{iA_L}\left[\frac{\boldsymbol{L}}{\mathbf{2}}\left(\mathbf{1}-\mathbf{cos}\,\tfrac{\theta}{2}\right)\right]\boldsymbol{E_1A_1(k_{l1})}+\boldsymbol{iA_I}\left[\frac{\boldsymbol{L}}{\mathbf{2}}\left(\mathbf{1}-\mathbf{cos}\,\tfrac{\theta}{2}\right)\right]\boldsymbol{E_1A_1(k_{l1})}$$

$$-\boldsymbol{iB_L}\left[\frac{\boldsymbol{L}}{\mathbf{2}}\left(\mathbf{1}-\mathbf{cos}\,\tfrac{\theta}{2}\right)\right]\boldsymbol{E_2A_2(k_{l2})}$$

$$\Bigg[\!\!\Bigg[A_4\underbrace{\left[-\left(E_1I_1\left(k_{f1}^2\right)\right)+\ i\left(\frac{L}{2}\left(\mathbf{sin}\,\tfrac{\theta}{2}\right)E_1I_1\left(k_{f1}^3\right)\right)+i\left(I_j\omega^2k_{f1}\right)\right]}_{S4a}$$

$$+A_I\underbrace{\boldsymbol{i}\left[\frac{\boldsymbol{L}}{\mathbf{2}}\left(\mathbf{1}-\mathbf{cos}\,\tfrac{\theta}{2}\right)\right]\boldsymbol{E_1A_1(k_{l1})}}_{S4b}$$

$$=-A_1\underbrace{\left[\left(E_1I_1\left(k_{f1}^2\right)\right)+\left(\frac{L}{2}\left(\mathbf{sin}\,\tfrac{\theta}{2}\right)E_1I_1\left(k_{f1}^3\right)\right)-\left(I_j\left(\omega^2k_{f1}\right)\right)\right]}_{S41}$$

$$+A_3\underbrace{\left[\left(E_1I_1\left(k_{f1}^2\right)\right)+i\left(\frac{L}{2}\left(\mathbf{sin}\,\tfrac{\theta}{2}\right)E_1I_1\left(k_{f1}^3\right)\right)+i\left(I_j\left(\omega^2k_{f1}\right)\right)\right]}_{S4}$$

$$-A_L\left[\underbrace{\boldsymbol{i}\left(\frac{\boldsymbol{L}}{\mathbf{2}}\left(\mathbf{1}-\mathbf{cos}\,\tfrac{\theta}{2}\right)\right)\boldsymbol{E_1A_1(k_{l1})}}_{\mathbf{S43}}\right]-B_L\left[\underbrace{\boldsymbol{i}\left(\frac{\boldsymbol{L}}{\mathbf{2}}\left(\mathbf{1}-\mathbf{cos}\,\tfrac{\theta}{2}\right)\right)\boldsymbol{E_2A_2(k_{l2})}}_{\mathbf{S44}}\right]$$

$$+B_2\underbrace{\left[\left(\ \ {}_2I_2\left(k_{f2}^2\right)\right)+\left(\frac{L}{2}\left(\mathbf{sin}\,\tfrac{\theta}{2}\right)E_2I_2\left(k_{f2}^3\right)\right)\right]}_{S45}$$

$$-B_4\underbrace{\left[\left(E_2I_2\left(k_{f2}^2\right)\right)+i\left(\frac{L}{2}\left(\mathbf{sin}\,\tfrac{\theta}{2}\right)E_2I_2\left(k_{f2}^3\right)\right)\right]}_{S4}\Bigg]\!\!\Bigg]$$

Equilibrium of compressive force

$$E_1A_1\frac{\partial U_-}{\partial x} = E_2A_2\frac{\partial U_+}{\partial \psi}\cos\theta + E_2I_2\frac{\partial^3 W_+}{\partial \psi^3}\sin\theta - m_j\frac{\partial^2}{\partial t^2}\left[U_- - \boldsymbol{L}\left(\mathbf{sin}\tfrac{\theta}{4}\right)^{\mathbf{2}}\frac{\boldsymbol{\partial W_-}}{\boldsymbol{\partial x}}\right]$$

$$\begin{aligned}E_1A_1(k_{l1})(iA_L - iA_I) &= E_2A_2(k_{l2})(-iB_L)\cos\theta + E_2I_2\left(-k_{f2}^3\right)(B_2 - iB_4)\sin\theta \\ &- m_j(-\omega^2)\left[(A_I + A_L) - \boldsymbol{L}\left(\mathbf{sin}\tfrac{\theta}{4}\right)^{\mathbf{2}}(\boldsymbol{k_{f1}})(\boldsymbol{A_1} + \boldsymbol{iA_3} - \boldsymbol{iA_4})\right]\end{aligned}$$

$$\begin{aligned}\Bigg[\!\!\Bigg[A_I \underbrace{\left[-i\left(E_1A_1(k_{l1})\right) - \left(m_j\omega^2\right)\right]}_{S5b} &- A_4\underbrace{\left[\left(m_j\omega^2\right)\boldsymbol{iL}\left(\mathbf{sin}\tfrac{\theta}{4}\right)^{\mathbf{2}}(\boldsymbol{k_{f1}})\right]}_{S5a} \\ &= -A_1\underbrace{\left[\left(m_j\omega^2\right)\boldsymbol{L}\left(\mathbf{sin}\tfrac{\theta}{4}\right)^{\mathbf{2}}(\boldsymbol{k_{f1}})\right]}_{S51} - A_3\underbrace{\left[\left(m_j\omega^2\right)\boldsymbol{iL}\left(\mathbf{sin}\tfrac{\theta}{4}\right)^{\mathbf{2}}(\boldsymbol{k_{f1}})\right]}_{S5} \\ &+ A_L\underbrace{\left[-i\left(E_1A_1(k_{l1})\right) + \left(m_j\omega^2\right)\right]}_{S53} - B_L\underbrace{\left[i\left(E_2A_2(k_{l2})\cos\theta\right)\right]}_{S54} \\ &- B_2\underbrace{\left[E_2I_2\left(k_{f2}^3\right)\sin\theta\right]}_{S55} + B_4\underbrace{\left[i\left(E_2I_2\left(k_{f2}^3\right)\sin\theta\right)\right]}_{S56}\Bigg]\!\!\Bigg]\end{aligned}$$

Note:

Equation for bending moment and compressive forces above were having both A_1 and A_4 as the input wave, to further simplify the equation for matrix arrangement, both equation need to be solve simultaneously.

The equation below being derived to simplify the matrix: -

$$5S = (S5a.S4b) + (S5b.S4a)$$

$$S5A1 = \frac{[(S41.S5a) + (S51.S4a)]}{S5}, \quad S5A3 = \frac{[(S42.S5a) - (S52.S4a)]}{S5},$$
$$S5AL = \frac{[-(S43.S5a) + (S53.S4a)]}{S5}$$

$$S5BL = \frac{[(S44.S5a) + (S54.S4a)]}{S5}, \quad S5B2 = \frac{[(S45.S5a) - (S55.S4a)]}{S5},$$
$$S5AL = \frac{[-(S46.S5a) + (S56.S4a)]}{S5}$$

$$S4A1 = -\left({}^{S41}/_{S4a}\right) + \left[S5A1.\left({}^{S4b}/_{S4a}\right)\right], \quad S4A3 = \left({}^{S42}/_{S4a}\right) + \left[S5A3.\left({}^{S4b}/_{S4a}\right)\right],$$
$$S4AL = -\left({}^{S43}/_{S4a}\right) - \left[S5AL.\left({}^{S4b}/_{S4a}\right)\right]$$

$$S4BL = -\left({}^{S44}/_{S4a}\right) + \left[S5BL.\left({}^{S4b}/_{S4a}\right)\right], \quad S4B2 = \left({}^{S45}/_{S4a}\right) + \left[S5B2.\left({}^{S4b}/_{S4a}\right)\right],$$
$$S4B4 = -\left({}^{S46}/_{S4a}\right) - \left[S5B4.\left({}^{S4b}/_{S4a}\right)\right]$$

Equilibrium of shear force

$$-E_1 I_1 \frac{\partial^3 W_-}{\partial x^3} = E_2 A_2 \frac{\partial U_+}{\partial \psi} \sin\theta - E_2 I_2 \frac{\partial^3 W_+}{\partial \psi^3} \cos\theta - m_j \frac{\partial^2}{\partial t^2}\left[W_- + \boldsymbol{L}\left(\mathbf{sin}\tfrac{\theta}{4}\right)\left(\mathbf{cos}\tfrac{\theta}{4}\right)\frac{\partial W_-}{\partial x}\right]$$

$$\begin{aligned}
&-E_1 I_1 \left(k_{f1}^3\right)(A_1 - iA_3 + iA_4) \\
&\qquad = E_2 A_2 (k_{l2})\,(-iB_L)\sin\theta - E_2 I_2\left(-k_{f2}^3\right)(B_2 - iB_4)\cos\theta \\
&\qquad - m_j\omega^2\left[-(A_1 + A_3 + A_4) + \left\langle \boldsymbol{L}\left(\mathbf{sin}\tfrac{\theta}{4}\right)\left(\mathbf{cos}\tfrac{\theta}{4}\right)\left(k_{f1}\right)(A_1 + iA_3 - iA_4)\right\rangle\right]
\end{aligned}$$

$$\begin{aligned}
&iA_4\left(-E_1 I_1\left(k_{f1}^3\right)\right) + A_1\left(-E_1 I_1\left(k_{f1}^3\right)\right) - iA_3\left(-E_1 I_1\left(k_{f1}^3\right)\right) \\
&\qquad = -iB_L\left(E_2 A_2 (k_{l2})\sin\theta\right) + B_2\left(E_2 I_2\left(k_{f2}^3\right)\cos\theta\right) - iB_4\left(E_2 I_2\left(k_{f2}^3\right)\cos\theta\right) \\
&\qquad\quad + A_4\left(m_j\omega^2\right) \qquad + A_1\left(m_j\omega^2\right) \qquad + A_3\left(m_j\omega^2\right) \\
&\qquad\quad + iA_4\left(\left(m_j\omega^2\right)\boldsymbol{L}\left(\mathbf{sin}\tfrac{\theta}{4}\right)\left(\mathbf{cos}\tfrac{\theta}{4}\right)\left(k_{f1}\right)\right) \\
&\qquad - A_1\left(\left(m_j\omega^2\right)\boldsymbol{L}\left(\mathbf{sin}\tfrac{\theta}{4}\right)\left(\mathbf{cos}\tfrac{\theta}{4}\right)\left(k_{f1}\right)\right) - iA_3\left(\left(m_j\omega^2\right)\boldsymbol{L}\left(\mathbf{sin}\tfrac{\theta}{4}\right)\left(\mathbf{cos}\tfrac{\theta}{4}\right)\left(k_{f1}\right)\right)
\end{aligned}$$

$$\left\Vert\begin{aligned}
&A_4 \underbrace{\left[\left(-iE_1 I_1\left(k_{f1}^3\right)\right) - \left(m_j\omega^2\right) - \left(i\left(m_j\omega^2\right)\boldsymbol{L}\left(\mathbf{sin}\tfrac{\theta}{4}\right)\left(\mathbf{cos}\tfrac{\theta}{4}\right)\left(k_{f1}\right)\right)\right]}_{S6} \\
&\qquad = A_1 \underbrace{\left[\left(E_1 I_1\left(k_{f1}^3\right)\right) + \left(m_j\omega^2\right) - \left(\left(m_j\omega^2\right)\boldsymbol{L}\left(\mathbf{sin}\tfrac{\theta}{4}\right)\left(\mathbf{cos}\tfrac{\theta}{4}\right)\left(k_{f1}\right)\right)\right]}_{S6A1} \\
&\qquad + A_3 \underbrace{\left[\left(-iE_1 I_1\left(k_{f1}^3\right)\right) + \left(m_j\omega^2\right) - \left(i\left(m_j\omega^2\right)\boldsymbol{L}\left(\mathbf{sin}\tfrac{\theta}{4}\right)\left(\mathbf{cos}\tfrac{\theta}{4}\right)\left(k_{f1}\right)\right)\right]}_{S6A3} \\
&\qquad - B_L \underbrace{\left[iE_2 A_2 (k_{l2})\sin\theta\right]}_{S6BL} + B_2 \underbrace{\left[E_2 I_2\left(k_{f2}^3\right)\cos\theta\right]}_{S6B2} - B_4 \underbrace{\left[iE_2 I_2\left(k_{f2}^3\right)\cos\theta\right]}_{S6B4}
\end{aligned}\right\Vert$$

Appendix: B-3 MATLAB coding for Variable Joint equation: -

```
%function Variable_Joint.m
%% Coupled and joint - (bending<flex> and compressive<long> waves)
clear all
clf
format long e

%Given
b=0.1;%0.05;                    %m
d=0.02;%0.006;                  %m
E1=1.75e9;%5.567e9;%            %N/m^2
I1=(b*(d^3))/12;                %m^4
A1=b*d;                         %m^2
E2=1.75e9;%5.567e9;%            %N/m^2
I2=(b*(d^3))/12;                %m^4
A2=b*d;                         %m^2
R=1170;                         %kg/m^3 (rho)
Rj=1170;                        %kg/m^3
Jw=1*b;                         %m
L=1*d;                          %m
Eta=0.00;
E1e=E1*(1+(1i*Eta));
E2e=E2*(1+(1i*Eta));

Q1=E1e*I1;
Q2=E2e*I2;
S1=E1e*A1;
S2=E2e*A2;

m1=R*A1;
m2=R*A2;

%Input
A4=1;                           %m
Ai=1;                           %m

%% Main

tht=zeros;
fqt=zeros;

nP1=zeros;
nP2=zeros;
nP3=zeros;
nP4=zeros;
nP5=zeros;
nP6=zeros;
nP7=zeros;
```

```
nP8=zeros;

Kf1=zeros;
Kf1t=zeros;
Kf2=zeros;
Kf2t=zeros;
Kl1=zeros;
Kl1t=zeros;
Kl2=zeros;
Kl2t=zeros;
Mj=zeros;
Mjt=zeros;
Ij=zeros;
Ijt=zeros;

afFF=zeros;
afFL=zeros;
btFF=zeros;
btFL=zeros;
afLL=zeros;
afLF=zeros;
btLL=zeros;
btLF=zeros;
afLN=zeros;
afFN=zeros;
btLN=zeros;
btFN=zeros;


Ioj=zeros;
Imj=zeros;

thcnt=0;
for thet=0:1:180;
    T=thet*pi/180;

    Mj=Rj*T/2*(L^2)*Jw;                          %kg
    %Ioj=((T-sin(T))*(L^4)/8);
    %Icj=L*(((4/3)*(sin(T/2)/(T)))-(1/2));
    %Ij=Mj*(Ioj-Icj);
    Ij=Mj*(L^2)/12;                              %kgm^2

    thcnt=thcnt+1;

    fqcnt=0;
    for fq=000:100:3000;%000:16.667:3000.06;                    %1/s
        w=2*pi*fq;                               %1/s (omega)

        %Kf1=(w^0.5)*((m1/Q1)^0.25);             %1/m
        %Kf2=(w^0.5)*((m2/Q2)^0.25);             %1/m
        %Kl1=w*sqrt(R/E1);                       %1/m
        %Kl2=w*sqrt(R/E2);                       %1/m

        Kf1=(w^0.5)*(((m1)/(E1e*I1))^0.25);%Kfa*(1-((i*Eta)/4));    %1/m
        Kf2=(w^0.5)*(((m1)/(E2e*I2))^0.25);%Kfb*(1-((i*Eta)/4));    %1/m
```

```
Kl1=w*sqrt(R/E1e);%Kla*(1-((i*Eta)/2));                              %1/m
Kl2=w*sqrt(R/E2e);%Klb*(1-((i*Eta)/2));                              %1/m

%
V1=L/2*(1-cos(T));
S1B2=(sin(T))+(Kf2*V1);
S1B4=(sin(T))+(i*Kf2*V1);

%
V2=L/2*(sin(T));
S2B2=(cos(T))+(Kf2*V2);
S2B4=(cos(T))+(i*Kf2*V2);

%
S3A1=1/i;
S3B2=(Kf2/Kf1)*1/i;
S3B4=Kf2/Kf1;

V5=L/2*(1-cos(T/2));
V6=L/2*(sin(T/2));
%
S4a=((i*Ij*(w^2)*Kf1)-(Q1*(Kf1^2))+(i*Q1*(Kf1^3)*V6));
S4b=-(i*S1*Kl1*V5);
S41=((Ij*Kf1*(w^2))-(Q1*(Kf1^2))-(Q1*(Kf1^3)*V6));
S42=((i*Ij*Kf1*(w^2))+(Q1*(Kf1^2))+(i*Q1*(Kf1^3)*V6));
S43=-(i*S1*Kl1*V5);
S44=-(i*S2*Kl2*V5);
S45=(Q2*(Kf2^2))+(Q2*(Kf2^3)*V6);
S46=(-(Q2*(Kf2^2))-(i*Q2*(Kf2^3)*V6));

%
S5a=(i*Mj*(w^2)*Kf1*V5);
S5b=((Mj*(w^2))+(i*S1*Kl1));
S51=(Mj*(w^2)*Kf1*V5);
S52=(i*Mj*(w^2)*Kf1*V5);
S53=-((Mj*(w^2))-(i*S1*Kl1));
S54=i*S2*Kl2*(cos(T));
S55=Q2*(Kf2^3)*(sin(T));
S56=-i*Q2*(Kf2^3)*(sin(T));

S5x=((S5a*S4b)-(S4a*S5b));
S4y=((S5b*S4a)-(S4b*S5a));

S4A1=((S51*S4a)-(S41*S5a))/S4y;
S4A3=((S52*S4a)-(S42*S5a))/S4y;
S4AL=((S53*S4a)-(S43*S5a))/S4y;
S4BL=((S54*S4a)-(S44*S5a))/S4y;
S4B2=((S55*S4a)-(S45*S5a))/S4y;
S4B4=((S56*S4a)-(S46*S5a))/S4y;

S5A1=((S51*S4b)-(S41*S5b))/S5x;
S5A3=((S52*S4b)-(S42*S5b))/S5x;
S5AL=((S53*S4b)-(S43*S5b))/S5x;
S5BL=((S54*S4b)-(S44*S5b))/S5x;
S5B2=((S55*S4b)-(S45*S5b))/S5x;
```

```
S5B4=((S56*S4b)-(S46*S5b))/S5x;

%
S6=((Mj*(w^2))-(Mj*(w^2)*i*Kf1*V6)+(i*Q1*(Kf1^3)));
S6A1=-((Mj*(w^2))+(Mj*(w^2)*Kf1*V6)+(Q1*(Kf1^3)));
S6A3=-((Mj*(w^2))+(i*Mj*(w^2)*Kf1*V6)-(i*Q1*(Kf1^3)));
S6BL=i*S2*Kl2*(sin(T));
S6B2=-Q2*(Kf2^3)*(cos(T));
S6B4=i*Q2*(Kf2^3)*(cos(T));

x(1,1)=0;
x(1,2)=0;
x(1,3)=-1;
x(1,4)=cos(T);
x(1,5)=-S1B2;
x(1,6)=-S1B4;

x(2,1)=-1;
x(2,2)=-1;
x(2,3)=0;
x(2,4)=sin(T);
x(2,5)=S2B2;
x(2,6)=S2B4;

x(3,1)=S3A1;
x(3,2)=1;
x(3,3)=0;
x(3,4)=0;
x(3,5)=S3B2;
x(3,6)=S3B4;

x(4,1)=S4A1;
x(4,2)=S4A3;
x(4,3)=S4AL;
x(4,4)=S4BL;
x(4,5)=S4B2;
x(4,6)=S4B4;

x(5,1)=S5A1;
x(5,2)=S5A3;
x(5,3)=S5AL;
x(5,4)=S5BL;
x(5,5)=S5B2;
x(5,6)=S5B4;

x(6,1)=(S6A1/S6);
x(6,2)=(S6A3/S6);
x(6,3)=0;
x(6,4)=(S6BL/S6);
x(6,5)=(S6B2/S6);
x(6,6)=(S6B4/S6);

zL=[Ai;0;0;Ai;0;0];
zF=[0;A4;A4;0;A4;A4];
```

```
        fqcnt=fqcnt+1;

        yL=x\zL;
        yF=x\zF;

        tht(thcnt)=T;
        sintht(thcnt)=sin(T);
        fqt(fqcnt)=fq;
        Kf1t(fqcnt)=Kf1;
        Kf2t(fqcnt)=Kf2;
        Kl1t(fqcnt)=Kl1;
        Kl2t(fqcnt)=Kl2;
        Mjt(thcnt)=Mj;
        Ijt(thcnt)=Ij;

        %Note that for the matrix of X;
        %y(1)      %A1 Nm/s  xxxx
        %y(2)      %A3 Nm/s
        %y(3)      %AL Nm/s
        %y(4)      %BL Nm/s
        %y(5)      %B2 Nm/s  xxxx
        %y(6)      %B4 Nm/s

        afFF(thcnt)=(imag(yF(2)))^2;
        afFL(thcnt)=(imag(yL(2)))^2;
        afLL(thcnt)=(imag(yL(3)))^2;
        afLF(thcnt)=(imag(yF(3)))^2;

        btFF(thcnt)=(imag(yF(6)))^2;
        btFL(thcnt)=(imag(yL(6)))^2;
        btLL(thcnt)=(imag(yL(4)))^2;
        btLF(thcnt)=(imag(yF(4)))^2;

        afLN(thcnt)=(imag(yL(1)))^2;
        afFN(thcnt)=(imag(yF(1)))^2;
        btLN(thcnt)=(imag(yL(5)))^2;
        btFN(thcnt)=(imag(yF(5)))^2;

        Pf1=E1*I1*(Kf1^3)*w*((abs(yF(2)))^2);        %Power in A due to
reflected flexural wave         yF(2)-> A3
        Pf2=E1*I1*(Kf1^3)*w*((abs(yL(2)))^2);        %Power in A due to
reflected flexural wave         yL(2)-> A3
        Pf3=E2*I2*(Kf2^3)*w*((abs(yF(6)))^2);        %Power in B due to
transmitted flexural wave       yF(6)-> B4
        Pf4=E2*I2*(Kf2^3)*w*((abs(yL(6)))^2);        %Power in B due to
transmitted flexural wave       yL(6)-> B4

        Pl1=0.5*E1*A1*w*Kl1*((abs(yL(3)))^2);        %Power in A due to
reflected longitudinal wave     yL(3)-> AL
        Pl2=0.5*E1*A1*w*Kl1*((abs(yF(3)))^2);        %Power in A due to
reflected longitudinal wave     yF(3)-> AL
        Pl3=0.5*E2*A2*w*Kl2*((abs(yL(4)))^2);        %Power in B due to
transmitted longitudinal wave   yL(4)-> BL
        Pl4=0.5*E2*A2*w*Kl2*((abs(yF(4)))^2);        %Power in B due to
transmitted longitudinal wave   yF(4)-> BL
```

```
        %Pf1=E1*I1*(Kf1^3)*w*(((real(yF(2)))^2)+((imag(yF(2)))^2));
%Power in A due to reflected flexural wave        yF(2)-> A3
        %Pf2=E1*I1*(Kf1^3)*w*(((real(yL(2)))^2)+((imag(yL(2)))^2));
%Power in A due to reflected flexural wave        yL(2)-> A3
        %Pf3=E2*I2*(Kf2^3)*w*(((real(yF(6)))^2)+((imag(yF(6)))^2));
%Power in B due to transmitted flexural wave      yF(6)-> B4
        %Pf4=E2*I2*(Kf2^3)*w*(((real(yL(6)))^2)+((imag(yL(6)))^2));
%Power in B due to transmitted flexural wave      yL(6)-> B4

        %Pl1=0.5*E1*A1*w*Kl1*(((real(yL(3)))^2)+((imag(yL(3)))^2));
%Power in A due to reflected longitudinal wave    yL(3)-> AL
        %Pl2=0.5*E1*A1*w*Kl1*(((real(yF(3)))^2)+((imag(yF(3)))^2));
%Power in A due to reflected longitudinal wave    yF(3)-> AL
        %Pl3=0.5*E2*A2*w*Kl2*(((real(yL(4)))^2)+((imag(yL(4)))^2));
%Power in B due to transmitted longitudinal wave  yL(4)-> BL
        %Pl4=0.5*E2*A2*w*Kl2*(((real(yF(4)))^2)+((imag(yF(4)))^2));
%Power in B due to transmitted longitudinal wave  yF(4)-> BL

        PFlex=E1*I1*Kf1^3*w*((abs(A4))^2);
        PLong=0.5*E1*A1*Kl1*w*((abs(Ai))^2);

        nP1(thcnt,fqcnt)=((Pf1)./(PFlex))*100;      % %power in A - flexural
incidence wave, flexural reflected wave
        nP2(thcnt,fqcnt)=((Pf2)./(PLong))*100;      % %power in A -
longitudinal incidence wave, flexural reflected wave
        nP3(thcnt,fqcnt)=((Pl2)./(PFlex))*100;      % %power in A - flexural
incidence wave, longitudinal reflected wave
        nP4(thcnt,fqcnt)=((Pl1)./(PLong))*100;      % %power in A -
longitudinal incidence wave, longitudinal reflected wave

        nP5(thcnt,fqcnt)=((Pf3)./(PFlex))*100;      % %power in B - flexural
incidence wave, flexural transmitted wave
        nP6(thcnt,fqcnt)=((Pf4)./(PLong))*100;      % %power in B -
longitudinal incidence wave, flexural transmitted wave
        nP7(thcnt,fqcnt)=((Pl4)./(PFlex))*100;      % %power in B - flexural
incidence wave, longitudinal transmitted wave
        nP8(thcnt,fqcnt)=((Pl3)./(PLong))*100;      % %power in B -
longitudinal incidence wave, longitudinal transmitted wave

        D=nP1+nP2;%nP1+nP3;%+nP2+nP4;
        E=nP5+nP6;%nP5+nP7;%+nP6+nP8;
        F=D+E;

        A=nP3+nP4;%+nP1+nP3;
        B=nP7+nP8;%+nP5+nP7;
        C=B+A;


    end

end

tht=0:1:180;
fqt=000:100:3000;%000:16.667:3000.06;
```

```
figure(1)
contour(fqt,tht,D);
xlabel('frequency /Hz')
ylabel('angle \theta')
zlabel('Flexural Power Reflected in Beam 1')
title('Flexural Power Reflected in Beam 1 vs angle \theta and frequency/Hz')
grid

figure(2)
contour(fqt,tht,E);
xlabel('frequency /Hz')
ylabel('angle \theta')
zlabel('Flexural Power Transmitted in Beam 2')
title('Flexural Power Transmitted in Beam 2 vs angle \theta and
frequency/Hz')
grid

figure(3)
contour(fqt,tht,A);
xlabel('frequency /Hz')
ylabel('angle \theta')
zlabel('Longitudinal Power Reflected in Beam 1')
title('Longitudinal Power Reflected in Beam 1 vs angle \theta and
frequency/Hz')
grid

figure(4)
contour(fqt,tht,B);
xlabel('frequency /Hz')
ylabel('angle \theta')
zlabel('Longitudinal Power Transmitted in Beam 2')
title('Longitudinal Power Transmitted in Beam 2 vs angle \theta and
frequency/Hz')
grid

figure(5)
plot(tht,A,'r')%Long-Alpha
hold on
plot(tht,B,'b')%Long-Beta
hold on
plot(tht,C,'k')
hold on
plot(tht,D,'.r')%Flex-Alpha
hold on
plot(tht,E,'.b')%Flex-Beta
hold on
plot(tht,F,'.k')
hold on
grid on
title 'Total Power in Alpha and Beta'
xlabel 'Angle of Arm 2 (Degrees)'
ylabel 'Percentage Power'
legend('Long-Alpha','Long-Beta','Total Long','Flex-Alpha','Flex-Beta','Total
Flex','Location','best');
```

```
figure(6)
surf(fqt,tht,nP1);
xlabel('frequency /Hz')
ylabel('angle \theta')
zlabel('FF - NP Reflected in Beam 1')
title('FF Power Reflected in Beam 1 vs angle \theta and frequency/Hz')
grid

figure (7)
surf(fqt,tht,nP2);
xlabel('frequency /Hz')
ylabel('angle \theta')
zlabel('LF - NP Reflected in Beam 1')
title('LF Power Reflected in Beam 1 vs angle \theta and frequency/Hz')
grid

figure (8)
surf(fqt,tht,nP3);
xlabel('frequency /Hz')
ylabel('angle \theta')
zlabel('FL - NP Reflected in Beam 1')
title('FL Power Reflected in Beam 1 vs angle \theta and frequency/Hz')
grid

figure (9)
surf(fqt,tht,nP4);
xlabel('frequency /Hz')
ylabel('angle \theta')
zlabel('LL - NP Reflected in Beam 1')
title('LL Power Reflected in Beam 1 vs angle \theta and frequency/Hz')
grid

figure (10)
surf(fqt,tht,nP5);
xlabel('frequency /Hz')
ylabel('angle \theta')
zlabel('FF - NP Transmitted to Beam 2')
title('FF Power Transmitted to Beam 2 vs angle \theta and frequency/Hz')
grid

figure (11)
surf(fqt,tht,nP6);
xlabel('frequency /Hz')
ylabel('angle \theta')
zlabel('LF - NP Transmitted to Beam 2')
title('LF Power Transmitted to Beam 2 vs angle \theta and frequency/Hz')
grid

figure (12)
surf(fqt,tht,nP7);
xlabel('frequency /Hz')
ylabel('angle \theta')
zlabel('FL - NP Transmitted to Beam 2')
title('FL Power Transmitted to Beam 2 vs angle \theta and frequency/Hz')
grid
```

```
figure (13)
surf(fqt,tht,nP8);
xlabel('frequency /Hz')
ylabel('angle \theta')
zlabel('LL - NP Transmitted to Beam 2')
title('LL Power Transmitted to Beam 2 vs angle \theta and frequency/Hz')
grid

figure(14)
plot(tht,nP1,'r')
hold on
plot(tht,nP2,'g')
hold on
plot(tht,nP3,'m')
hold on
plot(tht,nP4,'b')
hold on
grid on
title 'Percentage Power Reflected in Beam 1'
xlabel 'Angle of Arm 2 (Degrees)'
ylabel 'Percentage Power'
legend('FF','LF','FL','LL');

figure(15)
plot(tht,nP5,'r')
hold on
plot(tht,nP6,'g')
hold on
plot(tht,nP7,'m')
hold on
plot(tht,nP8,'b')
hold on
grid on
title 'Percentage Power Transmitted to Beam 2'
xlabel 'Angle of Arm 2 (Degrees)'
ylabel 'Percentage Power'
legend('FF','LF','FL','LL');

figure(16)
plot(tht,nP1,'r')
hold on
plot(tht,nP3,'m')
hold on
plot(tht,nP5,'r')
hold on
plot(tht,nP7,'m')
hold on
grid on
title 'Percentage Power Reflected from Flexural'
xlabel 'Angle of Arm 2 (Degrees)'
ylabel 'Percentage Power'
legend('FF1','FL1','FF2','FL2');

figure(17)
plot(tht,nP2,'g')
```

```
hold on
plot(tht,nP4,'b')
hold on
plot(tht,nP6,'g')
hold on
plot(tht,nP8,'b')
hold on
grid on
title 'Percentage Power Reflected from Longitudinal'
xlabel 'Angle of Arm 2 (Degrees)'
ylabel 'Percentage Power'
legend('LF1','LL1','LF2','LL2');


% fqMainCodeJointBeam
%*******************************************************************
% LOUGHBOROUGH UNIVERSITY
% PHD THESIS
% --------
% AUTHOR: SAIDDI ALI FIRDAUS BIN MOHAMED ISHAK
% SUPERVISORs: DR. JANE L.HORNER & DR.STEPHEN J.WALSH
%*******************************************************************
% MAIN PROGRAM: Reflection & Transmission - Power Measurements
%*******************************************************************
%
% THIS PROGRAM SOLVES FOR VIBRATION POWER IN BEAM WITH VARIABLE ANGLE
%

%
% DESCRIPTION OF INPUT PARAMETER
%
% E       is the Young's Modulus
% I       is the second moment of area
% A       is the area
% R       is the density of beam
% Rj      is density of joint
% Jw      is width of joint
% L       is height of joint
% Q       is the E x I
% S       is the E x A



%
% DESCRIPTION OF OTHER VARIABLES
%
% Kfa     is the flexural wavenumber in alpha
% Kfb     is the flexural wavenumber in beta
% Kfg     is the flexural wavenumber in gamma
% Kla     is the longitudinal wavenumber in alpha
% Klb     is the longitudinal wavenumber in beta
% Klg     is the longitudinal wavenumber in gamma

%
%% Ff & Fl input - (bending<flexural> and compressive<longitudinal> waves)
```

```
clear all
clf
format long e

%Given
b=0.1;                                            %m          %0.05;%
d=0.02;                                           %m          %0.006;%
E1=1.75e9;                                        %N/m^2      %60e9;%3.5e9;%5.567e9;%
I1=(b*(d^3))/12;                                  %m^4
A1=b*d;                                           %m^2
E2=1.75e9;                                        %N/m^2      %60e9;%3.5e9;%5.567e9;%
I2=(1.0*b*((1.0*d)^3))/12;                        %m^4
A2=1.0*b*1.0*d;                                   %m^2
R=1170;                                           %kg/m^3     %1500;%1190;%2500;
Rj=1170;                                          %kg/m^3     %1500;%1190;%2500;
Jw=1*b;                                           %m
L=1*d;                                            %m
Eta=0.07;

E1e=E1*(1+(1i*Eta));
E2e=E2*(1+(1i*Eta));

Q1=E1*I1;
Q2=E2*I2;
S1=E1*A1;
S2=E2*A2;

Q3=0;                                             %1.167e6*I1;

m1=R*A1;
m2=R*A2;

%% Main


thcnt=0;
for thet=0:1:180;
    T=thet*pi/180;

    thcnt=thcnt+1;


    fqcnt=0;
    for fq=00:100:3000;                             %1/s
        w=2*pi*fq;                                %1/s

        %Input
        Ff=1;%0.023*sqrt(2);                                  %m
%(1*i);%0.018;0.0038*sqrt(2);%(1);%
        Fl=1;%0.0020*sqrt(2);                                 %m
%(1*i);%0.018;0;%(1);%0;%
        m=-0.90;
        n=0.0;
```

```
Mj=Rj*Jw*(L^2)*T/2;                    %kg
%Ioj=((T-sin(T))*(L^4)/8);
%Icj=L*(((4/3)*(sin(T/2)/(T)))-(1/2));
%Ij=Mj*(Ioj-Icj);
Ij=Mj*(L^2)/12;                        %kgm^2

Kfa=(w^0.5)*(((R*A1)/(E1*I1))^0.25);      %1/m
Kfg=(w^0.5)*(((R*A1)/(E2*I1))^0.25);      %1/m
Kfb=(w^0.5)*(((R*A2)/(E2*I2))^0.25);      %1/m
Kla=w*sqrt(R/E1);                         %1/m
Klg=w*sqrt(R/E1);                         %1/m
Klb=w*sqrt(R/E2);                         %1/m

Kfax=(w^0.5)*(((R*A1)/(E1e*I1))^0.25);%Kfa*(1-((i*Eta)/4));     %1/m
Kfgx=(w^0.5)*(((R*A1)/(E1e*I1))^0.25);%Kfg*(1-((i*Eta)/4));     %1/m
Kfbx=(w^0.5)*(((R*A1)/(E2e*I2))^0.25);%Kfb*(1-((i*Eta)/4));     %1/m
Klax=w*sqrt(R/E1e);%Kla*(1-((i*Eta)/2));                        %1/m
Klgx=w*sqrt(R/E1e);%Klg*(1-((i*Eta)/2));                        %1/m
Klbx=w*sqrt(R/E2e);%Klb*(1-((i*Eta)/2));                        %1/m

%------%

nm=(n-m);   %finite length (fl)
mn=(m-n);

Lni=(exp(-i*Klax*nm));
Fn=(exp(-Kfa*nm));
Fni=(exp(-i*Kfax*nm));

Lpi=(exp(i*Klax*mn));
Fp=(exp(Kfa*mn));
Fpi=(exp(i*Kfax*mn));

%------%

%
V1=L/2*(1-cos(T));

g1=(sin(T)+(Kfb*V1));
h1=(sin(T)+(i*Kfbx*V1));
i1=cos(T);

%
V3=L/2*(sin(T));

g3=(cos(T))+(Kfb*V3);
h3=(cos(T))+(i*Kfbx*V3);
i3=sin(T);

%
a5=Kfa;
b5=i*Kfax;
d5=Kfa;
e5=i*Kfax;
```

```
        g5=Kfb;
        h5=i*Kfbx;

        %
        a6=Kfa;
        b6=i*Kfax;
        d6=Kfa;
        e6=i*Kfax;
        j6=Kfg;
        k6=i*Kfgx;

        %--------%
        V5=L/2*(1-cos(T/2));
        V6=L/2*(sin(T/2));
        %V5=L*((sin(T/4))^2);       %-same as above
        %V6=L*(sin(T/4))*(cos(T/4));%-same as above
        %--------%

        Mr=0.028;
        Ir=Mr*(L^2)/12;
        hs=1000;
        h=0.05;

        Dr =-(-(Mr*w^2)+(hs*(1+(i*h*w))));0;%
        Drm=-(-(Ir*w^2)+(hs*(1+(i*h*w))));0;%


        a7=((-Ij)  *Kfa *(w^2))+((-Q1)*(Kfa^2)) +(Q1  *(Kfa^3) *V6)        -
(Drm*  Kfa -Dr*V6);
        b7=((-Ij)*i*Kfax*(w^2))+(  Q1 *(Kfax^2))+(Q1*i*(Kfax^3)*(-V6))     -
(Drm*i*Kfax-Dr*V6);%
        c7=(S1*i*Klax*V5)
+(Dr*V5)         ;
        d7=(  Ij   *Kfa *(w^2))+((-Q1)*(Kfa^2)) +(Q1  *(Kfa^3) *(-V6))
+(Drm*  Kfa -Dr*V6);
        e7=(  Ij *i*Kfax*(w^2))+(  Q1 *(Kfax^2))+(Q1*i*(Kfax^3)*V6)
+(Drm*i*Kfax-Dr*V6);
        f7=(S1*i*Klax*(-V5))
+(Dr*V5)         ;
        g7=(  Q2 *(Kfb^2)) +(Q2  *(Kfb^3) *V6)                             -
(Drm*  Kfb -Dr*V6);
        h7=((-Q2)*(Kfbx^2))+(Q2*i*(Kfbx^3)*(-V6))                          -
(Drm*i*Kfbx-Dr*V6);
        i7=(S2*i*Klbx*(-V5))
+(Dr*V5)         ;


        %
        a8=(Kfa^2);     %*Q1;
        b8=(Kfax^2);    %*Q1;
        d8=(Kfa^2);     %*Q1;
        e8=(Kfax^2);    %*Q1;
        j8=(Kfg^2);     %*Q1;
        k8=(Kfgx^2);    %*Q1;

        %
```

```
        a9=( Mj*(w^2)  *Kfa *V5);
        b9=( Mj*(w^2)*i*Kfax*V5);
        c9=( Mj*(w^2))+(  S1 *i*Klax)
+Dr;
        d9=(-Mj*(w^2)  *Kfa *V5);
        e9=(-Mj*(w^2)*i*Kfax*V5);
        f9=( Mj*(w^2))+((-S1)*i*Klax)
+Dr;
        g9=((-Q2)*  (Kfb^3) *sin(T))
+Dr*sin(T);
        h9=(  Q2 *i*(Kfbx^3)*sin(T))
+Dr*sin(T);
        i9=((-S2)*i* Klbx   *cos(T))
+Dr*cos(T);

        %
        c10=(i*Klax);   %*(S1);%+ve
        f10=(i*Klax);   %*(S1);%-ve
        l10=(i*Klgx);   %*(S1);%+ve

        %
        a11=(Mj*(w^2))+((-Mj)*(w^2)  *Kfa *V6)+((-Q1)  *(Kfa^3))
+Dr;
        b11=(Mj*(w^2))+((-Mj)*(w^2)*i*Kfax*V6)+(  Q1 *i*(Kfax^3))
+Dr;
        d11=(Mj*(w^2))+(  Mj *(w^2)  *Kfa *V6)+(  Q1   *(Kfa^3))
+Dr;
        e11=(Mj*(w^2))+(  Mj *(w^2)*i*Kfax*V6)+((-Q1)*i*(Kfax^3))
+Dr;
        g11=(  Q2 *  (Kfb^3) *cos(T))
+Dr*cos(T);
        h11=((-Q2)*i*(Kfbx^3)*cos(T))
+Dr*cos(T);
        i11=((-S2)*i* Klbx   *sin(T))
+Dr*sin(T);

        %
        a12=(Kfa^3);    %*Q1;
        b12=i*(Kfax^3); %*Q1;
        d12=(Kfa^3);    %*Q1;
        e12=i*(Kfax^3); %*Q1;
        j12=(Kfg^3);    %*Q1;
        k12=i*(Kfgx^3); %*Q1;

        %------------------%

        %
        x(1,1)=0;
        x(1,2)=0;
        x(1,3)=-1*Lni;
        x(1,4)=0;
        x(1,5)=0;
        x(1,6)=-1;                  %*Lpi;
        x(1,7)=-g1;
        x(1,8)=-h1;
        x(1,9)=i1;
```

```
x(1,10)=0;
x(1,11)=0;
x(1,12)=0;

x(2,1)=0;
x(2,2)=0;
x(2,3)=1;
x(2,4)=0;
x(2,5)=0;
x(2,6)=1*(Lpi-0);
x(2,7)=0;
x(2,8)=0;
x(2,9)=0;
x(2,10)=0;
x(2,11)=0;
x(2,12)=-1;                        %xx*Lpi;

x(3,1)=-1*Fn;
x(3,2)=-1*Fni;
x(3,3)=0;
x(3,4)=-1;                 %*Fp;
x(3,5)=-1;                 %*Fpi;
x(3,6)=0;
x(3,7)=g3;
x(3,8)=h3;
x(3,9)=i3;
x(3,10)=0;
x(3,11)=0;
x(3,12)=0;

x(4,1)=1;
x(4,2)=1;
x(4,3)=0;
x(4,4)=1*(Fp-0);
x(4,5)=1*(Fpi-0);
x(4,6)=0;
x(4,7)=0;
x(4,8)=0;
x(4,9)=0;
x(4,10)=-1;                        %xx*Fp;
x(4,11)=-1;                        %xx*Fpi;
x(4,12)=0;

x(5,1)=a5*Fn;
x(5,2)=b5*Fni;
x(5,3)=0;
x(5,4)=-d5;                %*Fp;
x(5,5)=-e5;                %*Fpi;
x(5,6)=0;
x(5,7)=-g5;
x(5,8)=-h5;
x(5,9)=0;
x(5,10)=0;
x(5,11)=0;
x(5,12)=0;
```

```
x(6,1)=a6;
x(6,2)=b6;
x(6,3)=0;
x(6,4)=-d6*(Fp+0);
x(6,5)=-e6*(Fpi+0);
x(6,6)=0;
x(6,7)=0;
x(6,8)=0;
x(6,9)=0;
x(6,10)=j6;                         %xx*Fp;
x(6,11)=k6;                         %xx*Fpi;
x(6,12)=0;

x(7,1)=a7*Fn;
x(7,2)=b7*Fni;
x(7,3)=c7*Lni;
x(7,4)=d7;                  %*Fp;
x(7,5)=e7;                  %*Fpi;
x(7,6)=f7;                  %*Lpi;
x(7,7)=g7;
x(7,8)=h7;
x(7,9)=i7;
x(7,10)=0;
x(7,11)=0;
x(7,12)=0;

x(8,1)=-a8;
x(8,2)=b8;
x(8,3)=0;
x(8,4)=d8*(-Fp+0);
x(8,5)=e8*(Fpi-0);
x(8,6)=0;
x(8,7)=0;
x(8,8)=0;
x(8,9)=0;
x(8,10)=j8;                         %xx*Fp;
x(8,11)=-k8;                        %xx*Fpi;
x(8,12)=0;

x(9,1)=a9*Fn;
x(9,2)=b9*Fni;
x(9,3)=c9*Lni;
x(9,4)=d9;                  %*Fp;
x(9,5)=e9;                  %*Fpi;
x(9,6)=f9;                  %*Lpi;
x(9,7)=g9;
x(9,8)=h9;
x(9,9)=i9;
x(9,10)=0;
x(9,11)=0;
x(9,12)=0;

x(10,1)=0;
x(10,2)=0;
x(10,3)=-c10;
x(10,4)=0;
```

```
x(10,5)=0;
x(10,6)=f10*(Lpi+0);
x(10,7)=0;
x(10,8)=0;
x(10,9)=0;
x(10,10)=0;
x(10,11)=0;
x(10,12)=-l10;                      %xx*Lpi;

x(11,1)=a11*Fn;
x(11,2)=b11*Fni;
x(11,3)=0;
x(11,4)=d11;                %*Fp;
x(11,5)=e11;                %*Fpi;
x(11,6)=0;
x(11,7)=g11;
x(11,8)=h11;
x(11,9)=i11;
x(11,10)=0;
x(11,11)=0;
x(11,12)=0;

x(12,1)=a12;
x(12,2)=-b12;
x(12,3)=0;
x(12,4)=-d12*(Fp+0);
x(12,5)=e12*(Fpi+0);
x(12,6)=0;
x(12,7)=0;
x(12,8)=0;
x(12,9)=0;
x(12,10)=j12;                       %xx*Fp;
x(12,11)=-k12;                      %xx*Fpi;
x(12,12)=0;

zL=[0;0;0;0;0;0;0;0;0;(Fl/S1);0;0];     %(Fl/(4*E1*A1*Kla))
zF=[0;0;0;0;0;0;0;0;0;0;0;(Ff/Q1)];     %-(Ff/(4*E1*I1*Kfa^3))

yL=x\zL;
yF=x\zF;

%Note that for the matrix of X;
%y(1)      %A2 Nm/s  xxxx
%y(2)      %A4 Nm/s
%y(3)      %AL Nm/s
%y(4)      %B1 Nm/s  xxxx
%y(5)      %B3 Nm/s
%y(6)      %BL Nm/s
%y(7)      %C2 Nm/s  xxxx
%y(8)      %C4 Nm/s
%y(9)      %CL Nm/s
%y(10)     %D1 Nm/s  xxxx
%y(11)     %D3 Nm/s
%y(12)     %DL Nm/s

fqcnt=fqcnt+1;
```

```
        Pf1=1*E1*I1*w*(Kfax^3)*((abs(yF(2)))^2);     %Power in a due to trans
flexural wave            yF(2) -> A4
        Pf2=1*E1*I1*w*(Kfax^3)*((abs(yL(2)))^2);     %Power in a due to trans
flexural wave            yL(2) -> A4
        Pf3=1*E1*I1*w*(Kfax^3)*((abs(yF(5)))^2);     %Power in a due to
reflected flexural wave       yF(5) -> B3
        Pf4=1*E1*I1*w*(Kfax^3)*((abs(yL(5)))^2);     %Power in a due to
reflected flexural wave       yL(5) -> B3
        Pf5=1*E2*I2*w*(Kfbx^3)*((abs(yF(8)))^2);     %Power in b due to
transmitted flexural wave     yF(8) -> C4
        Pf6=1*E2*I2*w*(Kfbx^3)*((abs(yL(8)))^2);     %Power in b due to
transmitted flexural wave     yL(8) -> C4
        Pf7=1*E1*I1*w*(Kfgx^3)*((abs(yF(11)))^2);    %Power in g due to trans
flexural wave            yF(11)-> D3
        Pf8=1*E1*I1*w*(Kfgx^3)*((abs(yL(11)))^2);    %Power in g due to trans
flexural wave            yL(11)-> D3

        Pl1=0.5*E1*A1*w*Klax*((abs(yL(3)))^2);       %Power in a due to trans
longitudinal wave        yL(3) -> AL
        Pl2=0.5*E1*A1*w*Klax*((abs(yF(3)))^2);       %Power in a due to trans
longitudinal wave        yF(3) -> AL
        Pl3=0.5*E1*A1*w*Klax*((abs(yL(6)))^2);       %Power in a due to
reflected longitudinal wave   yL(6) -> BL
        Pl4=0.5*E1*A1*w*Klax*((abs(yF(6)))^2);       %Power in a due to
reflected longitudinal wave   yF(6) -> BL
        Pl5=0.5*E2*A2*w*Klbx*((abs(yL(9)))^2);       %Power in b due to
transmitted longitudinal wave yL(9) -> CL
        Pl6=0.5*E2*A2*w*Klbx*((abs(yF(9)))^2);       %Power in b due to
transmitted longitudinal wave yF(9) -> CL
        Pl7=0.5*E1*A1*w*Klgx*((abs(yL(12)))^2);      %Power in g due to trans
longitudinal wave        yL(12)-> DL
        Pl8=0.5*E1*A1*w*Klgx*((abs(yF(12)))^2);      %Power in g due to trans
longitudinal wave        yF(12)-> DL

        PFlex=(0.125*(((Ff)^2)*w))/(((E1*I1)*((Kfax)^3)));
        PLong=(0.25*(((Fl)^2)*w))/((E1*A1)*(Klax));
        %PFlexG=(0.125*(((Ff)^2)*w))/(((E1*I1)*((Kfg)^3)));
        %PLongG=(0.25*(((Fl)^2)*w))/((E1*A1)*(Klg));
        %lmbd=0.5;
        %Kfax2=2*pi/lmbd;
        %PFlex2=(0.125*((Ff)^2))/(m1*w/Kfax2);

        tht(thcnt)=T;
        wqt(fqcnt)=w;
        fqt(fqcnt)=fq;
        ndwave(fqcnt)=(Kfa*abs(m-n))/(2*pi);%((2*pi)/Kfa)*0.5;

        nP1(thcnt,fqcnt)=(Pf1)./(PFlex+0)*100;       %A%power in a - flexural
incidence wave, flexural reflected wave
        nP2(thcnt,fqcnt)=(Pf2)./(PLong+0)*100;       %A%power in a -
longitudinal incidence wave, flexural reflected wave
        nP3(thcnt,fqcnt)=(Pl2)./(PFlex+0)*100;       %A%power in a - flexural
incidence wave, longitudinal reflected wave
        nP4(thcnt,fqcnt)=(Pl1)./(PLong+0)*100;       %A%power in a -
longitudinal incidence wave, longitudinal reflected wave
```

```
        nP5(thcnt,fqcnt)=(Pf3)./(PFlex+0)*100;       %B%power in a - flexural
incidence wave, flexural reflected wave
        nP6(thcnt,fqcnt)=(Pf4)./(PLong+0)*100;       %B%power in a -
longitudinal incidence wave, flexural reflected wave
        nP7(thcnt,fqcnt)=(Pl4)./(PFlex+0)*100;       %B%power in a - flexural
incidence wave, longitudinal reflected wave
        nP8(thcnt,fqcnt)=(Pl3)./(PLong+0)*100;       %B%power in a -
longitudinal incidence wave, longitudinal reflected wave

        nP9(thcnt,fqcnt)=(Pf5)./(PFlex+0)*100;       %C%power in b - flexural
incidence wave, flexural transmitted wave
        nP10(thcnt,fqcnt)=(Pf6)./(PLong+0)*100;      %C%power in b -
longitudinal incidence wave, flexural transmitted wave
        nP11(thcnt,fqcnt)=(Pl6)./(PFlex+0)*100;      %C%power in b - flexural
incidence wave, longitudinal transmitted wave
        nP12(thcnt,fqcnt)=(Pl5)./(PLong+0)*100;      %C%power in b -
longitudinal incidence wave, longitudinal transmitted wave

%         nP13(thcnt,fqcnt)=(Pf7)./(PFlex+0)*100;      %D%power in g -
flexural incidence wave, flexural transmitted wave
%         nP14(thcnt,fqcnt)=(Pf8)./(PLong+0)*100;      %D%power in g -
longitudinal incidence wave, flexural transmitted wave
%         nP15(thcnt,fqcnt)=(Pl8)./(PFlex+0)*100;      %D%power in g -
flexural incidence wave, longitudinal transmitted wave
%         nP16(thcnt,fqcnt)=(Pl7)./(PLong+0)*100;      %D%power in g -
longitudinal incidence wave, longitudinal transmitted wave

        nP13(thcnt,fqcnt)=nP1(thcnt,fqcnt)+(Pf3)./(PFlex+0)*100;      %
%power in g - flexural incidence wave, flexural transmitted wave
        nP14(thcnt,fqcnt)=nP2(thcnt,fqcnt)+(Pf4)./(PLong+0)*100;      %
%power in g - longitudinal incidence wave, flexural transmitted wave
        nP15(thcnt,fqcnt)=nP3(thcnt,fqcnt)+(Pl4)./(PFlex+0)*100;      %
%power in g - flexural incidence wave, longitudinal transmitted wave
        nP16(thcnt,fqcnt)=nP4(thcnt,fqcnt)+(Pl3)./(PLong+0)*100;      %
%power in g - longitudinal incidence wave, longitudinal transmitted wave

        %-------------%

        fA=nP1+nP3;%+nP3;%nP1+nP3+nP5+nP7;
        fB=nP5+nP7;%+nP7;%nP9+nP11;

        fC=nP9+nP11;%+nP11;%nP13+nP15;
        fD=nP13+nP15;%+nP15;%nP17+nP18+nP19+nP20;

        fAl=fA-fB;
        fBe=fC;
        fGa=fD;
        ftot1=fAl+fGa;
        ftot2=fGa+fBe;
        %ftot3=fAl+fBe;
        fAla=fA;
        fAlb=fB;

        %-------------%
```

```
        lA=nP4+nP2;%=0
        lB=nP8+nP6;

        lC=nP12+nP10;
        lD=nP16+nP14;

        lAl=lA-lB;
        lBe=lC;
        lGa=lD;
        ltot1=lAl+lGa;
        ltot2=lGa+lBe;
        %ltot3=lAl+lBe;

        %-------------%

        tot1=ftot1+ltot1;
        tot2=ftot2+ltot2;
        %tot3=ftot3+ltot3;
        AlphaT=fAl+lAl;
        BetaT=fBe+lBe;
        GammaT=fGa+lGa;
        GammaTt=nP14+nP15;


        %nF=nP21+nP22+nP23+nP24;
        Tf=fGa+fAl;%fAl+
        Tl=lGa+lAl;%lAl+
        TOT1=GammaT+BetaT;%+AlphaT;%GammaT+fB+lB;BetaT+fA+lA;
        TOT2=GammaT+AlphaT;

        %-------------%

        xfcnt=0;
        for xf=m;
            Wf(thcnt,fqcnt)=(yF(1)*(exp(-Kfa*(xf-m))))+(yF(2)*(exp(-
1i*Kfax*(xf-m))))+(yF(4)*(exp(Kfa*(1*(xf-n)))))+(yF(5)*(exp(1i*Kfax*(1*(xf-
n)))));
            Uf(thcnt,fqcnt)=(yL(3)*(exp(-1i*Klax*(xf-
m))))+(yL(6)*(exp(1i*Klax*(1*(xf-n)))));

            xacnt=0;
            for xa=-0.45;
                Wa(thcnt,fqcnt)=(yF(1)*(exp(-Kfa*(xa-m))))+(yF(2)*(exp(-
1i*Kfax*(xa-m))))+(yF(4)*(exp(Kfa*(1*(xa-n)))))+(yF(5)*(exp(1i*Kfax*(1*(xa-
n)))));
                Ua(thcnt,fqcnt)=(yL(3)*(exp(-1i*Klax*(xa-
m))))+(yL(6)*(exp(1i*Klax*(1*(xa-n)))));

                xbcnt=0;
                for xb=0.45;

                    Wb(thcnt,fqcnt)=(yF(7)*(exp(-Kfb*(xb-n))))+(yF(8)*(exp(-
1i*Kfbx*(xb-n))));
```

```
                    Ub(thcnt,fqcnt)=(yL(9)*(exp(-1i*Klbx*(xb-n))));

                    xgcnt=0;
                    for xg=-1.35;

                        Wg(thcnt,fqcnt)=(yF(10)*(exp(Kfg*(xg-
m))))+(yF(11)*(exp(1i*Kfgx*(xg-m))));%+(yF(4)*(exp(-Kfa*(1*(xg-
n)))))+(yF(5)*(exp(-1i*Kfax*(1*(xg-n)))));
                        Ug(thcnt,fqcnt)=(yL(12)*(exp(1i*Klgx*(xg-
m))));%+(yL(6)*(exp(-1i*Klax*(1*(xg-n)))));

                        Va(thcnt,fqcnt)=1i*w*Wa(thcnt,fqcnt);
                        Vb(thcnt,fqcnt)=1i*w*Wb(thcnt,fqcnt);
                        Vg(thcnt,fqcnt)=1i*w*Wg(thcnt,fqcnt);
                        Aa(thcnt,fqcnt)=-1*w^2*Wa(thcnt,fqcnt);
                        Ab(thcnt,fqcnt)=-1*w^2*Wb(thcnt,fqcnt);
                        Ag(thcnt,fqcnt)=-1*w^2*Wg(thcnt,fqcnt);

                        xacnt=xacnt+1;
                        xWat(xacnt)=Wa(thcnt,fqcnt);
                        xUat(xacnt)=Ua(thcnt,fqcnt);
                        xWbt(xacnt)=Wb(thcnt,fqcnt);
                        xUbt(xacnt)=Ub(thcnt,fqcnt);
                        xWgt(xacnt)=Wg(thcnt,fqcnt);
                        xUgt(xacnt)=Ug(thcnt,fqcnt);



InPwrF(thcnt,fqcnt)=((((Ff)^2)*w)/(8*E1*I1*Kfax^3))*(1-Eta/4);
                        InPwr(thcnt,fqcnt)=-
0.5*real(Ff*(1i*w*(Wf(thcnt,fqcnt))));

ApPwr(thcnt,fqcnt)=((((1i*w*(Wa(thcnt,fqcnt))))^2*(E1*I1)*((Kfa)^3))/(w));

BtPwr(thcnt,fqcnt)=((((1i*w*(Wb(thcnt,fqcnt))))^2*(E2*I2)*((Kfb)^3))/(w));

GmPwr(thcnt,fqcnt)=((((1i*w*(Wg(thcnt,fqcnt))))^2*(E1*I1)*((Kfg)^3))/(w));
                        TotPwr=GmPwr+BtPwr;

                        Imp(fqcnt)=1/(1i*w*Wa(fqcnt));
                        Mob(fqcnt)=1/(Imp(fqcnt));

                        ReMob(fqcnt)=w/(4*E1*I1*Kfa^3);
                        ImMob(fqcnt)=(-1*w)/(4*E1*I1*Kfa^3);

                        Acc(fqcnt)=Wa(fqcnt)*(-(w^2));

                        Ar=(fAl)./(InPwr);
                        Gr=(fGa)./(InPwr);
                        Br=(fBe)./(InPwr);
                        %Ir=InPwr/fAl;
                        %Gr=fGa/fAl;
                        %Br=fBe/fAl;
                        tr=(Ar+Br)*1;
```

```
                    end

                end

            end

        end

    end

end

fqt=00:100:3000;
tht=0:1:180;

figure(1)
plot(tht,nP1,'r')
hold on
plot(tht,nP2,'g')
hold on
plot(tht,nP3,'m')
hold on
plot(tht,nP4,'b')
hold on
plot(tht,nP5,'r')
hold on
plot(tht,nP6,'g')
hold on
plot(tht,nP7,'m')
hold on
plot(tht,nP8,'b')
hold on
grid on
%axis([0 180 0 120])
title 'Percentage Power Transmitted&Reflected in alpha'
xlabel 'Angle'%'Frequency'
ylabel 'Percentage Power'
%legend('FF','LF','FL','LL','FF','LF','FL','LL','Location','best');

figure(2)
plot(tht,nP9,'r')
hold on
plot(tht,nP10,'g')
hold on
plot(tht,nP11,'m')
hold on
plot(tht,nP12,'b')
hold on
grid on
%axis([0 180 0 120])
title 'Percentage Power Transmitted in beta'
xlabel 'Angle'%'Frequency'
ylabel 'Percentage Power'
%legend('FF','LF','FL','LL','Location','best');
```

```
figure(3)
plot(tht,nP13,'r')
hold on
plot(tht,nP14,'g')
hold on
plot(tht,nP15,'m')
hold on
plot(tht,nP16,'b')
hold on
plot(tht,GammaTt,'k')
hold on
grid on
%axis([0 180 0 120])
title 'Percentage Power Transmitted in gamma'
xlabel 'Angle'%'Frequency'
ylabel 'Percentage Power'
%legend('FF','LF','FL','LL','Location','best');

figure(4)
plot(tht,nP1,'r')
hold on
plot(tht,nP2,'g')
hold on
plot(tht,nP3,'m')
hold on
plot(tht,nP4,'b')
hold on
grid on
%axis([0 180 0 120])
title 'Percentage Power Transmitted in Alpha'
xlabel 'Angle'%'Frequency'
ylabel 'Percentage Power'
%legend('FF','LF','FL','LL','Location','best');

figure(5)
plot(tht,nP9,'r')
hold on
plot(tht,nP11,'m')
hold on
plot(tht,nP13,'r')
hold on
plot(tht,nP15,'m')
hold on
grid on
%axis([0 180 0 120])
title 'Percentage Power from Flexural at beta and gamma'
xlabel 'Angle'%'Frequency'
ylabel 'Percentage Power'
%legend('FFb','FLb','FFg','FLg','Location','best');

figure(6)
plot(tht,nP10,'g')
hold on
plot(tht,nP12,'b')
hold on
plot(tht,nP14,'g')
```

```
hold on
plot(tht,nP16,'b')
hold on
grid on
%axis([0 180 0 120])
title 'Percentage Power from Longitudinal at beta and gamma'
xlabel 'Angle'%'Frequency'
ylabel 'Percentage Power'
%legend('LFb','LLb','LFg','LLg','Location','best');

figure(7)
plot(tht,AlphaT,'r')
hold on
plot(tht,BetaT,'b') %
hold on
plot(tht,GammaT,'g')
hold on
%plot(tht,nF,'k.')
%hold on
plot(tht,TOT2,'k')
hold on
grid on
title 'Percentage Power Total'
xlabel 'Angle'%'Frequency'
ylabel 'Percentage Power'
%legend('Al','Be','Ga','Total2','Location','best');%'nF',

figure(8)
plot(tht,fAl,'r.')
hold on
plot(tht,fBe,'b.') %
hold on
plot(tht,fGa,'g.')
hold on
plot(tht,Tf,'k.')
hold on
plot(tht,lAl,'r')
hold on
plot(tht,lBe,'b') %
hold on
plot(tht,lGa,'g')
hold on
plot(tht,Tl,'k')
hold on
grid on
title 'Percentage Power Total'
xlabel 'Angle'%'Frequency'
ylabel 'Percentage Power'
%legend('Al','Be','Ga','nF','Total','Location','best');

figure(9)
contour(fqt,tht,fAl);
xlabel('frequency /Hz')
ylabel('angle \theta')
zlabel('Power in Alpha')
title('Flexural Alpha Power vs angle \theta and frequency/Hz (with rubber)')
```

```
grid

figure (10)
contour(fqt,tht,fBe);
xlabel('frequency /Hz')
ylabel('angle \theta')
zlabel('Power in Beta')
title('Flexural Beta Power vs angle \theta and frequency/Hz (with rubber)')
grid

figure (11)
contour(fqt,tht,fGa);
xlabel('frequency /Hz')
ylabel('angle \theta')
zlabel('Power in Gamma')
title('Flexural Gamma Power vs angle \theta and frequency/Hz (with rubber)')
grid

figure(12)
contour(fqt,tht,lAl);
xlabel('frequency /Hz')
ylabel('angle \theta')
zlabel('Power in Alpha')
title('Longitudinal Alpha Power vs angle \theta and frequency/Hz (with
rubber)')
grid

figure (13)
contour(fqt,tht,lBe);
xlabel('frequency /Hz')
ylabel('angle \theta')
zlabel('Power in Beta')
title('Longitudinal Beta Power vs angle \theta and frequency/Hz (with
rubber)')
grid

figure (14)
contour(fqt,tht,lGa);
xlabel('frequency /Hz')
ylabel('angle \theta')
zlabel('Power in Gamma')
title('Longitudinal Gamma Power vs angle \theta and frequency/Hz (with
rubber)')
grid

figure (15)
contour(fqt,tht,AlphaT);
xlabel('frequency /Hz')
ylabel('angle \theta')
zlabel('Power in Alpha')
title('Total Alpha Power vs angle \theta and frequency/Hz (with rubber)')
grid

figure (16)
contour(fqt,tht,BetaT);
```

```
xlabel('frequency /Hz')
ylabel('angle \theta')
zlabel('Power in Beta')
title('Total Beta Power vs angle \theta and frequency/Hz (with rubber)')
grid
```

Appendix: $\boxed{\textbf{C-1}}$ ***Force-Input Joint equation derivation: -***

On the **incident side** of the bend for flexural displacement $W_\alpha(x,t)$ & $W_\gamma(x,t)$and longitudinal displacement $U_\alpha(x,t)$ & $U_\gamma(x,t)$

$$\boldsymbol{U_\alpha}(x,t) = \left\{A_L e^{-ik_{l\alpha*}(x-m)} + B_L e^{ik_{l\alpha*}(x-n)}\right\}\ e^{i\omega t};$$

$\boxed{2}$ $at\ x = m;\ \ \left\{A_L + B_L e^{ik_{l\alpha*}(m-n)}\right\};$

$\boxed{1}$ $at\ x = n;\ \ \left\{A_L e^{-ik_{l\alpha*}(n-m)} + B_L\right\};$

$$\frac{\partial U_\alpha}{\partial x} = k_{l\alpha*}\left\{-iA_L e^{-ik_{l\alpha*}(x-m)}\right\} + k_{l\alpha*}\left\{iB_L e^{ik_{l\alpha*}(x-n)}\right\};$$

$\boxed{10}$ $at\ x = m;\ \ k_{l\alpha*}\{-iA_L\} + k_{l\alpha*}\left\{iB_L e^{ik_{l\alpha*}(m-n)}\right\};$

$\boxed{7,9}$ $at\ x = n;\ \ k_{l\alpha*}\left\{-iA_L e^{-ik_{l\alpha*}(n-m)}\right\} + k_{l\alpha*}\{iB_L\};$

$$\boldsymbol{W_\alpha}(x,t) = \left\{A_2 e^{-k_{f\alpha}(x-m)} + A_4 e^{-ik_{f\alpha*}(x-m)} + B_1 e^{k_{f\alpha}(x-n)} + B_3 e^{ik_{f\alpha*}(x-n)}\right\}\ e^{i\omega t};$$

$\boxed{4}$ $at\ x = m;\ \ \left\{A_2 + A_4 + B_1 e^{k_{f\alpha}(m-n)} + B_3 e^{ik_{f\alpha*}(m-n)}\right\};$

$\boxed{3}$ $at\ x = n;\ \ \left\{A_2 e^{-k_{f\alpha}(n-m)} + A_4 e^{-ik_{f\alpha*}(n-m)} + B_1 + B_3\right\};$

$$\frac{\partial W_\alpha}{\partial x} = k_{f\alpha}\left\{-A_2 e^{-k_{f\alpha}(x-m)} + B_1 e^{k_{f\alpha}(x-n)}\right\} + k_{f\alpha*}\left\{-iA_4 e^{-ik_{f\alpha*}(x-m)} + iB_3 e^{ik_{f\alpha*}(x-n)}\right\};$$

$\boxed{6}$ $at\ x = m;\ \ k_{f\alpha}\left\{-A_2 + B_1 e^{k_{f\alpha}(m-n)}\right\} + k_{f\alpha*}\left\{-iA_4 + iB_3 e^{ik_{f\alpha*}(m-n)}\right\};$

$\boxed{3,5}$ $at\ x = n;\ \ k_{f\alpha}\left\{-A_2 e^{-k_{f\alpha}(n-m)} + B_1\right\} + k_{f\alpha*}\left\{-iA_4 e^{-ik_{f\alpha*}(n-m)} + iB_3\right\};$

$$\frac{\partial^2 W_\alpha}{\partial x^2} = {k_{f\alpha}}^2\left\{A_2 e^{-k_{f\alpha}(x-m)} + B_1 e^{k_{f\alpha}(x-n)}\right\} + {k_{f\alpha*}}^2\left\{-A_4 e^{-ik_{f\alpha*}(x-m)} - B_3 e^{ik_{f\alpha*}(x-n)}\right\};$$

$\boxed{8}$ $at\ x = m;\ \ {k_{f\alpha}}^2\left\{A_2 + B_1 e^{k_{f\alpha}(m-n)}\right\} + {k_{f\alpha*}}^2\left\{-A_4 - B_3 e^{ik_{f\alpha*}(m-n)}\right\};$

$\boxed{7}$ $at\ x = n;\ \ {k_{f\alpha}}^2\left\{A_2 e^{-k_{f\alpha}(n-m)} + B_1\right\} + {k_{f\alpha*}}^2\left\{-A_4 e^{-ik_{f\alpha*}(n-m)} - B_3\right\};$

$$\frac{\partial^3 W_\alpha}{\partial x^3} = {k_{f\alpha}}^3\left\{-A_2 e^{-k_{f\alpha}(x-m)} + B_1 e^{k_{f\alpha}(x-n)}\right\} + {k_{f\alpha*}}^3\left\{iA_4 e^{-ik_{f\alpha*}(x-m)} - iB_3 e^{ik_{f\alpha*}(x-n)}\right\};$$

$\boxed{12}$ $at\ x = m;\ \ {k_{f\alpha}}^3\left\{-A_2 + B_1 e^{k_{f\alpha}(m-n)}\right\} + {k_{f\alpha*}}^3\left\{iA_4 - iB_3 e^{k_{f\alpha*}(m-n)}\right\};$

$\boxed{7,11}$ $at\ x = n;\ \ {k_{f\alpha}}^3\left\{-A_2 e^{-k_{f\alpha}(n-m)} + B_1\right\} + {k_{f\alpha*}}^3\left\{iA_4 e^{-ik_{f\alpha*}(n-m)} - iB_3\right\};$

Differentiates $W_\alpha$and $U_\alpha$with respect to time (t);

$at: t = 0,\ x = n\ ,$ for $\frac{\partial^2 \boldsymbol{W_\alpha}}{\partial t^2}$,

$$\boldsymbol{W_\alpha}(x,t) = \left\{A_2 e^{-k_{f\alpha}(x-m)} + A_4 e^{-ik_{f\alpha*}(x-m)} + B_1 e^{k_{f\alpha}(x-n)} + B_3 e^{ik_{f\alpha*}(x-n)}\right\} e^{i\omega t} ;$$

$$\frac{\partial \boldsymbol{W_\alpha}}{\partial t} = i\omega\left\{A_2 e^{-k_{f\alpha}(n-m)} + A_4 e^{-ik_{f\alpha*}(n-m)} + B_1 + B_3\right\} e^{i\omega t} ;$$

$\boxed{11}$
$$\frac{\partial^2 \boldsymbol{W_\alpha}}{\partial t^2} = -\omega^2\left\{A_2 e^{-k_{f\alpha}(n-m)} + B_1\right\} - \omega^2\left\{A_4 e^{-ik_{f\alpha*}(n-m)} + B_3\right\} ;$$

$at: t = 0,\ x = n\ ,$ for $\frac{\partial^2}{\partial t^2}\frac{\partial \boldsymbol{W_\alpha}}{\partial x}$,

$$\frac{\partial W_\alpha}{\partial x} = k_{f\alpha}\left\{-A_2 e^{-k_{f\alpha}(x-m)} + B_1 e^{k_{f\alpha}(x-n)}\right\} + k_{f\alpha*}\left\{-iA_4 e^{-ik_{f\alpha*}(x-m)} + iB_3 e^{ik_{f\alpha*}(x-n)}\right\} ;$$

$$\frac{\partial}{\partial t}\frac{\partial \boldsymbol{W_\alpha}}{\partial x} = i\omega k_{f\alpha}\left\{-A_2 e^{-k_{f\alpha}(n-m)} + B_1\right\} e^{i\omega t} + i\omega k_{f\alpha*}\left\{-iA_4 e^{-ik_{f\alpha*}(n-m)} + iB_3\right\} e^{i\omega t} ;$$

$\boxed{7,9,11}$
$$\frac{\partial^2}{\partial t^2}\frac{\partial \boldsymbol{W_\alpha}}{\partial x} = -\omega^2 k_{f\alpha}\left\{-A_2 e^{-k_{f\alpha}(n-m)} + B_1\right\} -\omega^2 k_{f\alpha*}\left\{-iA_4 e^{-ik_{f\alpha*}(n-m)} + iB_3\right\} ;$$

$at: t = 0,\ x = n\ ,$ for $\frac{\partial^2 \boldsymbol{U_\alpha}}{\partial t^2}$,

$$\boldsymbol{U_\alpha}(x,t) = \left\{A_L e^{-ik_{l\alpha*}(x-m)} + B_L e^{ik_{l\alpha*}(x-n)}\right\} e^{i\omega t};$$

$$\frac{\partial U_\alpha}{\partial t} = i\omega\left\{A_L e^{-ik_{l\alpha*}(n-m)} + B_L\right\} e^{i\omega t} ;$$

$\boxed{9}$
$$\frac{\partial^2 \boldsymbol{U_\alpha}}{\partial t^2} = -\omega^2\left\{A_L e^{-ik_{l\alpha*}(n-m)} + B_L\right\} ;$$

$$\boldsymbol{W_\gamma}(x,t) = \left\{D_1 e^{k_{f\gamma}(x-m)} + D_3 e^{ik_{f\gamma*}(x-m)} + B_1 e^{-k_{f\alpha}(x-n)} + B_3 e^{-ik_{f\alpha*}(x-n)}\right\} e^{i\omega t} ;$$

$at\ x = m ;$ $\left\{D_1 + D_3 + B_1 e^{-k_{f\alpha}(m-n)} + B_3 e^{-ik_{f\alpha*}(m-n)}\right\} ;$ $\boxed{4}$

$$\frac{\partial W_\gamma}{\partial x} = k_{f\gamma}\left\{D_1 e^{k_{f\gamma}(x-m)} + iD_3 e^{ik_{f\gamma*}(x-m)}\right\} + k_{f\alpha}\left\{-B_1 e^{-k_{f\alpha}(x-m)} + (-iB_3) e^{-ik_{f\alpha*}(x-m)}\right\} ;$$

$at\ x = m ;$ $k_{f\gamma}\{D_1\} + k_{f\gamma*}\{iD_3\} - k_{f\alpha}\{B_1\}e^{-k_{f\alpha}(m-n)} - k_{f\alpha*}\{iB_3\}e^{-ik_{f\alpha*}(m-}$ $\boxed{6}$

$$\frac{\partial^2 W_\gamma}{\partial x^2} = k_{f\gamma}{}^2\left\{D_1 e^{k_{f\gamma}(x-m)} - D_3 e^{ik_{f\gamma*}(x-m)}\right\} + k_{f\alpha}{}^2\left\{B_1 e^{-k_{f\alpha}(x-m)} + (-B_3) e^{-ik_{f\alpha*}(x-m)}\right\} ;$$

$at\ x = m ;$ $k_{f\gamma}{}^2\{D_1\} - k_{f\gamma*}{}^2\{D_3\} + k_{f\alpha}{}^2\{B_1\}e^{-k_{f\alpha}(m-n)} - k_{f\alpha*}{}^2\{B_3\}e^{-ik_{f\alpha*}(m-n)}$ $\boxed{8}$

$$\frac{\partial^3 W_\gamma}{\partial x^3} = k_{f\gamma}{}^3\left\{D_1 e^{k_{f\gamma}(x-m)} - iD_3 e^{ik_{f\gamma*}(x-m)}\right\} + k_{f\alpha}{}^3\left\{-B_1 e^{-k_{f\alpha}(x-m)} + iB_3 e^{-ik_{f\alpha*}(x-m)}\right\} ;$$

$at\ x = m ;$ $k_{f\gamma}{}^3\{D_1\} - k_{f\gamma*}{}^3\{iD_3\} - k_{f\alpha}{}^3\{B_1\}e^{-k_{f\alpha}(m-n)} + k_{f\alpha*}{}^3\{iB_3\}e^{-ik_{f\alpha*}(m-}$ $\boxed{12}$

$$\boldsymbol{U_\gamma}(x,t) = \left\{D_L e^{ik_{l\gamma*}(x-m)} + B_L e^{-i\ \ l\alpha*(x-n)}\right\} e^{i\omega t} ;$$

$at\ x = m ;$ $\{D_L\} + \{B_L\}e^{-ik_{l\alpha*}(m-n)} ;$ $\boxed{2}$

$$\frac{\partial U_\gamma}{\partial x} = \ _{l\gamma*}\left\{iD_L e^{ik_{l\gamma*}(x-m)}\right\} - k_{l\alpha*}\left\{iB_L e^{-ik_{l\alpha*}(x-n)}\right\} ;$$

$at\ x = m ;$ $k_{l\gamma*}\{iD_L\} - k_{l\alpha*}\{iB_L\}e^{-ik_{l\alpha*}(m-}$ $\boxed{10}$

For the **transmitting side** of the bend for flexural $W_\beta(\psi,t)$ and longitudinal $U_\beta(\psi,t)$,

$$\boldsymbol{W_\beta}(\psi,t) = \left\{C_2 e^{-k_{f\beta}(\psi-n)} + C_4 e^{-ik_{f\beta*}(\psi-n)}\right\} e^{i\omega t} \;;$$

$at\ \psi = n\,;$ $\{C_2 + C_4\}\,;$

$$\frac{\partial W_\beta}{\partial \psi} = k_{f\beta}\left\{-C_2 e^{-k_{f\beta}(\psi-n)} - iC_4 e^{-ik_{f\beta*}(\psi-n)}\right\};$$

$\boxed{1{,}3}$

$at\ \psi = n\,;$ $k_{f\beta}\{-C_2\} + k_{f\beta*}\{-iC_4\}\ ;$

$$\frac{\partial^2 W_\beta}{\partial \psi^2} = {k_{f\beta}}^2\left\{C_2 e^{-k_{f\beta}(\psi-n)} - C_4 e^{-ik_{f\beta*}(\psi-n)}\right\};$$

$\boxed{1{,}3{,}5}$

$at\ \psi = n\,;$ ${k_{f\beta}}^2\{C_2\} - {k_{f\beta*}}^2\{C_4\}\ ;$

$$\frac{\partial^3 W_\beta}{\partial \psi^3} = {k_{f\beta}}^3\left\{-C_2 e^{-k_{f\beta}(\psi-n)} + iC_4 e^{-ik_{f\beta*}(\psi-n)}\right\};$$

$\boxed{7}$

$at\ \psi = n\,;$ ${k_{f\beta}}^3\{-C_2\} + {k_{f\beta*}}^3\{iC_4\}\,;$

$\boxed{7{,}9{,}1}$

$$\boldsymbol{U_\beta}(\psi,t) = \left\{C_L e^{-i\ \ l\beta*(\psi-n)}\right\} e^{i\omega t} \;;$$

$at\ \psi = n\,;$ $\{C_L\}\,;$

$\boxed{1{,}3}$

$$\frac{\partial U_\beta}{\partial \psi} = k_{l\beta*}\left\{-iC_L e^{-ik_{l\beta*}(\psi-n)}\right\};$$

$at\ \psi = n\,;$ $k_{l\beta*}\{-iC_L\}\,;$

$\boxed{7{,}9{,}1}$

Again, applying boundary condition at $x = m$, $x = n$ and $\psi = 0$, to all equation of continuity, summation of bending moments, shear forces and compressive forces, yields 12 governing equations as below:-

1.1.1.1 Continuity of displacement in axial direction (joint),

at $\boldsymbol{x = n}$

$$U_\alpha \quad = \quad U_\beta \cos\theta \quad - \quad W_\beta \sin\theta \quad + \quad \frac{L}{2}(\mathbf{1} - \mathbf{cos}\,\boldsymbol{\theta})\frac{\partial W_\beta}{\partial \psi}$$

$\boldsymbol{U_\alpha}(x,t)$	$\{A_L e^{-ik_{l\alpha*}(n-m)} + B_L\}\ ;$
$\boldsymbol{U_\beta}(\psi,t)$	$\{C_L\}\,;$
$\boldsymbol{W_\beta}(\psi,t)$	$\{C_2 + C_4\}\,;$
$\frac{\partial W_\beta}{\partial \psi}$	$k_{f\beta}\{-C_2\} + k_{f\beta*}\{-iC_4\}\ ;$

$$A_L e^{-ik_{l\alpha*}(n-m)} + B_L = C_L \cos\theta - (C_2 + C_4)\sin\theta + \frac{L}{2}(\mathbf{1} - \mathbf{cos}\,\boldsymbol{\theta})\left[k_{f\beta}\{-C_2\} + k_{f\beta*}\{-iC_4\}\right]$$

$$0 = -A_L e^{-ik_{l\alpha*}(n-m)} - B_L + C_L \cos\theta - C_2 \sin\theta - C_4 \sin\theta - (k_{f\beta})\frac{L}{2}\, C_2(\mathbf{1} - \mathbf{cos}\,\boldsymbol{\theta}) - (k_{f\beta*})\frac{L}{2}\, iC_4(\mathbf{1} - \mathbf{cos}\,\boldsymbol{\theta})$$

$$\left[\!\left[0 = (-A_L)\underbrace{e^{-ik_{l\alpha*}(n-m)}}_{1c} + -B_L + (-C_2)\underbrace{\left[\sin\theta + \left[(k_{f\beta})\frac{L}{2}\,(\mathbf{1} - \mathbf{cos}\,\boldsymbol{\theta})\right]\right]}_{1g} + (-C_4)\underbrace{\left[\sin\theta + \left[(ik_{f\beta*})\frac{L}{2}\,(\mathbf{1} - \mathbf{cos}\,\boldsymbol{\theta})\right]\right]}_{1h} + C_L \underbrace{\cos\theta}_{1i} \right]\!\right]$$

Equation for MATLAB:-

0 = [(-A$_L$)(Lni)]
+ (-B$_L$)
+ (-C$_2$)[Sin θ +($k_{f\beta}$ {V1})]
+ (-C$_4$)[Sin θ +(i$k_{f\beta*}$ {V1})]
+ (C$_L$)(Cos θ)

1.1.1.2 Continuity of displacement in axial direction,

$$\textbf{at } \boldsymbol{x = m}$$

$$U_\gamma = U_\alpha$$

$\boldsymbol{U_\gamma}(x,t)$ $\{D_L + B_L e^{-ikl\alpha*(m-n)}\}$;
$\boldsymbol{U_\alpha}(x,t)$ $\{A_L + B_L e^{ikl\alpha*(m-n)}\}$;

$$D_L + B_L e^{-ikl\ \ *(m-n)} = A_L + B_L e^{ikl\alpha*(m-n)}$$

$$\left[\!\left[0 = A_L + B_L\, e^{ikl\alpha*(m-n)} - D_L - B_L\, e^{-ikl\alpha*(m-n)} \right]\!\right]$$

0 = (A$_L$)
+ [(B$_L$) (Lpi)] + [(-B$_L$) (Lni)]
+ (-D$_L$)

Equation for MATLAB:-

0 = (A$_L$)
+ [(B$_L$) (Lpi - Lni)]
+ (-D$_L$)

1.1.1.3 Continuity of relative displacement in perpendicular direction (joint), at $x = n$

$$W_\alpha = U_\beta \sin\theta + W_\beta \cos\theta - \frac{L}{2}(\sin\theta)\frac{\partial W_\beta}{\partial \psi}$$

$\boldsymbol{W_\alpha}(x,t)$ $\{A_2 e^{-k_{f\alpha}(n-m)} + A_4 e^{-ik_{f\alpha*}(n-m)} + B_1 + B_3\}$;
$\boldsymbol{U_\beta}(\psi,t)$ $\{C_L\}$;
$\boldsymbol{W_\beta}(\psi,t)$ $\{C_2 + C_4\}$;
$\frac{\partial W_\beta}{\partial \psi}$ $k_{f\beta}\{-C_2\} + k_{f\beta*}\{-iC_4\}$;

$$A_2 e^{-k_{f\alpha}(n-m)} + A_4 e^{-ik_{f\alpha*}(n-m)} + B_1 + B_3 = C_L \sin\theta + (C_2 + C_4)\cos\theta - \frac{L}{2}(\sin\theta)[k_{f\beta}\{-C_2\} + k_{f\beta*}\{-iC_4\}]$$

$$0 = -B_1 - B_3 - A_4 e^{-ik_{f\alpha*}(n-m)} - A_2 e^{-k_{f\alpha}(n-m)} + C_L \sin\theta + C_2\cos\theta + C_4\cos\theta + C_2\left[(k_{f\beta})\frac{L}{2}(\sin\theta)\right] + C_4\left[(ik_{f\beta*})\frac{L}{2}(\sin\theta)\right]$$

$$\left[\left[0 = (-A_2)\underbrace{e^{-k_{f\alpha}(n-m)}}_{3a}(-A_4)\underbrace{e^{-ik_{f\alpha*}(n-m)}}_{3b} - B_1 - B_3 + C_2\underbrace{\left[\cos\theta + \left[(k_{f\beta})\frac{L}{2}(\sin\theta)\right]\right]}_{3g} + C_4\underbrace{\left[\cos\theta + \left[(ik_{f\beta*})\frac{L}{2}(\sin\theta)\right]\right]}_{3h} + C_L\underbrace{\sin\theta}_{3i}\right]\right]$$

Equation for MATLAB:-

0	=	**[(-A2)(Fn)]**
	+	**[(-A4) (Fni)]**
	+.	**(-B1)**
	+.	**(-B3)**
	+	**(C2)[Cos θ +(kfβ {V3})]**
	+	**(C4)[Cos θ +(ikfβ* {V3})]**
	+	**(CL)(Sin θ)**

1.1.1.4 Continuity of relative displacement in perpendicular direction, at $x = m$

$$W_\alpha = W_\gamma$$

$\boldsymbol{W_\gamma}(x,t)$ $\{D_1 + D_3 + B_1 e^{-kf\alpha*(m-n)} + B_3 e^{-ikf\alpha*(m-n)}\}$;
$\boldsymbol{W_\alpha}(x,t)$ $\{A_2 + A_4 + B_1 e^{kf\ \ *(m-n)} + B_3 e^{ikf\alpha*(m-n)}\}$;

$$\{A_2 + A_4 + B_1 e^{kf\alpha(m-n)} + B_3 e^{ikf\alpha*(m-n)}\} = \{D_1 + D_3 + B_1 e^{-kf\alpha(m-n)} + B_3 e^{-ikf\alpha*(m-n)}\}$$

$$[\![0 = A_2 + A_4 + B_1 e^{kf\ *(m-n)} + B_3 e^{ikf\alpha*(m-n)} - D_1 - D_3 - B_1 e^{-kf\alpha*(m-n)} - B_3 e^{-ikf\alpha*(m-n)}]\!]$$

0 = **(A2)**
\+ **(A4)**
\+ **[(B1) (Fp)]** + **[(B3) (Fpi)]**
\+ **(-D1)**
\+ **(-D3)**
\+ **[(-B1) (Fn)]** + **[(-B3) (Fni)]**

Equation for MATLAB:-

0 = **(A2)**
\+ **(A4)**
\+ **[(B1) (Fp - Fn)]**
\+ **[(B3) (Fpi - Fni)]**
\+ **(-D1)**
\+ **(-D3)**

1.1.1.5 Continuity of angular displacement/equal gradient (joint),

at $x = n$

$$\frac{\partial W_\alpha}{\partial x} = \frac{\partial W_\beta}{\partial \psi}$$

$\frac{\partial W_\alpha}{\partial x}$ $k_{f\alpha}\{-A_2 e^{-k_{f\alpha}(n-m)} + B_1\} + k_{f\alpha*}\{-iA_4 e^{-ik_{f\alpha*}(n-m)} + iB_3\};$

$\frac{\partial W_\beta}{\partial \psi}$ $k_{f\beta}\{-C_2\} + k_{f\beta*}\{-iC_4\};$

$$k_{f\alpha}\{-A_2 e^{-k_{f\alpha}(n-m)} + B_1\} + k_{f\alpha*}\{-iA_4 e^{-ik_{f\alpha*}(n-m)} + iB_3\} = k_{f\beta}\{-C_2\} + k_{f\beta*}\{-iC_4\}$$

$$-A_2 k_{f\alpha} e^{-k_{f\alpha}(n-m)} + B_1 k_{f\alpha} - A_4 ik_{f\alpha*} e^{-ik_{f\alpha*}(n-m)} + B_3 ik_{f\alpha*} = -C_2 k_{f\beta} - C_4 ik_{f\beta*}$$

$$[\![0 = (A_2)\underbrace{k_{f\alpha} e^{-k_{f\alpha}(n-m)}}_{5a} + (A_4)\underbrace{ik_{f\alpha*} e^{-ik_{f\alpha*}(n-m)}}_{5b} + (-B_1)\underbrace{(k_{f\alpha})}_{5d} + (-B_3)\underbrace{(ik_{f\alpha*})}_{5e} + (-C_2)\underbrace{(k_{f\beta})}_{5g} + (-C_4)\underbrace{(ik_{f\beta*})}_{5h}]\!]$$

Equation for MATLAB:-

0	=	**[(A2) kfα (Fn)]**
	+	**[(A4) ikfα* (Fni)]**
	+.	**(-B1) kfα**
	+.	**(-B3) ikfα***
	+	**(-C2) kfβ**
	+	**(-C4) ikfβ***

1.1.1.6 Continuity of angular displacement/equal gradient,

at $x = m$

$$\frac{\partial W_\alpha}{\partial x} = \frac{\partial W_\gamma}{\partial x}$$

$\frac{\partial W_\gamma}{\partial x}$ $k_{f\gamma}\{D_1\} + k_{f\gamma *}\{iD_3\} + k_{f\alpha}\{-B_1\}e^{-kf\alpha(m-n)} + k_{f\alpha *}\{-iB_3\}e^{-ikf\alpha *(m-n)}$;

$\frac{\partial W_\alpha}{\partial x}$ $k_{f\alpha}\{-A_2 + B_1 e^{kf\alpha(m-n)}\} + k_{f\alpha *}\{-iA_4 + iB_3\, e^{ikf\alpha *(m-n)}\}$;

$$k_{f\alpha}\{-A_2 + B_1 e^{kf\ (m-n)}\} + k_{f\alpha *}\{-iA_4 + iB_3 e^{ikf\alpha *(m-n)}\} = k_{f\gamma}\{D_1\} + k_{f\gamma *}\{iD_3\} + k_{f\alpha}\{-B_1\}e^{-kf\alpha(m-n)} + k_{f\alpha *}\{-iB_3\}e^{-ikf\alpha *(m-n)}$$

$$-A_2 k_{f\alpha} + B_1 k_{f\alpha} e^{kf\ (m-n)} - A_4 ik_{f\alpha *} + B_3 ik_{f\alpha *} e^{ikf\alpha *(m-n)}$$
$$= D_1 k_{f\gamma} + D_3 ik_{f\gamma *} - B_1 k_{f\alpha} e^{-kf\alpha(m-n)} - B_3 ik_{f\alpha *} e^{-ikf\alpha *(m-n)}$$

$$0 = (A_2)\underbrace{k_{f\alpha}}_{6a} + (A_4)\underbrace{ik_{f\alpha *}}_{6b} + (-B_1)\underbrace{k_{f\alpha}}_{6d} e^{kf\alpha(m-n)} + (-B_3)\underbrace{ik_{f\alpha *}}_{6e} e^{ikf\alpha *(m-n)}$$

$$+ D_1 \underbrace{k_{f\gamma}}_{6j} + D_3 \underbrace{ik_{f\gamma *}}_{6k} + (-B_1)\underbrace{k_{f\alpha}}_{6d} e^{-kf\alpha(m-n)} + (-B_3)\underbrace{ik_{f\alpha *}}_{6e} e^{-ikf\alpha *(m-n)}$$

0	=	**(A2) kfα**
	+	**(A4) ikfα***
	+	**[(-B1) kfα (Fp)] + [(-B3) ikfα* (Fpi)]**
	+	**(D1) kfγ**
	+	**(D3) ikfγ***
	+	**[(-B1) kfα (Fn)] + [(-B3) ikfα* (Fni)]**

Equation for MATLAB:-

0	=	**(A2) kfα**
	+	**(A4) ikfα***
	+	**[(-B1) kfα (Fp + Fn)]**

+ [(-B_3) $ik_{f\alpha*}$ (Fpi + Fni)]
+ (D_1) $k_{f\gamma}$
+ (D_3) $ik_{f\gamma*}$

1.1.1.7 Equilibrium of bending moment (joint), at $x = n$

$$E_1 I_1 \frac{\partial^2 W_\alpha}{\partial x^2} + \frac{L}{2}\left(\sin\tfrac{\theta}{2}\right) E_1 I_1 \frac{\partial^3 W_\alpha}{\partial x^3} = E_2 I_2 \frac{\partial^2 W_\beta}{\partial \psi^2} - \frac{L}{2}\left(\sin\tfrac{\theta}{2}\right) E_2 I_2 \frac{\partial^3 W_\beta}{\partial \psi^3} - I_j \frac{\partial^2 \partial W_\alpha}{\partial t^2 \partial x} - \boldsymbol{E_1 A_1 \frac{\partial U_\alpha}{\partial x}\left[\frac{L}{2}\left(1-\cos\tfrac{\theta}{2}\right)\right]} + \boldsymbol{E_2 A_2 \frac{\partial U_\beta}{\partial \psi}\left[\frac{L}{2}\left(1-\cos\tfrac{\theta}{2}\right)\right]}$$

$\frac{\partial^2 W_\alpha}{\partial x^2}$ $k_{f\alpha}{}^2\{A_2 e^{-k_{f\alpha}(n-m)} + B_1\} + k_{f\alpha*}{}^2\{-A_4 e^{-ik_{f\alpha*}(n-m)} - B_3\}$;

$\frac{\partial^3 W_\alpha}{\partial x^3}$ $k_{f\alpha}{}^3\{-A_2 e^{-k_{f\alpha}(n-m)} + B_1\} + k_{f\alpha*}{}^3\{iA_4 e^{-ik_{f\alpha*}(n-m)} - iB_3\}$;

$\frac{\partial^2 W_\beta}{\partial \psi^2}$ $k_{f\beta}{}^2\{C_2\} - k_{f\beta*}{}^2\{C_4\}$;

$\frac{\partial^3 W_\beta}{\partial \psi^3}$ $k_{f\beta}{}^3\{-C_2\} + k_{f\beta*}{}^3\{iC_4\}$;

$\frac{\partial^2}{\partial t^2}\frac{\partial \boldsymbol{W_\alpha}}{\partial x}$ $-\omega^2 k_{f\alpha}\{-A_2 e^{-k_{f\alpha}(n-m)} + B_1\} - \omega^2 k_{f\alpha*}\{-iA_4 e^{-ik_{f\alpha*}(n-m)} + iB_3\}$;

$\frac{\partial U_\alpha}{\partial x}$ $k_{l\alpha*}\{-iA_L e^{-ik_{l\alpha*}(n-m)}\} + k_{l\alpha*}\{iB_L\}$;

$\frac{\partial U_\beta}{\partial \psi}$ $k_{l\beta*}\{-iC_L\}$;

$$\begin{aligned}
&E_1 I_1\left[k_{f\alpha}{}^2\{A_2 e^{-k_{f\alpha}(n-m)} + B_1\} + k_{f\alpha*}{}^2\{-A_4 e^{-ik_{f\alpha*}(n-m)} - B_3\}\right] \\
&\quad + \frac{L}{2}\left(\sin\tfrac{\theta}{2}\right) E_1 I_1\left[k_{f\alpha}{}^3\{-A_2 e^{-k_{f\alpha}(n-m)} + B_1\} + k_{f\alpha*}{}^3\{iA_4 e^{-ik_{f\alpha*}(n-m)} - iB_3\}\right] \\
&= E_2 I_2\left[k_{f\beta}{}^2\{C_2\} - k_{f\beta*}{}^2\{C_4\}\right] - \frac{L}{2}\left(\sin\tfrac{\theta}{2}\right) E_2 I_2\left[k_{f\beta}{}^3\{-C_2\} + k_{f\beta*}{}^3\{iC_4\}\right] \\
&\quad - I_j\left[-\omega^2 k_{f\alpha}\{-A_2 e^{-k_{f\alpha}(n-m)} + B_1\} - \omega^2 k_{f\alpha*}\{-iA_4 e^{-ik_{f\alpha*}(n-m)} + iB_3\}\right] \\
&\quad - \left[\frac{L}{2}\left(1-\cos\tfrac{\theta}{2}\right)\right]\boldsymbol{E_1 A_1}\left[k_{l\alpha*}\{-iA_L e^{-ik_{l\alpha*}(n-m)}\} + k_{l\alpha*}\{iB_L\}\right] \\
&\quad + \left[\frac{L}{2}\left(1-\cos\tfrac{\theta}{2}\right)\right]\boldsymbol{E_2 A_2}\left[k_{l\beta*}\{-iC_L\}\right]
\end{aligned}$$

$$E_1I_1\left[k_{f\alpha}{}^2A_2e^{-k_{f\alpha}(n-m)}+k_{f\alpha}{}^2B_1-k_{f\alpha*}{}^2A_4e^{-ik_{f\alpha*}(n-m)}-k_{f\alpha*}{}^2B_3\right]$$
$$+\frac{L}{2}\left(\sin\tfrac{\theta}{2}\right)E_1I_1\left[-k_{f\alpha}{}^3A_2e^{-k_{f\alpha}(n-m)}+k_{f\alpha}{}^3B_1+k_{f\alpha*}{}^3iA_4e^{-ik_{f\alpha*}(n-m)}-k_{f\alpha*}{}^3iB_3\right]$$
$$=E_2I_2\left[k_{f\beta}{}^2C_2-k_{f\beta*}{}^2C_4\right]-\frac{L}{2}\left(\sin\tfrac{\theta}{2}\right)E_2I_2\left[-k_{f\beta}{}^3C_2+k_{f\beta*}{}^3iC_4\right]$$
$$-I_j\left[\omega^2k_{f\alpha}A_2e^{-k_{f\alpha}(n-m)}-\omega^2k_{f\alpha}B_1+\omega^2k_{f\alpha*}iA_4e^{-ik_{f\alpha*}(n-m)}-\omega^2k_{f\alpha*}iB_3\right]$$
$$-\left[\frac{L}{2}\left(1-\cos\tfrac{\theta}{2}\right)\right]E_1A_1\left[-k_{l\alpha*}iA_Le^{-ik_{l\alpha*}(n-m)}+k_{l\alpha*}iB_L\right]$$
$$+\left[\frac{L}{2}\left(1-\cos\tfrac{\theta}{2}\right)\right]E_2A_2\left[-k_{l\beta*}iC_L\right]$$

$$0$$
$$=A_2\underbrace{\left\{-\left(E_1I_1\left(k_{f\alpha}^2\right)\right)e^{-k_{f\alpha}(n-m)}+\left(\frac{L}{2}\left(\sin\tfrac{\theta}{2}\right)E_1I_1\left(k_{f\alpha}^3\right)\right)e^{-k_{f\alpha}(n-m)}-\left(I_j\omega^2\left(k_{f\alpha}\right)\right)e^{-k_{f\alpha}(n-m)}\right\}}_{7a}$$
$$+A_4\underbrace{\left\{\left(E_1I_1\left(k_{f\alpha*}^2\right)\right)e^{-ik_{f\alpha*}(n-m)}-\left(\frac{L}{2}\left(\sin\tfrac{\theta}{2}\right)E_1I_1\left(ik_{f\alpha*}^3\right)\right)e^{-ik_{f\alpha*}(n-m)}-\left(I_j\omega^2\left(ik_{f\alpha*}\right)\right)e^{-ik_{f\alpha*}(n-m)}\right\}}_{7b}$$
$$+A_L\underbrace{\left\{\left[\frac{L}{2}\left(1-\cos\tfrac{\theta}{2}\right)\right]E_1A_1\left(ik_{l\alpha*}\right)e^{-ik_{l\alpha*}(n-m)}\right\}}_{7c}$$
$$+B_1\underbrace{\left\{-\left(E_1I_1\left(k_{f\alpha}^2\right)\right)-\left(\frac{L}{2}\left(\sin\tfrac{\theta}{2}\right)E_1I_1\left(k_{f\alpha}^3\right)\right)+\left(I_j\omega^2\left(k_{f\alpha}\right)\right)\right\}}_{7d}$$
$$+B_3\underbrace{\left\{\left(E_1I_1\left(k_{f\alpha*}^2\right)\right)+\left(\frac{L}{2}\left(\sin\tfrac{\theta}{2}\right)E_1I_1\left(ik_{f\alpha*}^3\right)\right)+\left(I_j\omega^2\left(ik_{f\alpha*}\right)\right)\right\}}_{7e}$$
$$+B_L\underbrace{\left\{-\left[\frac{L}{2}\left(1-\cos\tfrac{\theta}{2}\right)\right]E_1A_1\left(ik_{l\alpha*}\right)\right\}}_{7f}$$
$$+C_2\underbrace{\left\{E_2I_2\left(k_{f\beta}{}^2\right)+\frac{L}{2}\left(\sin\tfrac{\theta}{2}\right)E_2I_2\left(k_{f\beta}{}^3\right)\right\}}_{7g}$$
$$+C_4\underbrace{\left\{-E_2I_2\left(k_{f\beta*}{}^2\right)-\frac{L}{2}\left(\sin\tfrac{\theta}{2}\right)E_2I_2\left(ik_{f\beta*}{}^3\right)\right\}}_{7h}$$
$$+C_L\underbrace{\left\{-\left[\frac{L}{2}\left(1-\cos\tfrac{\theta}{2}\right)\right]E_2A_2\left(ik_{l\beta*}\right)\right\}}_{7i}$$

Equation for MATLAB:-

$$
\begin{aligned}
0 \quad = \quad & (A_2)\ [\ \{V6\}(Q1)\ k_{f\alpha}^3\ (Fn) \quad + (-Q1)\ k_{f\alpha}^2\ (Fn) \quad + (-I_j w^2)\ k_{f\alpha}(Fn)\ ] \\
+ \quad & (A_4)\ [\ \{-V6\}(Q1)\ ik_{f\alpha^*}{}^3\ (Fni) + (Q1)\ k_{f\alpha^*}{}^2\ (Fni) + (-I_j w^2)\ ik_{f\alpha^*}\ (Fni)\ ] \\
+ \quad & (A_L)\ [\ \{V5\}(S1)\ ik_{l\alpha^*}\ (Lni)\ ] \\
+ \quad & (B_1)\ [\ \{-V6\}(Q1)\ k_{f\alpha}^3 + (-Q1)\ k_{f\alpha}^2 \quad + (I_j w^2)\ k_{f\alpha}\ ] \\
+ \quad & (B_3)\ [\ \{V6\}(Q1)\ ik_{f\alpha^*}{}^3 + (Q1)\ k_{f\alpha^*}{}^2 + (I_j w^2)\ ik_{f\alpha^*}\ ] \\
+ \quad & (B_L)\ [\ \{-V5\}(S1)\ ik_{l\alpha^*}\ ] \\
+ \quad & (C_2)\ [\ \{V6\}(Q2)\ k_{f\beta}^3 \quad + (Q2)\ k_{f\beta}{}^2\ ] \\
+ \quad & (C_4)\ [\ \{-V6\}(Q2)\ ik_{f\beta^*}{}^3 + (-Q2)\ k_{f\beta}{}^2] \\
+ \quad & (C_L)\ [\ \{-V5\}(S2)\ ik_{l\beta^*}\ ]
\end{aligned}
$$

$$
\begin{aligned}
0 \quad = \quad & (A_2)\ [\ \{V6\}(Q1)\ k_{f\alpha}^3 \quad + (-Q1)\ k_{f\alpha}^2 \quad + (-I_j w^2)\ k_{f\alpha}\ ]\ (Fn) \\
+ \quad & (A_4)\ [\ \{-V6\}(Q1)\ ik_{f\alpha^*}{}^3 \quad + (Q1)\ k_{f\alpha^*}{}^2 \quad + (-I_j w^2)\ ik_{f\alpha^*}]\ (Fni) \\
+ \quad & (A_L)\ [\ \{V5\}(S1)\ ik_{l\alpha^*}](Lni) \\
+ \quad & (B_1)\ [\ \{-V6\}(Q1)\ k_{f\alpha}^3 + (-Q1)\ k_{f\alpha}^2 \quad + (I_j w^2)\ k_{f\alpha}\ ] \\
+ \quad & (B_3)\ [\ \{V6\}(Q1)\ ik_{f\alpha^*}{}^3 + (Q1)\ k_{f\alpha^*}{}^2 + (I_j w^2)\ ik_{f\alpha^*}\ ] \\
+ \quad & (B_L)\ [\ \{-V5\}(S1)\ ik_{l\alpha^*}\ ] \\
+ \quad & (C_2)\ [\ \{V6\}(Q2)\ k_{f\beta}^3 \quad + (Q2)\ k_{f\beta}{}^2\ ] \\
+ \quad & (C_4)\ [\ \{-V6\}(Q2)\ ik_{f\beta^*}{}^3 + (-Q2)\ k_{f\beta}{}^2] \\
+ \quad & (C_L)\ [\ \{-V5\}(S2)\ ik_{l\beta^*}\ ]
\end{aligned}
$$

1.1.1.8 Equilibrium of bending moment, at $x = m$

$$E_1 I_1 \frac{\partial^2 W_\alpha}{\partial x^2} = E_1 I_1 \frac{\partial^2 W_\gamma}{\partial x^2}$$

$$\frac{\partial^2 W_\alpha}{\partial x^2} = \frac{\partial^2 W_\gamma}{\partial x^2}$$

$$\frac{\partial^2 W_\alpha}{\partial x^2} \qquad {k_{f\alpha}}^2\{A_2 + B_1 e^{kf\ \ (m-n)}\} + {k_{f\alpha*}}^2\{-A_4 - B_3 e^{ikf\alpha*(m-n)}\};$$

$$\frac{\partial^2 W_\gamma}{\partial x^2} \qquad {k_{f\gamma}}^2\{D_1\} - {k_{f\gamma*}}^2\{D_3\} + {k_{f\alpha}}^2\{B_1\}e^{-kf\alpha(m-n)} + {k_{f\alpha*}}^2\{-B_3\}e^{-ikf\alpha*(m-n)};$$

$$\begin{aligned} & {k_{f\alpha}}^2\{A_2 + B_1 e^{kf\alpha(m-n)}\} + {k_{f\alpha*}}^2\{-A_4 - B_3 e^{ikf\alpha*(m-n)}\} \\ = \ & {k_{f\gamma}}^2\{D_1\} - {k_{f\gamma*}}^2\{D_3\} + {k_{f\alpha}}^2\{B_1\}e^{-kf\alpha(m-n)} \\ + \ & {k_{f\alpha*}}^2\{-B_3\}e^{-ikf\alpha*(m-n)} \end{aligned}$$

$$\Bigg[\!\!\Bigg[0 = (-A_2)\underbrace{\{(k_{f\alpha}^2)\}}_{8a} + A_4\underbrace{\{(k_{f\alpha*}^2)\}}_{8b} + (-B_1)\underbrace{\{(k_{f\alpha}^2)\}}_{8d} e^{kf\ \ (m-n)} + B_3\underbrace{\{(k_{f\alpha*}^2)\}}_{8e} e^{ikf\alpha*(m-n)}$$

$$+ D_1\underbrace{\{(k_{f\gamma}^2)\}}_{8j} + (-D_3)\underbrace{\{(k_{f\gamma*}^2)\}}_{8k} + (B_1)\underbrace{\{(k_{f\alpha}^2)\}}_{8d} e^{-kf\alpha(m-n)}$$

$$+ (-B_3)\underbrace{\{(k_{f\alpha*}^2)\}}_{8e} e^{-ikf\alpha*(m-n)} \Bigg]\!\!\Bigg]$$

0	=	**($-A_2$) $k_{f\alpha}^2$**
	+	**(A_4) $ik_{f\alpha*}^2$**
	+	**[($-B_1$) $k_{f\alpha}^2$ (Fp)] + [(B_3) $ik_{f\alpha*}^2$ (Fpi)]**
	+	**(D_1) $k_{f\gamma}^2$**
	+	**($-D_3$) $ik_{f\gamma*}^2$**
	+	**[(B_1) $k_{f\alpha}^2$ (Fn)] + [($-B_3$) $ik_{f\alpha*}^2$ (Fni)]**

Equation for MATLAB:-

0	=	**($-A_2$) $k_{f\alpha}^2$**
	+	**(A_4) $ik_{f\alpha*}^2$**
	+	**[(B_1) $k_{f\alpha}^2$ (-Fp + Fn)]**
	+	**[(B_3) $ik_{f\alpha*}^2$ (Fpi - Fni)]**
	+	**(D_1) $k_{f\gamma}^2$**
	+	**($-D_3$) $ik_{f\gamma*}^2$**

1.1.1.9 Equilibrium of compressive force (joint), at $x = n$

$$E_1 A_1 \frac{\partial U_\alpha}{\partial x} = E_2 A_2 \frac{\partial U_\beta}{\partial \psi}\cos\theta + E_2 I_2 \frac{\partial^3 W_\beta}{\partial \psi^3}\sin\theta - m_j \frac{\partial^2}{\partial t^2}\left[U_\alpha - \boldsymbol{L}\left(\sin\tfrac{\theta}{4}\right)^2 \frac{\boldsymbol{\partial W_\alpha}}{\boldsymbol{\partial x}}\right]$$

$$\frac{\partial U_\alpha}{\partial x} \qquad k_{l\alpha*}\{-iA_L e^{-ik_{l\alpha*}(n-m)}\} + k_{l\alpha*}\{iB_L\};$$

$$\frac{\partial U_\beta}{\partial \psi} \qquad k_{l\beta*}\{-iC_L\};$$

$$\frac{\partial^3 W_\beta}{\partial \psi^3} \qquad {k_{f\beta}}^3\{-C_2\} + {k_{f\beta*}}^3\{iC_4\};$$

$$\frac{\partial^2 \boldsymbol{U_\alpha}}{\partial t^2} \quad -\omega^2\{A_L e^{-ik_{l\alpha*}(n-m)} + B_L\};$$
$$\frac{\partial^2}{\partial t^2}\frac{\partial \boldsymbol{W_\alpha}}{\partial x} \quad -\omega^2 k_{f\alpha}\{-A_2 e^{-k_{f\alpha}(n-m)} + B_1\} \; -\omega^2 k_{f\alpha*}\{-iA_4 e^{-ik_{f\alpha*}(n-m)} + iB_3\};$$

$$\begin{aligned}
E_1A_1\left(k_{l\alpha*}\{-iA_L e^{-ik_{l\alpha*}(n-m)}\} + k_{l\alpha*}\{iB_L\}\right) \\
= E_2A_2\left(k_{l\beta*}\{-iC_L\}\right)\cos\theta + E_2I_2\left(k_{f\beta}{}^3\{-C_2\} + k_{f\beta*}{}^3\{iC_4\}\right)\sin\theta \\
- m_j(-\omega^2)\left[\left(A_L e^{-ik_{l\alpha*}(n-m)} + B_L\right)\right. \\
\left. - \boldsymbol{L}\left(\boldsymbol{\sin}\tfrac{\theta}{4}\right)^2\left(k_{f\alpha}\{-A_2 e^{-k_{f\alpha}(n-m)} + B_1\} + k_{f\alpha*}\{-iA_4 e^{-i\ f\alpha*(n-m)} + iB_3\}\right)\right]
\end{aligned}$$

$$\begin{aligned}
0 = {} & A_2\underbrace{\left[(m_j\omega^2)\boldsymbol{L}\left(\boldsymbol{\sin}\tfrac{\theta}{4}\right)^2(\boldsymbol{k_{f\alpha}})\right]}_{9a} e^{-k_{f\alpha}(n-m)} + A_4\underbrace{\left[(m_j\omega^2)\boldsymbol{L}\left(\boldsymbol{\sin}\tfrac{\theta}{4}\right)^2(\boldsymbol{ik_{f\alpha*}})\right]}_{9b} e^{-ik_{f\alpha*}(n-m)} \\
& + A_L\underbrace{\left[\left(E_1A_1(ik_{l\alpha*})\right) + (m_j\omega^2)\right]}_{9c} e^{-ik_{l\alpha*}(n-m)} \\
& + B_1\underbrace{\left[-(m_j\omega^2)\boldsymbol{L}\left(\boldsymbol{\sin}\tfrac{\theta}{4}\right)^2(\boldsymbol{k_{f\alpha}})\right]}_{9d} + B_3\underbrace{\left[-(m_j\omega^2)\boldsymbol{L}\left(\boldsymbol{\sin}\tfrac{\theta}{4}\right)^2(\boldsymbol{ik_{f\alpha*}})\right]}_{9e} \\
& + B_L\underbrace{\left[-\left(E_1A_1(ik_{l\alpha*})\right) + (m_j\omega^2)\right]}_{9f} + C_2\underbrace{\left[-E_2I_2\left(k_{f\beta}^3\right)\sin\theta\right]}_{9g} \\
& + C_4\underbrace{\left[\left(E_2I_2\left(ik_{f\beta*}^3\right)\sin\theta\right)\right]}_{9h} + C_L\underbrace{\left[-\left(E_2A_2\left(ik_{l\beta*}\right)\cos\theta\right)\right]}_{9i}
\end{aligned}$$

Equation for MATLAB:-

0 = (A_2) [{ V5}($m_j w^2$) $k_{f\alpha}$] (Fn)

+ (A_4) [{ V5}($m_j w^2$) ik $_{f\alpha*}$] (Fni)

+ (A_L) [(S1) $ik_{l\alpha*}$ + ($m_j w^2$)] (Lni)

+ (B_1) [{ V5}(-$m_j w^2$) $k_{f\alpha}$]

+ (B_3) [{ V5}(-$m_j w^2$) ik $_{f\alpha*}$]

+ (B_L) [(-S1) $ik_{l\alpha*}$ + ($m_j w^2$)]

+ (C_2) [(-Q2) $k_{f\beta}^3$ Sin θ]

+ (C_4) [(Q2) $ik_{f\beta*}^3$ Sin θ]

+ (C_L) [(-S2) $ik_{l\beta*}$ Cos θ]

1.1.1.10 Equilibrium of compressive force, at $x = m$

$$- E_1 A_1 \frac{\partial U_\gamma}{\partial x} + E_1 A_1 \frac{\partial U_\alpha}{\partial x} = F_l$$

$\frac{\partial U_\alpha}{\partial x}$ $k_{l\alpha*}\{-iA_L\} + k_{l\alpha*}\{iB_L e^{ikl\alpha*(m-n)}\};$

$\frac{\partial U_\gamma}{\partial x}$ $k_{l\gamma*}\{iD_L\} + k_{l\alpha*}\{-iB_L e^{-ikl\alpha*(m-n)}\};$

$$-E_1 A_1 \left(k_{l\gamma*}\{iD_L\} + k_{l\alpha*}\{-iB_L\} e^{-ikl\alpha*(m-n)}\right) + E_1 A_1 \left(k_{l\alpha*}\{-iA_L\} + k_{l\alpha*}\{iB_L\} e^{ikl\ *(m-n)}\right) = F_l$$

$$-k_{l\gamma*}\{iD_L\} - k_{l\alpha*}\{-iB_L\} e^{-ikl\alpha*(m-n)} + k_{l\alpha*}\{-iA_L\} + k_{l\alpha*}\{iB_L\} e^{ikl\alpha*(m-n)} = \frac{F_l}{E_1 A_1}$$

$$\left[\!\left[\frac{F_l}{E_1 A_1} = (-A_L) \underbrace{[(ik_{l\alpha*})]}_{10c} + (B_L) \underbrace{[(ik_{l\alpha*})]}_{10} e^{-ikl\alpha*(m-n)} + (-D_L) \underbrace{[(ik_{l\gamma*})]}_{10l} + (B_L) \underbrace{[(ik_{l\alpha*})]}_{10f} e^{ikl\alpha*(m-n)} \right]\!\right]$$

Equation for MATLAB:-

$\frac{F_l}{E_1 A_1}$ = **(-A_L) $ik_{l\alpha*}$**

+ **[(B_L) $ik_{l\alpha*}$ (Lpi + Lni)]**

+ **(-D_L) $ik_{l\gamma*}$**

1.1.1.11 Equilibrium of shear force (joint), at $x = n$

$$-E_1 I_1 \frac{\partial^3 W_\alpha}{\partial x^3} = E_2 A_2 \frac{\partial U_\beta}{\partial \psi} \sin\theta - E_2 I_2 \frac{\partial^3 W_\beta}{\partial \psi^3} \cos\theta - m_j \frac{\partial^2}{\partial t^2}\left[W_\alpha + \boldsymbol{L}\left(\sin\tfrac{\theta}{4}\right)\left(\cos\tfrac{\theta}{4}\right)\frac{\partial W_\alpha}{\partial x}\right]$$

$\frac{\partial^3 W_\alpha}{\partial x^3}$ $k_{f\alpha}{}^3\{-A_2 e^{-k_{f\alpha}(n-m)} + B_1\} + k_{f\alpha*}{}^3\{iA_4 e^{-ik_{f\alpha*}(n-m)} - iB_3\};$

$\frac{\partial U_\beta}{\partial \psi}$ $k_{l\beta*}\{-iC_L\};$

$\frac{\partial^3 W_\beta}{\partial \psi^3}$ $k_{f\beta}{}^3\{-C_2\} + k_{f\beta*}{}^3\{iC_4\};$

$\frac{\partial^2 \boldsymbol{W_\alpha}}{\partial t^2}$ $-\omega^2\{A_2 e^{-k_{f\alpha}(n-m)} + B_1\} - \omega^2\{A_4 e^{-ik_{f\alpha*}(n-m)} + B_3\};$

$$\frac{\partial^2}{\partial t^2}\frac{\partial \boldsymbol{W_\alpha}}{\partial x} \quad -\omega^2 k_{f\alpha}\{-A_2 e^{-k_{f\alpha}(n-m)} + B_1\} \; -\omega^2 k_{f\alpha*}\{-iA_4 e^{-ik_{f\alpha*}(n-m)} + iB_3\} \; ;$$

$$\begin{aligned} -E_1 I_1\left(k_{f\alpha}{}^3\{-A_2 e^{-k_{f\alpha}(n-m)} + B_1\} + k_{f\alpha*}{}^3\{iA_4 e^{-ik_{f\alpha*}(n-m)} - iB_3\}\right) \\ = E_2 A_2\, k_{l\beta*}\{-iC_L\}\sin\theta \; - \; E_2 I_2\left(k_{f\beta}{}^3\{-C_2\} + k_{f\beta*}{}^3\{iC_4\}\right)\cos\theta \\ + \; m_j\omega^2\Big[\left(\{A_2 e^{-k_{f\alpha}(n-m)} + B_1\} + \{A_4 e^{-ik_{f\alpha*}(n-m)} + B_3\}\right) \\ + \Big(\boldsymbol{L}\left(\mathbf{sin}\tfrac{\theta}{4}\right)\left(\mathbf{cos}\tfrac{\theta}{4}\right)\left(k_{f\alpha}\{-A_2 e^{-k_{f\alpha}(n-m)} + B_1\} + k_{f\alpha*}\{-iA_4 e^{-ik_{f\alpha*}(n-m)} \\ + iB_3\}\right)\Big)\Big] \end{aligned}$$

$$\begin{aligned} 0 \\ = A_2 \underbrace{\left[-\left(E_1 I_1\left(k_{f\alpha}^3\right)\right) + \left(\left(m_j\omega^2\right)\right) - \left(\left(m_j\omega^2\right)\boldsymbol{L}\left(\mathbf{sin}\tfrac{\theta}{4}\right)\left(\mathbf{cos}\tfrac{\theta}{4}\right)\left(k_{f\alpha}\right)\right)\right]}_{11} e^{-k_{f\alpha}(n-m)} \\ + A_4 \underbrace{\left[\left(E_1 I_1\left(ik_{f\alpha*}^3\right)\right) + \left(\left(m_j\omega^2\right)\right) - \left(\left(m_j\omega^2\right)\boldsymbol{L}\left(\mathbf{sin}\tfrac{\theta}{4}\right)\left(\mathbf{cos}\tfrac{\theta}{4}\right)\left(ik_{f\alpha*}\right)\right)\right]}_{11b} e^{-ik_{f\alpha*}(n-m)} \\ + B_1 \underbrace{\left[\left(E_1 I_1\left(k_{f\alpha}^3\right)\right) + \left(\left(m_j\omega^2\right)\right) + \left(\left(m_j\omega^2\right)\boldsymbol{L}\left(\mathbf{sin}\tfrac{\theta}{4}\right)\left(\mathbf{cos}\tfrac{\theta}{4}\right)\left(k_{f\alpha}\right)\right)\right]}_{11d} \\ + B_3 \underbrace{\left[-\left(E_1 I_1\left(ik_{f\alpha*}^3\right)\right) + \left(\left(m_j\omega^2\right)\right) + \left(\left(m_j\omega^2\right)\boldsymbol{L}\left(\mathbf{sin}\tfrac{\theta}{4}\right)\left(\mathbf{cos}\tfrac{\theta}{4}\right)\left(ik_{f\alpha*}\right)\right)\right]}_{11} \\ + C_2 \underbrace{\left(E_2 I_2\left(k_{f\beta}^3\right)\cos\theta\right)}_{11} + C_4 \underbrace{\left[-\left(E_2 I_2\left(ik_{f\beta*}^3\right)\cos\theta\right)\right]}_{11h} + C_L \underbrace{\left[-\left(E_2 A_2\left(ik_{l\beta*}\right)\sin\theta\right)\right]}_{11} \end{aligned}$$

Equation for MATLAB:-

0	**=**	**(A_2) [(-Q1) $k_{f\alpha}{}^3$ + ($m_j w^2$) +(-$m_j w^2$){V6}($k_{f\alpha}$)] (Fn)**
	+	**(A_4) [(Q1) $ik_{f\alpha*}{}^3$ + ($m_j w^2$) +(-$m_j w^2$){V6}($ik_{f\alpha*}$)] (Fni)**
	+	**(B_1) [(Q1) $k_{f\alpha}{}^3$ + ($m_j w^2$) +($m_j w^2$){V6}($k_{f\alpha}$)]**
	+	**(B_3) [(-Q1) $ik_{f\alpha*}{}^3$ + ($m_j w^2$) +(-$m_j w^2$){V6}($ik_{f\alpha*}$)]**
	+	**(C_2) [(Q2) $k_{f\beta}{}^3$ Cos θ]**
	+	**(C_4) [(-Q2) $ik_{f\beta*}{}^3$ Cos θ]**
	+	**(C_L) [(-S2) $ik_{l\beta*}$ Sin θ]**

1.1.1.12 Equilibrium of shear force, $\boldsymbol{at\ x = m}$

$$-E_1 I_1 \frac{\partial^3 W_\alpha}{\partial x^3} + E_1 I_1 \frac{\partial^3 W_\gamma}{\partial x^3} \; = F_f$$

$$\frac{\partial^3 W_\alpha}{\partial x^3} \qquad {k_{f\alpha}}^3\{-A_2 + B_1 e^{kf\ (m-n)}\} + {k_{f\alpha*}}^3\{iA_4 - iB_3 e^{ikf\alpha*(m-n)}\};$$

$$\frac{\partial^3 W_\gamma}{\partial x^3} \qquad {k_{f\gamma}}^3\{D_1\} - {k_{f\gamma*}}^3\{iD_3\} + {k_{f\alpha}}^3\{-B_1 e^{-kf\alpha(m-n)}\} + {k_{f\alpha*}}^3\{iB_3 e^{-ikf\alpha*(m-n)}\};$$

$$\begin{aligned}
-E_1 I_1\Big({k_{f\alpha}}^3\{-A_2 + B_1\, e^{kf\alpha(m-n)}\} + {k_{f\alpha*}}^3\{iA_4 - iB_3 e^{ikf\alpha*(m-n)}\}\Big) \\
+ E_1 I_1\Big({k_{f\gamma}}^3\{D_1\} - {k_{f\gamma*}}^3\{iD_3\} + {k_{f\alpha}}^3\{-B_1 e^{-kf\ (m-n)}\} \\
+ {k_{f\alpha*}}^3\{iB_3 e^{-ikf\alpha*(m-n)}\}\Big) \; = F_f
\end{aligned}$$

$$\begin{aligned}
-\Big({k_{f\alpha}}^3\{-A_2 + B_1\, e^{kf\ (m-n)}\} + {k_{f\alpha*}}^3\{iA_4 - iB_3 e^{ikf\alpha*(m-n)}\}\Big) \\
+ \Big({k_{f\gamma}}^3\{D_1\} - {k_{f\gamma*}}^3\{iD_3\}\Big) + {k_{f\alpha}}^3\{-B_1 e^{-kf\ (m-n)}\} \\
+ {k_{f\alpha*}}^3\{iB_3 e^{-ikf\alpha*(m-n)}\} \; = \frac{F_f}{E_1 I_1}
\end{aligned}$$

$$\frac{F_f}{E_1 I_1} = A_2 \underbrace{\left(\left(k_{f\alpha}^3\right)\right)}_{12a} + (-A_4)\underbrace{\left(\left(ik_{f\alpha*}^3\right)\right)}_{12} + (-B_1)\underbrace{\left(\left(k_{f\alpha}^3\right)\right)}_{12} e^{kf\alpha(m-n)}$$

$$+ B_3 \underbrace{\left(\left(ik_{f\alpha*}^3\right)\right)}_{12} e^{ikf\alpha*(m-n)} + D_1 \underbrace{\left(k_{f\gamma}^3\right)}_{12j} + (-D_3)\underbrace{\left(ik_{f\gamma*}^3\right)}_{12k}$$

$$+ (-B_1)\underbrace{\left(\left(k_{f\alpha}^3\right)\right)}_{12d} e^{-kf\alpha(m-n)} + B_3 \underbrace{\left(\left(ik_{f\alpha*}^3\right)\right)}_{12} e^{-ikf\alpha*(m-n)}$$

$\frac{F_f}{E_1 I_1}$ = **(A_2) $k_{f\alpha}^3$**

\+ **($-A_4$) $ik_{f\alpha*}^3$**

\+ **[($-B_1$) $k_{f\alpha}^3$ (Fp) + (B_3) $ik_{f\alpha*}^3$ (Fpi)]**

\+ **(D_1) $k_{f\gamma}^3$**

\+ **($-D_3$) $ik_{f\gamma*}^3$**

\+ **[($-B_1$) $k_{f\alpha}^3$ (Fn) + (B_3) $ik_{f\alpha*}^3$ (Fni)]**

Equation for MATLAB:-

$\frac{F_f}{E_1 I_1}$ = **(A_2) $k_{f\alpha}^3$**

\+ **($-A_4$) $ik_{f\alpha*}^3$**

\+ **[($-B_1$) $k_{f\alpha}^3$ (Fp + Fn)]**

\+ **[(B_3) $ik_{f\alpha*}^3$ (Fpi + Fni)]**

\+ **(D_1) $k_{f\gamma}^3$**

\+ **($-D_3$) $ik_{f\gamma*}^3$**

Note :

Lni	-	$e^{-ik_{l\alpha*}(n-m)}$
Lpi	-	$e^{ikl\alpha*(m-n)}$
Fn	-	$e^{-k_{f\alpha}(n-m)}$
Fni	-	$e^{-ik_{f\alpha*}(n-m)}$
Fp	-	$e^{kf\alpha*(m-n)}$
Fpi	-	$e^{ikf\alpha*(m-n)}$

Appendix: C-2 MATLAB coding for Force-Input Joint equation: -

```
% MainCodeJointBeam
%*******************************************************************
% LOUGHBOROUGH UNIVERSITY
% PHD THESIS
% --------
% AUTHOR: SAIDDI ALI FIRDAUS BIN MOHAMED ISHAK
% SUPERVISORs: DR. JANE L.HORNER & DR.STEPHEN J.WALSH
%*******************************************************************
% MAIN PROGRAM: Reflection & Transmission - Power Measurements
%*******************************************************************
%

%
% DESCRIPTION OF INPUT PARAMETER
%
% E        is the Young's Modulus
% I        is the second moment of area
% A        is the area
% R        is the density of beam
% Rj       is density of joint
% Jw       is width of joint
% L        is height of joint
% Q        is the E x I
% S        is the E x A


%
% DESCRIPTION OF OTHER VARIABLES
%
% Kfa      is the flexural wavenumber in alpha
% Kfb      is the flexural wavenumber in beta
% Kfg      is the flexural wavenumber in gamma
% Kla      is the longitudinal wavenumber in alpha
% Klb      is the longitudinal wavenumber in beta
% Klg      is the longitudinal wavenumber in gamma

%
%% Ff & Fl input - (bending<flexural> and compressive<longitudinal> waves)

clear all
clf
format long e

%Given
b=0.1;%0.05;%                                 %m
d=0.02;%0.006;%                               %m
E1=1.75e9;%5.567e9;%60e9;%3.5e9;%   %N/m^2
I1=(b*(d^3))/12;                              %m^4
A1=b*d;                                       %m^2
E2=1.75e9;%5.567e9;%60e9;%3.5e9;%   %N/m^2
I2=(1.0*b*((1.0*d)^3))/12;                    %m^4
```

```
A2=1.0*b*1.0*d;                                    %m^2
R=1170;%1500;%1190;%2500;                           %kg/m^3
Rj=1170;%1500;%1190;%2500;                          %kg/m^3
Jw=1*b;                                             %m
L=1*d;                                              %m
Eta=0.07;
Mr=0.028;
Ir=Mr*(L^2)/12;
hs=3000;
h=0.2;

E1e=E1*(1+(1i*Eta));
E2e=E2*(1+(1i*Eta));

Q1=E1*I1;
Q2=E2*I2;
S1=E1*A1;
S2=E2*A2;

Q3=0;%1.167e6*I1;

m1=R*A1;
m2=R*A2;

%% Main


thcnt=0;
for thet=0:1:180;
    T=thet*pi/180;

        thcnt=thcnt+1;


    fqcnt=0;
    for fq=3000:500:3000;%000:16.667:3000.06;                %1/s  250:5:2250;
        w=2*pi*fq;                          %1/s

        %Input
        Ff=1;%*0.021*sqrt(2);%0.021*sqrt(2);%(1*i);%0.018;0.0038*sqrt(2);%
%m
        Fl=0;%*0.0105*sqrt(2);%0.0021*sqrt(2);%0;%(1*i);%0.018;
%m
        m=0.0;
        n=0.9;

        Mj=Rj*Jw*(L^2)*T/2;          %kg
        %Ioj=((T-sin(T))*(L^4)/8);
        %Icj=L*(((4/3)*(sin(T/2)/(T)))-(1/2));
        %Ij=Mj*(Ioj-Icj);
        Ij=Mj*(L^2)/12;                     %kgm^2

        Kfa=(w^0.5)*(((R*A1)/(E1*I1))^0.25);     %1/m
        Kfg=(w^0.5)*(((R*A1)/(E2*I1))^0.25);     %1/m
```

```
Kfb=(w^0.5)*(((R*A2)/(E2*I2))^0.25);      %1/m
Kla=w*sqrt(R/E1);                         %1/m
Klg=w*sqrt(R/E1);                         %1/m
Klb=w*sqrt(R/E2);                         %1/m

Kfax=(w^0.5)*(((R*A1)/(E1e*I1))^0.25);%Kfa*(1-((i*Eta)/4));     %1/m
Kfgx=(w^0.5)*(((R*A1)/(E1e*I1))^0.25);%Kfg*(1-((i*Eta)/4));     %1/m
Kfbx=(w^0.5)*(((R*A1)/(E2e*I2))^0.25);%Kfb*(1-((i*Eta)/4));     %1/m
Klax=w*sqrt(R/E1e);%Kla*(1-((i*Eta)/2));                        %1/m
Klgx=w*sqrt(R/E1e);%Klg*(1-((i*Eta)/2));                        %1/m
Klbx=w*sqrt(R/E2e);%Klb*(1-((i*Eta)/2));                        %1/m

%------%

fl=(n-m);   %finite length (fl)
fll=(m-n);

Lni=(exp(-i*Klax*fl));
Fn=(exp(-Kfa*fl));
Fni=(exp(-i*Kfax*fl));

Lpi=(exp(i*Klax*fll));
Fp=(exp(Kfa*fll));
Fpi=(exp(i*Kfax*fll));

Llni=(exp(i*1*Klax*fll));
Ffn=(exp(1*Kfa*fll));
Ffni=(exp(i*1*Kfax*fll));

%------%

%
V1=L/2*(1-cos(T));

g1=(sin(T)+(Kfb*V1));
h1=(sin(T)+(i*Kfbx*V1));
i1=cos(T);

%
V3=L/2*(sin(T));

g3=(cos(T))+(Kfb*V3);
h3=(cos(T))+(i*Kfbx*V3);
i3=sin(T);

%
a5=Kfa;
b5=i*Kfax;
d5=Kfa;
e5=i*Kfax;
g5=Kfb;
h5=i*Kfbx;

%
```

```
a6=Kfa;
b6=i*Kfax;
d6=Kfa;
e6=i*Kfax;
j6=Kfg;
k6=i*Kfgx;

%--------%
V5=L/2*(1-cos(T/2));
V6=L/2*(sin(T/2));
%V5=L*((sin(T/4))^2);        %-same as above
%V6=L*(sin(T/4))*(cos(T/4));%-same as above
%--------%

a7=((-Ij)  *Kfa *(w^2))+((-Q1)*(Kfa^2)) +(Q1  *(Kfa^3) *V6)
+(0);
b7=((-Ij)*i*Kfax*(w^2))+(  Q1 *(Kfax^2))+(Q1*i*(Kfax^3)*(-V6))
+(0);%
c7=(S1*i*Klax*V5)                                                  -
(0)       ;
d7=(  Ij   *Kfa *(w^2))+((-Q1)*(Kfa^2)) +(Q1  *(Kfa^3) *(-V6))     -
(0);
e7=(  Ij *i*Kfax*(w^2))+(  Q1 *(Kfax^2))+(Q1*i*(Kfax^3)*V6)        -
(0);
f7=(S1*i*Klax*(-V5))                                               -
(0)       ;
g7=(  Q2 *(Kfb^2)) +(Q2  *(Kfb^3) *V6)                             -
(0);
h7=((-Q2)*(Kfbx^2))+(Q2*i*(Kfbx^3)*(-V6))                          -
(0);
i7=(S2*i*Klbx*(-V5))
+(0)        ;

%
a8=(Kfa^2);%*Q1;
b8=(Kfax^2);%*Q1;
d8=(Kfa^2);%*Q1;
e8=(Kfax^2);%*Q1;
j8=(Kfg^2);%*Q1;
k8=(Kfgx^2);%*Q1;

%
a9=( Mj*(w^2)  *Kfa *V5);
b9=( Mj*(w^2)*i*Kfax*V5);
c9=( Mj*(w^2))+(  S1 *i*Klax)                                      -
0;
d9=(-Mj*(w^2)  *Kfa *V5);
e9=(-Mj*(w^2)*i*Kfax*V5);
f9=( Mj*(w^2))+((-S1)*i*Klax)                                      -
0;
g9=((-Q2)*  (Kfb^3) *sin(T))
+0;
h9=(  Q2 *i*(Kfbx^3)*sin(T))
+0;
i9=((-S2)*i* Klbx   *cos(T))
+0;
```

```
%
c10=(i*Klax);%*(S1);%+ve
f10=(i*Klax);%*(S1);%-ve
l10=(i*Klgx);%*(S1);%+ve

%
a11=(Mj*(w^2))+((-Mj)*(w^2)  *Kfa *V6)+((-Q1)  *(Kfa^3))          -
0;
b11=(Mj*(w^2))+((-Mj)*(w^2)*i*Kfax*V6)+(  Q1 *i*(Kfax^3))          -
0;
d11=(Mj*(w^2))+(  Mj  *(w^2)  *Kfa *V6)+(  Q1   *(Kfa^3))          -
0;
e11=(Mj*(w^2))+(  Mj  *(w^2)*i*Kfax*V6)+((-Q1)*i*(Kfax^3))          -
0;
g11=(  Q2 *  (Kfb^3) *cos(T))
+0;
h11=((-Q2)*i*(Kfbx^3)*cos(T))
+0;
i11=((-S2)*i* Klbx   *sin(T))
+0;

%
a12=(Kfa^3);%*Q1;
b12=i*(Kfax^3);%*Q1;
d12=(Kfa^3);%*Q1;
e12=i*(Kfax^3);%*Q1;
j12=(Kfg^3);%*Q1;
k12=i*(Kfgx^3);%*Q1;

%-------------------%

%
x(1,1)=0;
x(1,2)=0;
x(1,3)=-1*Lni;
x(1,4)=0;
x(1,5)=0;
x(1,6)=-1;%*Lpi;
x(1,7)=-g1;
x(1,8)=-h1;
x(1,9)=i1;
x(1,10)=0;
x(1,11)=0;
x(1,12)=0;

x(2,1)=0;
x(2,2)=0;
x(2,3)=1;
x(2,4)=0;
x(2,5)=0;
x(2,6)=1*(Lpi-Llni);
x(2,7)=0;
x(2,8)=0;
x(2,9)=0;
x(2,10)=0;
```

```
x(2,11)=0;
x(2,12)=-1;%*Lpi;

x(3,1)=-1*Fn;
x(3,2)=-1*Fni;
x(3,3)=0;
x(3,4)=-1;%*Fp;
x(3,5)=-1;%*Fpi;
x(3,6)=0;
x(3,7)=g3;
x(3,8)=h3;
x(3,9)=i3;
x(3,10)=0;
x(3,11)=0;
x(3,12)=0;

x(4,1)=1;
x(4,2)=1;
x(4,3)=0;
x(4,4)=1*(Fp-Ffn);
x(4,5)=1*(Fpi-Ffni);
x(4,6)=0;
x(4,7)=0;
x(4,8)=0;
x(4,9)=0;
x(4,10)=-1;%*Fp;
x(4,11)=-1;%*Fpi;
x(4,12)=0;

x(5,1)=a5*Fn;
x(5,2)=b5*Fni;
x(5,3)=0;
x(5,4)=-d5;%*Fp;
x(5,5)=-e5;%*Fpi;
x(5,6)=0;
x(5,7)=-g5;
x(5,8)=-h5;
x(5,9)=0;
x(5,10)=0;
x(5,11)=0;
x(5,12)=0;

x(6,1)=a6;
x(6,2)=b6;
x(6,3)=0;
x(6,4)=-d6*(Fp-Ffn);
x(6,5)=-e6*(Fpi-Ffni);
x(6,6)=0;
x(6,7)=0;
x(6,8)=0;
x(6,9)=0;
x(6,10)=j6;%*Fp;
x(6,11)=k6;%*Fpi;
x(6,12)=0;

x(7,1)=a7*Fn;
```

```
x(7,2)=b7*Fni;
x(7,3)=c7*Lni;
x(7,4)=d7;%*Fp;
x(7,5)=e7;%*Fpi;
x(7,6)=f7;%*Lpi;
x(7,7)=g7;
x(7,8)=h7;
x(7,9)=i7;
x(7,10)=0;
x(7,11)=0;
x(7,12)=0;

x(8,1)=-a8;
x(8,2)=b8;
x(8,3)=0;
x(8,4)=d8*(-Fp+Ffn);
x(8,5)=e8*(Fpi-Ffni);
x(8,6)=0;
x(8,7)=0;
x(8,8)=0;
x(8,9)=0;
x(8,10)=j8;%*Fp;
x(8,11)=-k8;%*Fpi;
x(8,12)=0;

x(9,1)=a9*Fn;
x(9,2)=b9*Fni;
x(9,3)=c9*Lni;
x(9,4)=d9;%*Fp;
x(9,5)=e9;%*Fpi;
x(9,6)=f9;%*Lpi;
x(9,7)=g9;
x(9,8)=h9;
x(9,9)=i9;
x(9,10)=0;
x(9,11)=0;
x(9,12)=0;

x(10,1)=0;
x(10,2)=0;
x(10,3)=-c10;
x(10,4)=0;
x(10,5)=0;
x(10,6)=f10*(Lpi-Llni);
x(10,7)=0;
x(10,8)=0;
x(10,9)=0;
x(10,10)=0;
x(10,11)=0;
x(10,12)=-l10;%*Lpi;

x(11,1)=a11*Fn;
x(11,2)=b11*Fni;
x(11,3)=0;
x(11,4)=d11;%*Fp;
x(11,5)=e11;%*Fpi;
```

```
        x(11,6)=0;
        x(11,7)=g11;
        x(11,8)=h11;
        x(11,9)=i11;
        x(11,10)=0;
        x(11,11)=0;
        x(11,12)=0;

        x(12,1)=a12;
        x(12,2)=-b12;
        x(12,3)=0;
        x(12,4)=-d12*(Fp-Ffn);
        x(12,5)=e12*(Fpi-Ffni);
        x(12,6)=0;
        x(12,7)=0;
        x(12,8)=0;
        x(12,9)=0;
        x(12,10)=j12;%*Fp;
        x(12,11)=-k12;%*Fpi;
        x(12,12)=0;

        zL=[0;0;0;0;0;0;0;0;0;(Fl/S1);0;0];%(Fl/(4*E1*A1*Kla))
        zF=[0;0;0;0;0;0;0;0;0;0;0;(Ff/Q1)];%-(Ff/(4*E1*I1*Kfa^3))

        yL=x\zL;
        yF=x\zF;

        %Note that for the matrix of X;
        %y(1)      %A2 Nm/s  xxxx
        %y(2)      %A4 Nm/s
        %y(3)      %AL Nm/s
        %y(4)      %B1 Nm/s  xxxx
        %y(5)      %B3 Nm/s
        %y(6)      %BL Nm/s
        %y(7)      %C2 Nm/s  xxxx
        %y(8)      %C4 Nm/s
        %y(9)      %CL Nm/s
        %y(10)     %D1 Nm/s  xxxx
        %y(11)     %D3 Nm/s
        %y(12)     %DL Nm/s

        fqcnt=fqcnt+1;


Pf1=1*E1*I1*w*(Kfax^3)*((abs(yF(2)))^2);%(((real(yF(2)))^2)+((imag(yF(2)))^2)
);%        %Power in a due to trans flexural wave           yF(2) -> A4

Pf2=1*E1*I1*w*(Kfax^3)*((abs(yL(2)))^2);%(((real(yL(2)))^2)+((imag(yL(2)))^2)
);%        %Power in a due to trans flexural wave           yL(2) -> A4

Pf3=1*E1*I1*w*(Kfax^3)*((abs(yF(5)))^2);%(((real(yF(5)))^2)+((imag(yF(5)))^2)
);%        %Power in a due to reflected flexural wave       yF(5) -> B3

Pf4=1*E1*I1*w*(Kfax^3)*((abs(yL(5)))^2);%(((real(yL(5)))^2)+((imag(yL(5)))^2)
);%        %Power in a due to reflected flexural wave       yL(5) -> B3
```

```
Pf5=1*E2*I2*w*(Kfbx^3)*((abs(yF(8)))^2);%(((real(yF(8)))^2)+((imag(yF(8)))^2)
);%        %Power in b due to transmitted flexural wave     yF(8) -> C4

Pf6=1*E2*I2*w*(Kfbx^3)*((abs(yL(8)))^2);%(((real(yL(8)))^2)+((imag(yL(8)))^2)
);%        %Power in b due to transmitted flexural wave     yL(8) -> C4

Pf7=1*E1*I1*w*(Kfgx^3)*((abs(yF(11)))^2);%(((real(yF(11)))^2)+((imag(yF(11)))
^2));%       %Power in g due to trans flexural wave           yF(11)-> D3

Pf8=1*E1*I1*w*(Kfgx^3)*((abs(yL(11)))^2);%(((real(yL(11)))^2)+((imag(yL(11)))
^2));%       %Power in g due to trans flexural wave           yL(11)-> D3


Pl1=0.5*E1*A1*w*Klax*((abs(yL(3)))^2);%(((real(yL(3)))^2)+((imag(yL(3)))^2));
%        %Power in a due to trans longitudinal wave       yL(3) -> AL

Pl2=0.5*E1*A1*w*Klax*((abs(yF(3)))^2);%(((real(yF(3)))^2)+((imag(yF(3)))^2));
%        %Power in a due to trans longitudinal wave       yF(3) -> AL

Pl3=0.5*E1*A1*w*Klax*((abs(yL(6)))^2);%(((real(yL(6)))^2)+((imag(yL(6)))^2));
%        %Power in a due to reflected longitudinal wave   yL(6) -> BL
        Pl4=0.5*E1*A1*w*Klax*((abs(yF(6)))^2);%
(((real(yF(6)))^2)+((imag(yF(6)))^2));%       %Power in a due to reflected
longitudinal wave   yF(6) -> BL

Pl5=0.5*E2*A2*w*Klbx*((abs(yL(9)))^2);%(((real(yL(9)))^2)+((imag(yL(9)))^2));
%        %Power in b due to transmitted longitudinal wave yL(9) -> CL

Pl6=0.5*E2*A2*w*Klbx*((abs(yF(9)))^2);%(((real(yF(9)))^2)+((imag(yF(9)))^2));
%      %Power in b due to transmitted longitudinal wave yF(9) -> CL

Pl7=0.5*E1*A1*w*Klgx*((abs(yL(12)))^2);%(((real(yL(12)))^2)+((imag(yL(12)))^2
));%       %Power in g due to trans longitudinal wave       yL(12)-> DL

Pl8=0.5*E1*A1*w*Klgx*((abs(yF(12)))^2);%(((real(yF(12)))^2)+((imag(yF(12)))^2
));%       %Power in g due to trans longitudinal wave       yF(12)-> DL

        PFlex=(0.125*(((Ff)^2)*w))/(((E1*I1)*((Kfax)^3)));
        PLong=(0.25*(((Fl)^2)*w))/((E1*A1)*(Klax));
        PFlexG=(0.125*(((Ff)^2)*w))/(((E1*I1)*((Kfg)^3)));
        PLongG=(0.25*(((Fl)^2)*w))/((E1*A1)*(Klg));
        %lmbd=0.5;
        %Kfax2=2*pi/lmbd;
        %PFlex2=(0.125*((Ff)^2))/(m1*w/Kfax2);

        tht(thcnt)=T;
        wqt(fqcnt)=w;
        fqt(fqcnt)=fq;
        ndwave(fqcnt)=(Kfa*0.9)/(2*pi);%((2*pi)/Kfa)*0.5;

        nP1(thcnt,fqcnt)=(Pf1-Pf3)/(PFlex+0)*100;       % %power in a -
flexural incidence wave, flexural reflected wave
        nP2(thcnt,fqcnt)=(Pf2-Pf4)/(PLong+0)*100;       % %power in a -
longitudinal incidence wave, flexural reflected wave
```

```
        nP3(thcnt,fqcnt)=(Pl2-Pl4)/(PFlex+0)*100;       % %power in a -
flexural incidence wave, longitudinal reflected wave
        nP4(thcnt,fqcnt)=(Pl1-Pl3)/(PLong+0)*100;       % %power in a -
longitudinal incidence wave, longitudinal reflected wave
        nP5(thcnt,fqcnt)=(Pf3)/(PFlex+0)*100;       % %power in a - flexural
incidence wave, flexural reflected wave
        nP6(thcnt,fqcnt)=(Pf4)/(PLong+0)*100;       % %power in a -
longitudinal incidence wave, flexural reflected wave
        nP7(thcnt,fqcnt)=(Pl4)/(PFlex+0)*100;       % %power in a - flexural
incidence wave, longitudinal reflected wave
        nP8(thcnt,fqcnt)=(Pl3)/(PLong+0)*100;       % %power in a -
longitudinal incidence wave, longitudinal reflected wave

        nP9(thcnt,fqcnt)=(Pf5)/(PFlex+0)*100;       % %power in b - flexural
incidence wave, flexural transmitted wave
        nP10(thcnt,fqcnt)=(Pf6)/(PLong+0)*100;      % %power in b -
longitudinal incidence wave, flexural transmitted wave
        nP11(thcnt,fqcnt)=(Pl6)/(PFlex+0)*100;      % %power in b - flexural
incidence wave, longitudinal transmitted wave
        nP12(thcnt,fqcnt)=(Pl5)/(PLong+0)*100;      % %power in b -
longitudinal incidence wave, longitudinal transmitted wave

        nP13(thcnt,fqcnt)=(Pf7+Pf3)/(PFlex+0)*100;      % %power in g -
flexural incidence wave, flexural transmitted wave
        nP14(thcnt,fqcnt)=(Pf8+Pf4)/(PLong+0)*100;      % %power in g -
longitudinal incidence wave, flexural transmitted wave
        nP15(thcnt,fqcnt)=(Pl8+Pl4)/(PFlex+0)*100;      % %power in g -
flexural incidence wave, longitudinal transmitted wave
        nP16(thcnt,fqcnt)=(Pl7+Pl3)/(PLong+0)*100;      % %power in g -
longitudinal incidence wave, longitudinal transmitted wave

        %nP13(thcnt,fqcnt)=nP25(thcnt,fqcnt)+(Pf3);%/(PFlexG+0)*100;      %
%power in g - flexural incidence wave, flexural transmitted wave
        %nP14(thcnt,fqcnt)=nP26(thcnt,fqcnt)+(Pf4);%/(PLongG+0)*100;      %
%power in g - longitudinal incidence wave, flexural transmitted wave
        %nP15(thcnt,fqcnt)=nP27(thcnt,fqcnt)+(Pl4);%/(PFlexG+0)*100;      %
%power in g - flexural incidence wave, longitudinal transmitted wave
        %nP16(thcnt,fqcnt)=nP28(thcnt,fqcnt)+(Pl3);%/(PLongG+0)*100;      %
%power in g - longitudinal incidence wave, longitudinal transmitted wave

        %nP17(thcnt,fqcnt)=(Pf1-Pf3);%/((PFlex+0))*100;       % %power in a -
flexural incidence wave, flexural reflected wave
        %nP18(thcnt,fqcnt)=(Pf4-Pf2);%/((PLong+0))*100;       % %power in a -
longitudinal incidence wave, flexural reflected wave
        %nP19(thcnt,fqcnt)=(Pl4-Pl2);%/((PFlex+0))*100;       % %power in a -
flexural incidence wave, longitudinal reflected wave
        %nP20(thcnt,fqcnt)=(Pl1-Pl3);%/((PLong+0))*100;       % %power in a -
longitudinal incidence wave, longitudinal reflected wave

        fB=nP5+nP7;%+nP7;%nP9+nP11;
        fA=nP1+nP3;%+nP3;%nP1+nP3+nP5+nP7;

        fC=nP9+nP11;%+nP11;%nP13+nP15;
        fD=nP13+nP15;%+nP15;%nP17+nP18+nP19+nP20;
```

```
        fAl=fA;
        fBe=fC;
        fGa=fD;
        ftot1=fAl+fGa;
        ftot2=fGa+fBe;
        %ftot3=fAl+fBe;
        fAla=fA;
        fAlb=fB;

        lB=nP8+nP6;
        lA=nP4+nP2;%=0

        lC=nP12+nP10;
        lD=nP16+nP14;

        lAl=lA;
        lBe=lC;
        lGa=lD;
        ltot1=lAl+lGa;
        ltot2=lGa+lBe;
        %ltot3=lAl+lBe;

        tot1=ftot1+ltot1;
        tot2=ftot2+ltot2;
        %tot3=ftot3+ltot3;
        AlphaT=fAl+lAl;
        BetaT=fBe+lBe;
        GammaT=fGa+lGa;


        %nF=nP21+nP22+nP23+nP24;
        Tf=fGa+fAl;%fAl+
        Tl=lGa+lAl;%lAl+
        TOT2=GammaT+BetaT;%+AlphaT;%GammaT+fB+lB;BetaT+fA+lA;
        TOT1=GammaT+AlphaT;

        xfcnt=0;
        for xf=0.00;
            Wf(thcnt,fqcnt)=(yF(1)*(exp(-Kfa*abs(xf-m))))+(yF(2)*(exp(-
1i*Kfax*abs(xf-m))))+(yF(4)*(exp(Kfa*(1*abs(xf-
m)))))+(yF(5)*(exp(1i*Kfax*(1*abs(xf-m)))));
            Uf(thcnt,fqcnt)=(yL(3)*(exp(-1i*Klax*abs(xf-
m))))+(yL(6)*(exp(1i*Klax*(1*abs(xf-m)))));

            xacnt=0;
            for xa=0.45;
                Wa(thcnt,fqcnt)=(yF(1)*(exp(-Kfa*abs(xa-m))))+(yF(2)*(exp(-
1i*Kfax*abs(xa-m))))+(yF(4)*(exp(Kfa*(1*abs(xa-
m)))))+(yF(5)*(exp(1i*Kfax*(1*abs(xa-m)))));
                Ua(thcnt,fqcnt)=(yL(3)*(exp(-1i*Klax*abs(xa-
m))))+(yL(6)*(exp(1i*Klax*(1*abs(xa-m)))));

                xbcnt=0;
                for xb=1.50;%0.25;
```

```
                    Wb(thcnt,fqcnt)=(yF(7)*(exp(-Kfb*(xb-n))))+(yF(8)*(exp(-
1i*Kfbx*(xb-n))));
                    Ub(thcnt,fqcnt)=(yL(9)*(exp(-1i*Klbx*(xb-n))));

                    xgcnt=0;
                    for xg=-0.30;%-0.75;

                        Wg(thcnt,fqcnt)=(yF(10)*(exp(Kfg*(xg-
m))))+(yF(11)*(exp(1i*Kfgx*(xg-m))));
                        Ug(thcnt,fqcnt)=(yL(12)*(exp(1i*Klgx*(xg-m))));

                        Va(thcnt,fqcnt)=1i*w*Wa(thcnt,fqcnt);
                        Vb(thcnt,fqcnt)=1i*w*Wb(thcnt,fqcnt);
                        Vg(thcnt,fqcnt)=1i*w*Wg(thcnt,fqcnt);
                        Aa(thcnt,fqcnt)=-1*w^2*Wa(thcnt,fqcnt);
                        Ab(thcnt,fqcnt)=-1*w^2*Wb(thcnt,fqcnt);
                        Ag(thcnt,fqcnt)=-1*w^2*Wg(thcnt,fqcnt);

                        xacnt=xacnt+1;
                        xWat(xacnt)=Wa(thcnt,fqcnt);
                        xUat(xacnt)=Ua(thcnt,fqcnt);
                        xWbt(xacnt)=Wb(thcnt,fqcnt);
                        xUbt(xacnt)=Ub(thcnt,fqcnt);
                        xWgt(xacnt)=Wg(thcnt,fqcnt);
                        xUgt(xacnt)=Ug(thcnt,fqcnt);



InPwrF(thcnt,fqcnt)=1*((((Ff)^2)*w)/(8*E1*I1*Kfax^3))*(1-Eta/4);
                        InPwr(thcnt,fqcnt)=-
0.5*real(Ff*(1i*w*(Wf(thcnt,fqcnt))));

ApPwr(thcnt,fqcnt)=1*(((real(1i*w*(Wa(thcnt,fqcnt))))^2*(E1*I1)*((Kfa)^3))/(w
));

BtPwr(thcnt,fqcnt)=1*(((real(1i*w*(Wb(thcnt,fqcnt))))^2*(E2*I2)*((Kfb)^3))/(w
));

GmPwr(thcnt,fqcnt)=1*(((real(1i*w*(Wg(thcnt,fqcnt))))^2*(E1*I1)*((Kfg)^3))/(w
));
                        TotPwr=GmPwr+BtPwr;

                        Imp(fqcnt)=1/(1i*w*Wa(fqcnt));
                        Mob(fqcnt)=1/(Imp(fqcnt));

                        ReMob(fqcnt)=w/(4*E1*I1*Kfa^3);
                        ImMob(fqcnt)=(-1*w)/(4*E1*I1*Kfa^3);

                        Acc(fqcnt)=Wa(fqcnt)*(-(w^2));

                        Ar=1*fAl./(InPwr.*1);
                        Gr=1*fGa./(InPwr.*1);
                        Br=1*fBe./(InPwr.*1);
                        %Ir=InPwr/fAl;
                        %Gr=fGa/fAl;
```

```
                        %Br=fBe/fAl;
                        tr=(0+Ar+Gr)*1;

                    end

                end

            end

        end

    end

end


fqt=3000:500:3000;%000:16.667:3000.06;
tht=0:1:180;

figure(1)
plot(tht,nP1,'r')
hold on
plot(tht,nP2,'g')
hold on
plot(tht,nP3,'m')
hold on
plot(tht,nP4,'b')
hold on
plot(tht,nP5,'r')
hold on
plot(tht,nP6,'g')
hold on
plot(tht,nP7,'m')
hold on
plot(tht,nP8,'b')
hold on
grid on
%axis([0 180 0 120])
title 'Percentage Power Transmitted&Reflected in alpha'
xlabel 'Angle'%'Frequency'
ylabel 'Percentage Power'
%legend('FF','LF','FL','LL','FF','LF','FL','LL','Location','best');

figure(2)
plot(tht,nP9,'r')
hold on
plot(tht,nP10,'g')
hold on
plot(tht,nP11,'m')
hold on
plot(tht,nP12,'b')
hold on
grid on
%axis([0 180 0 120])
title 'Percentage Power Transmitted in beta'
```

```
xlabel 'Angle'%'Frequency'
ylabel 'Percentage Power'
%legend('FF','LF','FL','LL','Location','best');

figure(3)
plot(tht,nP13,'r')
hold on
plot(tht,nP14,'g')
hold on
plot(tht,nP15,'m')
hold on
plot(tht,nP16,'b')
hold on
grid on
%axis([0 180 0 120])
title 'Percentage Power Transmitted in gamma'
xlabel 'Angle'%'Frequency'
ylabel 'Percentage Power'
%legend('FF','LF','FL','LL','Location','best');

figure(4)
plot(tht,nP1,'r')
hold on
plot(tht,nP2,'g')
hold on
plot(tht,nP3,'m')
hold on
plot(tht,nP4,'b')
hold on
grid on
%axis([0 180 0 120])
title 'Percentage Power Transmitted in Alpha'
xlabel 'Angle'%'Frequency'
ylabel 'Percentage Power'
%legend('FF','LF','FL','LL','Location','best');

figure(5)
plot(tht,nP9,'r')
hold on
plot(tht,nP11,'m')
hold on
plot(tht,nP13,'r')
hold on
plot(tht,nP15,'m')
hold on
grid on
%axis([0 180 0 120])
title 'Percentage Power from Flexural at beta and gamma'
xlabel 'Angle'%'Frequency'
ylabel 'Percentage Power'
%legend('FFb','FLb','FFg','FLg','Location','best');

figure(6)
plot(tht,nP10,'g')
hold on
plot(tht,nP12,'b')
```

```
hold on
plot(tht,nP14,'g')
hold on
plot(tht,nP16,'b')
hold on
grid on
%axis([0 180 0 120])
title 'Percentage Power from Longitudinal at beta and gamma'
xlabel 'Angle'%'Frequency'
ylabel 'Percentage Power'
%legend('LFb','LLb','LFg','LLg','Location','best');

figure(7)
plot(tht,AlphaT,'r')
hold on
plot(tht,BetaT,'b') %
hold on
plot(tht,GammaT,'g')
hold on
%plot(tht,nF,'k.')
%hold on
plot(tht,TOT2,'k')
hold on
grid on
title 'Percentage Power Total'
xlabel 'Angle'%'Frequency'
ylabel 'Percentage Power'
%legend('Al','Be','Ga','Total2','Location','best');%'nF',

figure(8)
plot(tht,fAl,'r.')
hold on
plot(tht,fBe,'b.') %
hold on
plot(tht,fGa,'g.')
hold on
plot(tht,Tf,'k.')
hold on
plot(tht,lAl,'r')
hold on
plot(tht,lBe,'b') %
hold on
plot(tht,lGa,'g')
hold on
plot(tht,Tl,'k')
hold on
grid on
title 'Percentage Power Total'
xlabel 'Angle'%'Frequency'
ylabel 'Percentage Power'
%legend('Al','Be','Ga','nF','Total','Location','best');

figure(9)
surf (fqt,tht,nP1);
xlabel('frequency /Hz')
ylabel('angle \theta')
```

```
zlabel('Power in Alpha')
title('(Figure-9)Alpha Power vs angle \theta and frequency/Hz')
grid

figure (10)
surf (fqt,tht,nP9);
xlabel('frequency /Hz')
ylabel('angle \theta')
zlabel('Power in Beta')
title('(Figure-10)Beta Power vs angle \theta and frequency/Hz')
grid

figure (11)
surf (fqt,tht,nP13);
xlabel('frequency /Hz')
ylabel('angle \theta')
zlabel('Power in Gamma')
title('(Figure-11)Gamma Power vs angle \theta and frequency/Hz')
grid
```

Appendix: C-3 MATLAB coding for measurement algorithm: -

```
%function ExpCode
%% Ff input to jointbeam beam
clear all
clf
format long e
%Given
b=0.1;                              %m
d=0.02;                             %m
Eta=0.00;
Eeta=(1+(1i*Eta));
E1=1.75e9;%60e9;%1.75e9;%           %N/m^2
I1=(b*(d^3))/12;                    %m^4
A1=b*d;                             %m^2
E2=1.75e9;%60e9;%1.75e9;%           %N/m^2
I2=(b*(d^3))/12;          %m^4
A2=b*d;                     %m^2
RHO=1170;%1190;%2500;                     %kg/m^3
RHOj=1170;%1190;%2500;                    %kg/m^3
Jw=1*b;                             %m
%L=1*d;                             %m
B=E1*I1;
ml=A1*RHO;

Ls=0.30;                            %depth in sand
Lb=1.50;                            %length beam exposed
Lt=Lb+(1*Ls);                       %total beam length
La=0.30;                            %distance force to accelerometer
Lx=0.30;                            %distance acclr to termination

%% Natural Frequency
fnt=zeros;
fncnt=0;
for n=1:1:20;
    fn=pi/2*sqrt(B/ml)*(n^2/Lb^2);
    fncnt=fncnt+1;
    fnt(fncnt)=fn;
end

    %% Freq limit
    %Lower Freq limit (due to termination)-t
    Wavet=2*Ls;                                 %Max wavelength W.R.T Ls
    kbt=(2*pi)/Wavet;                           %wavenumber for above
    omegat=kbt^2*(sqrt((E1*I1)/(A1*RHO)));      %
    %omegat=kbt*(sqrt((E1)/(RHO)));    %
    FqLwrt=omegat/(2*pi)

    %Lower Freq limit (due to force-acc midpoint)-f
    Wavef=La*2;
```

```
kbf=(2*pi)/Wavef;
omegaf=kbf^2*(sqrt((E1*I1)/(A1*RHO)));   %
%omegaf=kbf*(sqrt((E1)/(RHO)));   %
FqLwrf=omegaf/(2*pi)

%Upper Freq limit (due to acc spacing)-s
s=0.03;
Waves=s/0.2;
kbs=(2*pi)/Waves;
omegas=kbs^2*(sqrt((E1*I1)/(A1*RHO)));   %
%omegas=kbs*(sqrt((E1)/(RHO)));   %
FqUprs=omegas/(2*pi)

%% Theory - mobility

Freq=dlmread('H1_21.txt','','A34..A1833');%A134..A1833   %A74..A834 1634

omega=Freq.*(2*pi);
kb=(sqrt(omega))*(((ml)/(B))^0.25);
MobReTheory=omega./(4*B*(kb.^3));
MobImTheory=omega.*(-i)./(4*B*(kb.^3));
MobModTh=sqrt(((MobReTheory.^2)+abs(MobImTheory.^2)));

%% Read experiment data

H1_21Re=dlmread('H1_21.txt','','B34..B1833');
MobReal=-(H1_21Re.*1)./(Freq.*(2*pi));
H1_21Im=dlmread('H1_21.txt','','C34..C1833');
MobIm=(H1_21Im.*(1i))./(Freq.*(2*pi));
MobModMea=sqrt(((MobReal.^2)+abs(MobIm.^2)));

H1_21=sqrt(abs(((H1_21Re).^2)+((H1_21Im).^2)));
HdB=-20*log((H1_21));

HT=sqrt(abs(((MobReTheory).^2)+((MobImTheory).^2)));
HTdB=-20*log((HT));

G21Im=dlmread('G21.txt','','C34..C1833');
G21Re=dlmread('G21.txt','','B34..B1833');
G21=sqrt((G21Im.^2)+(G21Re.^2));
PwrIn=-0.5*(G21Im.*(1))./(Freq.*(2*pi))*1;

MIm=dlmread('G65.txt','','C34..C1833');
MRe=dlmread('G65.txt','','B34..B1833');
M=sqrt((MIm.^2)+(MRe.^2));
Ptrans1=2*((sqrt(ml*B))/(((2*pi)^2)*s))*((MIm.*(1))./Freq.^2);
Ptranstrue1=-1*Ptrans1.*(kb.*s)/(sin(kb.*s));

RIm=dlmread('G78.txt','','C34..C1833');
RRe=dlmread('G78.txt','','B34..B1833');
R=sqrt((RIm.^2)+(RRe.^2));
Ptrans2=2*((sqrt(ml*B))/(((2*pi)^2)*s))*((RIm.*(1))./Freq.^2);
Ptranstrue2=1*Ptrans2.*(kb.*s)/(sin(kb.*s));
```

```
    LIm=dlmread('G43.txt','','C34..C1833');
    LRe=dlmread('G43.txt','','B34..B1833');
    L=sqrt((LIm.^2)+(LRe.^2));
    Ptrans3=2*((sqrt(ml*B))/(((2*pi)^2)*s))*((LIm.*(1))./Freq.^2);
    Ptranstrue3=1*Ptrans3.*(kb.*s)/(sin(kb.*s));

    Ptotal=1*(Ptranstrue3+Ptranstrue2);

    Ar=Ptrans1./-PwrIn/1;
    Br=Ptrans2./PwrIn/1;
    Gr=Ptrans3./PwrIn/1;
    tr=(0+Br+Ar)/1;

    %Ir=-PwrIn./Ptrans1;
    %Gr=Ptrans3./Ptrans1;
    %Br=Ptrans2./Ptrans1;

    G33=dlmread('G33.txt','','B34..B1833');
    G44=dlmread('G44.txt','','B34..B1833');
    G43Re=dlmread('G43.txt','','B34..B1833');
    G34Im=dlmread('G43.txt','','C34..C1833');
    G34Re=dlmread('G34.txt','','B34..B1833');
    G3p4=G33+G44;
    Gp=((1/4)+((exp(1i*kb*s)).^(-2)));
    Gm=2*((1/4)-((exp(1i*kb*s)).^(-2)));
    GA=(Gp.*G3p4)+(Gm.*G34Re);
    GB=(G34Im.*(1i)).*(2/s);
    Rcp=abs(sqrt((GA+GB)./(GA-GB)));
    %Tcp=sqrt(1-((Rcp).^2));
    G4m3=G44-G33;
    argRcp=(atan(1/(kb.*s)*(G4m3./GA)))+2*(kb.*Lx);
    %DegRcp=wrap(argRcp);
    %DegRcp1=DegRcp.*180/pi;

    ejkd=exp(1i*kb.*s);%(1+(1i*(k*s)/2))/(1-(1i*(k*s)/2));
    Gpnp=2*G43Re.*ejkd;%exp(1i*k.*s);
    Gpnm=2*G43Re.*(-ejkd);%exp(-1i*k.*s);
    Rpn=abs(sqrt(((G3p4-Gpnp)/(G3p4-Gpnm))));
    %Tpn=sqrt(1-((Rpn).^2));
    argRpn=(atan((G4m3.*(sin(kb.*s)))./((G43Re.*2)-
(G3p4.*(cos(kb.*s))))))+2*(kb.*Lx);
    DegRpn=wrap(argRpn);
    DegRpn1=DegRpn.*180/pi;

    H1_34Re=dlmread('H1_34.txt','','B34..B1833');
    H1_34Im=dlmread('H1_34.txt','','C34..C1833');
    H1_34=sqrt((H1_34Re.^2)+(H1_34Im.^2));

    R3=(((H1_34)-(exp(-1i*kb.*s)))/(((exp(1i*kb.*s))-
(H1_34))));%*(exp(2i*kb.*(La+s)));
    %T3=sqrt(1-(R3));

    R4=(H1_34.*((1i*kb*s)+2)+(1i*kb*s)-2)./(H1_34.*((1i*kb*s)-
2)+(1i*kb*s)+2);
```

```
ndwave=(0.9)./((((2*pi)./Freq).^0.5)*((B/ml).^0.25));

%% Plot results

figure(1)
loglog(Freq,real(MobReal),'b')
hold on
loglog(Freq,real(MobReTheory),'k')
hold on
grid on
title 'Point Mobility (Real)';
xlabel 'Frequency, [Hz]'
ylabel 'Mobility-Re [m/s/N]'
legend('Real','Theory','Location','best');

figure(2)
loglog(Freq,imag(MobIm),'r')
hold on
loglog(Freq,imag(MobImTheory),'k')
hold on
grid on
title 'Point Mobility (Imaginary)';
xlabel 'Frequency, [Hz]'
ylabel 'Mobility-Im [m/s/N])'
legend('Imaginary','Theory','Location','best');

figure(3)
loglog(Freq,MobModMea,'m')
hold on
loglog(Freq,MobModTh,'k')
hold on
grid on
title 'Point Mobility (Modulus)';
xlabel 'Frequency, [Hz]'
ylabel '[Log] Mobility-Modulus'
legend('Measured','Theory','Location','best');

figure(7)
plot(Freq,PwrIn,'k')
hold on
plot(Freq,Ptotal,'m')
hold on
plot(Freq,Ptranstrue1,'r')
hold on
plot(Freq,Ptranstrue2,'b')
hold on
plot(Freq,Ptranstrue3,'g')
hold on
grid on
axis([250 2250 0 2.5e-6])
title 'Power Input and transmitted';
xlabel 'Frequency, [Hz]'
ylabel 'Power'
%legend('Power In','Power Trans
total','alpha','beta','gamma','Location','best');
```

```
figure(10)
plot(Freq,Rcp,'m')
hold on
%plot(Freq,Tcp,'c')
%hold on
plot(Freq,Rpn,'r')
hold on
%plot(Freq,Tpn,'b')
%hold on
%plot(Freq,R3,'r')
%hold on
%plot(Freq,T3,'b')
%hold on
%plot(Freq,R4,'h')
%hold on
grid on
title 'Reflection(red) & Transmission(blue) coefficient';
xlabel 'Frequency, [Hz]'
ylabel 'Magnitude [R]'
%legend('R3','T3');%('R1-C&P','T1-C&P','R2-P&N','T2-P&N');

figure(11)
plot(Freq,(DegRpn1),'r');grid
hold on
%plot(Freq,(DegRcp1),'b');grid
%hold on
grid on
title 'Reflection coefficient phase';
xlabel 'Frequency, [Hz]'
ylabel 'Phase in Degree'
legend('Method-1 Piaud&Nicholas','Method-2 Piaud&Nicholas');

figure(12)
plot(omega,HdB,'k');grid
hold on
plot(omega,HTdB,'k.');grid
hold on
grid minor
title 'Magnitude (dB) plot';
xlabel 'Frequency, [Hz]'
ylabel 'Magnitude (dB)'
%legend();

figure(14)
plot(ndwave,PwrIn,'k')
hold on
plot(ndwave,Ptotal,'m')
hold on
plot(ndwave,Ptranstrue1,'r')
hold on
plot(ndwave,Ptranstrue2,'b')
hold on
plot(ndwave,Ptranstrue3,'g')
hold on
grid on
axis([1 5 0 2.5e-6])
```

```
    title 'Power Input and transmitted';
    xlabel 'Dimensionless wavenumber'
    ylabel 'Power'
    %legend('Power In','Power Trans
total','alpha','beta','gamma','Location','best');

    figure(16)
    plot(Freq,Ar,'r')
    hold on
    plot(Freq,Br,'b')
    hold on
    plot(Freq,Gr,'g')
    hold on
    plot(Freq,tr,'k')
    hold on
    grid on
    axis([0 2250 0 2])
    title 'Ratio Power over Input';
    xlabel 'Frequency, [Hz]'
    ylabel 'Ratio of Power'
    %legend('Power In','Power Trans
total','alpha','beta','gamma','Location','best');

    figure(17)
```

```
%function ExpCode
%% Fl input to jointbeam beam
clear all
clf
format long e
%Given
b=0.1;                            %m
d=0.02;                           %m
Eta=0.00;
Eeta=(1+(1i*Eta));
E1=1.75e9;%60e9;%1.75e9;%         %N/m^2
I1=(b*(d^3))/12;                  %m^4
A1=b*d;                           %m^2
E2=1.75e9;%60e9;%1.75e9;%         %N/m^2
I2=(b*(d^3))/12;        %m^4
A2=b*d;                   %m^2
RHO=1170;%1190;%2500;                   %kg/m^3
RHOj=1170;%1190;%2500;                  %kg/m^3
Jw=1*b;                           %m
%L=1*d;                           %m
B=E1*I1;
ml=A1*RHO;

Ls=0.30;                          %depth in sand
Lb=1.50;                          %length beam exposed
Lt=Lb+(1*Ls);                     %total beam length
La=0.30;                          %distance force to accelerometer
Lx=0.30;                          %distance acclr to termination
```

```
%% Natural Frequency
fnt=zeros;
fncnt=0;
for n=1:1:20;
    fn=pi/2*sqrt(B/ml)*(n^2/Lb^2);
    fncnt=fncnt+1;
    fnt(fncnt)=fn;
end

    %% Freq limit
    %Lower Freq limit (due to termination)-t
    Wavet=2*Ls;                                %Max wavelength W.R.T Ls
    kbt=(2*pi)/Wavet;                          %wavenumber for above
    omegat=kbt^2*(sqrt((E1*I1)/(A1*RHO)));     %
    %omegat=kbt*(sqrt((E1)/(RHO)));    %
    FqLwrt=omegat/(2*pi)

    %Lower Freq limit (due to force-acc midpoint)-f
    Wavef=La*2;
    kbf=(2*pi)/Wavef;
    omegaf=kbf^2*(sqrt((E1*I1)/(A1*RHO)));     %
    %omegaf=kbf*(sqrt((E1)/(RHO)));    %
    FqLwrf=omegaf/(2*pi)

    %Upper Freq limit (due to acc spacing)-s
    s=0.03;
    Waves=s/0.2;
    kbs=(2*pi)/Waves;
    omegas=kbs^2*(sqrt((E1*I1)/(A1*RHO)));     %
    %omegas=kbs*(sqrt((E1)/(RHO)));    %
    FqUprs=omegas/(2*pi)

    %% Theory - mobility

    Freq=dlmread('H1_21.txt','','A34..A1833');%A134..A1833   %A74..A834 1634

    omega=Freq.*(2*pi);
    kb=(sqrt(omega))*(((ml)/(B))^0.25);
    MobReTheory=omega./(4*B*(kb.^3));
    MobImTheory=omega.*(-i)./(4*B*(kb.^3));
    MobModTh=sqrt(((MobReTheory.^2)+abs(MobImTheory.^2)));

    %% Read experiment data

    H1_21Re=dlmread('H1_21.txt','','B34..B1833');
    MobReal=-(H1_21Re.*1)./(Freq.*(2*pi));
    H1_21Im=dlmread('H1_21.txt','','C34..C1833');
    MobIm=(H1_21Im.*(1i))./(Freq.*(2*pi));
    MobModMea=sqrt(((MobReal.^2)+abs(MobIm.^2)));

    H1_21=sqrt(abs(((H1_21Re).^2)+((H1_21Im).^2)));
    HdB=-20*log((H1_21));

    HT=sqrt(abs(((MobReTheory).^2)+((MobImTheory).^2)));
    HTdB=-20*log((HT));
```

```
G21Im=dlmread('G21.txt','','C34..C1833');
G21Re=dlmread('G21.txt','','B34..B1833');
G21=sqrt((G21Im.^2)+(G21Re.^2));
PwrIn=-0.5*(G21Im.*(1))./(Freq.*(2*pi))*1;

MIm=dlmread('G65.txt','','C34..C1833');
MRe=dlmread('G65.txt','','B34..B1833');
M=sqrt((MIm.^2)+(MRe.^2));
Ptrans1=2*((sqrt(ml*B))/(((2*pi)^2)*s))*((MIm.*(1))./Freq.^2);
Ptranstrue1=-1*Ptrans1.*(kb.*s)/(sin(kb.*s));

RIm=dlmread('G78.txt','','C34..C1833');
RRe=dlmread('G78.txt','','B34..B1833');
R=sqrt((RIm.^2)+(RRe.^2));
Ptrans2=2*((sqrt(ml*B))/(((2*pi)^2)*s))*((RIm.*(1))./Freq.^2);
Ptranstrue2=1*Ptrans2.*(kb.*s)/(sin(kb.*s));

LIm=dlmread('G43.txt','','C34..C1833');
LRe=dlmread('G43.txt','','B34..B1833');
L=sqrt((LIm.^2)+(LRe.^2));
Ptrans3=2*((sqrt(ml*B))/(((2*pi)^2)*s))*((LIm.*(1))./Freq.^2);
Ptranstrue3=1*Ptrans3.*(kb.*s)/(sin(kb.*s));

Ptotal=1*(Ptranstrue3+Ptranstrue2);

Ar=Ptrans1./-PwrIn/1;
Br=Ptrans2./PwrIn/1;
Gr=Ptrans3./PwrIn/1;
tr=(0+Br+Ar)/1;

%Ir=-PwrIn./Ptrans1;
%Gr=Ptrans3./Ptrans1;
%Br=Ptrans2./Ptrans1;

G33=dlmread('G33.txt','','B34..B1833');
G44=dlmread('G44.txt','','B34..B1833');
G43Re=dlmread('G43.txt','','B34..B1833');
G34Im=dlmread('G43.txt','','C34..C1833');
G34Re=dlmread('G34.txt','','B34..B1833');
G3p4=G33+G44;
Gp=((1/4)+((exp(1i*kb*s)).^(-2)));
Gm=2*((1/4)-((exp(1i*kb*s)).^(-2)));
GA=(Gp.*G3p4)+(Gm.*G34Re);
GB=(G34Im.*(1i)).*(2/s);
Rcp=abs(sqrt((GA+GB)./(GA-GB)));
%Tcp=sqrt(1-((Rcp).^2));
G4m3=G44-G33;
argRcp=(atan(1/(kb.*s)*(G4m3./GA)))+2*(kb.*Lx);
%DegRcp=wrap(argRcp);
%DegRcp1=DegRcp.*180/pi;

ejkd=exp(1i*kb.*s);%(1+(1i*(k*s)/2))/(1-(1i*(k*s)/2));
Gpnp=2*G43Re.*ejkd;%exp(1i*k.*s);
Gpnm=2*G43Re.*(-ejkd);%exp(-1i*k.*s);
```

```
    Rpn=abs(sqrt(((G3p4-Gpnp)/(G3p4-Gpnm))));
    %Tpn=sqrt(1-((Rpn).^2));
    argRpn=(atan((G4m3.*(sin(kb.*s)))./((G43Re.*2)-
(G3p4.*(cos(kb.*s))))))+2*(kb.*Lx);
    DegRpn=wrap(argRpn);
    DegRpn1=DegRpn.*180/pi;

    H1_34Re=dlmread('H1_34.txt','','B34..B1833');
    H1_34Im=dlmread('H1_34.txt','','C34..C1833');
    H1_34=sqrt((H1_34Re.^2)+(H1_34Im.^2));

    R3=(((H1_34)-(exp(-1i*kb.*s)))/(((exp(1i*kb.*s))-
(H1_34))));%*(exp(2i*kb.*(La+s)));
    %T3=sqrt(1-(R3));

    R4=(H1_34.*((1i*kb*s)+2)+(1i*kb*s)-2)./(H1_34.*((1i*kb*s)-
2)+(1i*kb*s)+2);

    ndwave=(0.9)./((((2*pi)./Freq).^0.5)*((B/ml).^0.25));

    %% Plot results

    figure(1)
    loglog(Freq,real(MobReal),'b')
    hold on
    loglog(Freq,real(MobReTheory),'k')
    hold on
    grid on
    title 'Point Mobility (Real)';
    xlabel 'Frequency, [Hz]'
    ylabel 'Mobility-Re [m/s/N]'
    legend('Real','Theory','Location','best');

    figure(2)
    loglog(Freq,imag(MobIm),'r')
    hold on
    loglog(Freq,imag(MobImTheory),'k')
    hold on
    grid on
    title 'Point Mobility (Imaginary)';
    xlabel 'Frequency, [Hz]'
    ylabel 'Mobility-Im [m/s/N])'
    legend('Imaginary','Theory','Location','best');

    figure(3)
    loglog(Freq,MobModMea,'m')
    hold on
    loglog(Freq,MobModTh,'k')
    hold on
    grid on
    title 'Point Mobility (Modulus)';
    xlabel 'Frequency, [Hz]'
    ylabel '[Log] Mobility-Modulus'
    legend('Measured','Theory','Location','best');
```

```
    figure(7)
    plot(Freq,PwrIn,'k')
    hold on
    plot(Freq,Ptotal,'m')
    hold on
    plot(Freq,Ptranstrue1,'r')
    hold on
    plot(Freq,Ptranstrue2,'b')
    hold on
    plot(Freq,Ptranstrue3,'g')
    hold on
    grid on
    axis([250 2250 0 2.5e-6])
    title 'Power Input and transmitted';
    xlabel 'Frequency, [Hz]'
    ylabel 'Power'
    %legend('Power In','Power Trans
total','alpha','beta','gamma','Location','best');

    figure(10)
    plot(Freq,Rcp,'m')
    hold on
    %plot(Freq,Tcp,'c')
    %hold on
    plot(Freq,Rpn,'r')
    hold on
    %plot(Freq,Tpn,'b')
    %hold on
    %plot(Freq,R3,'r')
    %hold on
    %plot(Freq,T3,'b')
    %hold on
    %plot(Freq,R4,'h')
    %hold on
    grid on
    title 'Reflection(red) & Transmission(blue) coefficient';
    xlabel 'Frequency, [Hz]'
    ylabel 'Magnitude [R]'
    %legend('R3','T3');%('R1-C&P','T1-C&P','R2-P&N','T2-P&N');

    figure(11)
    plot(Freq,(DegRpn1),'r');grid
    hold on
    %plot(Freq,(DegRcp1),'b');grid
    %hold on
    grid on
    title 'Reflection coefficient phase';
    xlabel 'Frequency, [Hz]'
    ylabel 'Phase in Degree'
    legend('Method-1 Piaud&Nicholas','Method-2 Piaud&Nicholas');

    figure(12)
    plot(omega,HdB,'k');grid
    hold on
    plot(omega,HTdB,'k.');grid
    hold on
```

```
    grid minor
    title 'Magnitude (dB) plot';
    xlabel 'Frequency, [Hz]'
    ylabel 'Magnitude (dB)'
    %legend();

    figure(14)
    plot(ndwave,PwrIn,'k')
    hold on
    plot(ndwave,Ptotal,'m')
    hold on
    plot(ndwave,Ptranstrue1,'r')
    hold on
    plot(ndwave,Ptranstrue2,'b')
    hold on
    plot(ndwave,Ptranstrue3,'g')
    hold on
    grid on
    axis([1 5 0 2.5e-6])
    title 'Power Input and transmitted';
    xlabel 'Dimensionless wavenumber'
    ylabel 'Power'
    %legend('Power In','Power Trans
total','alpha','beta','gamma','Location','best');

    figure(16)
    plot(Freq,Ar,'r')
    hold on
    plot(Freq,Br,'b')
    hold on
    plot(Freq,Gr,'g')
    hold on
    plot(Freq,tr,'k')
    hold on
    grid on
    axis([0 2250 0 2])
    title 'Ratio Power over Input';
    xlabel 'Frequency, [Hz]'
    ylabel 'Ratio of Power'
    %legend('Power In','Power Trans
total','alpha','beta','gamma','Location','best');

    figure(17)




FqLwrt =

    1.232374869692417e+002


FqLwrf =

    1.232374869692417e+002
```

```
FqUprs =

    1.971799791507868e+003


function[phase] = wrap(phase)
%the wrap function as:
%   a wrap function
phase = atan2(sin(phase),cos(phase));
phase = phase + 2*pi*(phase <= -pi);

end
```

Appendix: $\boxed{\textbf{\textit{D-1}}}$ ***Force-Input Joint (with rubber) equation: -***

Equilibrium of bending moment (joint), **at $x = n$**

$$\overbrace{E_1 I_1 \frac{\partial^2 W_\alpha}{\partial x^2}}^{M-} + \overbrace{\frac{L}{2}\left(\sin\frac{\theta}{2}\right)}^{e}\overbrace{E_1 I_1 \frac{\partial^3 W_\alpha}{\partial x^3}}^{V-} = E_2 I_2 \frac{\partial^2 W_\beta}{\partial \psi^2} - \frac{L}{2}\left(\sin\frac{\theta}{2}\right) E_2 I_2 \frac{\partial^3 W_\beta}{\partial \psi^3} - I_j \frac{\partial^2 \partial W_\alpha}{\partial t^2 \partial x} - \boldsymbol{E_1 A_1 \frac{\partial U_\alpha}{\partial x}\left[\frac{L}{2}\left(1-\cos\frac{\theta}{2}\right)\right]} + \boldsymbol{E_2 A_2 \frac{\partial U_\beta}{\partial \psi}\left[\frac{L}{2}\left(1-\cos\frac{\theta}{2}\right)\right]}$$

Which is in the form of: -

$$(M_-) + [(e)(V_-)] = (M_+) - [(e)(V_+)] - I_j\ddot{\theta} - [(F_-)(f)] + [(F_+)(f)]$$

$\frac{\partial^2 W_\alpha}{\partial x^2}$ $\quad {k_{f\alpha}}^2\{A_2 e^{-k_{f\alpha}(n-m)} + B_1\} + {k_{f\alpha*}}^2\{-A_4 e^{-ik_{f\alpha*}(n-m)} - B_3\};$

$\frac{\partial^3 W_\alpha}{\partial x^3}$ $\quad {k_{f\alpha}}^3\{-A_2 e^{-k_{f\alpha}(n-m)} + B_1\} + {k_{f\alpha*}}^3\{iA_4 e^{-ik_{f\alpha*}(n-m)} - iB_3\};$

$\frac{\partial^2 W_\beta}{\partial \psi^2}$ $\quad {k_{f\beta}}^2\{C_2\} - {k_{f\beta*}}^2\{C_4\};$

$\frac{\partial^3 W_\beta}{\partial \psi^3}$ $\quad {k_{f\beta}}^3\{-C_2\} + {k_{f\beta*}}^3\{iC_4\};$

$\frac{\partial^2}{\partial t^2}\frac{\partial \boldsymbol{W_\alpha}}{\partial x}$ $\quad -\omega^2 k_{f\alpha}\{-A_2 e^{-k_{f\alpha}(n-m)} + B_1\} - \omega^2 k_{f\alpha*}\{-iA_4 e^{-ik_{f\alpha*}(n-m)} + iB_3\};$

$\frac{\partial U_\alpha}{\partial x}$ $\quad k_{l\alpha*}\{-iA_L e^{-ik_{l\alpha*}(n-m)}\} + k_{l\alpha*}\{iB_L\};$

$\frac{\partial U_\beta}{\partial \psi}$ $\quad k_{l\beta*}\{-iC_L\};$

$$\begin{aligned}
&E_1 I_1\left[{k_{f\alpha}}^2\{A_2 e^{-k_{f\alpha}(n-m)} + B_1\} + {k_{f\alpha*}}^2\{-A_4 e^{-ik_{f\alpha*}(n-m)} - B_3\}\right] \\
&\qquad + \frac{L}{2}\left(\sin\frac{\theta}{2}\right) E_1 I_1\left[{k_{f\alpha}}^3\{-A_2 e^{-k_{f\alpha}(n-m)} + B_1\} \right. \\
&\qquad \left. + {k_{f\alpha*}}^3\{iA_4 e^{-ik_{f\alpha*}(n-m)} - iB_3\}\right] \\
&= E_2 I_2\left[{k_{f\beta}}^2\{C_2\} - {k_{f\beta*}}^2\{C_4\}\right] - \frac{L}{2}\left(\sin\frac{\theta}{2}\right) E_2 I_2\left[{k_{f\beta}}^3\{-C_2\} + {k_{f\beta*}}^3\{iC_4\}\right] \\
&\qquad - I_j\left[-\omega^2 k_{f\alpha}\{-A_2 e^{-k_{f\alpha}(n-m)} + B_1\} - \omega^2 k_{f\alpha*}\{-iA_4 e^{-ik_{f\alpha*}(n-m)} + iB_3\}\right] \\
&\qquad - \left[\frac{\boldsymbol{L}}{\boldsymbol{2}}\left(\boldsymbol{1} - \boldsymbol{\cos}\frac{\theta}{2}\right)\right] \boldsymbol{E_1 A_1}\left[k_{l\alpha*}\{-iA_L e^{-ik_{l\alpha*}(n-m)}\} + k_{l\alpha*}\{iB_L\}\right] \\
&\qquad + \left[\frac{\boldsymbol{L}}{\boldsymbol{2}}\left(\boldsymbol{1} - \boldsymbol{\cos}\frac{\theta}{2}\right)\right] \boldsymbol{E_2 A_2}\left[k_{l\beta*}\{-iC_L\}\right]
\end{aligned}$$

$$E_1I_1\left[k_{f\alpha}{}^2A_2e^{-k_{f\alpha}(n-m)} + k_{f\alpha}{}^2B_1 - k_{f\alpha*}{}^2A_4e^{-ik_{f\alpha*}(n-m)} - k_{f\alpha*}{}^2B_3\right]$$
$$+ \frac{L}{2}\left(\sin\tfrac{\theta}{2}\right)E_1I_1\left[-k_{f\alpha}{}^3A_2e^{-k_{f\alpha}(n-m)} + k_{f\alpha}{}^3B_1 + k_{f\alpha*}{}^3iA_4e^{-ik_{f\alpha*}(n-m)} - k_{f\alpha*}{}^3iB_3\right]$$
$$= E_2I_2\left[k_{f\beta}{}^2C_2 - k_{f\beta*}{}^2C_4\right] - \frac{L}{2}\left(\sin\tfrac{\theta}{2}\right)E_2I_2\left[-k_{f\beta}{}^3C_2 + k_{f\beta*}{}^3iC_4\right]$$
$$- I_j\left[\omega^2k_{f\alpha}A_2e^{-k_{f\alpha}(n-m)} - \omega^2k_{f\alpha}B_1 + \omega^2k_{f\alpha*}iA_4e^{-ik_{f\alpha*}(n-m)} - \omega^2k_{f\alpha*}iB_3\right]$$
$$- \left[\frac{\boldsymbol{L}}{\boldsymbol{2}}\left(\mathbf{1} - \mathbf{cos}\tfrac{\theta}{2}\right)\right]\boldsymbol{E_1A_1}\left[-k_{l\alpha*}iA_Le^{-ik_{l\alpha*}(n-m)} + k_{l\alpha*}iB_L\right]$$
$$+ \left[\frac{\boldsymbol{L}}{\boldsymbol{2}}\left(\mathbf{1} - \mathbf{cos}\tfrac{\theta}{2}\right)\right]\boldsymbol{E_2A_2}\left[-k_{l\beta*}iC_L\right]$$

$$\left[\!\left[0 \right.\right.$$

$$= A_2\underbrace{\left\{-\left(E_1I_1\left(k_{f\alpha}^2\right)\right)e^{-k_{f\alpha}(n-m)} + \left(\frac{L}{2}\left(\mathbf{sin}\tfrac{\theta}{2}\right)E_1I_1\left(k_{f\alpha}^3\right)\right)e^{-k_{f\alpha}(n-m)} - \left(I_j\omega^2\left(k_{f\alpha}\right)\right)e^{-k_{f\alpha}(n-m)}\right\}}_{7a}$$
$$+ A_4\underbrace{\left\{\left(E_1I_1\left(k_{f\alpha*}^2\right)\right)e^{-ik_{f\alpha*}(n-m)} - \left(\frac{L}{2}\left(\mathbf{sin}\tfrac{\theta}{2}\right)E_1I_1\left(ik_{f\alpha*}^3\right)\right)e^{-ik_{f\alpha*}(n-m)} - \left(I_j\omega^2\left(ik_{f\alpha*}\right)\right)e^{-ik_{f\alpha*}(n-m)}\right\}}_{7b}$$
$$+ A_L\underbrace{\left\{\left[\frac{\boldsymbol{L}}{\boldsymbol{2}}\left(\mathbf{1} - \boldsymbol{cos}\tfrac{\theta}{2}\right)\right]E_1A_1\left(ik_{l\alpha*}\right)e^{-ik_{l\alpha*}(n-m)}\right\}}_{7c}$$
$$+ B_1\underbrace{\left\{-\left(E_1I_1\left(k_{f\alpha}^2\right)\right) - \left(\frac{L}{2}\left(\mathbf{sin}\tfrac{\theta}{2}\right)E_1I_1\left(k_{f\alpha}^3\right)\right) + \left(I_j\omega^2\left(k_{f\alpha}\right)\right)\right\}}_{7d}$$
$$+ B_3\underbrace{\left\{\left(E_1I_1\left(k_{f\alpha*}^2\right)\right) + \left(\frac{L}{2}\left(\mathbf{sin}\tfrac{\theta}{2}\right)E_1I_1\left(ik_{f\alpha*}^3\right)\right) + \left(I_j\omega^2\left(ik_{f\alpha*}\right)\right)\right\}}_{7e}$$
$$+ B_L\underbrace{\left\{-\left[\frac{\boldsymbol{L}}{\boldsymbol{2}}\left(\mathbf{1} - \boldsymbol{cos}\tfrac{\theta}{2}\right)\right]E_1A_1\left(ik_{l\alpha*}\right)\right\}}_{7f}$$
$$+ C_2\underbrace{\left\{E_2I_2\left(k_{f\beta}{}^2\right) + \frac{L}{2}\left(\mathbf{sin}\tfrac{\theta}{2}\right)E_2I_2\left(k_{f\beta}{}^3\right)\right\}}_{7g}$$
$$+ C_4\underbrace{\left\{-E_2I_2\left(k_{f\beta*}{}^2\right) - \frac{L}{2}\left(\mathbf{sin}\tfrac{\theta}{2}\right)E_2I_2\left(ik_{f\beta*}{}^3\right)\right\}}_{7h}$$
$$+ C_L\underbrace{\left\{-\left[\frac{\boldsymbol{L}}{\boldsymbol{2}}\left(\mathbf{1} - \mathbf{cos}\tfrac{\theta}{2}\right)\right]\boldsymbol{E_2A_2}\left(ik_{l\beta*}\right)\right\}}_{7i}\left.\right]\!\!\right]$$

Equation for MATLAB:-

$$0 = (A_2)\,[\,\{V6\}(Q1)\,k_{f\alpha}^3\,(Fn) + (-Q1)\,k_{f\alpha}^2\,(Fn) + (-I_j w^2)\,k_{f\alpha}(Fn)\,]$$
$$+ (A_4)\,[\,\{-V6\}(Q1)\,ik_{f\alpha^*}^{\ 3}\,(Fni) + (Q1)\,k_{f\alpha^*}^{\ 2}\,(Fni) + (-I_j w^2)\,ik_{f\alpha^*}\,(Fni)\,]$$
$$+ (A_L)\,[\,\{V5\}(S1)\,ik_{l\alpha^*}\,(Lni)\,]$$
$$+ (B_1)\,[\,\{-V6\}(Q1)\,k_{f\alpha}^3 + (-Q1)\,k_{f\alpha}^2 + (I_j w^2)\,k_{f\alpha}\,]$$
$$+ (B_3)\,[\,\{V6\}(Q1)\,ik_{f\alpha^*}^{\ 3} + (Q1)\,k_{f\alpha^*}^{\ 2} + (I_j w^2)\,ik_{f\alpha^*}\,]$$
$$+ (B_L)\,[\,\{-V5\}(S1)\,ik_{l\alpha^*}\,]$$
$$+ (C_2)\,[\,\{V6\}(Q2)\,k_{f\beta}^3 + (Q2)\,k_{f\beta}^{\ 2}\,]$$
$$+ (C_4)\,[\,\{-V6\}(Q2)\,ik_{f\beta^*}^{\ 3} + (-Q2)\,k_{f\beta}^{\ 2}\,]$$
$$+ (C_L)\,[\,\{-V5\}(S2)\,ik_{l\beta^*}\,]$$

$$0 = (A_2)\,[\,\{V6\}(Q1)\,k_{f\alpha}^3 + (-Q1)\,k_{f\alpha}^2 + (-I_j w^2)\,k_{f\alpha}\,]\,(Fn)$$

`+(Drm*  Kfa -Dr*V6)` **(Fn)**

$$+ (A_4)\,[\,\{-V6\}(Q1)\,ik_{f\alpha^*}^{\ 3} + (Q1)\,k_{f\alpha^*}^{\ 2} + (-I_j w^2)\,ik_{f\alpha^*}\,]\,(Fni)$$

`+(Drm*i*Kfax-Dr*V6)` **(Fni)**

$$+ (A_L)\,[\,\{V5\}(S1)\,ik_{l\alpha^*}\,]\,(Lni)$$

`+(DrL*V5)` **(Lni)**

$$+ (B_1)\,[\,\{-V6\}(Q1)\,k_{f\alpha}^3 + (-Q1)\,k_{f\alpha}^2 + (I_j w^2)\,k_{f\alpha}\,]$$

`(-Drm*  Kfa -Dr*V6)`

$$+ (B_3)\,[\,\{V6\}(Q1)\,ik_{f\alpha^*}^{\ 3} + (Q1)\,k_{f\alpha^*}^{\ 2} + (I_j w^2)\,ik_{f\alpha^*}\,]$$

`(-Drm*i*Kfax-Dr*V6)`

$+ (B_L)\,[\,\{-V5\}(S1)\,ik_{l\alpha^*}\,]$ `+(DrL*V5)`

$+ (C_2)\,[\,\{V6\}(Q2)\,k_{f\beta}^3 + (Q2)\,k_{f\beta}^{\ 2}\,]$ `+(-Drm*  Kfb +Dr*V6)`

$+ (C_4)\,[\,\{-V6\}(Q2)\,ik_{f\beta^*}^{\ 3} + (-Q2)\,k_{f\beta}^{\ 2}\,]$ `+(-Drm*i*Kfbx+Dr*V6)`

$+ (C_L)\,[\,\{-V5\}(S2)\,ik_{l\beta^*}\,]$ `+(DrL*V5)`

Equilibrium of compressive force (joint), **at $x = n$**

$$E_1 A_1 \frac{\partial U_\alpha}{\partial x} = E_2 A_2 \frac{\partial U_\beta}{\partial \psi}\cos\theta + E_2 I_2 \frac{\partial^3 W_\beta}{\partial \psi^3}\sin\theta - m_j \frac{\partial^2}{\partial t^2}\left[U_\alpha - \boldsymbol{L}\left(\mathbf{sin}\,\tfrac{\theta}{4}\right)^2 \frac{\boldsymbol{\partial W_\alpha}}{\boldsymbol{\partial x}}\right]$$

Which is in the form of: -

$$(F_-) = (F_+)cos\theta + (V_+)sin\theta - M_j\ddot{U}$$

$\frac{\partial U_\alpha}{\partial x}$ $\quad k_{l\alpha*}\{-iA_L e^{-ik_{l\alpha*}(n-m)}\} + k_{l\alpha*}\{iB_L\}$;

$\frac{\partial U_\beta}{\partial \psi}$ $\quad k_{l\beta*}\{-iC_L\}$;

$\frac{\partial^3 W_\beta}{\partial \psi^3}$ $\quad {k_{f\beta}}^3\{-C_2\} + {k_{f\beta*}}^3\{iC_4\}$;

$\frac{\partial^2 \boldsymbol{U_\alpha}}{\partial t^2}$ $\quad -\omega^2\{A_L e^{-ik_{l\alpha*}(n-m)} + B_L\}$;

$\frac{\partial^2}{\partial t^2}\frac{\boldsymbol{\partial W_\alpha}}{\partial x}$ $\quad -\omega^2 k_{f\alpha}\{-A_2 e^{-k_{f\alpha}(n-m)} + B_1\} - \omega^2 k_{f\alpha*}\{-iA_4 e^{-ik_{f\alpha*}(n-m)} + iB_3\}$;

$$\begin{aligned}
E_1 A_1 &\left(k_{l\alpha*}\{-iA_L e^{-ik_{l\alpha*}(n-m)}\} + k_{l\alpha*}\{iB_L\}\right) \\
&= E_2 A_2\left(k_{l\beta*}\{-iC_L\}\right)\cos\theta + E_2 I_2\left({k_{f\beta}}^3\{-C_2\} + {k_{f\beta*}}^3\{iC_4\}\right)\sin\theta \\
&- m_j(-\omega^2)\Big[\left(A_L e^{-ik_{l\alpha*}(n-m)} + B_L\right) \\
&- \boldsymbol{L}\left(\mathbf{sin}\,\tfrac{\theta}{4}\right)^2\left(k_{f\alpha}\{-A_2 e^{-k_{f\alpha}(n-m)} + B_1\} + k_{f\alpha*}\{-iA_4 e^{-i\ f\alpha*(n-m)} + iB_3\}\right)\Big]
\end{aligned}$$

$$\begin{aligned}
0 = \; & A_2 \underbrace{\left[(m_j\omega^2)\boldsymbol{L}\left(\mathbf{sin}\,\tfrac{\theta}{4}\right)^2(\boldsymbol{k_{f\alpha}})\right]}_{9a} e^{-k_{f\alpha}(n-m)} + A_4 \underbrace{\left[(m_j\omega^2)\boldsymbol{L}\left(\mathbf{sin}\,\tfrac{\theta}{4}\right)^2(\boldsymbol{ik_{f\alpha*}})\right]}_{9b} e^{-ik_{f\alpha*}(n-m)} \\
& + A_L \underbrace{\left[\left(E_1 A_1(ik_{l\alpha*})\right) + (m_j\omega^2)\right]}_{9c} e^{-ik_{l\alpha*}(n-m)} \\
& + B_1 \underbrace{\left[-(m_j\omega^2)\boldsymbol{L}\left(\mathbf{sin}\,\tfrac{\theta}{4}\right)^2(\boldsymbol{k_{f\alpha}})\right]}_{9d} + B_3 \underbrace{\left[-(m_j\omega^2)\boldsymbol{L}\left(\mathbf{sin}\,\tfrac{\theta}{4}\right)^2(\boldsymbol{ik_{f\alpha*}})\right]}_{9e} \\
& + B_L \underbrace{\left[-\left(E_1 A_1(ik_{l\alpha*})\right) + (m_j\omega^2)\right]}_{9f} + C_2 \underbrace{\left[-E_2 I_2\left(k_{f\beta}^3\right)\sin\theta\right]}_{9g} \\
& + C_4 \underbrace{\left[\left(E_2 I_2\left(ik_{f\beta*}^3\right)\sin\theta\right)\right]}_{9h} + C_L \underbrace{\left[-\left(E_2 A_2\left(ik_{l\beta*}\right)\cos\theta\right)\right]}_{9i}
\end{aligned}$$

Equation for MATLAB:-

$$
\begin{aligned}
\mathbf{0} \quad = \quad & (A_2)\ [\ \{\ V5\}(m_j w^2)\ k_{f\alpha}]\ (Fn) \\
+ \quad & (A_4)\ [\ \{\ V5\}(m_j w^2)\ ik_{\ f\alpha^*}]\ (Fni) \\
+ \quad & (A_L)\ [\ (S1)\ ik_{l\alpha^*} + (m_j w^2)]\ \underline{\texttt{+DrL}}\ \ (Lni) \\
+ \quad & (B_1)\ [\ \{\ V5\}(-m_j w^2)\ k_{f\alpha}] \\
+ \quad & (B_3)\ [\ \{\ V5\}(-m_j w^2)\ ik_{\ f\alpha^*}] \\
+ \quad & (B_L)\ [\ (-S1)\ ik_{l\alpha^*} + (m_j w^2)]\ \underline{\texttt{+DrL}} \\
+ \quad & (C_2)\ [\ (-Q2)\ k_{f\beta}^3\ Sin\ \theta]\ \underline{\texttt{-Dr*sin(T)}} \\
+ \quad & (C_4)\ [\ (Q2)\ ik_{f\beta^*}^3\ Sin\ \theta]\ \underline{\texttt{-Dr*sin(T)}} \\
+ \quad & (C_L)\ [(-S2)\ ik_{l\beta^*}\ Cos\ \theta]\ \underline{\texttt{+DrL*cos(T)}}
\end{aligned}
$$

Equilibrium of shear force (joint), **at $x = n$**

$$-E_1 I_1 \frac{\partial^3 W_\alpha}{\partial x^3} = E_2 A_2 \frac{\partial U_\beta}{\partial \psi}\sin\theta - E_2 I_2 \frac{\partial^3 W_\beta}{\partial \psi^3}\cos\theta - m_j \frac{\partial^2}{\partial t^2}\left[W_\alpha + \boldsymbol{L}\left(\mathbf{sin}\tfrac{\theta}{4}\right)\left(\mathbf{cos}\tfrac{\theta}{4}\right)\frac{\partial W_\alpha}{\partial x}\right]$$

Which is in the form of: -

$$-(V_-) = (F_+)sin\theta - (V_+)cos\theta - M_j\ddot{W}$$

$\frac{\partial^3 W_\alpha}{\partial x^3}$ $\quad k_{f\alpha}{}^3\{-A_2 e^{-k_{f\alpha}(n-m)} + B_1\} + k_{f\alpha*}{}^3\{iA_4 e^{-ik_{f\alpha*}(n-m)} - iB_3\}$;

$\frac{\partial U_\beta}{\partial \psi}$ $\quad k_{l\beta*}\{-iC_L\}$;

$\frac{\partial^3 W_\beta}{\partial \psi^3}$ $\quad k_{f\beta}{}^3\{-C_2\} + k_{f\beta*}{}^3\{iC_4\}$;

$\frac{\partial^2 \boldsymbol{W_\alpha}}{\partial t^2}$ $\quad -\omega^2\{A_2 e^{-k_{f\alpha}(n-m)} + B_1\} - \omega^2\{A_4 e^{-ik_{f\alpha*}(n-m)} + B_3\}$;

$\frac{\partial^2}{\partial t^2}\frac{\partial \boldsymbol{W_\alpha}}{\partial x}$ $\quad -\omega^2 k_{f\alpha}\{-A_2 e^{-k_{f\alpha}(n-m)} + B_1\} - \omega^2 k_{f\alpha*}\{-iA_4 e^{-ik_{f\alpha*}(n-m)} + iB_3\}$;

$$\begin{aligned}
-E_1 I_1\left(k_{f\alpha}{}^3\{-A_2 e^{-k_{f\alpha}(n-m)} + B_1\} + k_{f\alpha*}{}^3\{iA_4 e^{-ik_{f\alpha*}(n-m)} - iB_3\}\right) \\
= E_2 A_2\, k_{l\beta*}\{-iC_L\}\sin\theta - E_2 I_2\left(k_{f\beta}{}^3\{-C_2\} + k_{f\beta*}{}^3\{iC_4\}\right)\cos\theta \\
+ m_j\omega^2\Big[\left(\{A_2 e^{-k_{f\alpha}(n-m)} + B_1\} + \{A_4 e^{-ik_{f\alpha*}(n-m)} + B_3\}\right) \\
+ \Big(\boldsymbol{L}\left(\mathbf{sin}\tfrac{\theta}{4}\right)\left(\mathbf{cos}\tfrac{\theta}{4}\right)\Big(k_{f\alpha}\{-A_2 e^{-k_{f\alpha}(n-m)} + B_1\} + k_{f\alpha*}\{-iA_4 e^{-ik_{f\alpha*}(n-m)} \\
+ iB_3\}\Big)\Big)\Big]
\end{aligned}$$

$$\begin{aligned}
0 &= A_2\underbrace{\left[-\left(E_1 I_1 (k_{f\alpha}^3)\right) + \left((m_j\omega^2)\right) - \left((m_j\omega^2)\boldsymbol{L}\left(\mathbf{sin}\tfrac{\theta}{4}\right)\left(\mathbf{cos}\tfrac{\theta}{4}\right)(k_{f\alpha})\right)\right]}_{11} e^{-k_{f\alpha}(n-m)} \\
&+ A_4\underbrace{\left[\left(E_1 I_1 (ik_{f\alpha*}^3)\right) + \left((m_j\omega^2)\right) - \left((m_j\omega^2)\boldsymbol{L}\left(\mathbf{sin}\tfrac{\theta}{4}\right)\left(\mathbf{cos}\tfrac{\theta}{4}\right)(ik_{f\alpha*})\right)\right]}_{11b} e^{-ik_{f\alpha*}(n-m)} \\
&+ B_1\underbrace{\left[\left(E_1 I_1 (k_{f\alpha}^3)\right) + \left((m_j\omega^2)\right) + \left((m_j\omega^2)\boldsymbol{L}\left(\mathbf{sin}\tfrac{\theta}{4}\right)\left(\mathbf{cos}\tfrac{\theta}{4}\right)(k_{f\alpha})\right)\right]}_{11d} \\
&+ B_3\underbrace{\left[-\left(E_1 I_1 (ik_{f\alpha*}^3)\right) + \left((m_j\omega^2)\right) + \left((m_j\omega^2)\boldsymbol{L}\left(\mathbf{sin}\tfrac{\theta}{4}\right)\left(\mathbf{cos}\tfrac{\theta}{4}\right)(ik_{f\alpha*})\right)\right]}_{11e} \\
&+ C_2\underbrace{\left(E_2 I_2 (k_{f\beta}^3)\cos\theta\right)}_{11} + C_4\underbrace{\left[-\left(E_2 I_2 (ik_{f\beta*}^3)\cos\theta\right)\right]}_{11h} + C_L\underbrace{\left[-\left(E_2 A_2 (ik_{l\beta*})\sin\theta\right)\right]}_{11i}
\end{aligned}$$

Equation for MATLAB:-

0	=	**(A_2) [(-Q1) $k_{f\alpha}^3$ + ($m_j w^2$) +(-$m_j w^2$){V6}($k_{f\alpha}$)]** +Dr **(Fn)**
	+	**(A_4) [(Q1) $ik_{f\alpha*}^3$ + ($m_j w^2$) +(-$m_j w^2$){V6}($ik_{f\alpha*}$)]** +Dr **(Fni)**
	+	**(B_1) [(Q1) $k_{f\alpha}^3$ + ($m_j w^2$) +($m_j w^2$){V6}($k_{f\alpha}$)]** +Dr
	+	**(B_3) [(-Q1) $ik_{f\alpha*}^3$ + ($m_j w^2$) +(-$m_j w^2$){V6}($ik_{f\alpha*}$)]** +Dr
	+	**(C_2) [(Q2) $k_{f\beta}^3$ Cos θ]** +Dr*cos(T)
	+	**(C_4) [(-Q2) $ik_{f\beta*}^3$ Cos θ]** +Dr*cos(T)
	+	**(C_L) [(-S2) $ik_{l\beta*}$ Sin θ]** +DrL*sin(T)

Note :

Lni	-	$e^{-ik_{l\alpha*}(n-m)}$
Lpi	-	$e^{ikl\alpha*(m-n)}$
Fn	-	$e^{-k_{f\alpha}(n-m)}$
Fni	-	$e^{-ik_{f\alpha*}(n-m)}$
Fp	-	$e^{kf\ \ *(m-n)}$
Fpi	-	$e^{ikf\alpha*(m-n)}$

Where,

```
Mr=0.028;
Ir=Mr*(L^2)/12;
hsf=10000;
hf=0.05;

Dr  =(-(Mr*w^2)+(hsf*(1+(i*hf*w))))
DrL =(-(Mr*w^2)+(hsl*(1+(i*hl*w))))
Drm =(-(Ir*w^2)+(hsm*(1+(i*hm*w))))
```

Appendix: D-2 MATLAB coding for Force-Input Joint (with rubber) equation: -

```
% MainCodeJointBeam
%*******************************************************************
% LOUGHBOROUGH UNIVERSITY
% PHD THESIS
% --------
% AUTHOR: SAIDDI ALI FIRDAUS BIN MOHAMED ISHAK
% SUPERVISORs: DR. JANE L.HORNER & DR.STEPHEN J.WALSH
%*******************************************************************
% MAIN PROGRAM: Reflection & Transmission - Power Measurements
%*******************************************************************
%

%
% DESCRIPTION OF INPUT PARAMETER
%
% E       is the Young's Modulus
% I       is the second moment of area
% A       is the area
% R       is the density of beam
% Rj      is density of joint
% Jw      is width of joint
% L       is height of joint
% Q       is the E x I
% S       is the E x A


%
% DESCRIPTION OF OTHER VARIABLES
%
% Kfa     is the flexural wavenumber in alpha
% Kfb     is the flexural wavenumber in beta
% Kfg     is the flexural wavenumber in gamma
% Kla     is the longitudinal wavenumber in alpha
% Klb     is the longitudinal wavenumber in beta
% Klg     is the longitudinal wavenumber in gamma

%
%% Ff & Fl input - (bending<flexural> and compressive<longitudinal> waves)

clear all
clf
format long e

%Given
b=0.1;%0.05;%                                   %m
d=0.02;%0.006;%                                 %m
E1=1.75e9;%5.567e9;%60e9;%3.5e9;%   %N/m^2
I1=(b*(d^3))/12;                                %m^4
A1=b*d;                                         %m^2
E2=1.75e9;%5.567e9;%60e9;%3.5e9;%   %N/m^2
```

```
I2=(1.0*b*((1.0*d)^3))/12;                    %m^4
A2=1.0*b*1.0*d;                               %m^2
R=1170;%1500;%1190;%2500;                     %kg/m^3
Rj=1170;%1500;%1190;%2500;                    %kg/m^3
Jw=1*b;                                       %m
L=1*d;                                        %m
Eta=0.07;
Mr=0.028;
Ir=Mr*(L^2)/12;
hs=3000;
h=0.2;

E1e=E1*(1+(1i*Eta));
E2e=E2*(1+(1i*Eta));

Q1=E1*I1;
Q2=E2*I2;
S1=E1*A1;
S2=E2*A2;

Q3=0;%1.167e6*I1;

m1=R*A1;
m2=R*A2;

%% Main


thcnt=0;
for thet=0:1:180;
    T=thet*pi/180;

        thcnt=thcnt+1;


    fqcnt=0;
    for fq=3000:500:3000;%000:16.667:3000.06;              %1/s  250:5:2250;
        w=2*pi*fq;                          %1/s

        %Input
        Ff=1;%*0.021*sqrt(2);%0.021*sqrt(2);%(1*i);%0.018;0.0038*sqrt(2);%
%m
        Fl=0;%*0.0105*sqrt(2);%0.0021*sqrt(2);%0;%(1*i);%0.018;
%m
        m=0.0;
        n=0.9;

        Mj=Rj*Jw*(L^2)*T/2;         %kg
        %Ioj=((T-sin(T))*(L^4)/8);
        %Icj=L*(((4/3)*(sin(T/2)/(T)))-(1/2));
        %Ij=Mj*(Ioj-Icj);
        Ij=Mj*(L^2)/12;                     %kgm^2

        Kfa=(w^0.5)*(((R*A1)/(E1*I1))^0.25);     %1/m
```

```
Kfg=(w^0.5)*(((R*A1)/(E2*I1))^0.25);     %1/m
Kfb=(w^0.5)*(((R*A2)/(E2*I2))^0.25);     %1/m
Kla=w*sqrt(R/E1);                        %1/m
Klg=w*sqrt(R/E1);                        %1/m
Klb=w*sqrt(R/E2);                        %1/m

Kfax=(w^0.5)*(((R*A1)/(E1e*I1))^0.25);%Kfa*(1-((i*Eta)/4));     %1/m
Kfgx=(w^0.5)*(((R*A1)/(E1e*I1))^0.25);%Kfg*(1-((i*Eta)/4));     %1/m
Kfbx=(w^0.5)*(((R*A1)/(E2e*I2))^0.25);%Kfb*(1-((i*Eta)/4));     %1/m
Klax=w*sqrt(R/E1e);%Kla*(1-((i*Eta)/2));                        %1/m
Klgx=w*sqrt(R/E1e);%Klg*(1-((i*Eta)/2));                        %1/m
Klbx=w*sqrt(R/E2e);%Klb*(1-((i*Eta)/2));                        %1/m

%------%

fl=(n-m);   %finite length (fl)
fll=(m-n);

Lni=(exp(-i*Klax*fl));
Fn=(exp(-Kfa*fl));
Fni=(exp(-i*Kfax*fl));

Lpi=(exp(i*Klax*fll));
Fp=(exp(Kfa*fll));
Fpi=(exp(i*Kfax*fll));

Llni=(exp(i*1*Klax*fll));
Ffn=(exp(1*Kfa*fll));
Ffni=(exp(i*1*Kfax*fll));

%------%

%
V1=L/2*(1-cos(T));

g1=(sin(T)+(Kfb*V1));
h1=(sin(T)+(i*Kfbx*V1));
i1=cos(T);

%
V3=L/2*(sin(T));

g3=(cos(T))+(Kfb*V3);
h3=(cos(T))+(i*Kfbx*V3);
i3=sin(T);

%
a5=Kfa;
b5=i*Kfax;
d5=Kfa;
e5=i*Kfax;
g5=Kfb;
h5=i*Kfbx;
```

```
%
a6=Kfa;
b6=i*Kfax;
d6=Kfa;
e6=i*Kfax;
j6=Kfg;
k6=i*Kfgx;

%--------%
V5=L/2*(1-cos(T/2));
V6=L/2*(sin(T/2));
%V5=L*((sin(T/4))^2);       %-same as above
%V6=L*(sin(T/4))*(cos(T/4));%-same as above
%--------%

Dr=0;%-(-(Mr*w^2)+(hs*(1+(i*h*w))));
Drm=0;%-(-(Ir*w^2)+(hs*(1+(i*h*w))));


        a7=((-Ij)  *Kfa *(w^2))+((-Q1)*(Kfa^2)) +(Q1  *(Kfa^3) *V6)
+(Drm*  Kfa -Dr*V6);
        b7=((-Ij)*i*Kfax*(w^2))+(  Q1 *(Kfax^2))+(Q1*i*(Kfax^3)*(-V6))
+(Drm*i*Kfax-Dr*V6);%
        c7=(S1*i*Klax*V5)                                               -
(Dr*V5)         ;
        d7=(  Ij   *Kfa *(w^2))+((-Q1)*(Kfa^2)) +(Q1  *(Kfa^3) *(-V6))  -
(Drm*  Kfa -Dr*V6);
        e7=(  Ij *i*Kfax*(w^2))+(  Q1 *(Kfax^2))+(Q1*i*(Kfax^3)*V6)     -
(Drm*i*Kfax-Dr*V6);
        f7=(S1*i*Klax*(-V5))                                            -
(Dr*V5)         ;
        g7=(  Q2 *(Kfb^2)) +(Q2  *(Kfb^3) *V6)                          -
(Drm*  Kfb -Dr*V6);
        h7=((-Q2)*(Kfbx^2))+(Q2*i*(Kfbx^3)*(-V6))                       -
(Drm*i*Kfbx-Dr*V6);
        i7=(S2*i*Klbx*(-V5))
+(Dr*V5)         ;

%
a8=(Kfa^2);%*Q1;
b8=(Kfax^2);%*Q1;
d8=(Kfa^2);%*Q1;
e8=(Kfax^2);%*Q1;
j8=(Kfg^2);%*Q1;
k8=(Kfgx^2);%*Q1;

%
a9=( Mj*(w^2)  *Kfa *V5);
b9=( Mj*(w^2)*i*Kfax*V5);
c9=( Mj*(w^2))+(  S1 *i*Klax)                                           -
Dr;
d9=(-Mj*(w^2)  *Kfa *V5);
e9=(-Mj*(w^2)*i*Kfax*V5);
f9=( Mj*(w^2))+((-S1)*i*Klax)                                           -
Dr;
```

```
        g9=((-Q2)*  (Kfb^3) *sin(T))
+Dr*sin(T);
        h9=(  Q2 *i*(Kfbx^3)*sin(T))
+Dr*sin(T);
        i9=((-S2)*i* Klbx   *cos(T))
+Dr*cos(T);

        %
        c10=(i*Klax);%*(S1);%+ve
        f10=(i*Klax);%*(S1);%-ve
        l10=(i*Klgx);%*(S1);%+ve

        %
        a11=(Mj*(w^2))+((-Mj)*(w^2)  *Kfa *V6)+((-Q1)  *(Kfa^3))          -
Dr;
        b11=(Mj*(w^2))+((-Mj)*(w^2)*i*Kfax*V6)+(  Q1 *i*(Kfax^3))          -
Dr;
        d11=(Mj*(w^2))+(  Mj  *(w^2)  *Kfa *V6)+(  Q1   *(Kfa^3))          -
Dr;
        e11=(Mj*(w^2))+(  Mj  *(w^2)*i*Kfax*V6)+((-Q1)*i*(Kfax^3))          -
Dr;
        g11=(  Q2 *  (Kfb^3) *cos(T))
+Dr*cos(T);
        h11=((-Q2)*i*(Kfbx^3)*cos(T))
+Dr*cos(T);
        i11=((-S2)*i* Klbx   *sin(T))
+Dr*sin(T);

        %
        a12=(Kfa^3);%*Q1;
        b12=i*(Kfax^3);%*Q1;
        d12=(Kfa^3);%*Q1;
        e12=i*(Kfax^3);%*Q1;
        j12=(Kfg^3);%*Q1;
        k12=i*(Kfgx^3);%*Q1;

        %------------------%

        %
        x(1,1)=0;
        x(1,2)=0;
        x(1,3)=-1*Lni;
        x(1,4)=0;
        x(1,5)=0;
        x(1,6)=-1;%*Lpi;
        x(1,7)=-g1;
        x(1,8)=-h1;
        x(1,9)=i1;
        x(1,10)=0;
        x(1,11)=0;
        x(1,12)=0;

        x(2,1)=0;
        x(2,2)=0;
        x(2,3)=1;
        x(2,4)=0;
```

```
x(2,5)=0;
x(2,6)=1*(Lpi-Llni);
x(2,7)=0;
x(2,8)=0;
x(2,9)=0;
x(2,10)=0;
x(2,11)=0;
x(2,12)=-1;%*Lpi;

x(3,1)=-1*Fn;
x(3,2)=-1*Fni;
x(3,3)=0;
x(3,4)=-1;%*Fp;
x(3,5)=-1;%*Fpi;
x(3,6)=0;
x(3,7)=g3;
x(3,8)=h3;
x(3,9)=i3;
x(3,10)=0;
x(3,11)=0;
x(3,12)=0;

x(4,1)=1;
x(4,2)=1;
x(4,3)=0;
x(4,4)=1*(Fp-Ffn);
x(4,5)=1*(Fpi-Ffni);
x(4,6)=0;
x(4,7)=0;
x(4,8)=0;
x(4,9)=0;
x(4,10)=-1;%*Fp;
x(4,11)=-1;%*Fpi;
x(4,12)=0;

x(5,1)=a5*Fn;
x(5,2)=b5*Fni;
x(5,3)=0;
x(5,4)=-d5;%*Fp;
x(5,5)=-e5;%*Fpi;
x(5,6)=0;
x(5,7)=-g5;
x(5,8)=-h5;
x(5,9)=0;
x(5,10)=0;
x(5,11)=0;
x(5,12)=0;

x(6,1)=a6;
x(6,2)=b6;
x(6,3)=0;
x(6,4)=-d6*(Fp-Ffn);
x(6,5)=-e6*(Fpi-Ffni);
x(6,6)=0;
x(6,7)=0;
x(6,8)=0;
```

```
x(6,9)=0;
x(6,10)=j6;%*Fp;
x(6,11)=k6;%*Fpi;
x(6,12)=0;

x(7,1)=a7*Fn;
x(7,2)=b7*Fni;
x(7,3)=c7*Lni;
x(7,4)=d7;%*Fp;
x(7,5)=e7;%*Fpi;
x(7,6)=f7;%*Lpi;
x(7,7)=g7;
x(7,8)=h7;
x(7,9)=i7;
x(7,10)=0;
x(7,11)=0;
x(7,12)=0;

x(8,1)=-a8;
x(8,2)=b8;
x(8,3)=0;
x(8,4)=d8*(-Fp+Ffn);
x(8,5)=e8*(Fpi-Ffni);
x(8,6)=0;
x(8,7)=0;
x(8,8)=0;
x(8,9)=0;
x(8,10)=j8;%*Fp;
x(8,11)=-k8;%*Fpi;
x(8,12)=0;

x(9,1)=a9*Fn;
x(9,2)=b9*Fni;
x(9,3)=c9*Lni;
x(9,4)=d9;%*Fp;
x(9,5)=e9;%*Fpi;
x(9,6)=f9;%*Lpi;
x(9,7)=g9;
x(9,8)=h9;
x(9,9)=i9;
x(9,10)=0;
x(9,11)=0;
x(9,12)=0;

x(10,1)=0;
x(10,2)=0;
x(10,3)=-c10;
x(10,4)=0;
x(10,5)=0;
x(10,6)=f10*(Lpi-Llni);
x(10,7)=0;
x(10,8)=0;
x(10,9)=0;
x(10,10)=0;
x(10,11)=0;
x(10,12)=-l10;%*Lpi;
```

```
        x(11,1)=a11*Fn;
        x(11,2)=b11*Fni;
        x(11,3)=0;
        x(11,4)=d11;%*Fp;
        x(11,5)=e11;%*Fpi;
        x(11,6)=0;
        x(11,7)=g11;
        x(11,8)=h11;
        x(11,9)=i11;
        x(11,10)=0;
        x(11,11)=0;
        x(11,12)=0;

        x(12,1)=a12;
        x(12,2)=-b12;
        x(12,3)=0;
        x(12,4)=-d12*(Fp-Ffn);
        x(12,5)=e12*(Fpi-Ffni);
        x(12,6)=0;
        x(12,7)=0;
        x(12,8)=0;
        x(12,9)=0;
        x(12,10)=j12;%*Fp;
        x(12,11)=-k12;%*Fpi;
        x(12,12)=0;

        zL=[0;0;0;0;0;0;0;0;0;(Fl/S1);0;0];%(Fl/(4*E1*A1*Kla))
        zF=[0;0;0;0;0;0;0;0;0;0;0;(Ff/Q1)];%-(Ff/(4*E1*I1*Kfa^3))

        yL=x\zL;
        yF=x\zF;

        %Note that for the matrix of X;
        %y(1)       %A2 Nm/s  xxxx
        %y(2)       %A4 Nm/s
        %y(3)       %AL Nm/s
        %y(4)       %B1 Nm/s  xxxx
        %y(5)       %B3 Nm/s
        %y(6)       %BL Nm/s
        %y(7)       %C2 Nm/s  xxxx
        %y(8)       %C4 Nm/s
        %y(9)       %CL Nm/s
        %y(10)      %D1 Nm/s  xxxx
        %y(11)      %D3 Nm/s
        %y(12)      %DL Nm/s

        fqcnt=fqcnt+1;


Pf1=1*E1*I1*w*(Kfax^3)*((abs(yF(2)))^2);%(((real(yF(2)))^2)+((imag(yF(2)))^2)
);%        %Power in a due to trans flexural wave          yF(2) -> A4

Pf2=1*E1*I1*w*(Kfax^3)*((abs(yL(2)))^2);%(((real(yL(2)))^2)+((imag(yL(2)))^2)
);%        %Power in a due to trans flexural wave          yL(2) -> A4
```

```
Pf3=1*E1*I1*w*(Kfax^3)*((abs(yF(5)))^2);%(((real(yF(5)))^2)+((imag(yF(5)))^2)
);%        %Power in a due to reflected flexural wave       yF(5) -> B3

Pf4=1*E1*I1*w*(Kfax^3)*((abs(yL(5)))^2);%(((real(yL(5)))^2)+((imag(yL(5)))^2)
);%        %Power in a due to reflected flexural wave       yL(5) -> B3

Pf5=1*E2*I2*w*(Kfbx^3)*((abs(yF(8)))^2);%(((real(yF(8)))^2)+((imag(yF(8)))^2)
);%        %Power in b due to transmitted flexural wave     yF(8) -> C4

Pf6=1*E2*I2*w*(Kfbx^3)*((abs(yL(8)))^2);%(((real(yL(8)))^2)+((imag(yL(8)))^2)
);%        %Power in b due to transmitted flexural wave     yL(8) -> C4

Pf7=1*E1*I1*w*(Kfgx^3)*((abs(yF(11)))^2);%(((real(yF(11)))^2)+((imag(yF(11)))
^2));%       %Power in g due to trans flexural wave           yF(11)-> D3

Pf8=1*E1*I1*w*(Kfgx^3)*((abs(yL(11)))^2);%(((real(yL(11)))^2)+((imag(yL(11)))
^2));%       %Power in g due to trans flexural wave           yL(11)-> D3


Pl1=0.5*E1*A1*w*Klax*((abs(yL(3)))^2);%(((real(yL(3)))^2)+((imag(yL(3)))^2));
%         %Power in a due to trans longitudinal wave       yL(3) -> AL

Pl2=0.5*E1*A1*w*Klax*((abs(yF(3)))^2);%(((real(yF(3)))^2)+((imag(yF(3)))^2));
%         %Power in a due to trans longitudinal wave       yF(3) -> AL

Pl3=0.5*E1*A1*w*Klax*((abs(yL(6)))^2);%(((real(yL(6)))^2)+((imag(yL(6)))^2));
%         %Power in a due to reflected longitudinal wave   yL(6) -> BL
        Pl4=0.5*E1*A1*w*Klax*((abs(yF(6)))^2);%
(((real(yF(6)))^2)+((imag(yF(6)))^2));%       %Power in a due to reflected
longitudinal wave   yF(6) -> BL

Pl5=0.5*E2*A2*w*Klbx*((abs(yL(9)))^2);%(((real(yL(9)))^2)+((imag(yL(9)))^2));
%         %Power in b due to transmitted longitudinal wave yL(9) -> CL

Pl6=0.5*E2*A2*w*Klbx*((abs(yF(9)))^2);%(((real(yF(9)))^2)+((imag(yF(9)))^2));
%       %Power in b due to transmitted longitudinal wave yF(9) -> CL

Pl7=0.5*E1*A1*w*Klgx*((abs(yL(12)))^2);%(((real(yL(12)))^2)+((imag(yL(12)))^2
));%       %Power in g due to trans longitudinal wave       yL(12)-> DL

Pl8=0.5*E1*A1*w*Klgx*((abs(yF(12)))^2);%(((real(yF(12)))^2)+((imag(yF(12)))^2
));%       %Power in g due to trans longitudinal wave       yF(12)-> DL

        PFlex=(0.125*(((Ff)^2)*w))/(((E1*I1)*((Kfax)^3)));
        PLong=(0.25*(((Fl)^2)*w))/((E1*A1)*(Klax));
        PFlexG=(0.125*(((Ff)^2)*w))/(((E1*I1)*((Kfg)^3)));
        PLongG=(0.25*(((Fl)^2)*w))/((E1*A1)*(Klg));
        %lmbd=0.5;
        %Kfax2=2*pi/lmbd;
        %PFlex2=(0.125*((Ff)^2))/(m1*w/Kfax2);

        tht(thcnt)=T;
        wqt(fqcnt)=w;
        fqt(fqcnt)=fq;
        ndwave(fqcnt)=(Kfa*0.9)/(2*pi);%((2*pi)/Kfa)*0.5;
```

```
        nP1(thcnt,fqcnt)=(Pf1-Pf3)/(PFlex+0)*100;       % %power in a -
flexural incidence wave, flexural reflected wave
        nP2(thcnt,fqcnt)=(Pf2-Pf4)/(PLong+0)*100;       % %power in a -
longitudinal incidence wave, flexural reflected wave
        nP3(thcnt,fqcnt)=(Pl2-Pl4)/(PFlex+0)*100;       % %power in a -
flexural incidence wave, longitudinal reflected wave
        nP4(thcnt,fqcnt)=(Pl1-Pl3)/(PLong+0)*100;       % %power in a -
longitudinal incidence wave, longitudinal reflected wave
        nP5(thcnt,fqcnt)=(Pf3)/(PFlex+0)*100;       % %power in a - flexural
incidence wave, flexural reflected wave
        nP6(thcnt,fqcnt)=(Pf4)/(PLong+0)*100;       % %power in a -
longitudinal incidence wave, flexural reflected wave
        nP7(thcnt,fqcnt)=(Pl4)/(PFlex+0)*100;       % %power in a - flexural
incidence wave, longitudinal reflected wave
        nP8(thcnt,fqcnt)=(Pl3)/(PLong+0)*100;       % %power in a -
longitudinal incidence wave, longitudinal reflected wave

        nP9(thcnt,fqcnt)=(Pf5)/(PFlex+0)*100;       % %power in b - flexural
incidence wave, flexural transmitted wave
        nP10(thcnt,fqcnt)=(Pf6)/(PLong+0)*100;      % %power in b -
longitudinal incidence wave, flexural transmitted wave
        nP11(thcnt,fqcnt)=(Pl6)/(PFlex+0)*100;      % %power in b - flexural
incidence wave, longitudinal transmitted wave
        nP12(thcnt,fqcnt)=(Pl5)/(PLong+0)*100;      % %power in b -
longitudinal incidence wave, longitudinal transmitted wave

        nP13(thcnt,fqcnt)=(Pf7+Pf3)/(PFlex+0)*100;      % %power in g -
flexural incidence wave, flexural transmitted wave
        nP14(thcnt,fqcnt)=(Pf8+Pf4)/(PLong+0)*100;      % %power in g -
longitudinal incidence wave, flexural transmitted wave
        nP15(thcnt,fqcnt)=(Pl8+Pl4)/(PFlex+0)*100;      % %power in g -
flexural incidence wave, longitudinal transmitted wave
        nP16(thcnt,fqcnt)=(Pl7+Pl3)/(PLong+0)*100;      % %power in g -
longitudinal incidence wave, longitudinal transmitted wave

        %nP13(thcnt,fqcnt)=nP25(thcnt,fqcnt)+(Pf3);%/(PFlexG+0)*100;      %
%power in g - flexural incidence wave, flexural transmitted wave
        %nP14(thcnt,fqcnt)=nP26(thcnt,fqcnt)+(Pf4);%/(PLongG+0)*100;      %
%power in g - longitudinal incidence wave, flexural transmitted wave
        %nP15(thcnt,fqcnt)=nP27(thcnt,fqcnt)+(Pl4);%/(PFlexG+0)*100;      %
%power in g - flexural incidence wave, longitudinal transmitted wave
        %nP16(thcnt,fqcnt)=nP28(thcnt,fqcnt)+(Pl3);%/(PLongG+0)*100;      %
%power in g - longitudinal incidence wave, longitudinal transmitted wave

        %nP17(thcnt,fqcnt)=(Pf1-Pf3);%/((PFlex+0))*100;       % %power in a -
flexural incidence wave, flexural reflected wave
        %nP18(thcnt,fqcnt)=(Pf4-Pf2);%/((PLong+0))*100;       % %power in a -
longitudinal incidence wave, flexural reflected wave
        %nP19(thcnt,fqcnt)=(Pl4-Pl2);%/((PFlex+0))*100;       % %power in a -
flexural incidence wave, longitudinal reflected wave
        %nP20(thcnt,fqcnt)=(Pl1-Pl3);%/((PLong+0))*100;       % %power in a -
longitudinal incidence wave, longitudinal reflected wave

        fB=nP5+nP7;%+nP7;%nP9+nP11;
        fA=nP1+nP3;%+nP3;%nP1+nP3+nP5+nP7;
```

```
        fC=nP9+nP11;%+nP11;%nP13+nP15;
        fD=nP13+nP15;%+nP15;%nP17+nP18+nP19+nP20;

        fAl=fA;
        fBe=fC;
        fGa=fD;
        ftot1=fAl+fGa;
        ftot2=fGa+fBe;
        %ftot3=fAl+fBe;
        fAla=fA;
        fAlb=fB;

        lB=nP8+nP6;
        lA=nP4+nP2;%=0

        lC=nP12+nP10;
        lD=nP16+nP14;

        lAl=lA;
        lBe=lC;
        lGa=lD;
        ltot1=lAl+lGa;
        ltot2=lGa+lBe;
        %ltot3=lAl+lBe;

        tot1=ftot1+ltot1;
        tot2=ftot2+ltot2;
        %tot3=ftot3+ltot3;
        AlphaT=fAl+lAl;
        BetaT=fBe+lBe;
        GammaT=fGa+lGa;


        %nF=nP21+nP22+nP23+nP24;
        Tf=fGa+fAl;%fAl+
        Tl=lGa+lAl;%lAl+
        TOT2=GammaT+BetaT;%+AlphaT;%GammaT+fB+lB;BetaT+fA+lA;
        TOT1=GammaT+AlphaT;

        xfcnt=0;
        for xf=0.00;
            Wf(thcnt,fqcnt)=(yF(1)*(exp(-Kfa*abs(xf-m))))+(yF(2)*(exp(-
1i*Kfax*abs(xf-m))))+(yF(4)*(exp(Kfa*(1*abs(xf-
m)))))+(yF(5)*(exp(1i*Kfax*(1*abs(xf-m)))));
            Uf(thcnt,fqcnt)=(yL(3)*(exp(-1i*Klax*abs(xf-
m))))+(yL(6)*(exp(1i*Klax*(1*abs(xf-m)))));

            xacnt=0;
            for xa=0.45;
                Wa(thcnt,fqcnt)=(yF(1)*(exp(-Kfa*abs(xa-m))))+(yF(2)*(exp(-
1i*Kfax*abs(xa-m))))+(yF(4)*(exp(Kfa*(1*abs(xa-
m)))))+(yF(5)*(exp(1i*Kfax*(1*abs(xa-m)))));
                Ua(thcnt,fqcnt)=(yL(3)*(exp(-1i*Klax*abs(xa-
m))))+(yL(6)*(exp(1i*Klax*(1*abs(xa-m)))));
```

```
            xbcnt=0;
            for xb=1.50;%0.25;

                Wb(thcnt,fqcnt)=(yF(7)*(exp(-Kfb*(xb-n))))+(yF(8)*(exp(-
1i*Kfbx*(xb-n))));
                Ub(thcnt,fqcnt)=(yL(9)*(exp(-1i*Klbx*(xb-n))));

                xgcnt=0;
                for xg=-0.30;%-0.75;

                    Wg(thcnt,fqcnt)=(yF(10)*(exp(Kfg*(xg-
m))))+(yF(11)*(exp(1i*Kfgx*(xg-m))));
                    Ug(thcnt,fqcnt)=(yL(12)*(exp(1i*Klgx*(xg-m))));

                    Va(thcnt,fqcnt)=1i*w*Wa(thcnt,fqcnt);
                    Vb(thcnt,fqcnt)=1i*w*Wb(thcnt,fqcnt);
                    Vg(thcnt,fqcnt)=1i*w*Wg(thcnt,fqcnt);
                    Aa(thcnt,fqcnt)=-1*w^2*Wa(thcnt,fqcnt);
                    Ab(thcnt,fqcnt)=-1*w^2*Wb(thcnt,fqcnt);
                    Ag(thcnt,fqcnt)=-1*w^2*Wg(thcnt,fqcnt);

                    xacnt=xacnt+1;
                    xWat(xacnt)=Wa(thcnt,fqcnt);
                    xUat(xacnt)=Ua(thcnt,fqcnt);
                    xWbt(xacnt)=Wb(thcnt,fqcnt);
                    xUbt(xacnt)=Ub(thcnt,fqcnt);
                    xWgt(xacnt)=Wg(thcnt,fqcnt);
                    xUgt(xacnt)=Ug(thcnt,fqcnt);



InPwrF(thcnt,fqcnt)=1*((((Ff)^2)*w)/(8*E1*I1*Kfax^3))*(1-Eta/4);
                    InPwr(thcnt,fqcnt)=-
0.5*real(Ff*(1i*w*(Wf(thcnt,fqcnt))));

ApPwr(thcnt,fqcnt)=1*(((real(1i*w*(Wa(thcnt,fqcnt))))^2*(E1*I1)*((Kfa)^3))/(w
));

BtPwr(thcnt,fqcnt)=1*(((real(1i*w*(Wb(thcnt,fqcnt))))^2*(E2*I2)*((Kfb)^3))/(w
));

GmPwr(thcnt,fqcnt)=1*(((real(1i*w*(Wg(thcnt,fqcnt))))^2*(E1*I1)*((Kfg)^3))/(w
));
                    TotPwr=GmPwr+BtPwr;

                    Imp(fqcnt)=1/(1i*w*Wa(fqcnt));
                    Mob(fqcnt)=1/(Imp(fqcnt));

                    ReMob(fqcnt)=w/(4*E1*I1*Kfa^3);
                    ImMob(fqcnt)=(-1*w)/(4*E1*I1*Kfa^3);

                    Acc(fqcnt)=Wa(fqcnt)*(-(w^2));
```

```
                        Ar=1*fAl./(InPwr.*1);
                        Gr=1*fGa./(InPwr.*1);
                        Br=1*fBe./(InPwr.*1);
                        %Ir=InPwr/fAl;
                        %Gr=fGa/fAl;
                        %Br=fBe/fAl;
                        tr=(0+Ar+Gr)*1;

                    end

                end

            end

        end

    end

end


fqt=3000:500:3000;%000:16.667:3000.06;
tht=0:1:180;

figure(1)
plot(tht,nP1,'r')
hold on
plot(tht,nP2,'g')
hold on
plot(tht,nP3,'m')
hold on
plot(tht,nP4,'b')
hold on
plot(tht,nP5,'r')
hold on
plot(tht,nP6,'g')
hold on
plot(tht,nP7,'m')
hold on
plot(tht,nP8,'b')
hold on
grid on
%axis([0 180 0 120])
title 'Percentage Power Transmitted&Reflected in alpha'
xlabel 'Angle'%'Frequency'
ylabel 'Percentage Power'
%legend('FF','LF','FL','LL','FF','LF','FL','LL','Location','best');

figure(2)
plot(tht,nP9,'r')
hold on
plot(tht,nP10,'g')
hold on
plot(tht,nP11,'m')
hold on
```

```
plot(tht,nP12,'b')
hold on
grid on
%axis([0 180 0 120])
title 'Percentage Power Transmitted in beta'
xlabel 'Angle'%'Frequency'
ylabel 'Percentage Power'
%legend('FF','LF','FL','LL','Location','best');

figure(3)
plot(tht,nP13,'r')
hold on
plot(tht,nP14,'g')
hold on
plot(tht,nP15,'m')
hold on
plot(tht,nP16,'b')
hold on
grid on
%axis([0 180 0 120])
title 'Percentage Power Transmitted in gamma'
xlabel 'Angle'%'Frequency'
ylabel 'Percentage Power'
%legend('FF','LF','FL','LL','Location','best');

figure(4)
plot(tht,nP1,'r')
hold on
plot(tht,nP2,'g')
hold on
plot(tht,nP3,'m')
hold on
plot(tht,nP4,'b')
hold on
grid on
%axis([0 180 0 120])
title 'Percentage Power Transmitted in Alpha'
xlabel 'Angle'%'Frequency'
ylabel 'Percentage Power'
%legend('FF','LF','FL','LL','Location','best');

figure(5)
plot(tht,nP9,'r')
hold on
plot(tht,nP11,'m')
hold on
plot(tht,nP13,'r')
hold on
plot(tht,nP15,'m')
hold on
grid on
%axis([0 180 0 120])
title 'Percentage Power from Flexural at beta and gamma'
xlabel 'Angle'%'Frequency'
ylabel 'Percentage Power'
%legend('FFb','FLb','FFg','FLg','Location','best');
```

```
figure(6)
plot(tht,nP10,'g')
hold on
plot(tht,nP12,'b')
hold on
plot(tht,nP14,'g')
hold on
plot(tht,nP16,'b')
hold on
grid on
%axis([0 180 0 120])
title 'Percentage Power from Longitudinal at beta and gamma'
xlabel 'Angle'%'Frequency'
ylabel 'Percentage Power'
%legend('LFb','LLb','LFg','LLg','Location','best');

figure(7)
plot(tht,AlphaT,'r')
hold on
plot(tht,BetaT,'b') %
hold on
plot(tht,GammaT,'g')
hold on
%plot(tht,nF,'k.')
%hold on
plot(tht,TOT2,'k')
hold on
grid on
title 'Percentage Power Total'
xlabel 'Angle'%'Frequency'
ylabel 'Percentage Power'
%legend('Al','Be','Ga','Total2','Location','best');%'nF',

figure(8)
plot(tht,fAl,'r.')
hold on
plot(tht,fBe,'b.') %
hold on
plot(tht,fGa,'g.')
hold on
plot(tht,Tf,'k.')
hold on
plot(tht,lAl,'r')
hold on
plot(tht,lBe,'b') %
hold on
plot(tht,lGa,'g')
hold on
plot(tht,Tl,'k')
hold on
grid on
title 'Percentage Power Total'
xlabel 'Angle'%'Frequency'
ylabel 'Percentage Power'
%legend('Al','Be','Ga','nF','Total','Location','best');
```

```
figure(9)
surf (fqt,tht,nP1);
xlabel('frequency /Hz')
ylabel('angle \theta')
zlabel('Power in Alpha')
title('(Figure-9)Alpha Power vs angle \theta and frequency/Hz')
grid

figure (10)
surf (fqt,tht,nP9);
xlabel('frequency /Hz')
ylabel('angle \theta')
zlabel('Power in Beta')
title('(Figure-10)Beta Power vs angle \theta and frequency/Hz')
grid

figure (11)
surf (fqt,tht,nP13);
xlabel('frequency /Hz')
ylabel('angle \theta')
zlabel('Power in Gamma')
title('(Figure-11)Gamma Power vs angle \theta and frequency/Hz')
grid
```

Appendix: E Other MATLAB coding: -

Plot Frequency Domain

```
figure(1)
plot(tht,nP1,'r')
hold on
plot(tht,nP2,'g')
hold on
plot(tht,nP3,'m')
hold on
plot(tht,nP4,'b')
hold on
plot(tht,nP5,'r')
hold on
plot(tht,nP6,'g')
hold on
plot(tht,nP7,'m')
hold on
plot(tht,nP8,'b')
hold on
grid on
%axis([0 180 0 120])
title 'Percentage Power Transmitted&Reflected in alpha'
xlabel 'Angle'%'Frequency'
ylabel 'Percentage Power'
%legend('FF','LF','FL','LL','FF','LF','FL','LL','Location','best');

figure(2)
plot(tht,nP9,'r')
hold on
plot(tht,nP10,'g')
hold on
plot(tht,nP11,'m')
hold on
plot(tht,nP12,'b')
hold on
grid on
%axis([0 180 0 120])
title 'Percentage Power Transmitted in beta'
xlabel 'Angle'%'Frequency'
ylabel 'Percentage Power'
%legend('FF','LF','FL','LL','Location','best');

figure(3)
plot(tht,nP13,'r')
hold on
plot(tht,nP14,'g')
hold on
plot(tht,nP15,'m')
hold on
plot(tht,nP16,'b')
```

```
hold on
plot(tht,GammaTt,'k')
hold on
grid on
%axis([0 180 0 120])
title 'Percentage Power Transmitted in gamma'
xlabel 'Angle'%'Frequency'
ylabel 'Percentage Power'
%legend('FF','LF','FL','LL','Location','best');

figure(4)
plot(tht,nP1,'r')
hold on
plot(tht,nP2,'g')
hold on
plot(tht,nP3,'m')
hold on
plot(tht,nP4,'b')
hold on
grid on
%axis([0 180 0 120])
title 'Percentage Power Transmitted in Alpha'
xlabel 'Angle'%'Frequency'
ylabel 'Percentage Power'
%legend('FF','LF','FL','LL','Location','best');

figure(5)
plot(tht,nP9,'r')
hold on
plot(tht,nP11,'m')
hold on
plot(tht,nP13,'r')
hold on
plot(tht,nP15,'m')
hold on
grid on
%axis([0 180 0 120])
title 'Percentage Power from Flexural at beta and gamma'
xlabel 'Angle'%'Frequency'
ylabel 'Percentage Power'
%legend('FFb','FLb','FFg','FLg','Location','best');

figure(6)
plot(tht,nP10,'g')
hold on
plot(tht,nP12,'b')
hold on
plot(tht,nP14,'g')
hold on
plot(tht,nP16,'b')
hold on
grid on
%axis([0 180 0 120])
title 'Percentage Power from Longitudinal at beta and gamma'
xlabel 'Angle'%'Frequency'
ylabel 'Percentage Power'
```

```
%legend('LFb','LLb','LFg','LLg','Location','best');

figure(7)
plot(tht,AlphaT,'r')
hold on
plot(tht,BetaT,'b') %
hold on
plot(tht,GammaT,'g')
hold on
%plot(tht,nF,'k.')
%hold on
plot(tht,TOT2,'k')
hold on
grid on
title 'Percentage Power Total'
xlabel 'Angle'%'Frequency'
ylabel 'Percentage Power'
%legend('Al','Be','Ga','Total2','Location','best');%'nF',

figure(8)
plot(tht,fAl,'r.')
hold on
plot(tht,fBe,'b.') %
hold on
plot(tht,fGa,'g.')
hold on
plot(tht,Tf,'k.')
hold on
plot(tht,lAl,'r')
hold on
plot(tht,lBe,'b') %
hold on
plot(tht,lGa,'g')
hold on
plot(tht,Tl,'k')
hold on
grid on
title 'Percentage Power Total'
xlabel 'Angle'%'Frequency'
ylabel 'Percentage Power'
%legend('Al','Be','Ga','nF','Total','Location','best');

figure(9)
surf (fqt,tht,nP1);
xlabel('frequency /Hz')
ylabel('angle \theta')
zlabel('Power in Alpha')
title('(Figure-9)Alpha Power vs angle \theta and frequency/Hz')
grid

figure (10)
surf (fqt,tht,nP9);
xlabel('frequency /Hz')
ylabel('angle \theta')
zlabel('Power in Beta')
title('(Figure-10)Beta Power vs angle \theta and frequency/Hz')
```

```
grid

figure (11)
surf (fqt,tht,nP13);
xlabel('frequency /Hz')
ylabel('angle \theta')
zlabel('Power in Gamma')
title('(Figure-11)Gamma Power vs angle \theta and frequency/Hz')
grid

%%%%%%%%%%%%%%%%%%%%%%%%%%%%%%%%%%%%%%%%%%%%

figure(1)
plot(fqt,nP1,'r')
hold on
plot(fqt,nP2,'g')
hold on
plot(fqt,nP3,'m')
hold on
plot(fqt,nP4,'b')
hold on
plot(fqt,nP5,'r')
hold on
plot(fqt,nP6,'g')
hold on
plot(fqt,nP7,'m')
hold on
plot(fqt,nP8,'b')
hold on
grid on
title 'Percentage Power Transmitted&Reflected in alpha'
xlabel 'Frequency'
ylabel 'Percentage Power'
%legend('FF','LF','FL','LL','FF','LF','FL','LL','Location','best');

figure(2)
plot(fqt,nP9,'r')
hold on
plot(fqt,nP10,'g')
hold on
plot(fqt,nP11,'m')
hold on
plot(fqt,nP12,'b')
hold on
grid on
title 'Percentage Power Transmitted in beta'
xlabel 'Frequency'
ylabel 'Percentage Power'
%legend('FF','LF','FL','LL','Location','best');

figure(3)
plot(fqt,nP13,'r')
hold on
plot(fqt,nP14,'g')
hold on
plot(fqt,nP15,'m')
```

```
hold on
plot(fqt,nP16,'b')
hold on
grid on
title 'Percentage Power Transmitted in gamma'
xlabel 'Frequency'
ylabel 'Percentage Power'
%legend('FF','LF','FL','LL','Location','best');

figure(5)
plot(fqt,nP9,'r')
hold on
plot(fqt,nP11,'m')
hold on
plot(fqt,nP13,'r')
hold on
plot(fqt,nP15,'m')
hold on
grid on
title 'Percentage Power from Flexural at beta and gamma'
xlabel 'Frequency'
ylabel 'Percentage Power'
%legend('FFb','FLb','FFg','FLg','Location','best');

figure(6)
plot(fqt,nP10,'g')
hold on
plot(fqt,nP12,'b')
hold on
plot(fqt,nP14,'g')
hold on
plot(fqt,nP16,'b')
hold on
grid on
title 'Percentage Power from Longitudinal at beta and gamma'
xlabel 'Frequency'
ylabel 'Percentage Power'
%legend('LFb','LLb','LFg','LLg','Location','best');

figure(7)
plot(fqt,fAl,'r')
hold on
%plot(fqt,fAla,'r')
%hold on
%plot(fqt,fAlb,'rx')
%hold on
plot(fqt,fBe,'b')
hold on
plot(fqt,fGa,'g')
hold on
plot(fqt,ftot2,'m')
hold on
plot(fqt,InPwr,'k')
hold on
%plot(fqt,InPwrf,'o')
%hold on
```

```
plot(fqt,InPwrF,'x')
hold on
grid on
title 'Total Flexural Power at Alpha, Beta, Gamma'
xlabel 'Frequency'
ylabel 'Power Reflected & Transmitted'
%legend('fAl','fBe','fGa','Total','Pwr FV','PwrForce','Location','best');
%legend('fAla','fAlb','fBe','fGa','Total','Pwr
FV','PwrForce','Location','best');

figure(8)
plot(fqt,AlphaT,'r')
hold on
plot(fqt,BetaT,'b') %plot(fqt,nP17,'r')
hold on
grid on
title 'Percentage Power Total'
xlabel 'Frequency'
ylabel 'Percentage Power'
%legend('Al','Be','Location','best');

figure(9)
plot(fqt,Wa,'r')
hold on
plot(fqt,Wb,'b')
hold on
plot(fqt,Wg,'g')
hold on
grid on
title 'Disp W at alpha, beta, gamma'
xlabel 'Frequency'
ylabel 'Displacement (W)'
%legend('Wa','Wb','Wg','Location','best');

figure(10)
plot(fqt,Ua,'r')
hold on
plot(fqt,Ub,'b')
hold on
plot(fqt,Ug,'g')
hold on
grid on
title 'Disp U at alpha, beta, gamma'
xlabel 'Frequency'
ylabel 'Displacement (U)'
%legend('Ua','Ub','Ug','Location','best');

figure(11)
plot(fqt,InPwr,'o')
hold on
plot(fqt,InPwrF,'x')
hold on
grid on
title 'InputPower'
xlabel 'Frequency'%'Angle of Arm 2 (Degrees)'
ylabel 'Power'
```

```
%legend('InPwr','InPwrF','Location','best');

figure(12)
plot(fqt,ApPwr,'r')%ndwave
hold on
plot(fqt,BtPwr,'b')
hold on
plot(fqt,GmPwr,'g')
hold on
plot(fqt,InPwr,'k')
hold on
plot(fqt,TotPwr,'m')
grid on
title 'Power at Alpha, Beta, Gamma'
xlabel 'Frequency'
ylabel 'Power'
%legend('ApPwr','BtPwr','GmPwr','Pwr(FxV)','TotPwr','Location','best');

figure(13)
plot(ndwave,ApPwr,'r')
hold on
plot(ndwave,BtPwr,'b')
hold on
plot(ndwave,GmPwr,'g')
hold on
plot(ndwave,InPwr,'k')
hold on
plot(ndwave,TotPwr,'m')
grid on
title 'Power at Alpha, Beta, Gamma'
xlabel 'Dimensionless wavenumber (*abs(m-n)/(2*pi)'
ylabel 'Power Reflected & Transmitted'
%legend('ApPwr','BtPwr','GmPwr','Pwr(FxV)','TotPwr','Location','best');

figure(14)
plot(ndwave,fAl,'r')
hold on
plot(ndwave,fBe,'b')
hold on
plot(ndwave,fGa,'g')
hold on
plot(ndwave,lAl,'r')
hold on
plot(ndwave,lBe,'b')
hold on
plot(ndwave,lGa,'g')
hold on
plot(ndwave,tot2,'m')
hold on
plot(ndwave,InPwr,'k')
hold on
%plot(ndwave,InPwrf,'o')
%hold on
plot(ndwave,InPwrF,'x')
hold on
%plot(ndwave,AlphaT,'x')
```

```
%hold on
%plot(ndwave,BetaT,'o')
%hold on
grid on
title 'Total Power at Alpha, Beta, Gamma'
xlabel 'Dimensionless wavenumber (*abs(m-n)/(2*pi)'
ylabel 'Power Reflected & Transmitted'
%legend('fAl','fBe','fGa','lAl','lBe','lGa','Total','Pwr(FxV)','Pwr(inFinite)
','Location','best');

figure(15)
plot(ndwave,lAl,'r')
hold on
plot(ndwave,lBe,'b')
hold on
plot(ndwave,lGa,'g')
hold on
hold on
grid on
title 'Total Longitudinal Power at Alpha, Beta, Gamma'
xlabel 'Dimensionless wavenumber (*abs(m-n)/(2*pi)'
ylabel 'Power Reflected & Transmitted'
%legend('lAl','lBe','lGa','Location','best');

figure(16)
plot(fqt,Ar,'r')
hold on
plot(fqt,Br,'b')
hold on
plot(fqt,Gr,'g')
hold on
plot(fqt,tr,'k')
hold on
plot(fqt,InPwr,'k.')
%hold on
grid on
%axis([0 2250 0 2])
title 'Ratio Flexural Power over Input'
xlabel 'Frequency'
ylabel 'Ratio of Power'
%legend('fAl','fBe','fGa','Total','Pwr FV','PwrForce','Location','best');
%legend('fAla','fAlb','fBe','fGa','Total','Pwr
%FV','PwrForce','Location','best');




%function rubbermobility
%% Fl input to jointbeam beam
clear all
clf


    %% Theory - mobility

    Freq=dlmread('H1_21.txt','','A34..A1833');%A134..A1833  %A74..A834 1634
```

```
omega=Freq.*(2*pi);
%kb=(sqrt(omega))*(((ml)/(B))^0.25);
%MobReTheory=omega./(4*B*(kb.^3));
%MobImTheory=omega.*(-i)./(4*B*(kb.^3));
%MobModTh=sqrt(((MobReTheory.^2)+abs(MobImTheory.^2)));

%% Read experiment data

H1_21Re=dlmread('H1_21.txt','','B34..B1833');
MobReal=-(H1_21Re.*1)./(Freq.*(2*pi)).^2;
H1_21Im=dlmread('H1_21.txt','','C34..C1833');
MobIm=(H1_21Im.*1)./(Freq.*(2*pi)*i).^2;
MobModMea=sqrt(((MobReal.^2)+abs(MobIm.^2)));

H1_21=sqrt(abs(((H1_21Re).^2)+((H1_21Im).^2)));
HdB=-20*log((H1_21));

%HT=sqrt(abs(((MobReTheory).^2)+((MobImTheory).^2)));
%HTdB=-20*log((HT));


%% Plot results

figure(1)
loglog(Freq,real(MobReal),'b')
hold on
%loglog(Freq,real(MobReTheory),'k')
%hold on
grid on
title 'Point Mobility (Real)';
xlabel 'Frequency, [Hz]'
ylabel 'Mobility-Re [m/s/N]'
legend('Real','Theory','Location','best');

figure(2)
loglog(Freq,imag(MobIm),'r')
hold on
%loglog(Freq,imag(MobImTheory),'k')
%hold on
grid on
title 'Point Mobility (Imaginary)';
xlabel 'Frequency, [Hz]'
ylabel 'Mobility-Im [m/s/N])'
legend('Imaginary','Theory','Location','best');

figure(3)
loglog(Freq,MobModMea,'m')
hold on
%loglog(Freq,MobModTh,'k')
%hold on
grid on
title 'Point Mobility (Modulus)';
xlabel 'Frequency, [Hz]'
ylabel '[Log] Mobility-Modulus'
```

```
legend('Measured','Theory','Location','best');

figure(12)
plot(omega,HdB,'k');grid
hold on
plot(omega,HTdB,'k.');grid
hold on
grid minor
title 'Magnitude (dB) plot';
xlabel 'Frequency, [Hz]'
ylabel 'Magnitude (dB)'
%legend();
```

```
%function Wavelength_calculation
%% Wavenumber calculation
clear all
clf
format long e

%Given
b=0.1;                              %m
d=0.02;                             %m
E1=1.75e9;%5.567e9;                         %N/m^2
I1=(b*(d^3))/12;                    %m^4
A1=b*d;                             %m^2
RHO=1190;                           %kg/m^3
L=1*d;                              %m

%Input
Fl=1;%0.707;                               %m
Ff=1;%0.707;                               %m
LbdLt=zeros;
LbdFt=zeros;
fqt=zeros;

%% Main

fqcnt=0;
    for fq=0:100:10000;
        omega=2*pi*fq;

LbdL=(sqrt(E1/RHO))/fq;
LbdF=(sqrt(omega*sqrt(E1*I1/RHO*A1)))/fq;

fqcnt=fqcnt+1;

fqt(fqcnt)=fq;
LbdLt(fqcnt)=LbdL;
LbdFt(fqcnt)=LbdF;

    end

figure(1)
semilogx(fqt,LbdLt,'b')
hold on
grid on
title 'Longitudinal Wavelength vs Frequency'
xlabel 'Frequency'
ylabel 'Longitudinal wavelength'
figure(2)
semilogx(fqt,LbdFt,'r')
hold on
grid on
title 'Flexural Wavelength vs Frequency'
xlabel 'Frequency'
ylabel 'Flexural wavelength'
```

Appendix: F Miscellaneous

Calibration

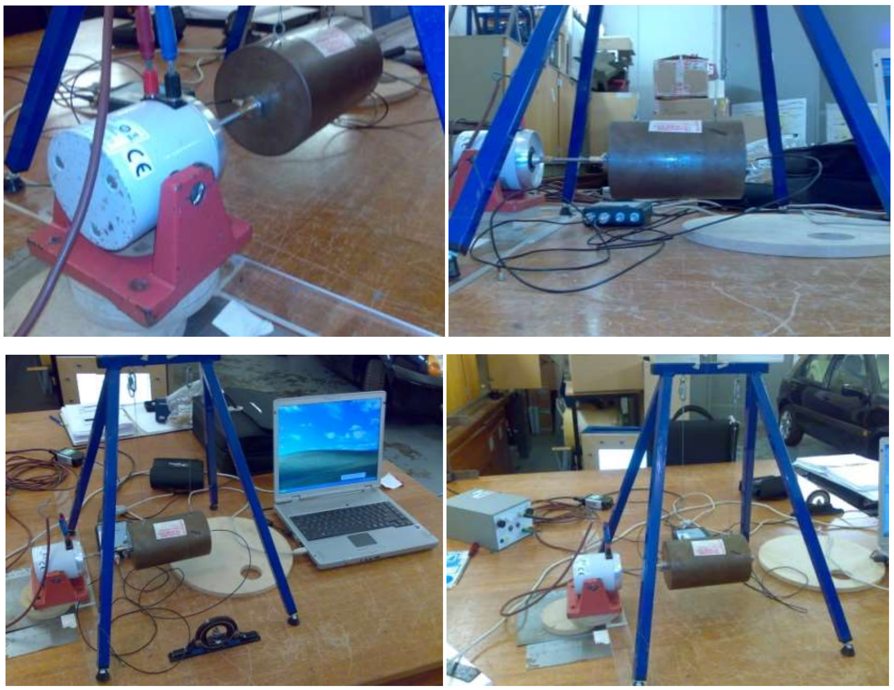

Calibration set-up and measurement in vibration laboratory

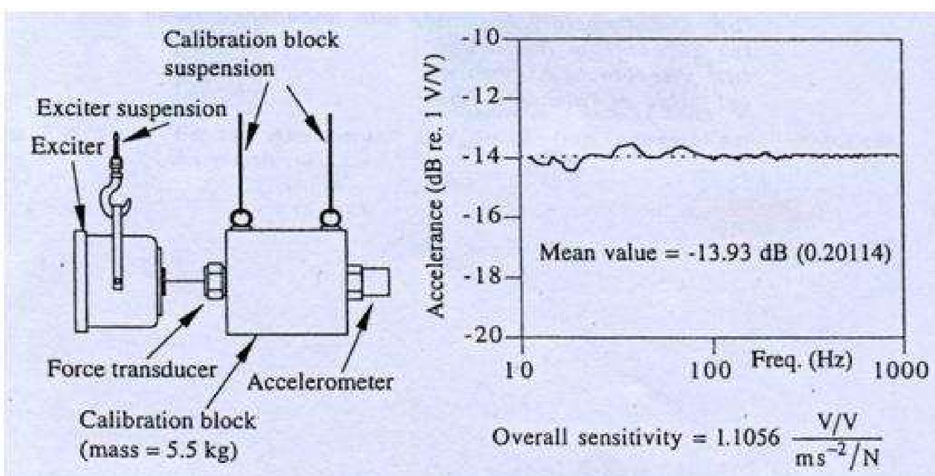

Example of calibration set-up and expected result (Dossing 1988)

Measurement activity can either be using shaker or impact hammer to the set-up mass as shown in figure below.

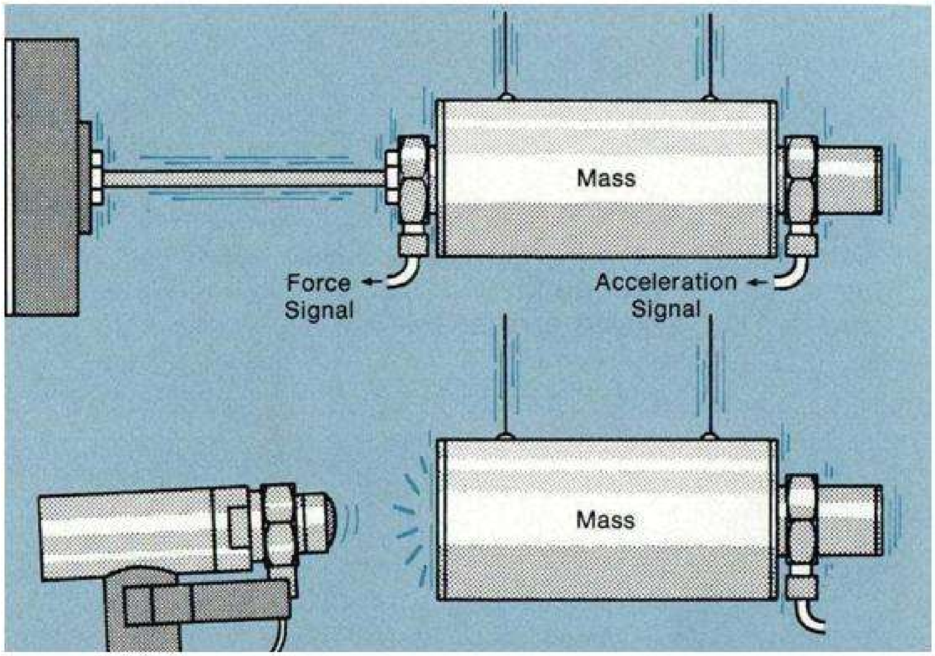

Excitation option (using shaker or hammer) for calibration of transducer (Dossing 1988)

From Newton's second law;

$$\text{Force} = (\text{m})\ \text{mass} \times (\ddot{x})\ \text{acceleration}$$

It is known that accelerance;

$$A(\omega) = \frac{\ddot{x}}{F} = \frac{1}{m}$$

For any frequency the accelerance has amplitude of $1/_{mass}$ and a phase of 0 degrees. Using the shaker and mass of 10kg,

$$A(\omega) = \frac{1}{10} = 0.1$$

The calibration for transducer above was conducted and giving satisfactory result as displayed below.

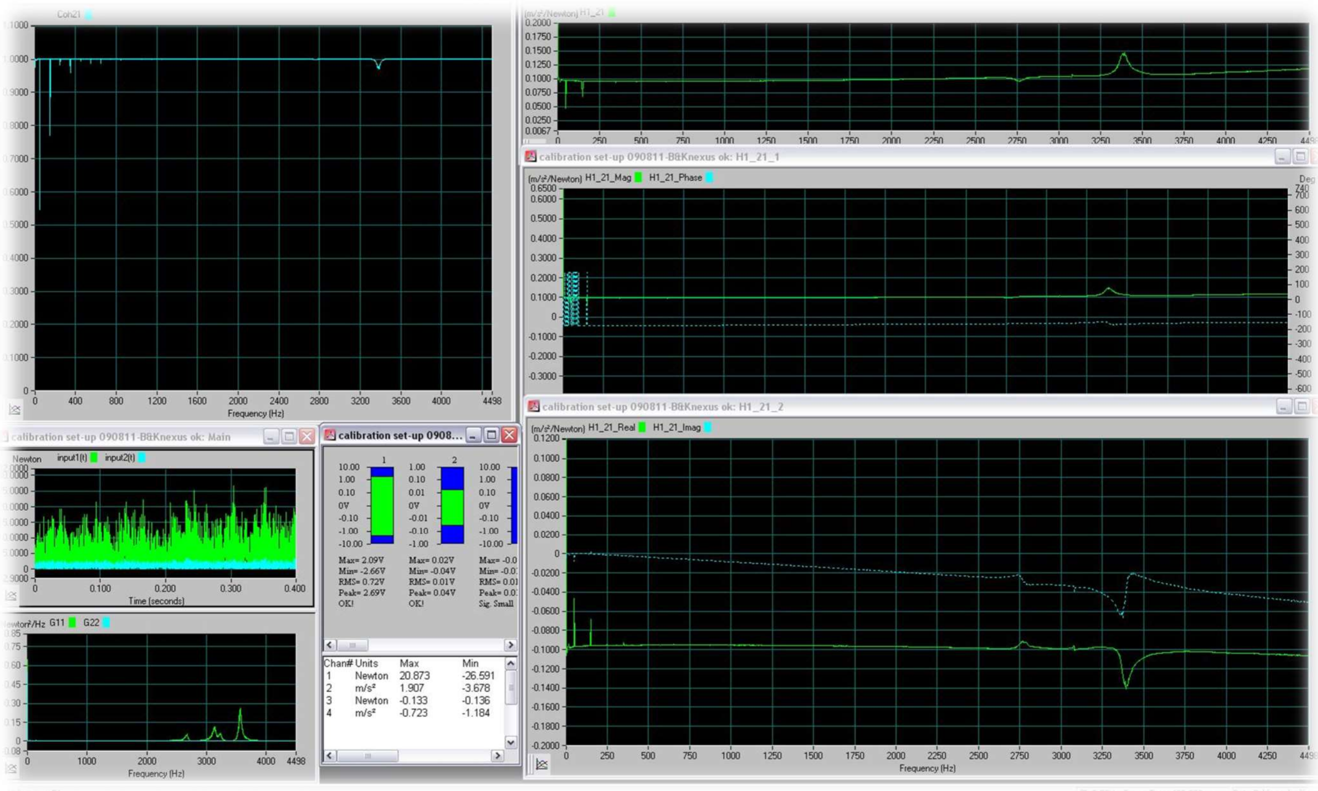

Result displayed for calibration of accelerometer used in measurement

Amplifiers used in measurement activity

Initial Measurement - mobility

Mobility of a similar material for experimentation later was tested for its linearity against theoretical value, in attempt to fully understand equipment's capability and display selection. It is known that from equation of structure point mobility for infinite beam – flexural wave motion force excitation,

$$M_{11} = \frac{(1-i)k}{4\omega\rho A}$$

From calculation of mobility, at 100Hz and 2000Hz, mobility value was at -34.4dB and -47.4dB as plotted on the displayed result from laboratory measurement below. This shown close similarity (poor measurement result after 3000Hz due to material's imperfection) for measurement and theoretical beam of infinite length.

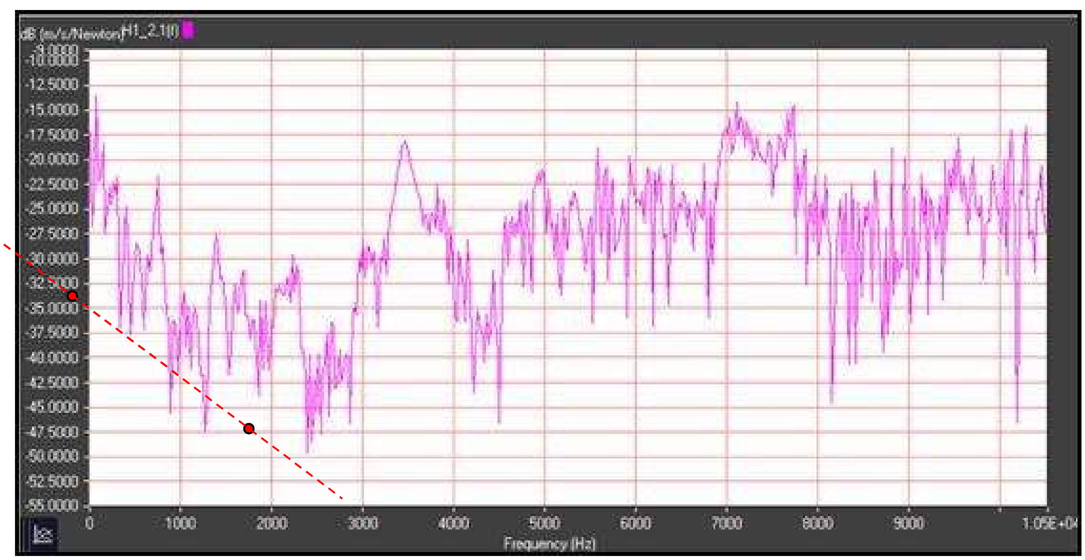

Mobility for sample Perspex beam measured compared to theoretical value (linear dotted line)

Another measurement were taken from the angled beam giving a better mobility results as displayed below

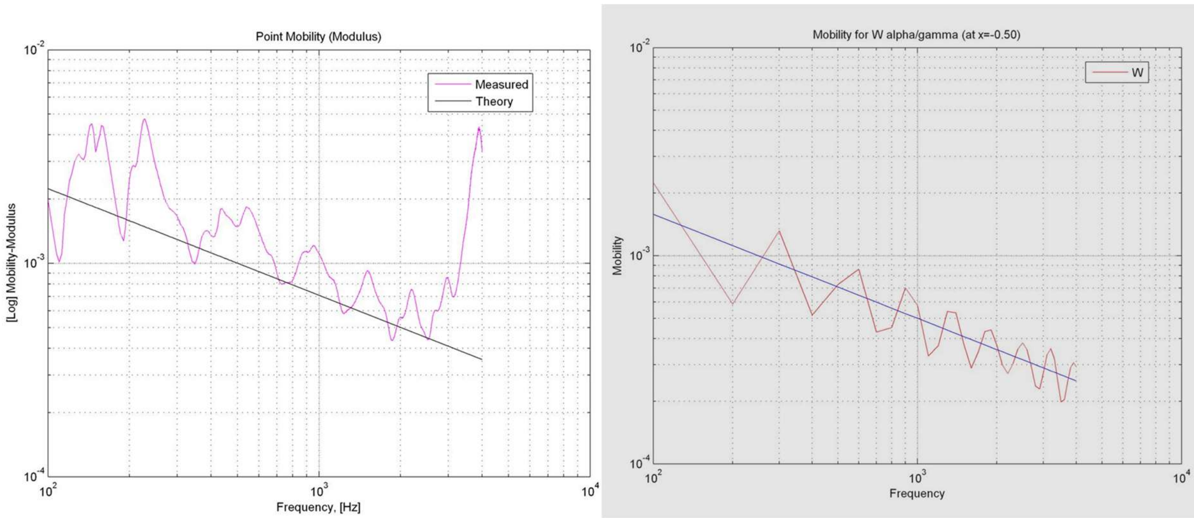

Point Mobility comparison between measurement (left) and modelling (right) at 120^o angle beam – Frequency 100Hz-4000Hz

Measurement set-up using Focus analyser in the lab

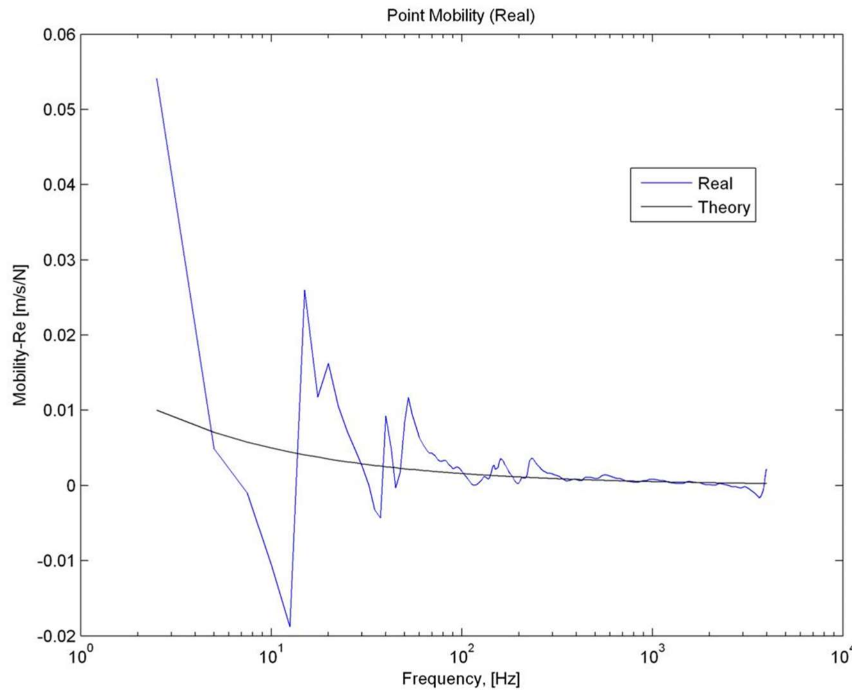

Mobility-Real against log frequency

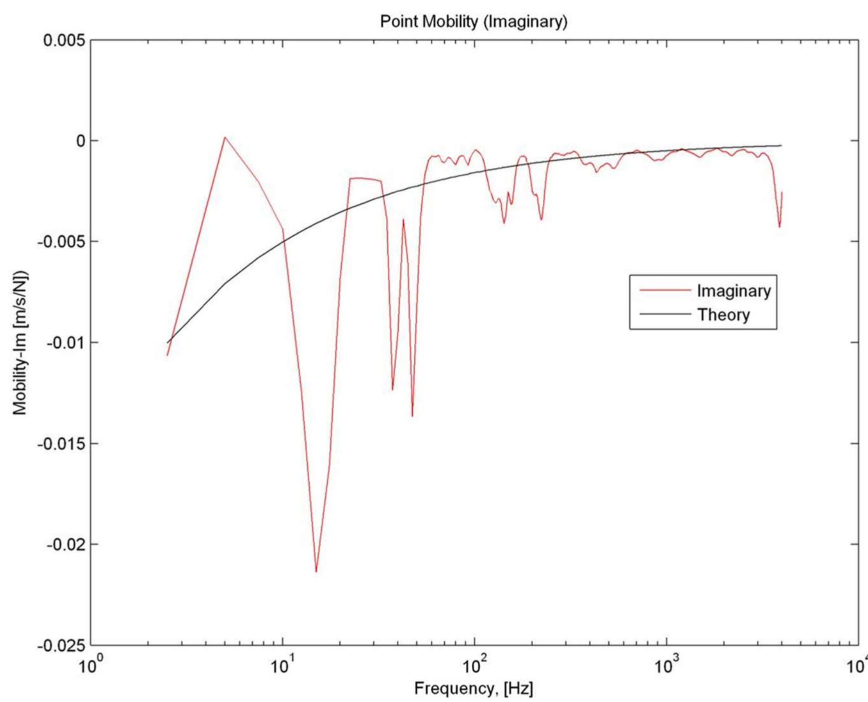

Mobility-Imaginary against log frequency

Errors and averaging

Apart from random and bias errors in measurements, the further consideration would also to include calculation for amplitude error and phase error in mathematical model and provide clear bridge to the measurement in experiment.

From the ideal displacement equation,

$$x(t) = A\sin\big(\omega t - k(x+d)\big),$$

Where d is distance between two transducers (0.03m).

Consideration for the amplitude error, A_e and phase error, $\emptyset_e$ into the above equation,

$$x(t) = (A + A_e)\sin(\omega t - k(x+d) + \emptyset_e)$$

Measurement display for all variable angles and set-up of experimentation

Figures shows samples of response data obtained during measurements

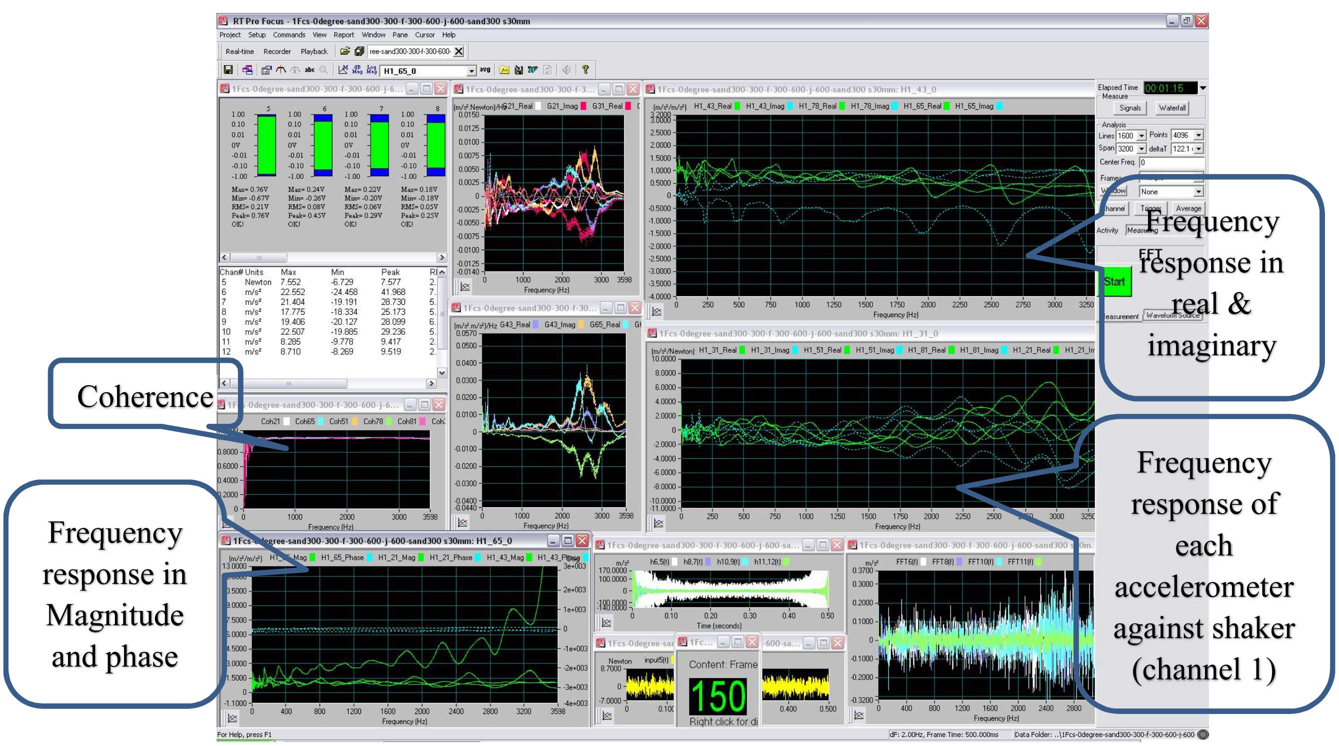

Measurement display for 0º angle set-up (two straight beams connected)

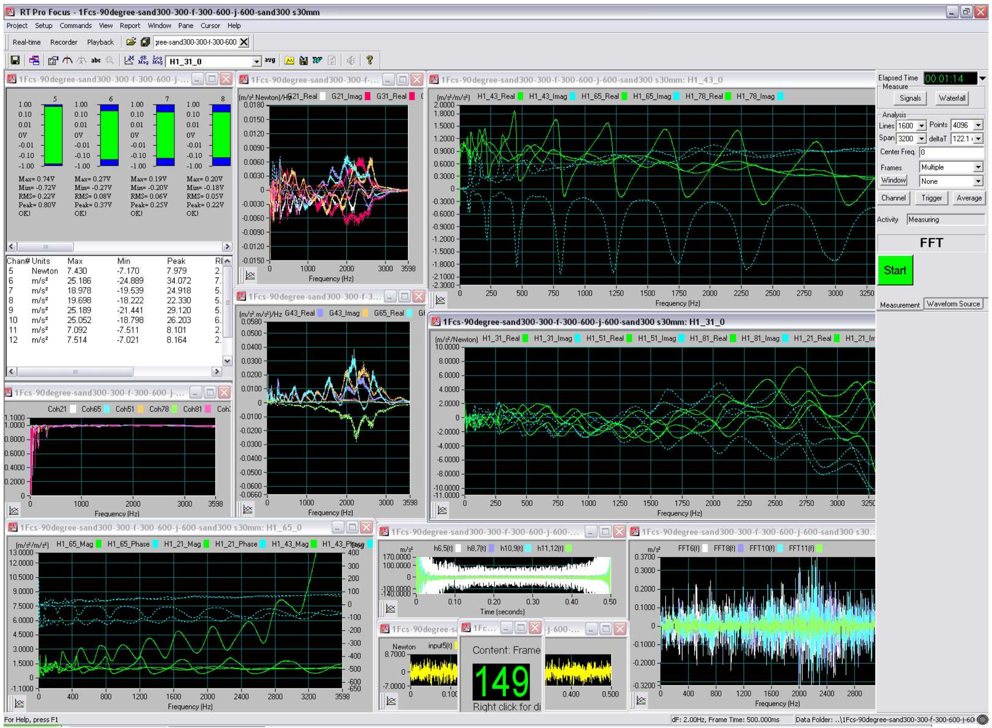

Measurement display for 90º set-up of beam angle

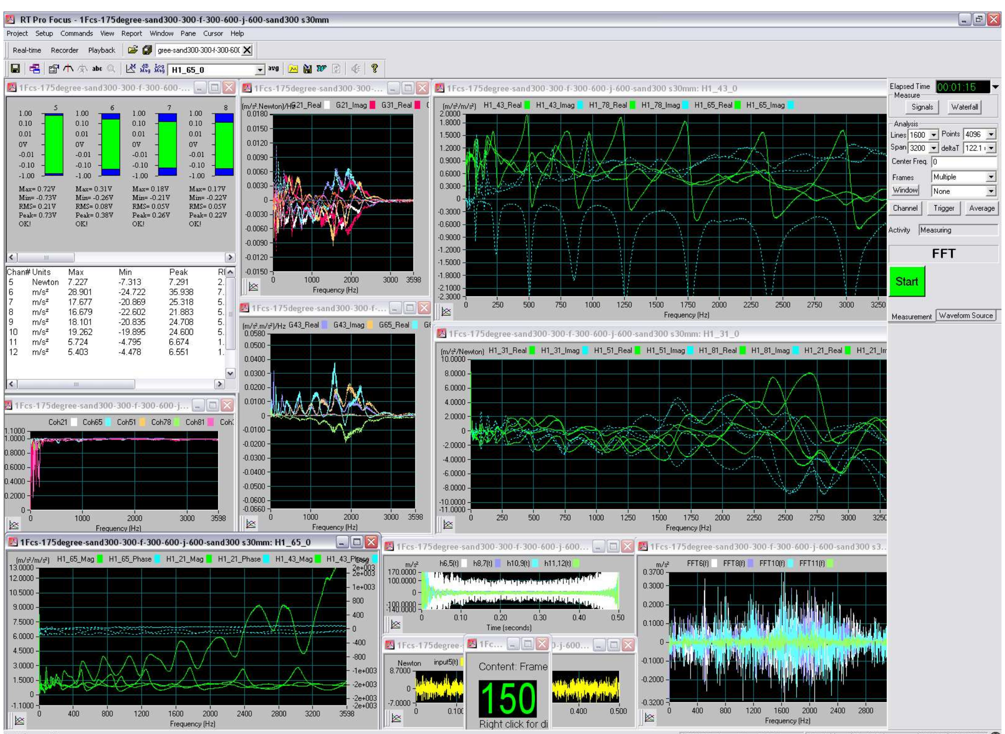

Measurement display for 175º set-up of beam angle

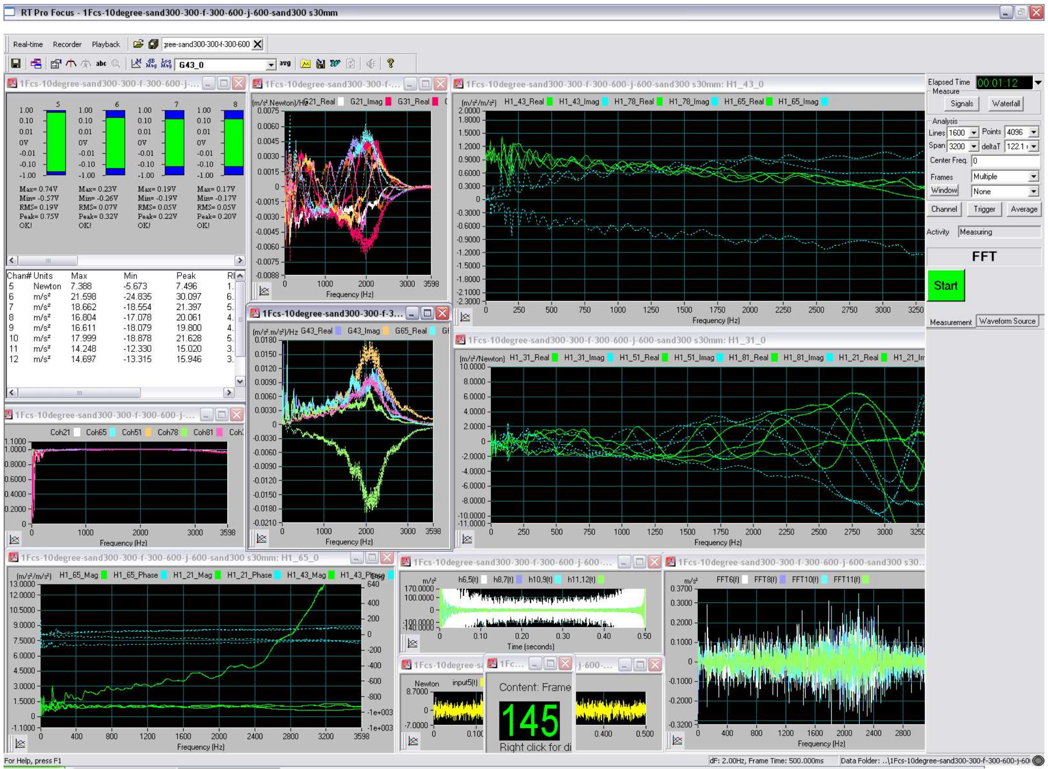

Measurement display for 10º set-up of beam angle

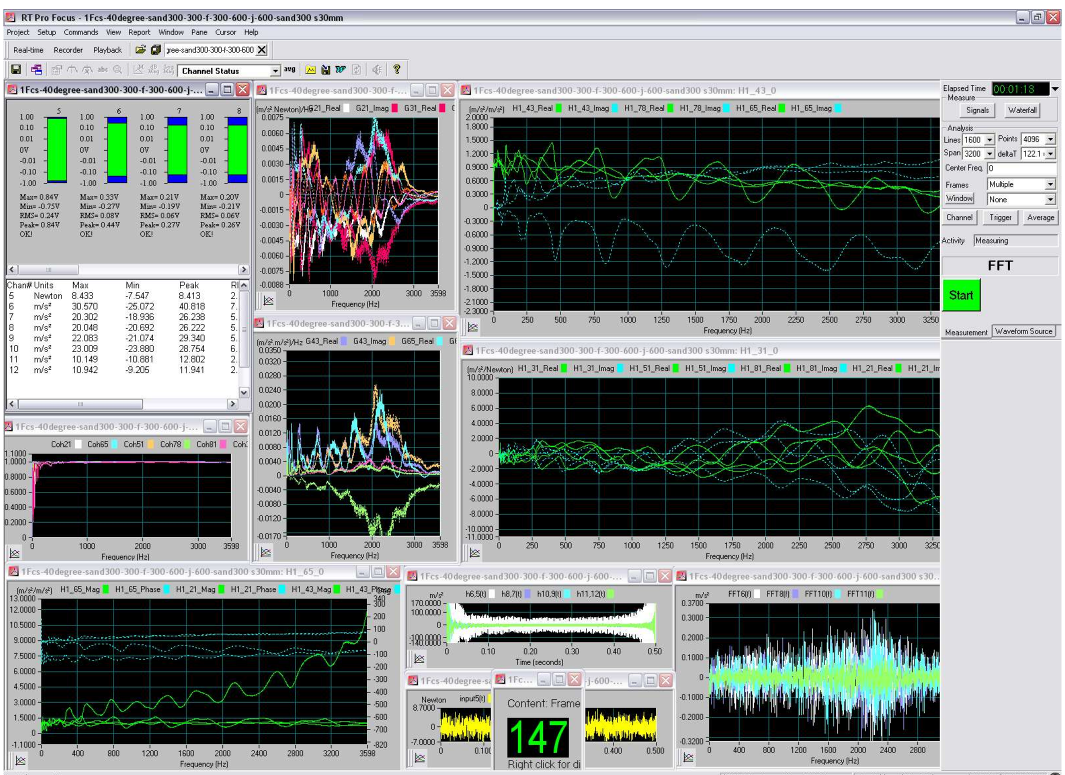

Measurement display for 40º set-up of beam angle

Measurement display for 60º set-up of beam angle

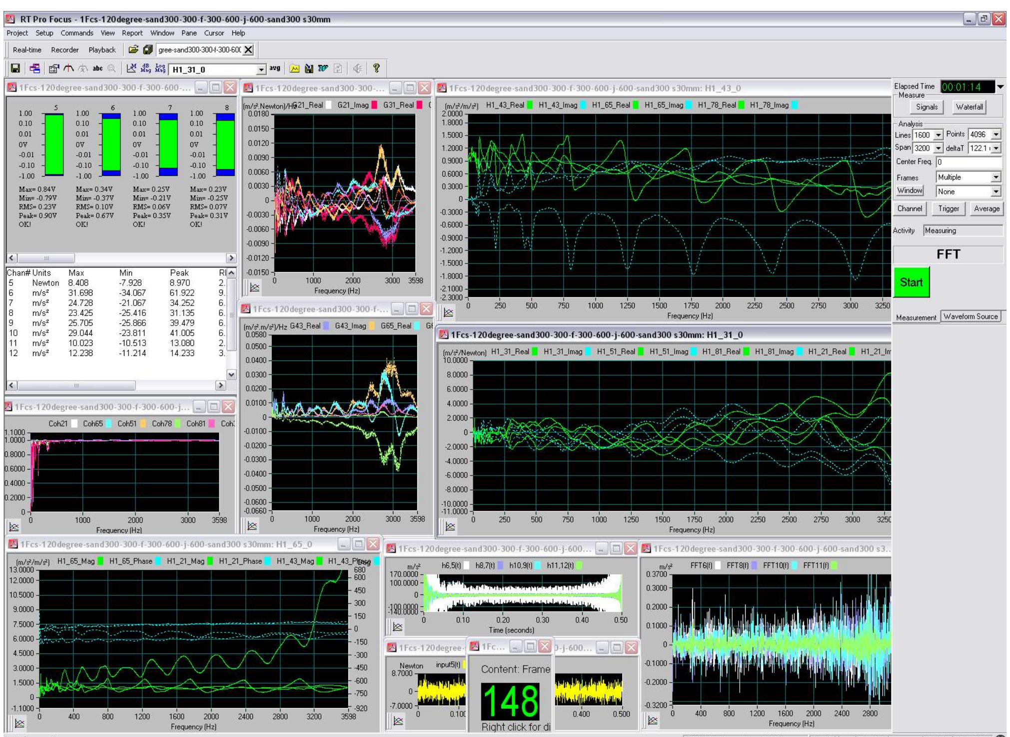

Measurement display for 120º set-up of beam angle

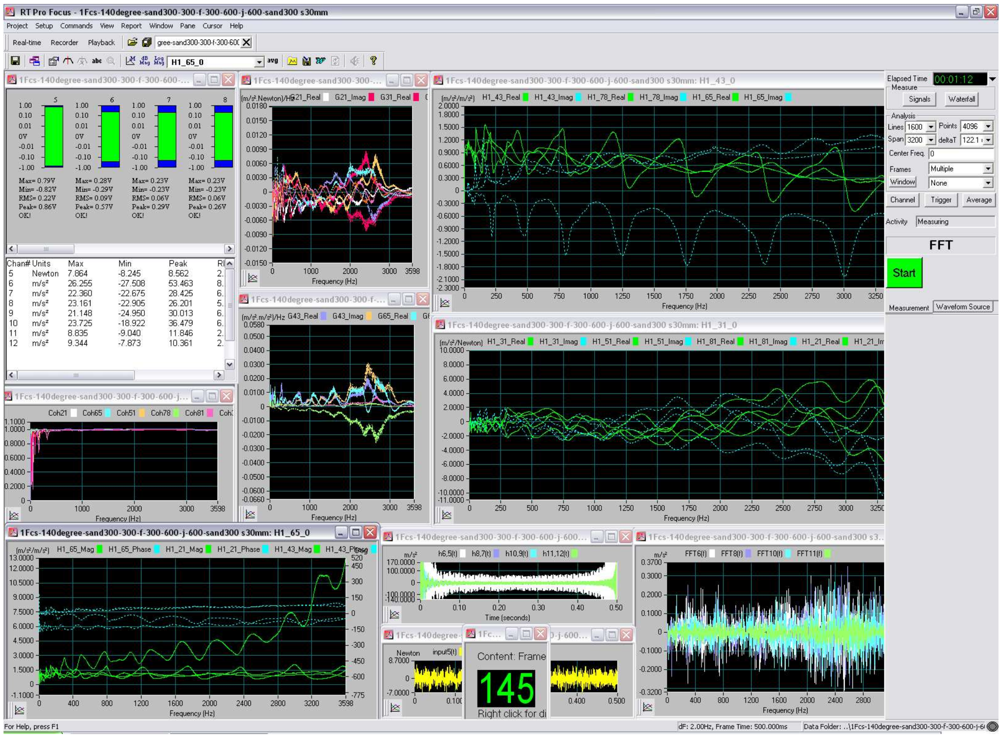

Measurement display for 140º set-up of beam angle

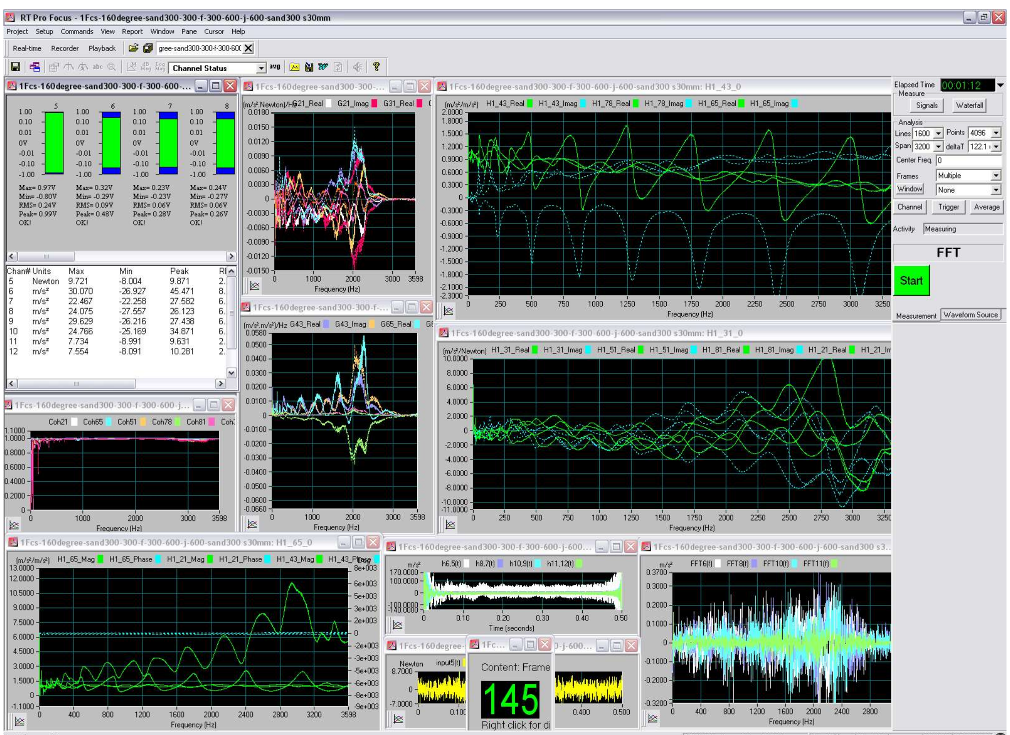

Measurement display for 160º set-up of beam angle

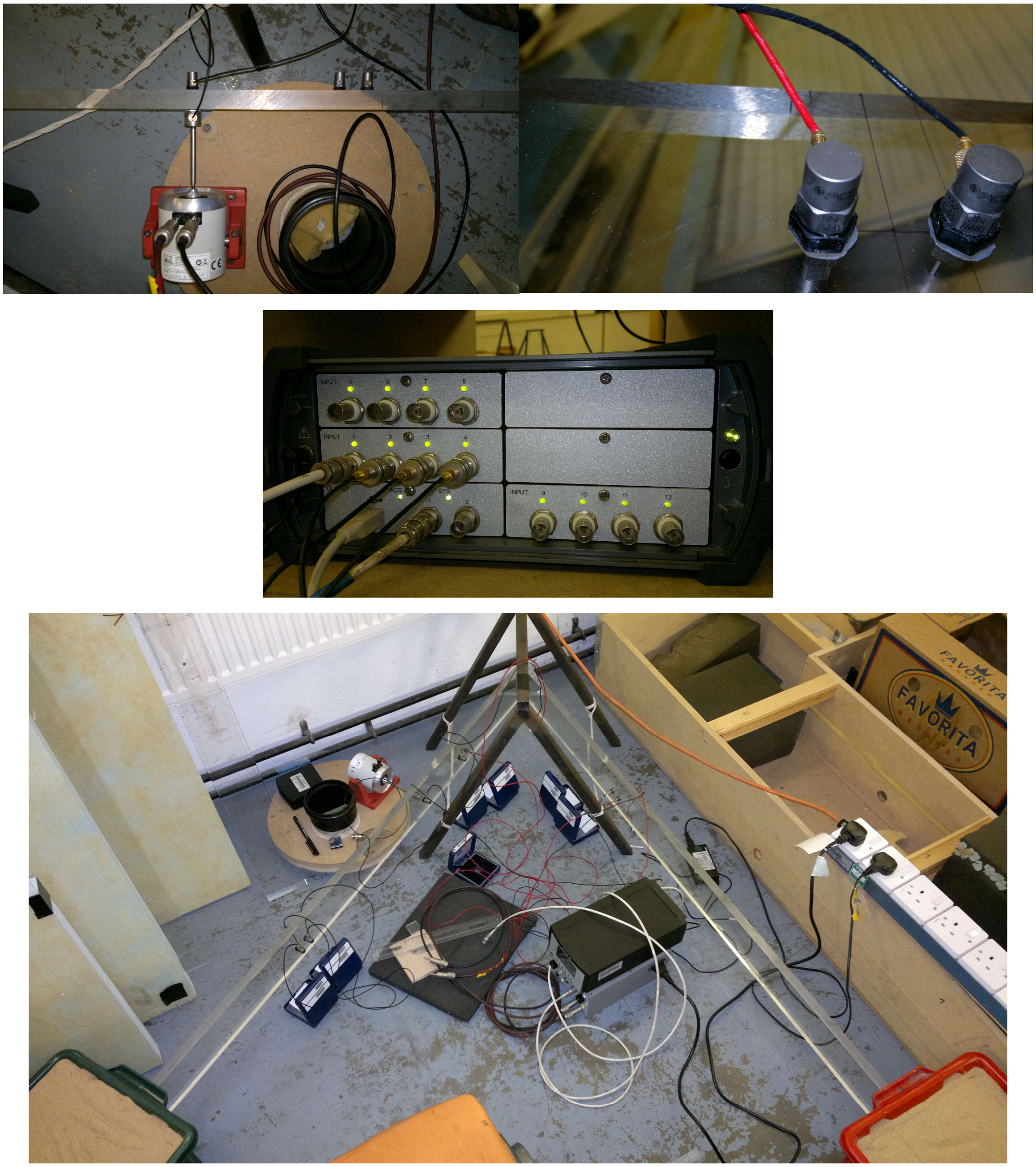

Measurement set-up with Focus analyser for 120º angle

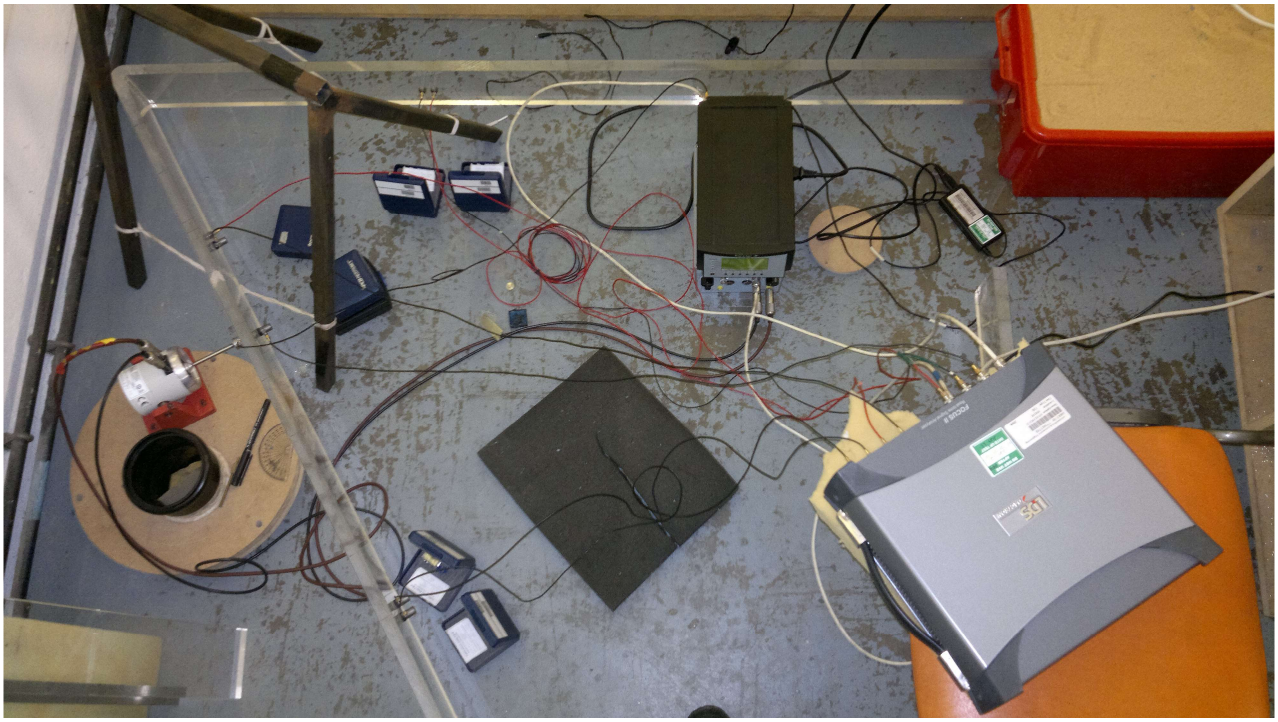

Measurement set-up for 120º angle

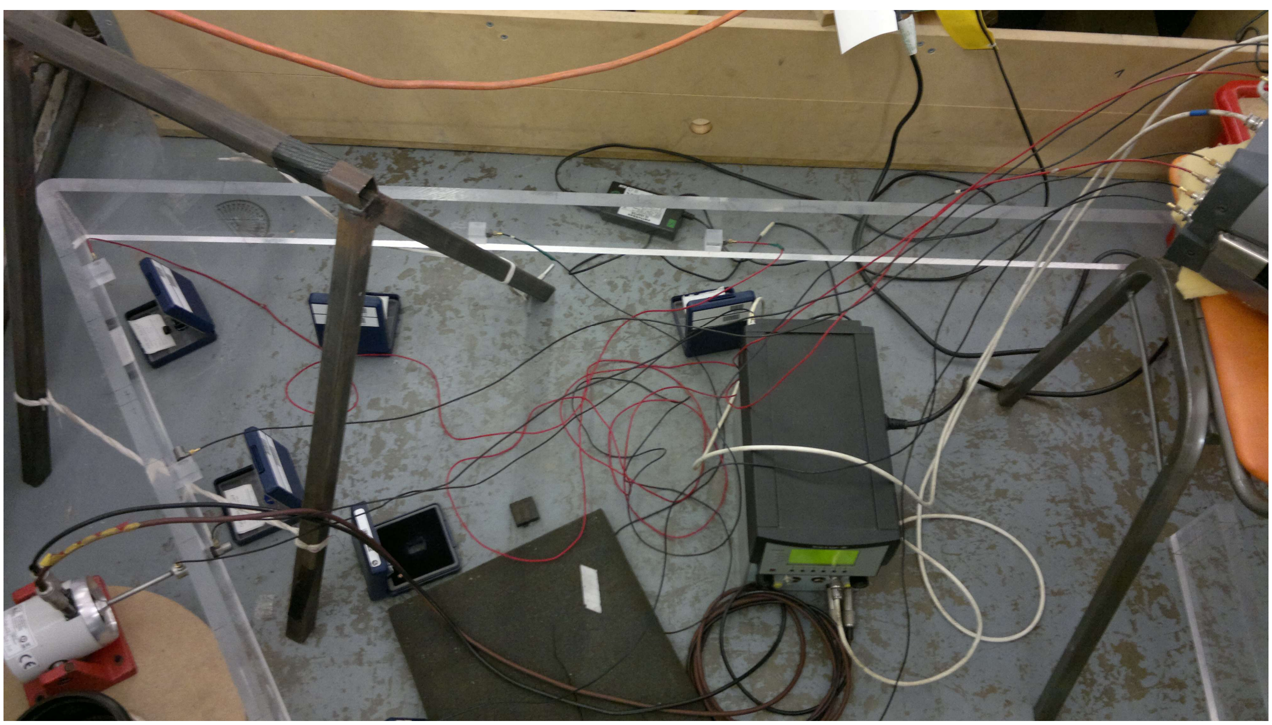

Measurement attempt to obtain longitudinal power responses.

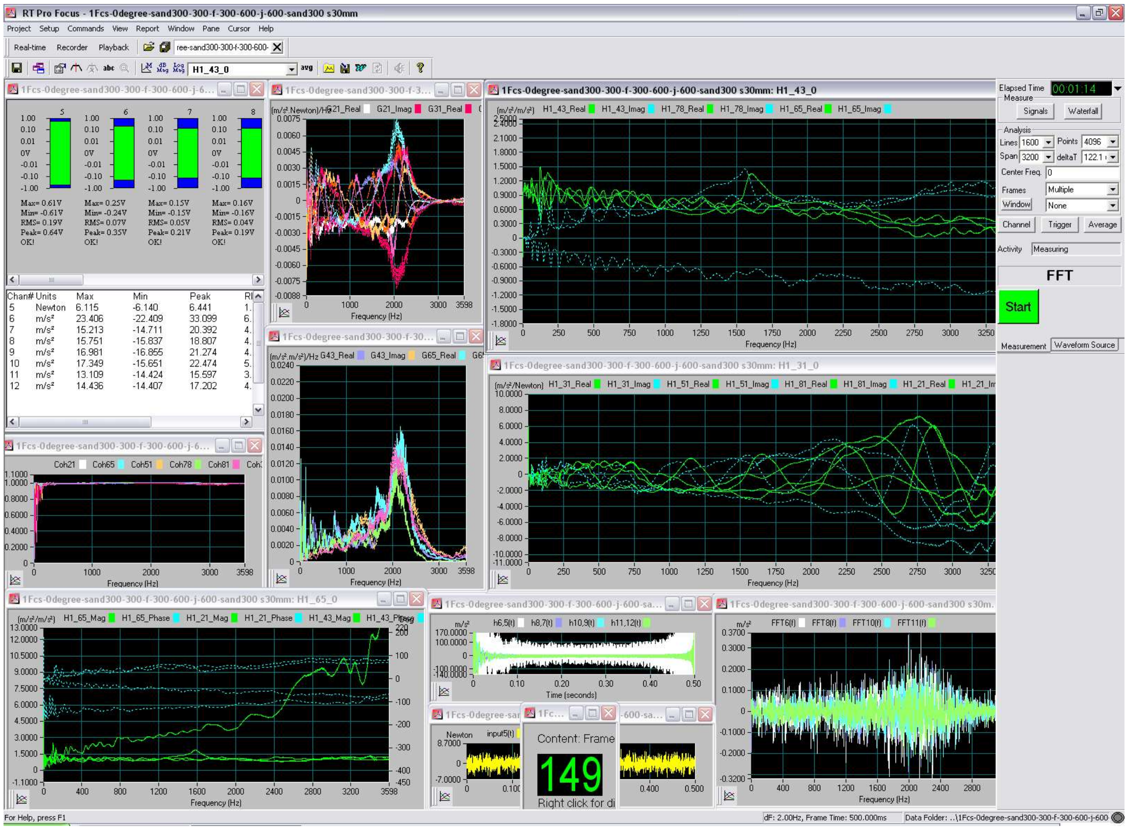

0 degree setup for joint with rubber layer

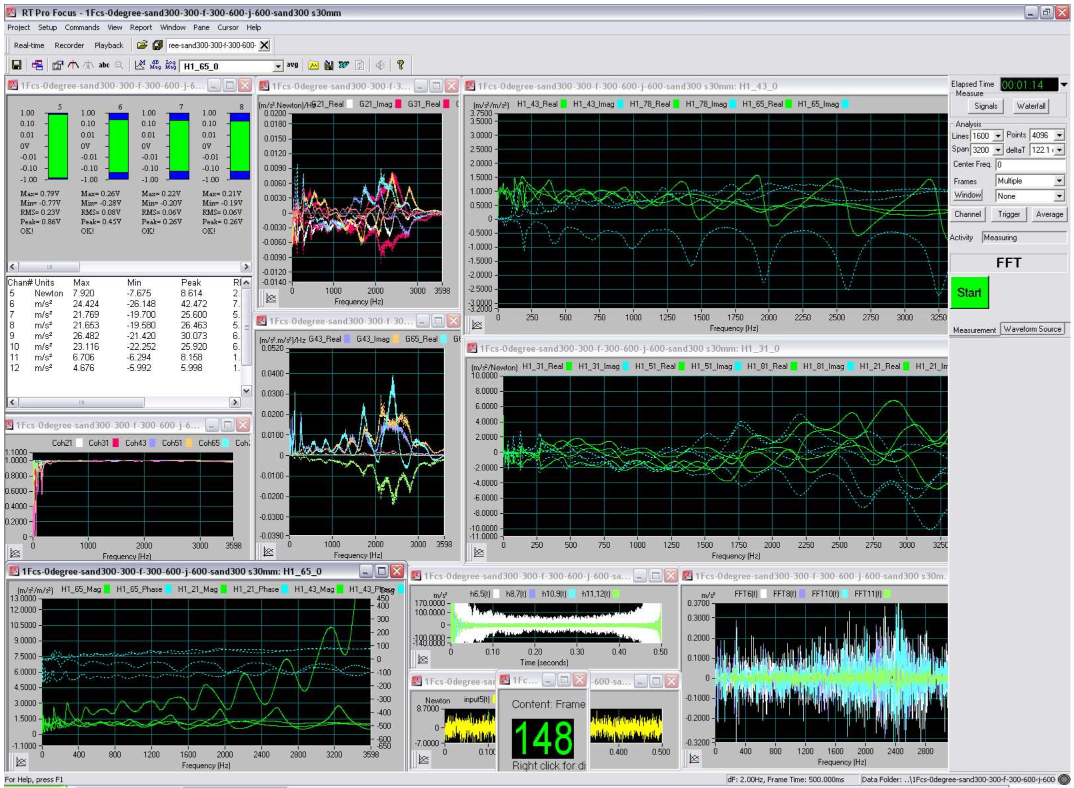

40 degree setup for joint with rubber layer

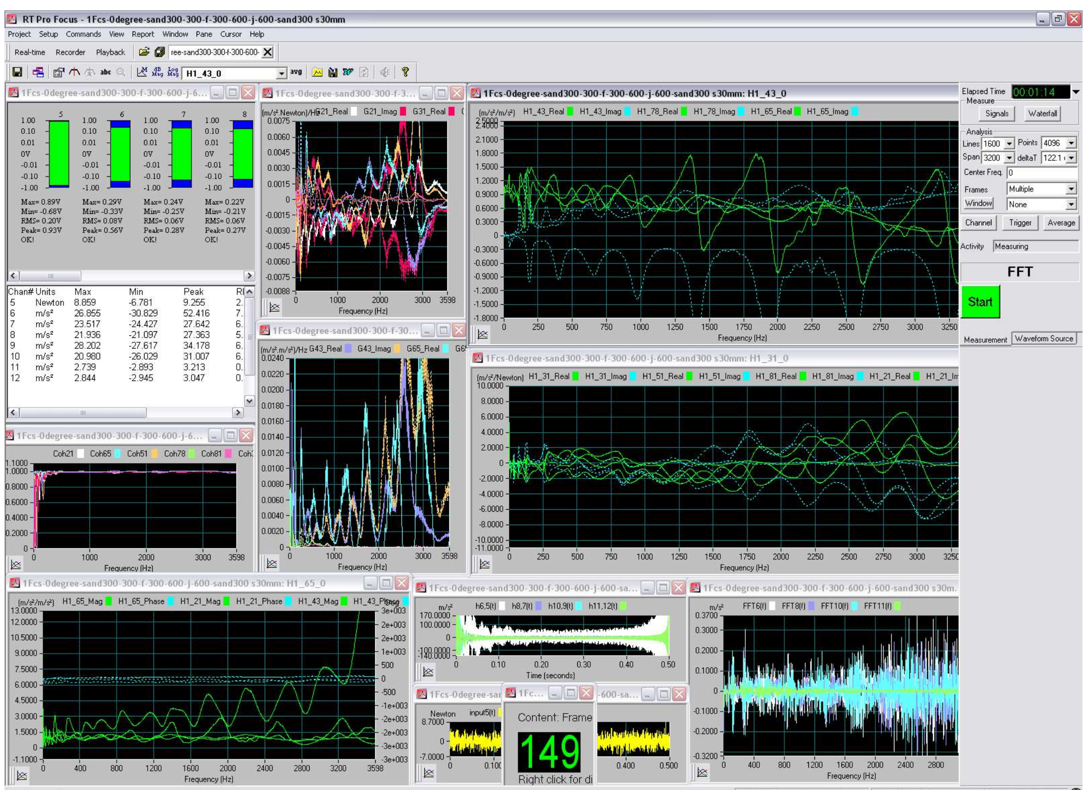

90 degree setup for joint with rubber layer

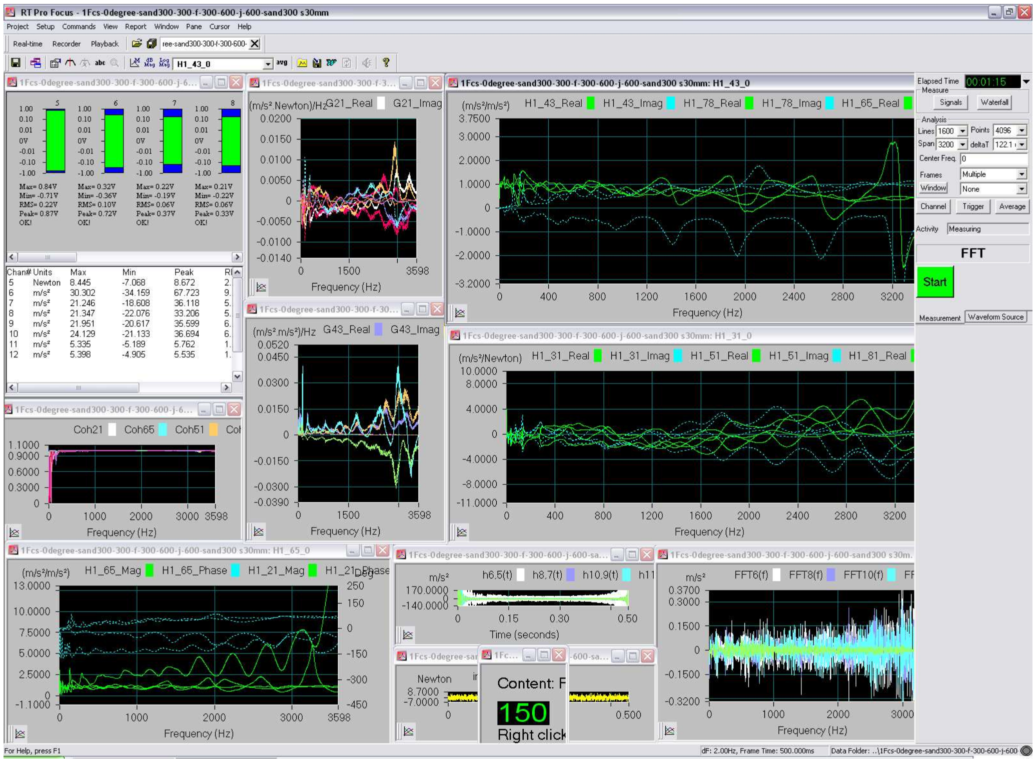

140 degree setup for joint with rubber layer

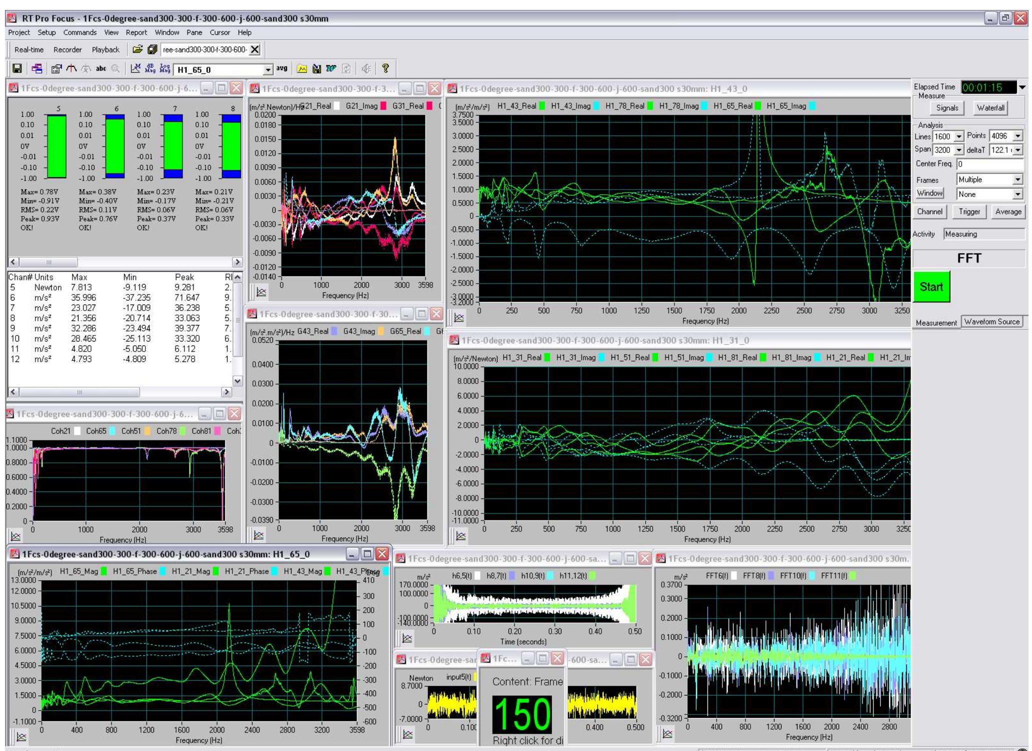

175 degree setup for joint with rubber layer